NASA Reference Publication 1017

Stratospheric Warmings: Synoptic, Dynamic and General-Circulation Aspects

Raymond M. McInturff, Editor

JANUARY 1978

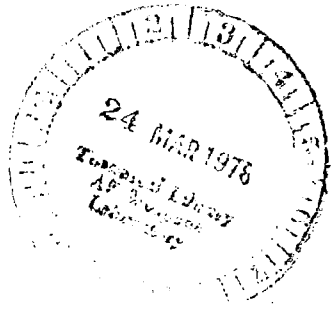

NASA Reference Publication 1017

Stratospheric Warmings: Synoptic, Dynamic and General-Circulation Aspects

Raymond M. McInturff, Editor
National Meteorological Center
Washington, D.C.

National Aeronautics
and Space Administration

**Scientific and Technical
Information Office**

1978

PREFACE

Much has been learned about stratospheric warmings (often called STRATWARMS) during the past quarter-century, thanks largely to the improved observational basis. At the same time, advances in the theory of the general circulation have made possible studies of stratospheric energetics and of stratospheric-tropospheric interaction which are crucial to a fundamental understanding of STRATWARMS. Thus, theoretical meteorologists have made notable contributions in pointing out ways in which the available data may be used to best advantage and in formulating hypotheses, while applied meteorologists have come to a better position for testing the hypotheses.

Up to now, reports of observational and theoretical research on STRATWARMS have been widely scattered in a variety of publications. Some results have not been documented at all. It seems to us that the time has come to summarize some of the present information on STRATWARMS and their relationships with other phenomena. The purpose of this monograph, then, is to consolidate currently available information on STRATWARMS. We include other pertinent aspects in order to provide background information for the non-specialist. Hopefully this will show where the meteorological community presently stands in this area of stratospheric research.

We realize that such an account could include many more items and more detailed discussion. In the selection of material, we were guided largely by considerations of accessibility of the pertinent literature. For example, there now exist rather detailed accounts of climatology (e.g., publications of the Stratospheric Research Group at the Free University of Berlin, Meteorologische Abhandlunger, Bd. 100, Hefte 4 and 5), which we saw no reason to duplicate. Similarly, with regard to the ionosphere, we wished merely to give the barest introduction to the subject, since our area of concern is confined, as we see it, to the neutral atmosphere. Finally, our concern with ozone is restricted to its role in stratospheric warmings.

The rather comprehensive lists of references should serve to guide the reader in obtaining additional information.

This monograph was prepared by the Staff of the Upper Air Branch, Development Division, National Meteorological Center, National Weather Service, National Oceanic and Atmospheric Administration. The principal contributors, along with principal subjects, are as follows:

Raymond M. McInturff - Data-basis; Energetics; Mesosphere

Roderick S. Quiroz - Synoptic Description

Alvin J. Miller and Keith W. Johnson - Numerical Modeling

James D. Laver - Climatology

Ronald M. Nagatani - Ozone; Introduction

Melvyn E. Gelman - Stratospheric Warmings in Relation to Man's Activities

Frederick G. Finger, Chief
Upper Air Branch
National Meteorological Center
National Weather Service, NOAA

ACKNOWLEDGMENTS

The editor wishes to express thanks to Mrs. Joyce Peters, who typed the manuscript in exemplary fashion and provided considerable editorial assistance. Her diligence and independent good judgment greatly facilitated the production of this monograph.

The authors and editor are grateful to the following publishers, for permission to reproduce material in this monograph which had previously appeared elsewhere: The Pergamon Press, Oxford, England; the American Meteorological Society, Boston, U.S.A.; the Royal Meteorological Society, Bracknell, England; Birkhäuser Verlag, Basel, Switzerland; Verlag von Dietrich Reimer, Berlin; and the U.S. Naval Weather Service Command. Each piece of material is identified as it is presented in the text by reference to the source, given in the list of papers beginning on page 156.

CONTENTS

STRATOSPHERIC WARMINGS: SYNOPTIC, DYNAMIC AND GENERAL-CIRCULATION ASPECTS

Edited by Raymond M. McInturff[1]
Upper Air Branch
NOAA, National Weather Service, National Meteorological Center

SUMMARY

Both observational and theoretical aspects of stratospheric warmings (STRATWARMS) are reviewed. From an historical viewpoint, it is shown how radiosondes, rocketsondes, and finally satellites have aided in the depiction of stratospheric phenomena and the interaction of the layers above and below (the mesosphere and troposphere). Matters of nomenclature are discussed for the sake of clarity. By way of background, a stratospheric climatology is sketched, though this is based on only samples from about 30 years of data for the lower stratosphere (16-20 km), 25 years for the middle stratosphere (20-30 km), and 15 years for the upper stratosphere (30-50 km). The "normal" warm and cold seasons are described, along with average interhemispheric differences. Thus the stage is set for a discussion of anomalies--i.e., warmings and coolings, with emphasis on the type of mid-winter warming which results in circulation reversals at 10 mb or lower, since this phenomenon is rather irregular in nature and must be explained in terms of dynamic effects rather than radiative effects. (The latter appear paramount during the more regular springtime and autumnal circulation reversals.)

Case-studies dominate the sections on synoptic description. No two warmings have been exactly alike, but there are similarities which suggest similar causes.

The discussion of stratospheric energetics serves as a necessary prelude to a discussion of theoretical aspects. The flux of geopotential from troposphere to stratosphere (along with quantities which may be derived therefrom) appears to hold greatest promise for the prediction of STRATWARMS; thus, tropospheric-stratospheric interaction is given considerable emphasis.

Less is known about stratospheric-mesospheric interaction, and consequently little is said on this topic, although interesting stratospheric-ionospheric relationships have been discovered.

---

[1]See Preface for contributors to the various sections of this report.

As elsewhere in meteorology, numerical modeling provides the most fruitful approach to theoretical analysis of the sTRATWARM phenomenon. Three types of models are discussed--forecast models, general-circulation models, and analytical (hypothesis-testing) models. Wave-zonal flow interaction (critical layer) theory has provided much insight into STRATWARMS, just as in the case of tropical phenomena (the quasi-biennial and semi-annual oscillations).

Physical considerations make it clear that there are close correlations between changes in ozone concentrations and changes in temperatures at stratospheric levels. The backscatter Ultraviolet (BUV) instrument on board the Nimbus 4 satellite has yielded a great deal of data on world-wide ozone concentration and distribution, and while these data are still largely preliminary, it seems certain that the BUV will ultimately be useful in clarifying the relationships between ozone and the STRATWARM phenomenon.

Perhaps the most interesting but also the most difficult of topics in this connection is that of the impact of stratospheric disturbances on man's activities, and the possible reverse impact of man's activities on the stratosphere. The latter in particular has been given wide publicity. It is hoped that the remarks on this subject, indeed, that the entire monograph, will help place this question in better perspective.

INTRODUCTION

Throughout the past few decades an increasing amount of information has been accumulated on the stratospheric circulation, in particular on the so-called wintertime "stratospheric warming" phenomenon. A greater knowledge of the stratosphere is evolving from studies utilizing the world-wide radiosonde network, a more limited number of high-altitude rocketsonde observations, and more recently a massive amount of data gathered by meteorological satellites.

The purpose of this paper is to consolidate present knowledge of stratospheric circulation behavior, with a primary emphasis on the warming phenomenon. Some of the important works of past years will be highlighted, defining the role of stratospheric warmings in the processes of the atmosphere and the role the phenomenon plays in redistributing mass and important trace constituents in the stratosphere.

One of the goals of this monograph will be to determine the impact that stratospheric warmings might have on practical problems associated with SST and space shuttle flights, forecast problems, and infrared horizon sensing for satellite navigation. The monograph will also attempt to lay some groundwork for future studies on stratospheric warmings, to examine options open for future investigators, and to examine some of the data sources that might be available for studies of future warmings.

In order to introduce the subject of stratospheric warmings, some history of the event and a few words on the various observational methods

used for the stratosphere may be in order. Scherhag's first documentation of a mid-winter stratospheric warming in 1952 (ref. 1) stimulated the use of higher altitude balloons, and by the late 1950's rawinsonde observations reaching levels as high as 10 mb were fairly common. By the end of that decade a number of studies had been completed and several other warming events and circulation changes had been documented (refs. 2, 3 and 4). With a number of warmings having been documented to present, it is now well known that the most intense events are accompanied by large-scale temperature variations exceeding 50°C within a deep stratospheric layer and within the period of about a week. The stratospheric circulation also undergoes tremendous upheavals, with the normal polar cyclone and associated strong westerlies being replaced by circumpolar anticyclonic flow. What was once thought to be a highly stratified, quiescent medium has now been shown to be strongly dynamic in character. A growing number of scientists have become interested in the stratosphere with the point of view of relating stratospheric warmings with solar events or relating tropospheric events with high-level warmings. These topics are still being actively investigated.

Technological advances in rocketry yielded an expansion in high-level observational capabilities in the 1960's, allowing, by the last half of that decade, the derivation of at least the large-scale circulation of the Northern Hemisphere upper stratosphere. Only through painstaking research and development has the instrumental concept proven itself in an operational meteorological network and we now have a more complete picture of stratospheric meteorology. For the lower stratospheric levels (100-10 mb), the number of rawinsonde observations increased dramatically. Conscious efforts were directed toward reducing the effects of solar radiation on the instrument or thermistor at very high levels. The U.S. National Weather Service, for example, adopted a more efficient high-altitude thermistor.

The addition of the higher-level rocketsonde data allows analysis of the very-large scale circulation features to the top of the stratosphere and higher into the mesosphere. Rocket data have shown that the greatest wintertime variations take place at about 40 to 45 km and that warmings can be traced to even higher altitudes.

Most recently, a large volume of satellite data has become available for analyses of stratospheric warmings. The use of satellite data has already yielded new information, but full exploitation of the observations from various types of instrumentation is still in the future. Problems of compatibility of data are created with each new data source, and at present the relative usefulness of the data from the various satellite instruments is being evaluated. Satellites have revealed evidence of a series of pulses throughout the winter, some stronger at higher levels, some at lower levels. The pulses appear at approximately bi-weekly intervals, suggesting some sort of solar influence on stratospheric warmings.

The synoptics and energetics of many individual warmings have been closely examined, and the evidence compiled suggests that the major energy source of stratospheric warmings lies in the troposphere. The basic questions of where and how the troposphere is coupled to the stratosphere and what mechanisms are involved in producing and maintaining the warming are slowly being answered but much work remains to be done. Trenberth (ref. 5) addresses himself to these questions in his review of various theoretical and observational works relating primarily to causes and effects of the phenomenon. That orography plays an important part in stratospheric

warmings can be seen by the differences in circulation patterns between the Northern and Southern Hemispheres. The Aleutian anticyclone and a displaced polar vortex in the Northern Hemisphere are nearly stationary wave-one features resulting from orographic influences and nonzonal heating. The Southern Hemisphere, on the other hand, has a nearly circumpolar vortex because of lesser orographic and nonzonal heating contrasts, and consequently does not have as strong a stationary wave feature as in the Northern Hemisphere. Both hemispheres have transient features, and the interaction between the transient and stationary features appears to produce stratospheric warmings with more explosive effects in the Northern Hemisphere while the absence of a strong stationary features in the Southern Hemisphere produces warmings having lesser impact. Questions that need to be answered are related to the tropospheric causes and effects of these stationary waves in the stratosphere, the sources or origins of the transient waves, and the mode of interaction between the two types of waves.

Other interesting questions to be raised are the interactions between various levels of the atmosphere. As mentioned earlier, the troposphere appears to be the major energy source of stratospheric warmings, with the eddy flux of geopotential of prime importance (refs. 6, 7, 8). There is no unique relationship, however, between the eddy flux of geopotential and the type of warming one sees in the stratosphere, and the relationship is probably further complicated by wave energy fluxes. Interactions with mesospheric and ionospheric levels are also intriguing with even less known about these interactions.

The meteorological satellite has aided greatly in the monitoring and understanding of warmings. An interesting feature revealed by data from SIRS and SCR is the global extent of stratospheric warmings (refs. 9 and 10), but the mode of interhemispheric relationships remains to be solved. Quiroz (ref. 11) has documented several cases of warmings seen from satellite data, and this massive amount of data has made it possible to do more extensive analyses of warmings, raising more questions than ever before. The satellite is also yielding Backscatter Ultraviolet (BUV) ozone data from Nimbus IV, and efforts are now being directed toward a study of the 1970-71 warming. Other data from satellites are also forthcoming, including Pressure Modulated Radiometer (PMR) information, and these should yield more information about stratospheric warmings to even higher altitudes.

Perhaps the most important questions to be answered concern the relationship of stratospheric warmings on man's activities, the effects warmings have on designs of vehicles, and their fuel consumption; what the prospects are for forecasting at the higher levels, and what the long range effects may be of stratospheric warmings on the troposphere, and the predictability of these effects.

A Table of Acronyms and Abbreviations appears on pages 154-155 for the convenience of the reader.

DATA USED IN MONITORING AND STUDYING STRATOSPHERIC WARMINGS

Background

The data used thus far in real-time monitoring of STRATWARMS have generally coincided with those used in carrying out research studies of the phenomenon. These data have come from essentially three sources: (1) balloon-sounding devices (rawinsondes), currently with an effective upper limit of 30 km, (2) rocket-sounding devices (rocketsondes) with an effective upper limit in the Western Hemisphere of about 60 km, and (3) satellite-borne remote sensors. Up to 1960, the network of rocket-sounding stations was too sparse to permit anything more ambitious than single-station analysis for levels above 30 km. Consequently, stratospheric warmings which occurred between 1952† and 1960 were studied mainly by means of subjective analyses of synoptic rawinsonde data (mostly for 100-30 mb, but extending more and more frequently, with the passage of time, up to the 10-mb or approximately 30-km level), supplemented by some time-sections for those few rocket stations which provided higher-level data.* Between 1960 and 1964, the Meteorological Rocketsonde Network (MRN)** was greatly expanded in preparation for the intensive data-gathering period (1964-65) that comprised the International Years of the Quiet Sun (IQSY). By 1964 it became possible to perform weekly synoptic analyses of rocketsonde data at constant-pressure surfaces near 36 km (5 mb), near 42 km (2 mb), and near 55 km (0.4 mb), for a portion of the Northern Hemisphere including principally North America. Such a series was accomplished for the years 1964 through 1968 (ref. 13).

The analysis of rocketsonde data up to the 0.4-mb level permitted a partial view of the upper stratosphere, though limited geographically through the 1960's because of lack of data from the Eastern Hemisphere. However, rawinsonde coverage has been adequate since 1957 (the beginning of the IGY) for the daily subjective analyses of lower stratospheric data up to 10 mb for the entire Northern Hemisphere (ref. 14). In 1964 daily objective analyses of the 100-, 50-, 30-, and 10-mb surfaces were begun, and have continued to the present, with the addition of the 70-mb level (refs. 15 and 16)††.

Owing to the data-limitations outlined above, studies of stratospheric warmings, insofar as they require hemispheric coverage, were largely confined to levels below 10 mb up to the time Nimbus 3 was launched in April 1969. Then, with supportive infrared-radiation data from satellites, the increasing amounts of rocketsonde data available from both Eastern and Western Hemispheres made it possible to increase the upper limits of analysis and the geographical limits of coverage. In 1972 another series of weekly charts was begun for the 5-, 2-, and 0.4-mb surfaces, this time

---

†The year the phenomenon was discovered and documented.

*For the role of grenade- and sphere-soundings in the early years of stratospheric-mesospheric studies, see ref. 12.

**Inaugurated in 1959.

††The daily maps are available on roll microfilm from the National Climatic Center, Asheville, North Carolina.

with the area of analysis extended to include the entire Northern Hemisphere; and this series has continued, on a quasi-real-time basis, to the present day (ref. 17). (Details on how both satellite and rocketsonde data are used in this series are given in the section below on Synoptic Description.) A series of weekly meridional cross-sections for the stratosphere and lower mesosphere was also begun, with nominal pole-to-pole coverage near 70W and 70E.

In order to evaluate the present data-acquisition systems with reference to their ability to provide adequate information on STRATWARMS, it is instructive to consider that even a question as elementary as that concerning the direction of propagation of warmings--upward or downward--cannot be decisively answered in all cases. The upper-stratospheric data (30-60 km) obtained by direct-sounding techniques are still too sparse for definitive analyses. Satellite-measured radiances measure the energy emanating from relatively thick atmospheric layers, and are thus not uniquely suited for such studies.

Since most available evidence indicates that the energy required for stratospheric warmings is propagated upward from the troposphere, one might ask whether it would be sufficient to have reasonably good observational coverage up to the highest levels for which STRATWARMS have been observed. No doubt it is necessary to investigate the energy budget of the mesosphere along with the energy budget of the stratosphere during STRATWARM periods, since it is not known whether the mesosphere undergoes an infusion of energy at the same time as the stratosphere. Whatever happens, it seems clear, on the basis of such studies as Labitzke's (ref. 18), that the mesosphere cannot be ignored in any comprehensive investigation of the stratospheric warming phenomenon. Yet the upper limit to reliable temperature data is between 60 and 70 km from the current operational meteorological rockets employed by the U.S.A. (Super-Loki Datasonde) and by the U.S.S.R. (M100). Furthermore, geographical coverage remains far from adequate. Thus there is a clear need for more mesospheric data.

How, then, should the observational system be improved? Will satellites soon provide adequate stratospheric-mesospheric soundings? Or will improvement require augmentation of both the rawinsonde and rocketsonde networks?--We will try to prepare the basis for answers to these questions in the paragraphs which follow.

Current Data Sources

Rawinsonde, for levels 15-30 km (approximately 100-10 mb). - A rawinsonde report characteristically includes wind, temperature, and pressure data. The pressure data can be readily converted to geopotential-height data for constant-pressure surfaces; i.e., p(z) can be converted to gz(p), through integration of the hydrostatic equation. While occasionally one or more of these parameters will be missing, the overwhelming majority of observations include all three.

Rawinsonde coverage falls off rapidly above 100 mb during typical winters. While approximately 70% of all soundings reach 100 mb, only about 10% reach 10 mb. For this reason, it is desirable for analysis-purposes to use both 0000 GMT and 1200 GMT data sets at 30 mb and above. At the

National Meteorological Center, the first choice of the analysis program for a nominal map-time of 1200 GMT will be 1200 GMT data; if these are missing for a particular station, then the data for the previous time (0000 GMT) are used. It is believed that changes occur slowly enough at stratospheric levels to justify this procedure.

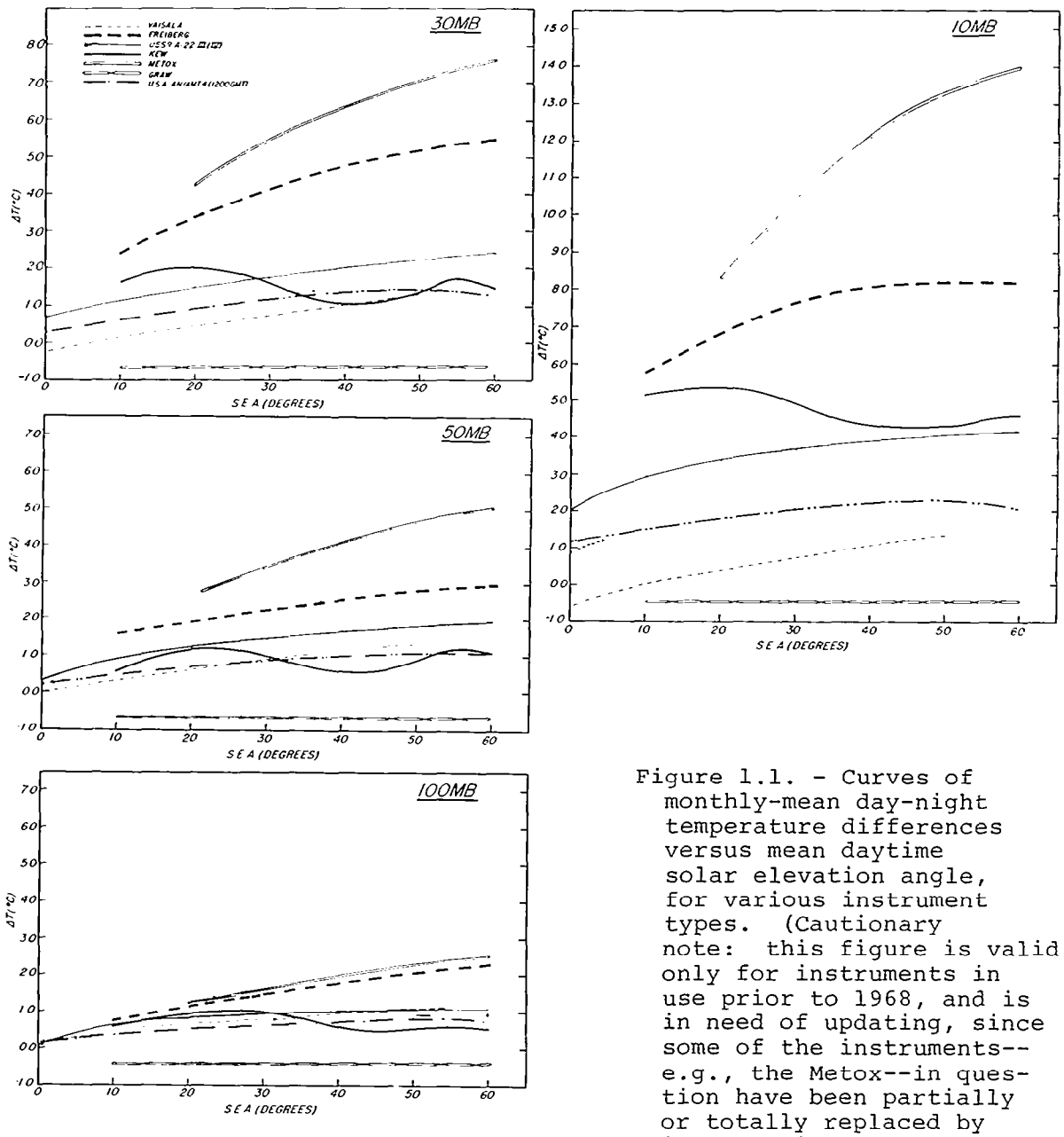

Figure 1.1. - Curves of monthly-mean day-night temperature differences versus mean daytime solar elevation angle, for various instrument types. (Cautionary note: this figure is valid only for instruments in use prior to 1968, and is in need of updating, since some of the instruments--e.g., the Metox--in question have been partially or totally replaced by improved instruments.)

Analysis at stratospheric levels is hampered not only by the diminution in data-quantity, but also by problems of instrumental errors. From the beginning of stratospheric soundings by balloons, it was known, on theoretical and experimental grounds, that radiation errors would become more and more significant with increased sounding heights (ref. 19). The role of solar radiation in particular was demonstrated conclusively through day-night difference studies (refs. 20, 21, 22). These studies have stimulated the development of improved instrument systems in several countries. However, rather large differences between measurements made in daytime and those made at night by various instrument types persist to the present day at stratospheric levels. These differences cannot be explained as manifestations of a true diurnal variation, which has been shown to have a daily range of at most 1°C at 10 mb (ref. 23). The decision was therefore made very early in synoptic stratospheric analysis--even prior to 1964--to "reduce" all data to nighttime levels, by subtracting average day-night differences (as functions of solar elevation angle) from daytime reports (ref. 22). Examples of these differences for selected instrument types are shown in Figure 1.1. While this procedure does not ensure "correctness"--an impossible goal as long as there is no absolute standard--at least it does ensure world-wide compatibility of daytime observations.

Rocketsondes, for levels 20-60 km. - As can be seen from Figure 1.2, the system of rocketsonde stations is rather sparse as compared to that of rawinsonde stations. In an average 24-hour period, more than 100 rawinsonde reports are received for the Northern Hemisphere 30-km level. By contrast, routine synoptic Rocket Network firings are scheduled only once a week (on Wednesdays). With only about 20 stations in the Northern Hemisphere, and not all of these firings as scheduled, it is evident that the number of rocket soundings is an order of magnitude less than the number of balloon soundings.

Table 1.1 summarizes the sounding-records for most Northern Hemisphere meteorological rocket sites for the year 1974. For each station it shows the ratio of the number of actual soundings usable in synoptic analysis (whether of constant levels, constant-pressure surfaces or cross-sections) to the total possible number of soundings. This ratio varies between .35 and 1.00. The average for all stations is 0.71, or approximately two-thirds. This means that the average number of weekly rocket soundings for the Northern Hemisphere is 0.71 x 19 $\sim$13--the number which should be contrasted with the more than 100 soundings available from the rawinsonde network for 30 km, during a typical 24-hour period.

It is primarily because of this difference in data-coverage that the synoptic maps for 10 mb (30 km) and below are based primarily on rawinsonde data. Above 10 mb, however, rawinsonde reports are rare and sporadic, and synoptic analysis is based mainly on rocketsonde data at these higher levels--5 mb (near 36 km), 2 mb (or 42 km), and 0.4 mb (or 55 km).

Just as the rawinsonde instruments were designed principally for tropospheric measurements, so were rocketsonde instruments designed primarily for stratospheric-mesospheric measurements. Thus a special effort has been made to minimize the susceptibility of rocketsonde thermistors to radiation error. Nevertheless, it is still necessary to correct rocketsonde reports for a number of factors: convective heat exchange of the thermistor with its environment; radiative heat exchange; heating by the measuring current; aerodynamic heating; and thermal conductivity of the lead wires (ref. 24).

Not only is there a problem of correcting observations obtained by using a single instrument type, but there is also, as in the case of rawinsondes, the problem of compatibility between rocketsonde instruments of different manufacture. There are several different rocketsonde systems in use throughout the world, each with usually more than one designation. For the sake of brevity we shall usually refer to each of them by merely naming the country of its origin.

Figure 1.2. The current network of active meteorological rocketsonde stations in the Northern Hemisphere.

TABLE 1.1. - RATIO OF NUMBER OF ROCOBS USABLE FOR WEEKLY SYNOPTIC ANALYSIS TO TOTAL NUMBER OF POSSIBLE ROCOBS FOR THIS PURPOSE (NORTHERN HEMISPHERE, 1974)*

Antigua, B.W.I.	0.81	Pt. Mugu, U.S.A.	0.77
Barking Sands, U.S.A.	0.80	Poker Flat, U.S.A.	0.87
C. Canaveral, U.S.A.	0.98	Primrose Lake, Canada	0.38
Ft. Churchill, Canada	1.00	Ryori, Japan	0.54
Ft. Sherman, C.Z.	0.87	Thule, Greenland	0.40
Heiss Island, U.S.S.R.	0.96	Thumba, India	0.44
Kourou, Fr. Guiana	0.35	Volgograd, U.S.S.R.	0.75
Kwajalein, Marshall Is.	0.80	Wallops Flt. Ctr., U.S.A.	0.98
		White Sands, U.S.A.	0.98

*West Geirinish, U.K. and El Arenosillo, Spain are experimental stations, hence not strictly comparable to the others listed here.

Series of "intercomparison tests" have been made of meteorological rockets. The latest took place at the Guiana Space Center, Kourou, French Guiana, in September 1973. Participating were France with the Super-Arcas DMN Sonde, the United Kingdom (UK) with the SKUA system, the United States (USA) with the Super Loki Datasonde, and the Union of Soviet Socialist Republics (USSR) with the M100 system. Figure 1.3 shows the principal results. Compatibility is evidently quite good approximately up to the stratopause level (45-50 km). Above this level, the USSR-US difference is rather pronounced. It is indeed apparent that adjustments are needed to make the US observations compatibile with the USSR observations, and these, based on the September 1973 intercomparisons, are given in Table 1.2. Also included in this table are adjustments to be applied to the French instrument.

It is gratifying that the UK-US differences are very small. Even though the UK operates only one rocket station, at West Geirinish, Scotland, this is a very important station for observing STRATWARMS because of its location (see Figure 1.2). Some of the highest winds ever reported have been observed at this station.

It has been mentioned that a) there are relatively few balloonsonde (rawinsonde) observations above 10 mb, and that b) the rawinsonde thermistor was designed primarily for tropospheric measurements. The fact of the matter is that b) is a more cogent reason than a) for basing charts above 10 mb principally on rocketsonde data. There is a substantial number of balloon sounding observations at the 7- and 5-mb levels, and these can be used to advantage in constructing high-level charts. However, it has been reported (ref. 26) that "errors make balloonsonde temperature data above 30 km unsuitable for many types of study," while "systematic errors in the rocketsonde have been largely eliminated (at least for the region from 20 to 45 km)."

Radiosonde-reported temperatures above 10 mb are consistently lower than rocketsonde reports, more so by night than by day, as is to be expected from considerations of solar-radiation error. When it is elected to use these very high-level radiosonde reports in synoptic analysis, appropriate corrections are applied. At the National Meteorological Center in Washington, the problem is circumvented by not using rawinsonde data above 30 km for STRATWARM studies. Consequently the matter will not be discussed further here.

The question of augmenting the rocketsonde network, and of improving rocket soundings, can be adequately answered only after satellite data have been discussed.

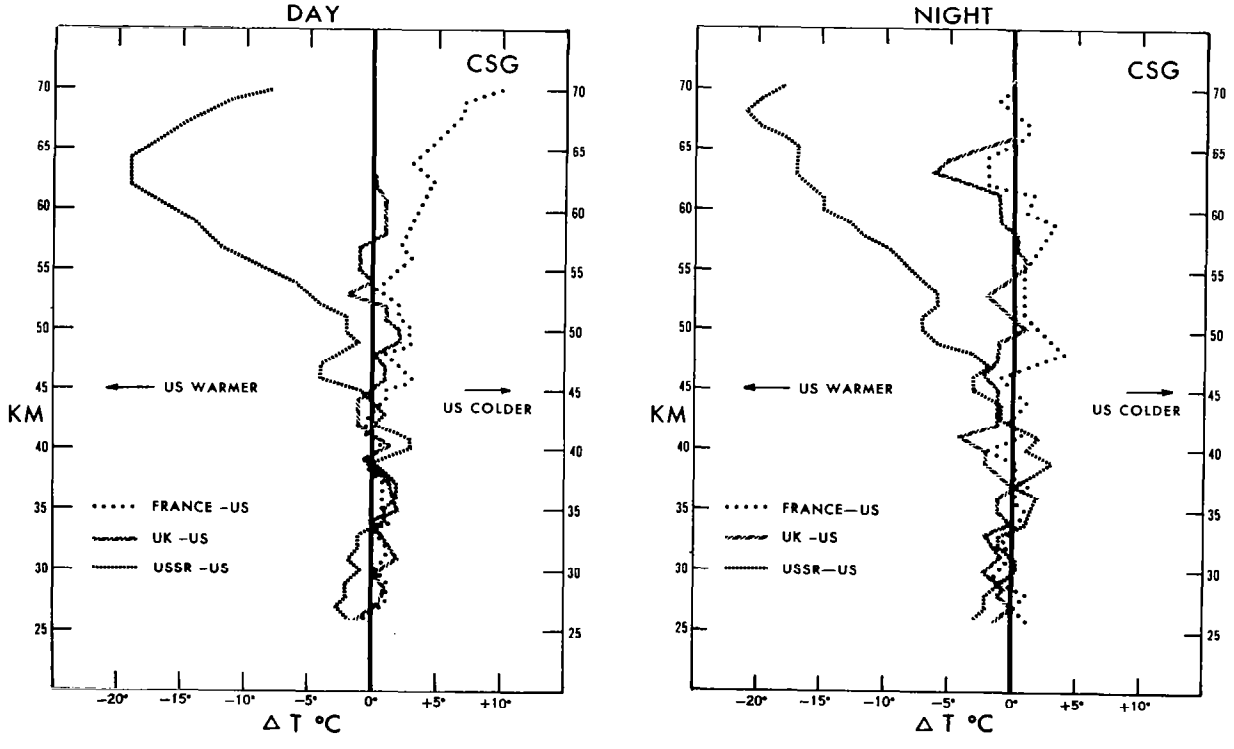

Figure 1.3. - Average temperature differences as reported by various rocketsonde instruments during the Kourou intercomparisons, September 1973. a) Daytime; b) nighttime. (Source: Ref. 25.)

TABLE 1.2. - AVERAGE ADJUSTMENT NECESSARY TO OBTAIN COMPATIBILITY TO US CORRECTED ROCKETSONDE TEMPERATURES

	USSR Adjustment	French Adjustment
70	+18	-10
69	+18	- 8
68	+18	- 7
67	+18	- 6
66	+18	- 5
65	+18	- 4
64	+18	- 4
63	+18	- 4
62	+17	- 4
61	+16	- 4
60	+15	- 4
59	+14	- 3
58	+13	- 3
57	+11	- 3
56	+10	- 3
55	+ 8	- 2
54	+ 7	- 2
53	+ 6	- 2
52	+ 5	- 2
51	+ 5	- 2
50	+ 4	- 2
49	+ 4	- 2
48	+ 3	- 2
47	+ 3	- 2
46	+ 2	- 2
45	+ 1	- 2
44	0	- 1
43	0	0
42		
41		
40		

Satellite Data. - Satellite data are presently useful in depicting atmospheric conditions from the surface up to at least 55 km. Above this level, some information can be obtained (e.g., from the pressure-modulated radiometer (PMR) on Nimbus 6), but it is not straightforward or unambiguous. However, the situation is rapidly changing. Various new sounding units are scheduled for launch on TIROS-N in 1978, and should provide temperature profiles for levels above those presently attainable. At present, limb-radiance and microwave-sensing techniques appear most promising.

Satellite information forms a useful part of the data base for STRATWARM monitoring and for research studies of the phenomenon. A distinction must be made between raw satellite data in the form of radiances, and processed data in the form of temperatures for particular levels. Many problems have arisen in connection with the latter, mainly owing to the fact that, given radiance reports from the various instrument-channels, no unique solution exists in terms of a temperature profile for the radiative transfer equation. The raw radiance data, on the other hand, insofar as they provide

weighted mean temperatures over rather thick atmospheric layers, are very useful in delineating large-scale changes, and in estimating levels of activity within broad limits.

Figure 1.4 shows typical coverage of derived temperatures for 100 mb over the Northern Hemisphere, as provided by the Vertical Temperature Profile Radiometer (VTPR) on board NOAA 3. Coverage is restricted to ocean areas owing to the need for having well-specified surface temperatures, which are more readily obtainable over water than over land. However, for present purposes of stratospheric synoptic meteorology, the radiance fields are more important than the derived temperature fields, and one can obtain a fairly accurate picture of Northern Hemisphere VTPR radiance coverage by envisaging the pattern of Figure 1.4 for the oceans extended and repeated over land areas. Selective Chopper Radiometer (SCR) radiance data from Nimbus 5 are also available from over both land and sea, but coverage is not quite so complete as from VTPR.

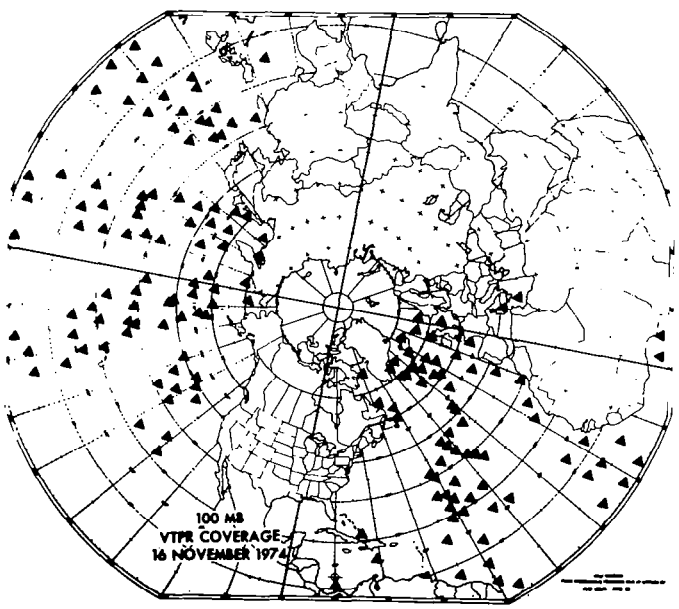

Figure 1.4. - VTPR reports for the 100-mb level, 16 November 1974, illustrating how satellite data may help to "fill the gaps" in otherwise data-sparse oceanic areas.

There are two VTPR channels which are of greatest interest for stratospheric studies - VTPR-1 with its weighting function (w.f.) peaking between 30 and 50 mb, and VTPR-2 with its w.f. peaking between 50 and 100 mb (Figure 1.5). The two uppermost SCR channels have w.f.'s peaking at near 2 mb and at 10 mb respectively, so that obviously they have the potential of providing information on the upper stratosphere. Radiance data from the uppermost VTPR and SCR channels, together with rocketsonde data, can delineate areas and levels of warmings and aid in determining the amplitude of the warmings (ref. 27).

Specific examples of STRATWARM monitoring will be given in a later section.

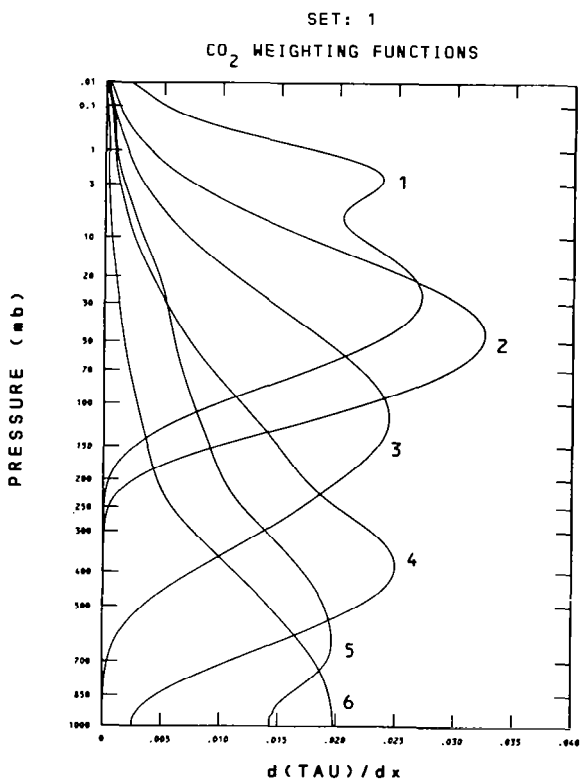

Figure 1.5. - The set of "weighting functions" used to obtain temperature profiles from the radiances measured in the six CO_2 channels of the first VTPR instrument. Each weighting function d(TAU)/dx is shown as a function of atmospheric pressure; the term "weighting function" is due to its occurrence in the radiative transfer equation for a cloudless atmosphere,

$$I(\nu) = B[\nu,T(x_0)]TAU(\nu,x_0) - \int_0^{x_0} B[\nu,T(x)]\frac{dTAU(\nu,x)}{dx}\,dx$$

where I = measured radiance, B = Planck radiance, ν = spectral frequency, T = temperature. The subscript zero refers to the lower boundary, and x is any single-valued function of pressure.

The principal application of satellite data to stratospheric meteorology, and thus, by implication, to STRATWARM studies, lies in the supportive role of radiance data in providing first-guess fields for maps of geopotential heights and temperatures at the 5-, 2-, and 0.4-mb levels. It has been established that good correlations exist between radiance values (obtained from certain channels) and layer-thicknesses (ref. 28). By adding the thicknesses of, say, the 100-2 mb layer to the heights of the 100-mb surface, one obtains an approximation to the height-field of the 2-mb surface. Other such regressions and radiance data aid in the depiction of the 5-mb surface. Correlations have also been found between radiance-values and temperatures at constant-pressure surfaces, and first-guess fields of temperature are accordingly derived.

As explained above, satellite data have, since 1972, permitted the extension of coverage of upper-stratospheric maps (5, 2, and 0.4-mb) from the North American area to the entire Northern Hemisphere. With the first-guess fields as outlined above, the sparse rocketsonde data are used to adjust these fields wherever possible. Where no in situ data are available, the first-guess values are allowed to stand unaltered.

Rocket-Satellite Comparisons

Two of the data-systems discussed (the radiosonde and the rocketsonde) provide in situ measurements of atmospheric parameters, while the third depends upon remote sounding (satellite systems). The future of satellites as a means of providing meteorological information is well-assured; and it can be safely assumed that remote-sensing techniques, whether ground-based or carried by vehicles in the air or in outer space, will provide, as time goes by, more and more of the data needed for the increasingly sophisticated forecast models to be used in many countries of the world.

For the present, however, we are faced with the necessity of utilizing all three data sources. The rawinsonde is so far indispensable at levels below 30 km. The rocketsonde is likewise indispensable above 30 km. The satellite has made possible closer and better monitoring of stratospheric phenomena, while at the same time contributing to the improvement of charts based primarily on rawinsonde or rocketsonde data.

In this chapter, we have discussed the various ways in which data from the various sources get utilized. However, while we have discussed problems of compatibility between various radiosonde types, and similar problems between rocketsonde types, and have briefly considered some radiosonde-rocketsonde comparisons, we have yet to consider the compatibility between satellites and radiosondes, and between satellites and rocketsondes. Such a discussion will perhaps provide some indication of future developments, along with the time-scale of those developments.

It has already been pointed out that, as far as the stratosphere is concerned, satellite data are most important above 30 km (10 mb). Below that level rawinsonde data provide adequate coverage, and there are problems in deriving temperatures from satellite radiances for the particular levels of interest. On the other hand, above that level, the available in situ data are almost exclusively rocketsonde data; and, although sparse,

they cover the whole altitude range 30-60 km. With only 12 rocketsonde reports (on the average) available at any one analysis-time per week, and with no data at all available from most of Eurasia and North Africa, as well as the oceans, obviously even gross upper-stratospheric and mesospheric features may escape attention. This is the point where satellite data come in most effectively. As discussed above, the raw radiances values from various channels aid in the day-to-day monitoring of stratospheric events (warmings and coolings, with their implications for circulation changes), while at the same time they form the basis for first-approximation fields for upper stratospheric charts (the final analyses being for rocketsonde data).

One of the most important questions left to be answered, in connection with current usage, is: How well do the satellite and rocket data agree? It is also important to ask the corresponding question concerning satellite and radiosonde data. Even after six years of study, these questions have not been definitively answered. The situation is roughly as follows: At tropospheric levels, there appears to be reasonable agreement between radiosonde and satellite-derived data. This agreement is good enough to permit the inclusion of satellite data in tropospheric analysis programs. However, at stratospheric levels, the lower information content of satellite-derived data makes it more difficult to use them. For a quantitative discussion of this matter, the reader is referred to reference 29.

To estimate the degree of compatibility between satellite and rocket data, the following approach was used. It was reasoned that a particular temperature profile as determined by rocket and radiosonde, will, if it reflects the true state of the atmosphere, correspond to a particular set of radiances from the various channels of the satellite instruments. Thus, given each weighting function and a temperature profile, the radiative transfer equation can be integrated to obtain a calculated radiance. The calculated radiance may then be compared with the measured satellite radiance. The calculated radiances will be equal to the measured radiances only if (1) the observations are coincident in space and time, (2) there are no instrumental errors in the rocketsonde, radiosonde, or satellite sounder, and (3) the atmospheric transmittance is known perfectly. Since none of these conditions can be satisfied, some differences must be expected.

Figure 1.6 shows the results from a sample of observations satisfying condition (1) as well as possible. It may be noted that results are shown not only for the VTPR, but also for the research instrument called the Infrared Temperature Profile Radiometer (ITPR) flown on Nimbus 5; in addition a comparison of calculated and measured temperatures for the Nimbus E Microwave Spectrometer (NEMS 5) on Nimbus 5 is given.

For the VTPR and ITPR scatter diagrams, if the measured satellite radiances were perfectly compatible with the rocketsonde-radiosonde calculated radiance, a distribution of points precisely along the Y=X line could be expected. Instead, for each of the satellite channels a distribution with some bias and some scatter is indicated. The distribution is in general, however, approximately parallel to the line with relatively little scatter.

It has been pointed out that the radiances for the uppermost VTPR channels are well correlated with temperatures at the 2 mb (42 km) and 5 mb (36 km) levels. A further check on satellite-rocketsonde compatibility was made by comparing radiance-deduced temperatures with rocketsonde-reported

temperatures along a meridian near 70°W for the period March 15, 1972 to April 12, 1972. The result is shown in Figure 1.7, which gives some indication of how well the first guess field fits the data which are to be analyzed. (Refer to Fig. 1.2 for station locations.)

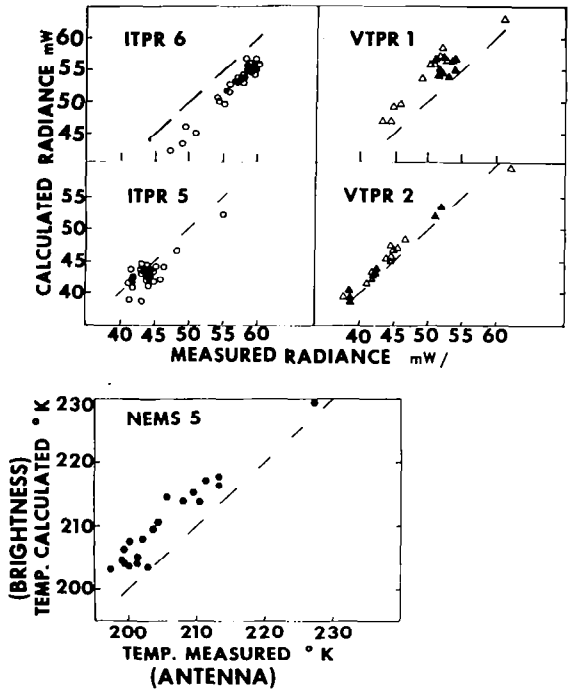

Figure 1.6. - Comparisons of calculated with measured radiances (temperatures in the case of NEMS) for the instruments and channels shown. See Figure 1.5 for transmittance weighting functions.

From the tests that have been conducted to date, we conclude that radiosonde-rocketsonde-satellite compatibility is sufficiently good to justify the kinds of current applications of the three data-sources discussed in this section.

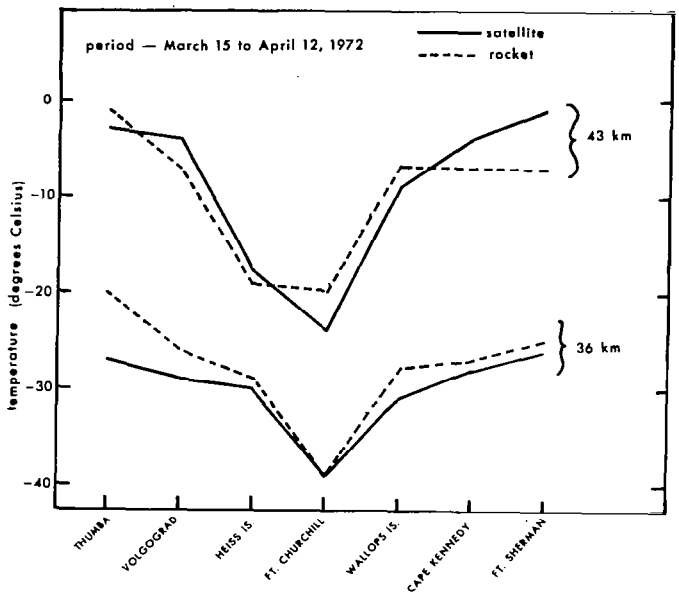

Figure 1.7. - Comparison of first-guess satellite information with rocketsonde data.

CLIMATOLOGICAL DESCRIPTION

Purpose

The purpose of this section is to define the term stratospheric warming (STRATWARM) and to enhance our understanding of the phenomenon by contrasting the warming situation with the various seasonal mean circulation patterns observed. Maximum deviations from climatological means are referenced to facilitate understanding of typical stratospheric events. For proper perspective, climatological means for seasons other than winter should be consulted. For completeness, both Northern and Southern Hemisphere are discussed. It should be kept in mind that much less climatological information is available for the Southern Hemisphere.

Definitions

During the years immediately following the discovery of the stratospheric warming phenomenon (1952), an attempt was made to categorize STRATWARMS as "major" and "minor", since in some years the events were of sufficient magnitude to cause circulation reversals, while in other years temperature changes were not large enough to result in significant disruption of the wind-field at the levels observed. Diverse judgments of researchers making use of the terms "major" and "minor" have unfortunately led to some confusion. Moreover, the constantly changing techniques for observing stratospheric parameters (as described in other sections of this monograph), have compounded the difficulty of attempting to categorize individual events as "major" or "minor".

In an attempt to standardize the use of the terms "major" and "minor" the World Meteorological Organization's Commission for Atmospheric Sciences has adopted the following definitions:

"1. A stratospheric warming is called minor if a significant temperature increase is observed (i.e., at least 25 degrees in a period of a week or less) at any stratospheric level in any area of the wintertime hemisphere, measured by radiosonde or rocketsonde data and/or indicated by satellite data; and if criteria for major warmings (see below) are not met. Less extreme warmings will be referred to as warming pulses."

"2. A stratospheric warming can be said to be major if at 10 mb or below the latitudinal mean temperature increases poleward from 60 degrees latitude and an associated circulation reversal is observed (i.e., mean westerly winds poleward of 60° latitude are succeeded by mean easterlies in the same area)."

It might seem that the mode of establishing categories ought to depend on the special interests of particular research groups. However, since consistency in nomenclature is essential, and a certain degree of arbitrariness is inevitable in any taxonomical system, the WMO definition will be adhered to throughout this paper.

Recent studies have revealed that throughout the entire winter, in either hemisphere, a series of warming pulses occurs. The significance or strength of these pulses may be greater at higher or lower stratospheric levels, depending on the event. A particularly strong event, occurring during a one to two week period, cannot be completely understood unless one considers the pulses leading up to such an event. Various sections of this monograph will discuss phenomena and parameters observed by in situ and remote-sensing devices.

For the sake of completeness, in this monograph we will define stratospheric warming (STRATWARM) as a thermal pulse which exhibits itself as a warm anomaly (relative to neighboring values in space and time) at any level in the stratosphere. Our principal interest, however, will be in the major and minor STRATWARMS defined above.

As we attempt to describe stratospheric warmings with the tools of climatology, we find it useful to keep in mind some factors contributing to climatological patterns. The Aleutian Anticyclone and displaced polar vortex in the wintertime Northern Hemisphere are quasi-stationary wave-one features that may be attributed to orographic influence and zonally asymmetric heating. These effects appear to be weaker in the Southern Hemisphere, resulting in weaker stationary wave features and a deeper vortex in winter.

Both hemispheres have transient features, and the interaction between the transient and stationary features appears to produce more significant stratospheric warmings in the Northern Hemisphere. The absence of strong stationary features in the Southern Hemisphere may account for the fact that up to now no major warming has been observed there. (Physical origin and interactions between transient and stationary features are discussed in other sections of this monograph.)

Summer Stratosphere

For the sake of comparison and reference, a brief description of the summer stratosphere may be useful. During the entire year, a distinct polar vortex maintains itself from surface through 100 mb in the Northern Hemisphere and through 70 mb in the Southern Hemisphere. (Superimposed on the prevailing westerlies, of course, are various synoptic and subsynoptic scale features.) Mean summertime circulation patterns at 70 mb and 50 mb, in the Northern Hemisphere and Southern Hemisphere respectively, show broad troughs amid weak pressure gradients over the polar area, accompanied by weak mid-latitude ridging. Above these transition levels, a summertime circulation reversal (circumpolar easterly winds with warmest air over polar regions) increases in intensity with height in accordance with the thermal-wind relation, reaching a maximum intensity in the lower mesosphere. The summer season will be arbitrarily considered to run roughly from May to October in the Northern Hemisphere and from November to April in the Southern Hemisphere.

The warm season begins as differential solar heating of the ozone layer causes a breakdown in the polar vortex above 100 mb, and ends as the decrease in solar heating results in a reversal of temperature gradient and a consequent return of westerly winds.

At 50 mb and above, peak anticyclonic circulation is reached in July in the Northern Hemisphere and in January in the Southern Hemisphere.

Figures 2.1 and 2.2 are typical Northern Hemisphere means for mid-summer, at 100 and 10 mb respectively. The anticyclone at 100 mb over Southern Asia has been documented by Mason and Anderson (ref. 30). The 10-mb patterns consists essentially in anticyclonic flow centered near the pole, with warmest air near the pole and with only minor perturbations.

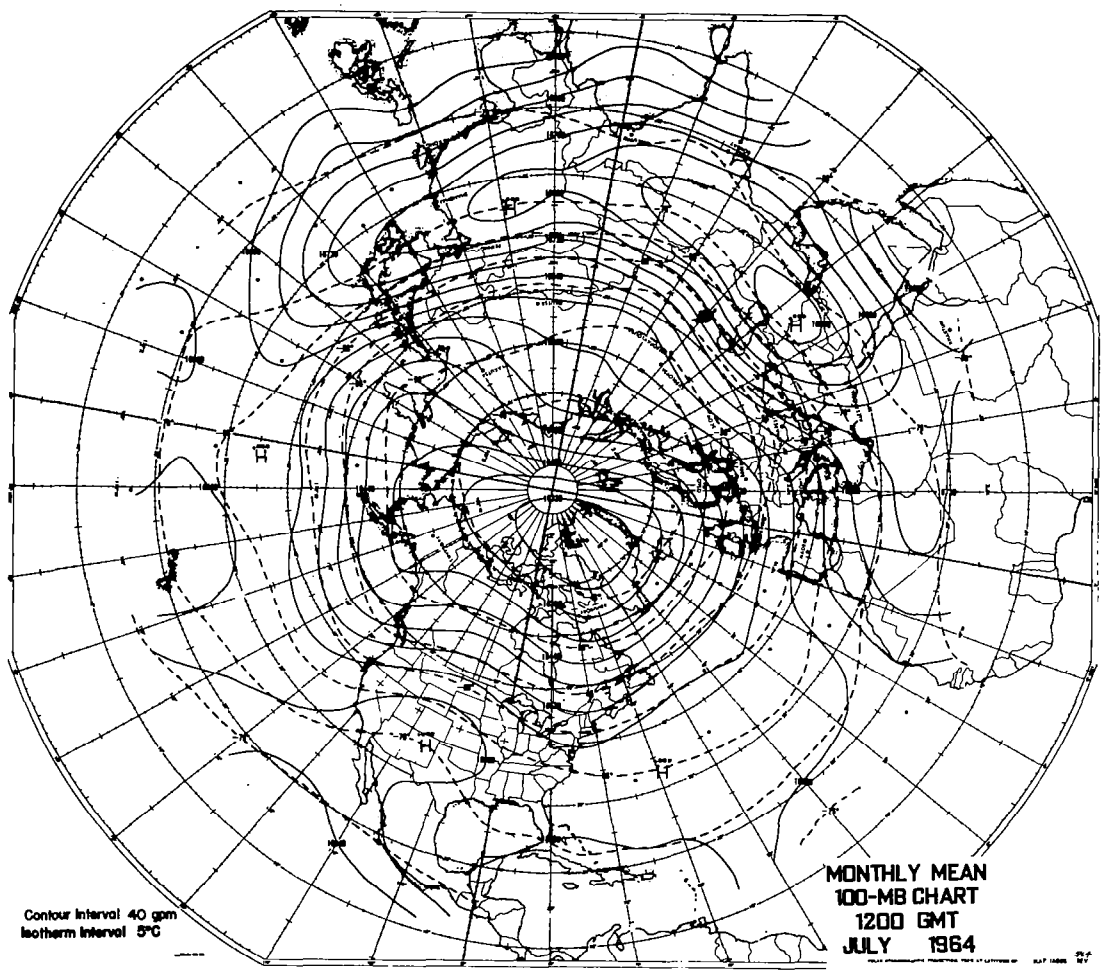

Figure 2.1. - Monthly mean of objective analyses of 100-mb surface heights and temperatures, for July 1964, 1200 GMT. (Northern Hemisphere) Source: Ref. 16.

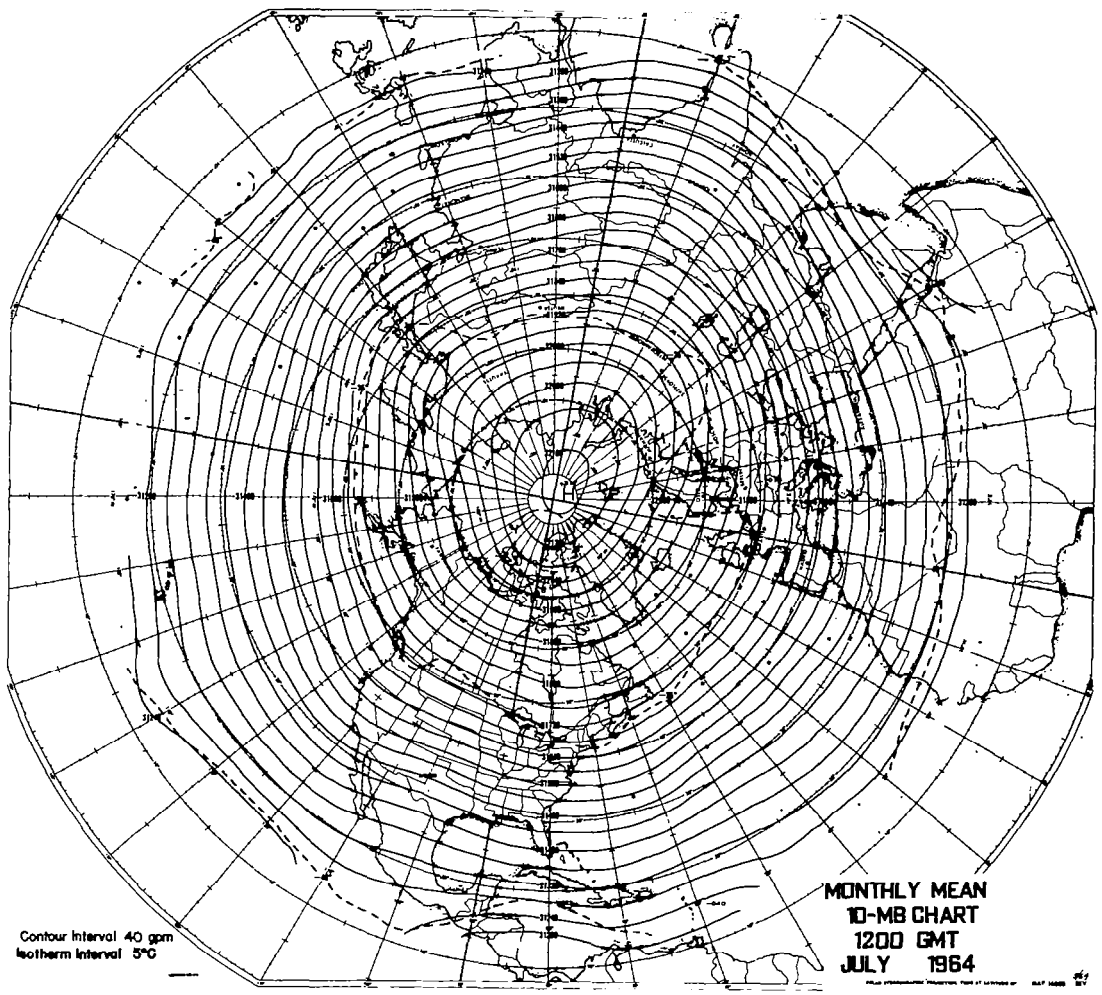

Figure 2.2. - Monthly mean of objective analyses of 10-mb surface heights and temperatures, for July 1964, 1200 GMT. (Northern Hemisphere) Source: Ref. 16.

Transition from Summer to Winter

In contrast to the extratropical transition from wintertime to summertime stratospheric circulation, which is greatly complicated by dynamic events (related, no doubt, to the springtime ozone maximum and its highly variable distribution), the transition from summer to winter is fairly regular and lends itself to simple pictorial representation. Figure 2.3

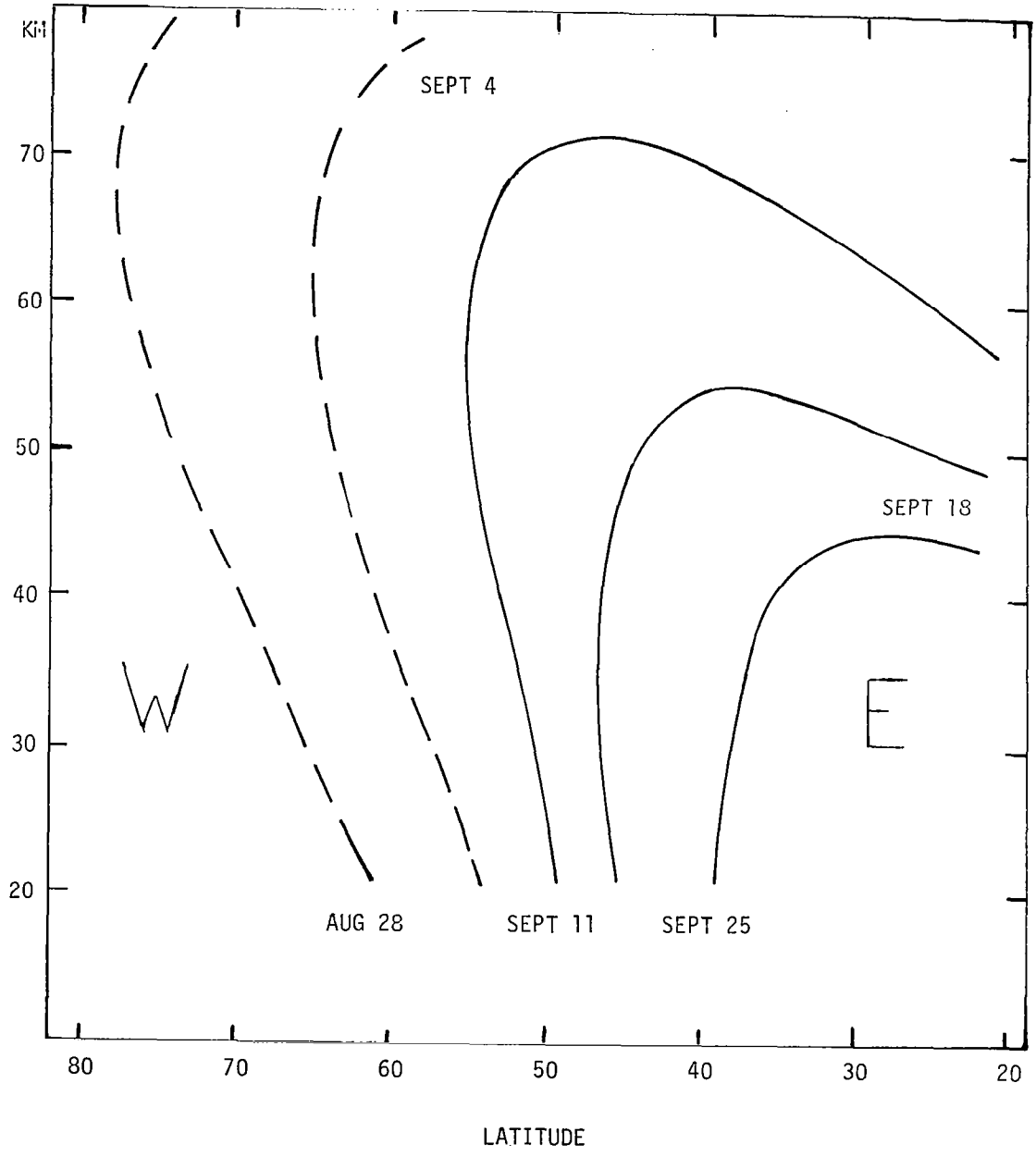

Figure 2.3. - Schematic illustration of zero-zonal wind lines (separating easterly from westerly winds between 20 and 80 km and between 20°N and 80°N).

illustrates this latter transition. It is based on several years of rocketsonde data, and shows schematically that westerlies appear at lower stratospheric levels at high latitudes as the sun retreats southward and cooling progresses in the polar regions (it should be noted, however, that the zero-zonal wind lines at high latitudes are nearly vertical). It is suggested that westerlies prevail always at the very highest levels (well above 70 km). At middle and low latitudes (southward of 45°N), these westerlies descend to lower levels, and, as autumn progresses, the region of easterlies becomes confined more and more to lower latitudes and lower altitudes. (The graph is not extended southward of 20°N, owing to the complicating factors at equatorial latitudes of the quasi-biennial and semi-annual oscillations.)

Winter Stratosphere

From the autumn transition until the following spring, the dominant planetary-scale feature in either winter hemisphere is the polar vortex. Warm perturbations over significantly thick stratospheric layers may occasionally disturb the predominantly westerly circulation. The winter season occurs usually from October to April (approximately) in the Northern Hemisphere and from May to October in the Southern Hemisphere. Figures 2.4 and 2.5 show Southern Hemisphere wintertime mean height and temperature (based on mean 100 mb data). (Some Southern Hemisphere mean charts for single winter months are available.)

Maximum wintertime temperature variations occur near 45 km. Figures 2.6 and 2.7 show typical mid-winter 100- and 10-mb patterns of geopotential height and temperature over the Northern Hemisphere. Detailed statistics on temperature, height, and wind variability at various stratospheric levels have been published by the University of Berlin (see ref. 14).

The presence of the Aleutian anticyclone, with its peak amplitude near 30 km in the mean, is evident in Figure 2.7. Orography, land-sea contrasts, earth distance from the sun, and other lesser known factors may contribute to this Northern Hemisphere feature which appears to have a somewhat weaker counterpart in the Southern Hemisphere. During the Northern Hemisphere winter, lower-stratosphere polar area temperatures average 10-15°C warmer than their Southern Hemisphere winter counterparts (compare Figures 2.5 and 2.6, 100-mb mean temperature). This partially explains the increased depth of the Southern Hemisphere polar vortex at midstratospheric levels. Moving perturbations which frequently reinforce the standing anticyclone feature during warming occurrences in the Northern Hemisphere are often masked in climatological means. Warming intensity and the time of the season during which warming occurs affect the degree to which the polar low becomes reestablished follow warming events. The range of effects from STRATWARMS can be depicted in a multitude of ways, only a few of which are discussed below.

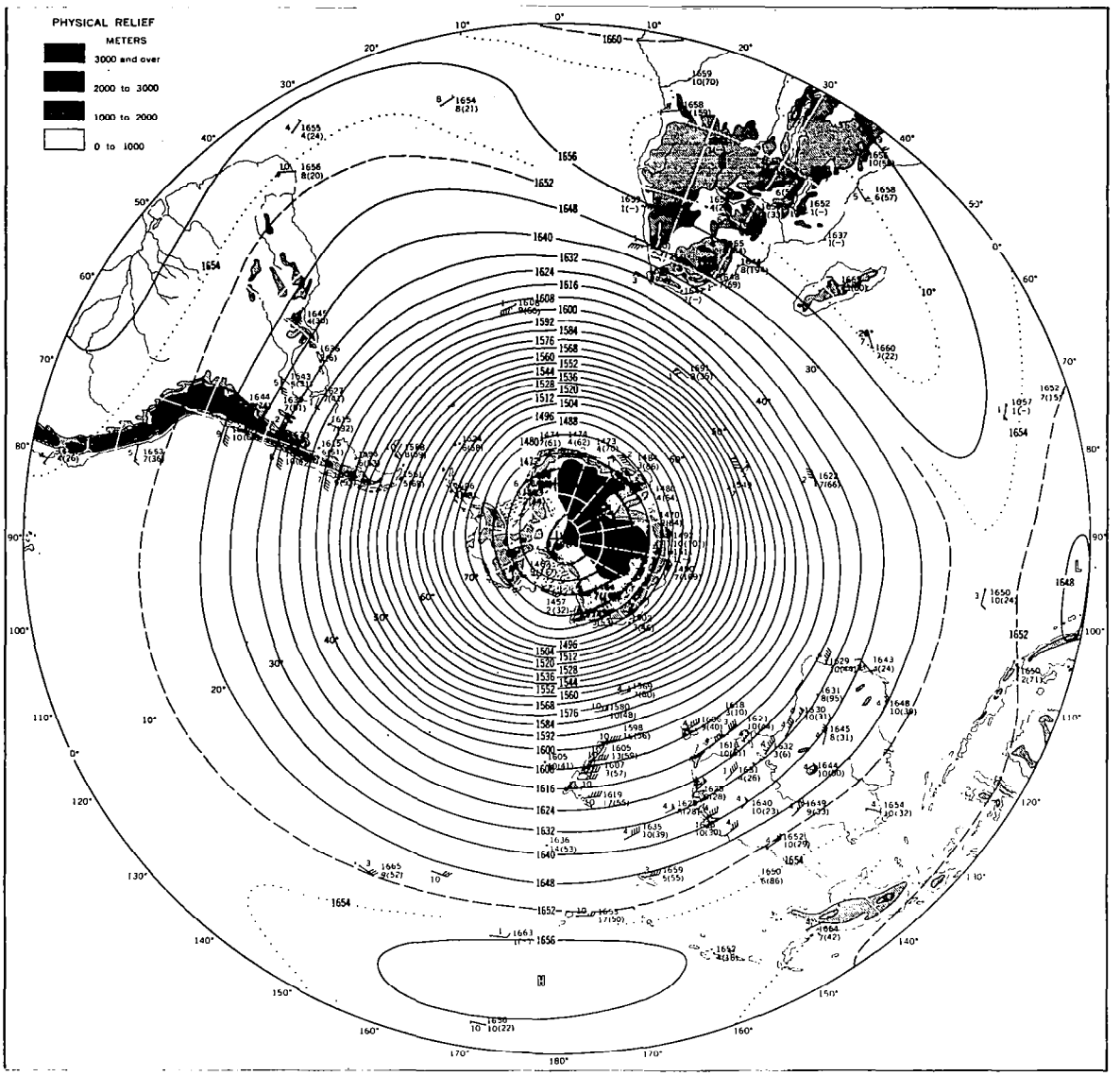

Figure 2.4. - Mean geopotential heights (in decameters) of the 100-mb surface for July (midwinter) Southern Hemisphere. (Source: Ref. 31.)

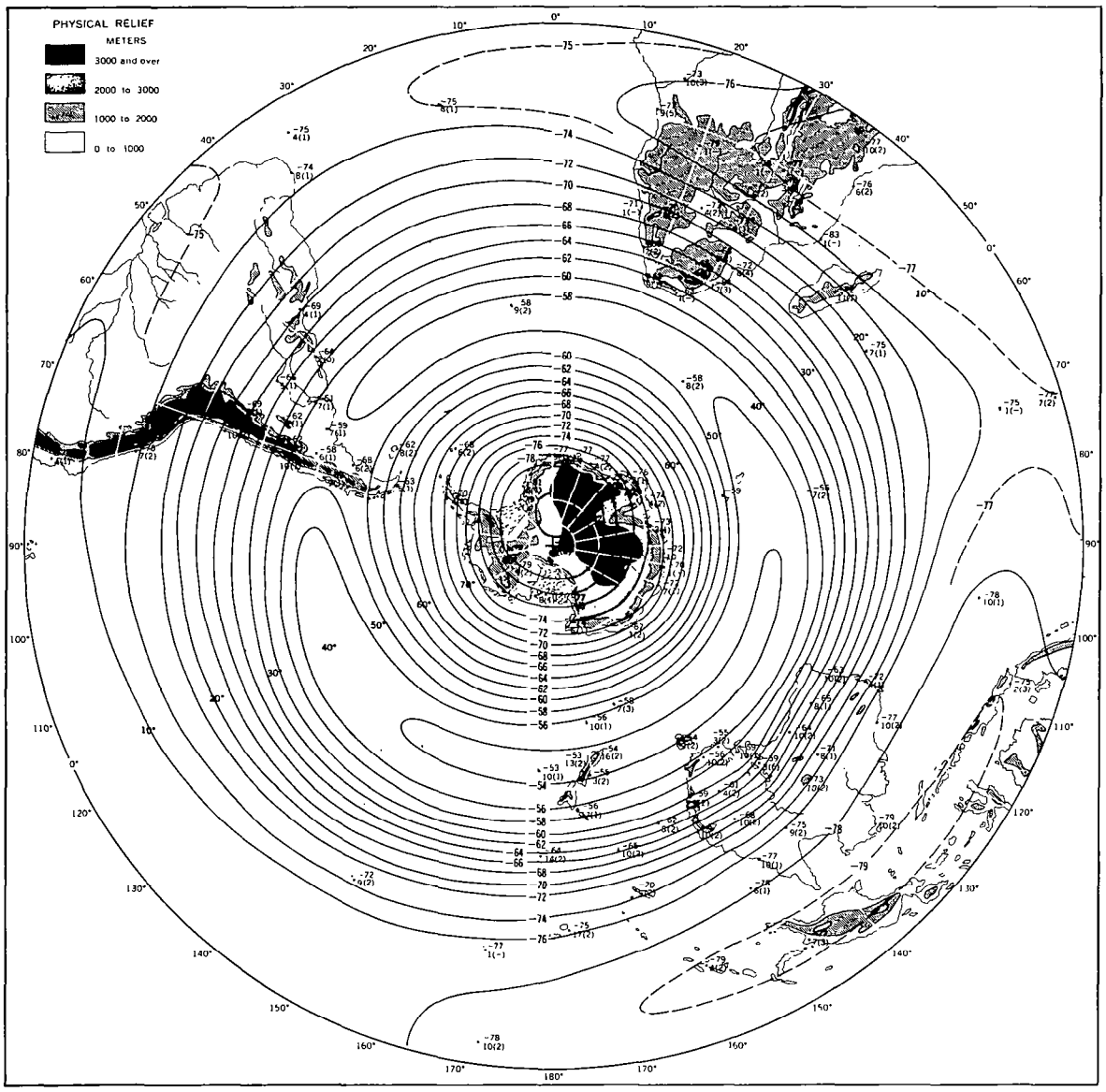

Figure 2.5. - Mean temperatures (in degrees C) at the 100-mb surfaces for July (midwinter), Southern Hemisphere. (Source: Ref. 31.)

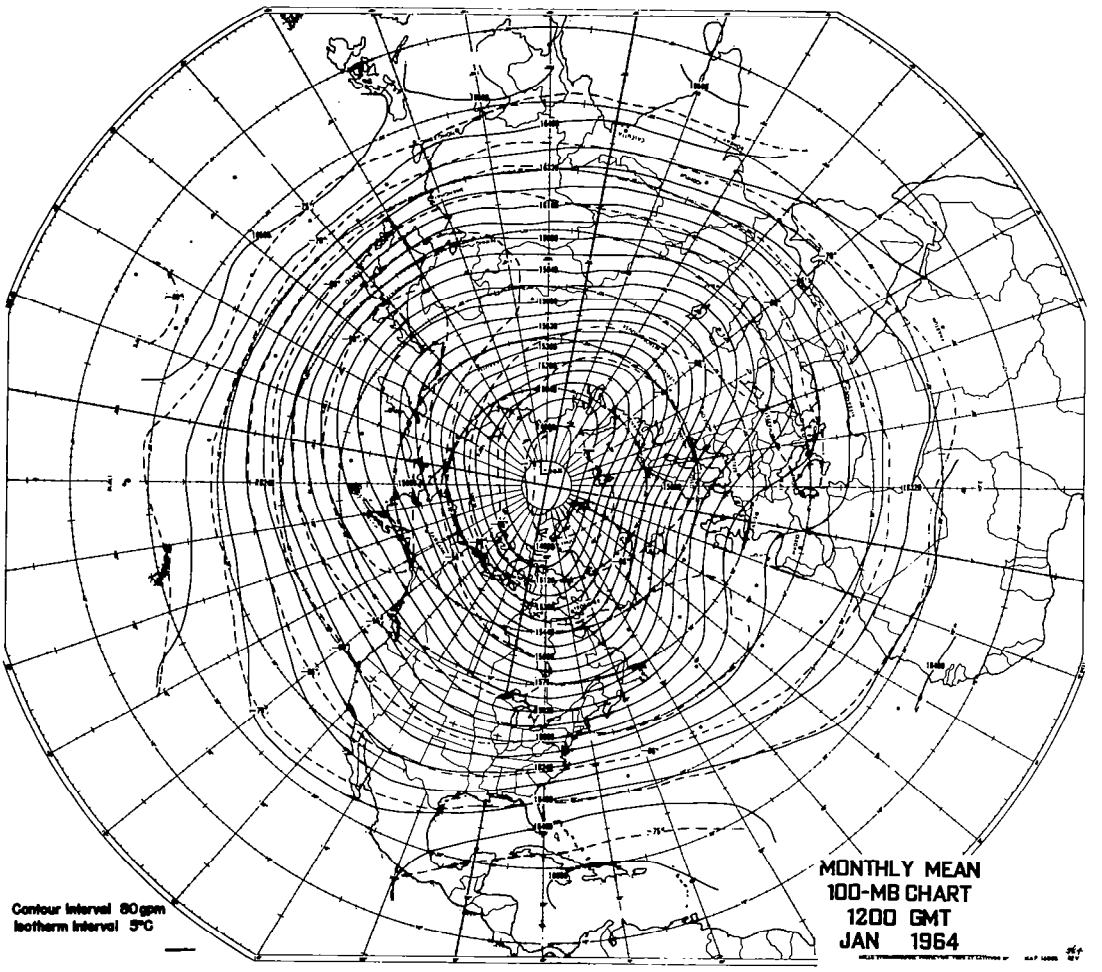

Figure 2.6. - Monthly mean of objective analyses of 100-mb surface heights (in meters) and temperatures (in degrees C) for January 1964, 1200 GMT, Northern Hemisphere. (Source: Ref. 16.)

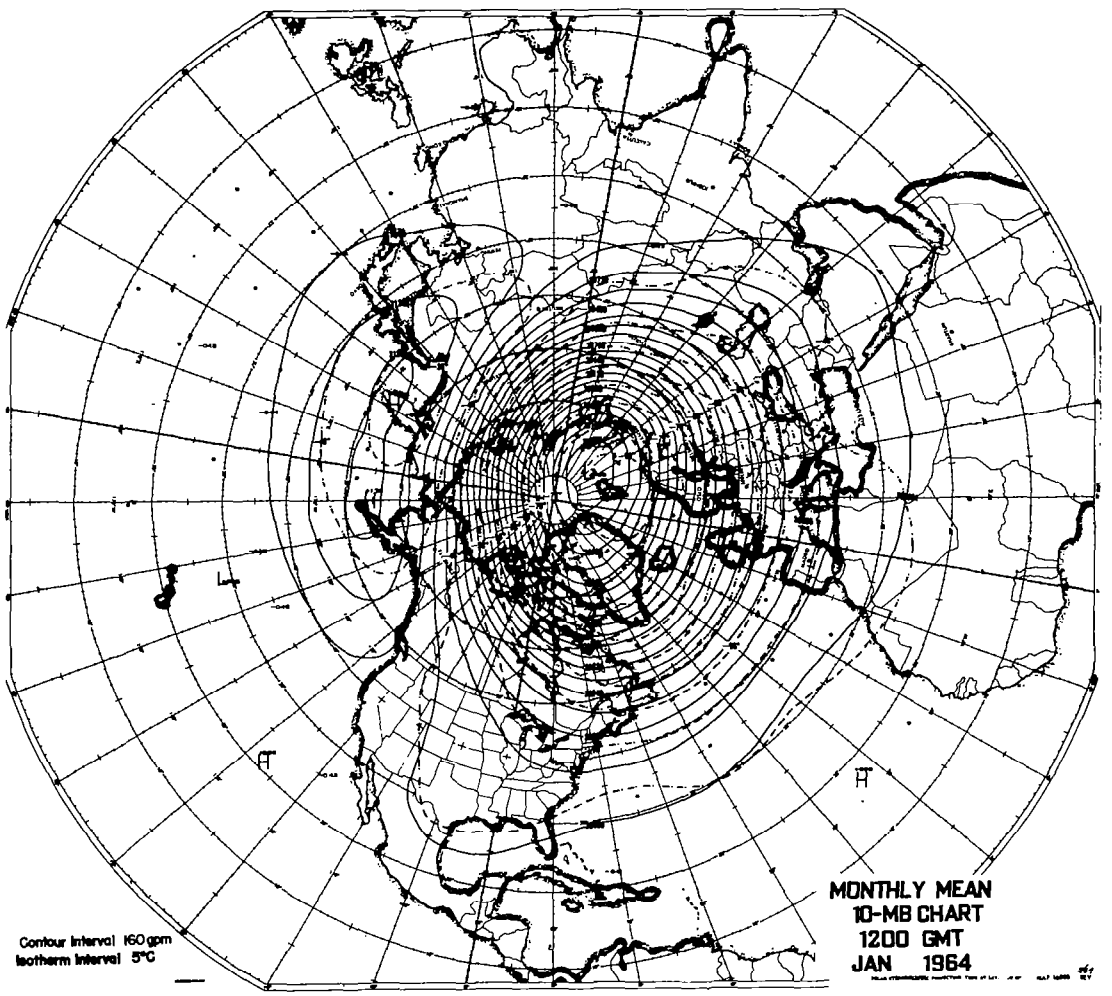

Figure 2.7. - Monthly mean of objective analyses of 10-mb surface heights (in meters) and temperatures (in degrees C) for January 1964, 1200 GMT, Northern Hemisphere. (Source: Ref. 16.)

Table 2.1 summarizes some salient features of warming events that have occurred since 1952. For each winter only that warming which was considered most significant is represented. Although this table was constructed as objectively as possible, it is difficult to present all the details. The 10-mb level was used as a basis for categorizing the types of warmings because it is the highest level for which a long series of maps is available. Every effort was made to apply the definitions of the Commission for Atmospheric Sciences (see text); however, paucity of data and different analyses (subjective and objective) might lead other researchers to results somewhat at variance with those given here. It should be noted that warmings are observed to altitudes of at least 50 km and, in many cases, strong high altitude events may not be classified as major in accordance with the definition we have adopted. However, all major warmings at 10 mb have been preceded, or accompanied, by strong warmings above that level. Thus, at least the entire stratospheric layer is significantly involved in major warming events. Rather arbitrary criteria were used for definition of the columns entitled "warming began" and "warming moved" in the table. The former is based on the approximate date when 10-mb temperatures exceeded -35°C in a cell which later became a major or minor warming; the latter on movement during the initial warming stages (approximately the first 3 days). In addition, the period of the phenomenon included only days when 10-mb temperatures exceeded -35°C. A direct indication of the warming intensity can be obtained from the temperature and wind information in this table. The peak temperature and temperature changes over the polar area provide a good index of the particular event, even though these values may have been exceeded in various other areas. Also of interest are the maximum temperatures at 5 and 2 mb during the warmings. This information from the rocketsonde network is based on considerably fewer observations than at 10 mb, where a great amount of rawinsonde data and indeed daily analyses are available. The 2-mb temperature +43°C, which was measured by a rocketsonde at West Geirinish, Scotland on December 21, 1967, appears to be the highest recorded by this type of observation. A wind of 182 m/s was recorded at a slightly higher level a week previous (the strongest known wind of 198 m/s was measured at 39 km over Heiss Island on February 1, 1966). Unfortunately, very little rocketsonde temperature information is available for the warming of early 1963, which appears to be the most pronounced on record.

Circulation breakdown must be preceded by a temperature reversal at lower levels. The warmest temperature ever measured in the stratosphere, +43°C or +316°K, occurred near 60°N at ≈2 mb during the 1967-68 warming. This is ≈90°K warmer than the average winter temperature, at that latitude, in a non-warming situation. Temperature gradient reversals during winter, in the mid and upper stratosphere, are fairly commonplace, and are accompanied by westerly circulation breakdowns of varying degrees of magnitude, along with altitude shifts in the polar night jet.

Southern Hemisphere data are sparse above 100 mb. Enough is known, however, to suggest that the deeper polar vortex inhibits wintertime circulation breakdowns. Occasionally, late winter dynamic events may couple with increased springtime solar radiation activity. Greater clarification of tropical stratosphere climatology is a prerequisite to an understanding of hemispheric interaction.

TABLE 2.1

STRATOSPHERIC WARMINGS

Winter Years	Warming Intensity	Warming Began	Warming Moved	Warming Peaked	Warming Period (Days)	Max. 10 mb Temp.	POLAR TEMPERATURES			Strongest East Wind at 10 mb (Major Warm)	Max. Temp. 5 mb/2 mb (Rocket Data)	Springtime Change over
							Begin Date	Peak Polar	ΔT °C (Pole)			
1951-52	MAJOR	unk	unk	unk	unk	unk	unk	unk	unk	unk	unk	unk
1955-56	minor	Jan 9	unk	Jan 20	unk	unk	unk	unk	unk	---	unk	unk
1956-57	MAJOR	Jan 19	E	Feb 6	27	-3°C	unk	unk	unk	unk	unk	unk
1957-58	MAJOR	Jan 22	NW	Jan 30	21	-14°C	-70	-30	+40	unk	unk	Mid May
1958-59	minor	Jan 23	NE	Jan 28	9	-32°C	-65	-50	+15	---	unk	Early May
1959-60	minor	Feb 21	N	Feb 24	10	-19°C	-65	-55	+10	---	unk	Late Apr
1960-61	minor	Jan 25	N	Jan 28	6	-16°C	-60	-50	+10	---	unk	Late Apr
1961-62	minor	Feb 15	NW	Feb 17	5	-28°C	-45	-35	+10	---	unk/-6°C	Mid May
1962-63	MAJOR	Jan 18	NW	Jan 27	19	0°C	-78	-15	+63	100 KTS	unk	Mid May
1963-64	minor	Jan 27	N	Jan 30	9	-23°C	-78	-68	+10	---	-7°C/-5°C	Early May
1964-65	minor	Dec 30	NE	Jan 6	13	-25°C	-75	-55	+20	---	unk/-5°C	Early May
1965-66	MAJOR	Jan 19	NW	Jan 31	43	-15°C	-81	-33	+48	120 KTS	+14°C/+14°C	Mid May
1966-67	minor	Dec 29	N	Jan 5	25	-16°C	-82	-66	+16	---	-8°C/+10°C	Late Apr
1967-68	MAJOR	Dec 17	NW	Jan 1	29	-15°C	-75	-19	+56	120 KTS	+3°C/+43°C	Mid May
1968-69	minor	Nov 29	N	Dec 14	23	-16°C	-57	-49	+8	---	unk/+36°C	Late Apr
1969-70	MAJOR	Dec 17	NE	Jan 2	49	-6°C	-77	-31	+46	140 KTS	+16°C/+38°C	Mid May
1970-71	MAJOR	Dec 7	NE	Jan 7	48	-8°C	-68	-26	+42	120 KTS	+25°C/+35°C	Mid May
1971-72	minor	Feb 8	N	Feb 15	24	-18°C	-68	-35	+33	---	+8°C/+2°C	Early May
1972-73	MAJOR	Jan 4	N	Feb 6	33	-12°C	-69	-31	+38	90 KTS	+11°C/+11°C	Mid May
1973-74	MAJOR	Feb 20	NW	Mar 3	28	+7°C	-70	-30	+40	---	-17°C/+3°C	Early Apr
1974-75	MAJOR	Feb 22	NW	Mar 2	21	-3°C	-65	-35	+30	---	-2°C/+2°C	Late Mar
1975-76	minor	Jan 30	NW	Feb 6	16	-3°C	-80	-65	+15	---	-11°C/±0°C	Early Apr

SYNOPTIC DESCRIPTION

Thermal Patterns in the Stratosphere

For many years the "breakdown" of the polar night vortex has been considered the chief characteristic of a major stratospheric warming. The occurrence of a circulation breakdown in high latitudes might suggest that warming occurs mainly in the polar region. However, the thermal disturbances which develop on a planetary scale, commonly in wavenumbers 1 or 2, result in significant warming in subpolar latitudes first (at least in middle and low latitudes of the stratosphere). These major warmings, usually exhibiting a westward slope with height and sometimes a poleward inclination, then proceed to higher latitudes.

Radiosonde data at 10 mb and below frequently permit the detection of a significant warming at an early stage of development. Indeed, in the early years of observation of the phenomenon, descriptions were necessarily based on patterns given by constant-pressure maps at 50 mb (about 20 km) or below. Figure 3.1, based on 50-mb temperature data, indicates the development of a stratospheric warming in late February 1974, over Siberia. At 65°N, there is warming by 40-50°C at 100-150°E, February 18-28. At 55°N, the amount of warming is less, about 20-30°C. Figure 3.2 shows that warming by up to 70°C occurred at 10 mb (about 30 km) near 65°N, 110°E, February 18-25. From February 25 to March 1, the warm center moved northeastward to a position near 80°N.

Figure 3.3 shows selected information from daily 50-mb maps for February 14, 18, 24, and 28. Note the strongly elongated polar vortex on February 14 and the re-orientation of the major axis on successive dates. Since hydrostatically the morphology of the 50-mb surface must reflect thermal conditions at lower altitudes, it seems plausible that the pattern of warming in late February is linked with events in the troposphere and/or lower stratosphere. Stratospheric-tropospheric interactions will be discussed in another chapter of this monograph.

Also noteworthy are details of the thermal patterns on these maps (Figure 3.3). Even before the warming a warm anomaly is evident on February 14 in the far North Pacific, centered at 50-60°N. This is a semi-permanent feature of the stratosphere, associated with the "Aleutian" or "Siberian" anticyclone, which has been simulated through dynamic modeling by Matsuno (ref. 32) and from general circulation models by Kasahara et al. (ref. 33) and Manabe and Terpstra (ref. 34). The anticyclone was simulated in a case "with mountains" but not in a case "with no mountains" in their circulation model (Kasahara, op. cit.), so it may be reasonable to assume that the standing wave may be linked to the orography of east Asia. At the same time, the eastward progression of thermal changes required by the counterclockwise rotation of the vortex at 50 mb suggests the possibility of interaction between traveling waves and the standing wave in the Far East, a process which is discernible in maps of satellite radiation data, as will be shown later.

Still another link is suggested between warming in high latitudes on the one hand, and thermal changes in equatorial latitudes and latitudes of the opposite hemisphere, on the other. Such a link was first seen in

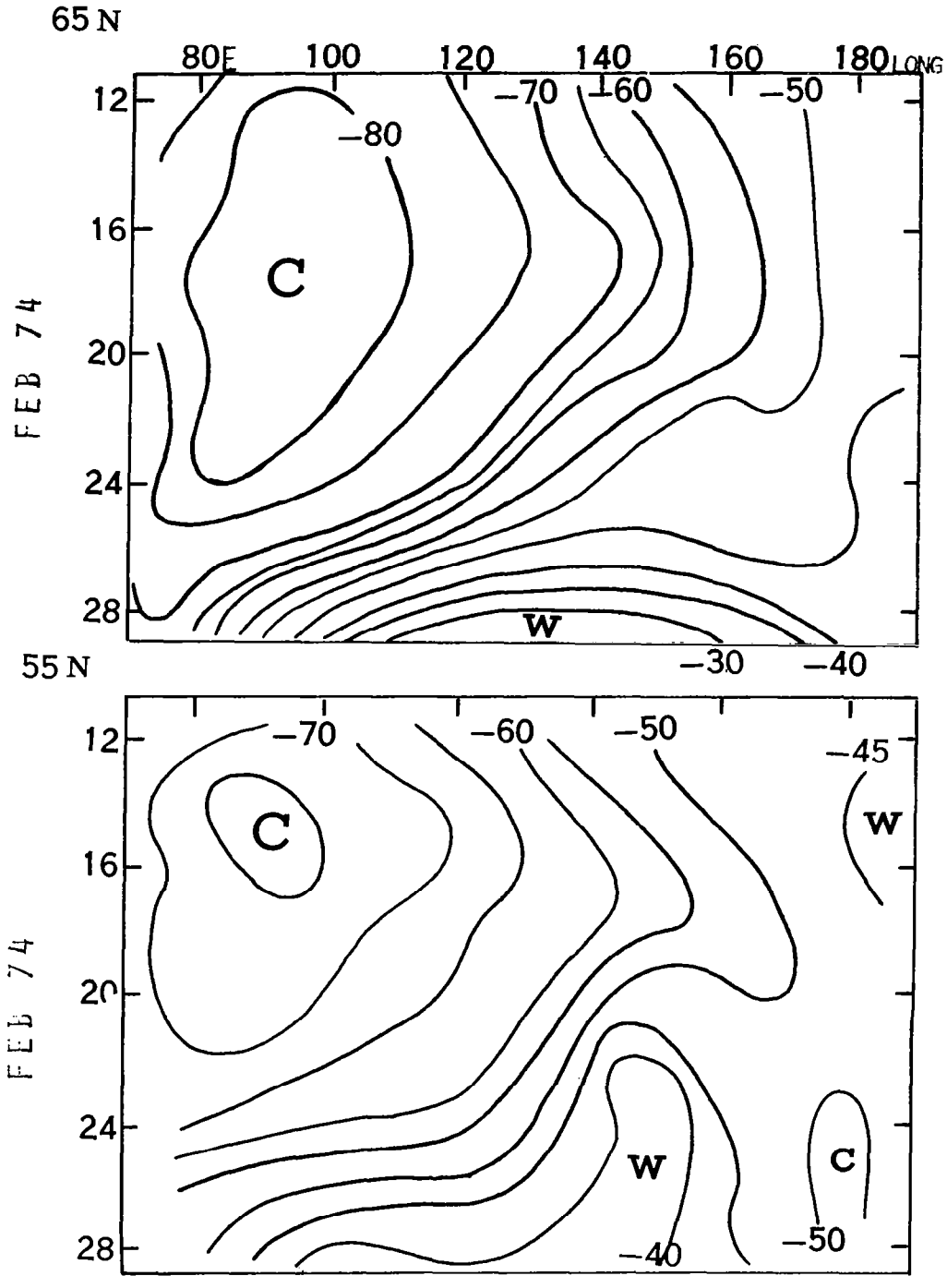

Figure 3.1. - Longitudinal time-sections of 50-mb temperature (degrees C) at 55°N and 65°N, 12-28 February 1974.

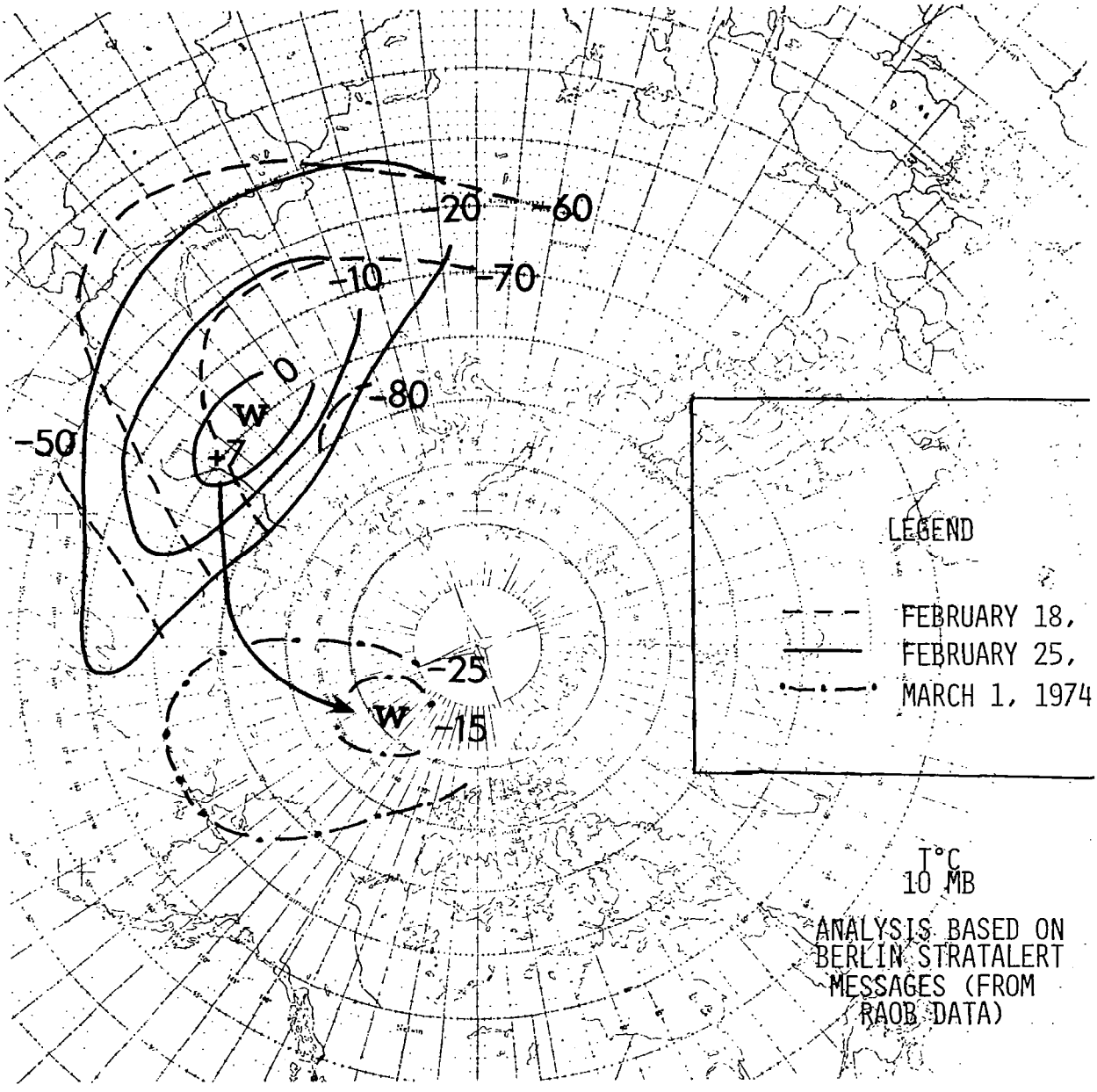

Figure 3.2. - Temperature patterns at 10 mb for 18 and 25 February and 1 March 1974, showing warming by 70°C during period 18-25 February near 65°N, 110°E and apparent movement of warm cell to position near 80°N.

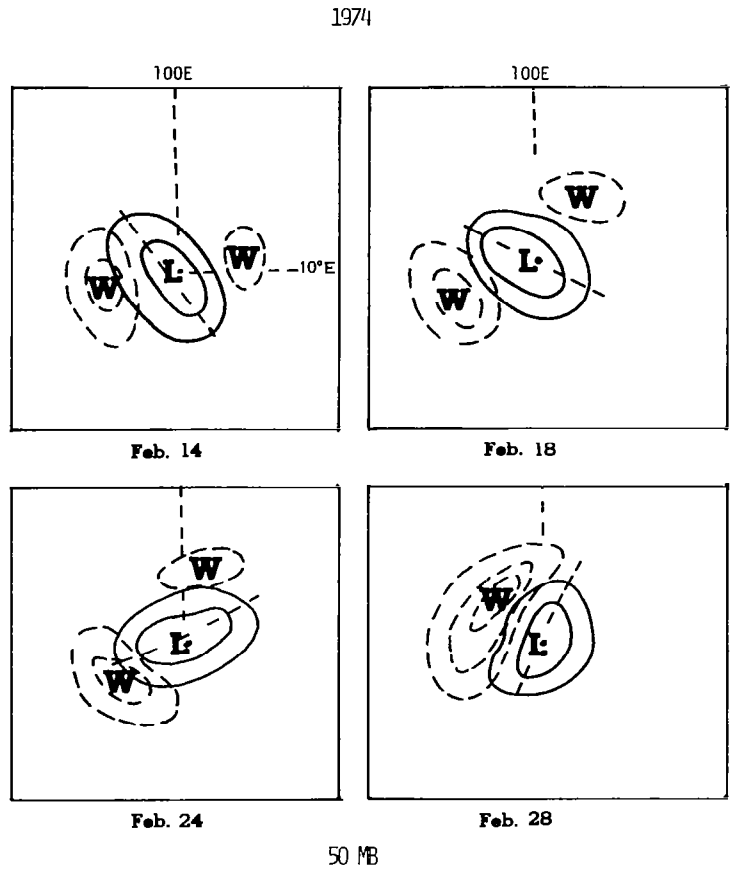

Figure 3.3. - Schematic illustration of 50-mb height and temperature patterns 14-28 February 1974. Note eastward rotation of polar-vortex axis, and formation of single thermal wave by 28 February. North Pole is at center of each diagram.

satellite radiation measurements during the major warming of December 1969 - January 1970 and has been observed in numerous cases, minor and major, since then. Figure 3.4, from Fritz and Soules (ref. 9), shows means zonal radiances observed by the Nimbus 3 SIRS instrument, expressed as departures from values in the annual cycle. A strong positive departure in December 1969 - January 1970 in high northern latitudes reflects major warming during that winter (ref. 26). A simultaneous decrease occurred in low latitudes of both hemispheres and, possibly more important, a phase lag was observed in the radiance maxima from low to high latitudes. The mechanism accounting for these effects will be examined below with the aid of synoptic radiance maps.

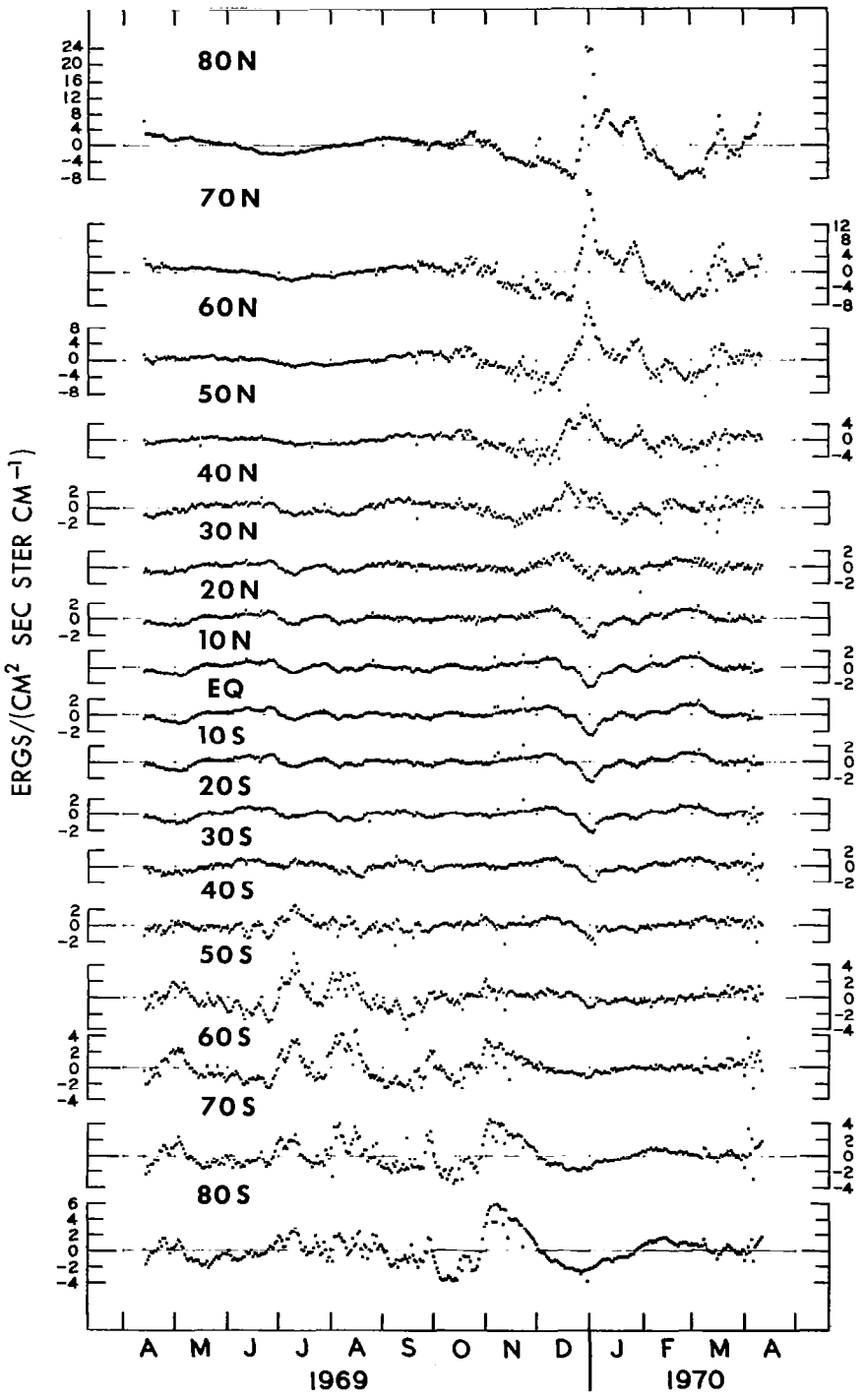

Figure 3.4. - Daily values of mean zonal radiance measured in SIRS Channel 8 (weighting function maximum in middle stratosphere), expressed as deviation from value in annual cycle. (Source: Ref. 9.)

In Figures 3.1-3.2 we determined the occurrence of warming in Siberia, at latitudes near 60°N, and tracked the warm centers to 80°N, from February 25 to March 1. Figure 3.4 suggests that we might be able to track the centers from lower latitudes earlier in the month. This is not easy to do, because the thermal changes in low latitudes are of relatively small amplitude and the dominant component of motion is zonal. The low-latitude tracking of thermal changes is also difficult, from maps based on radiosonde data, because of the sparse distribution of stations in the tropics.

Satellite radiation measurements since 1969 have provided useful insights into this problem. The picture most commonly observed is represented schematically in Figure 3.5, showing the trajectory of high radiance centers (VTPR Channel 1), December 24, 1972 - February 10, 1973. In the Far East, a quasi-stationary thermal wave is indicated by centers which undergo very little longitudinal displacement, December 24 - January 26. On the other hand, the high-radiance system centered near 55°N, 100°E can be tracked back all the way to South America on December 27. By January 27, the two systems merged together in NE Siberia and thence the amplified system moved to the North Pole. The eastward progression of the traveling wave and the superposition with the standing wave are shown in VTPR Channel 2 radiance maps for selected days during January 22 - February 6 (Figure 3.6). Figure 3.7 shows the trajectories of radiance centers in channels with maximum weighting at levels from the lower stratosphere (VTPR 2) to the upper stratosphere (SCR B12).

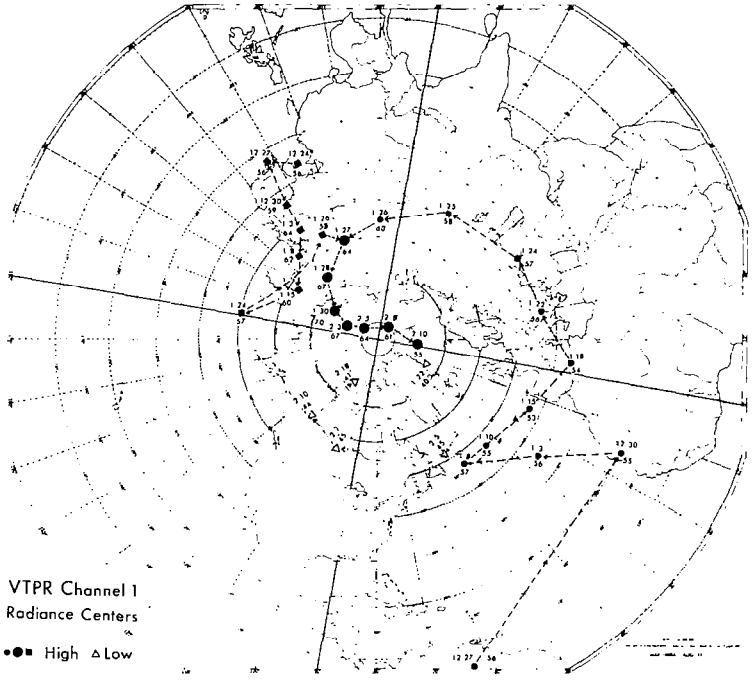

Figure 3.5. - Trajectories of radiance centers (VTPR Channel 1, similar to SIRS Channel 8) in winter 1972-73. (Source: Ref. 11.) Central values are in mW $(m^2\ sr\ cm^{-1})^{-1}$.

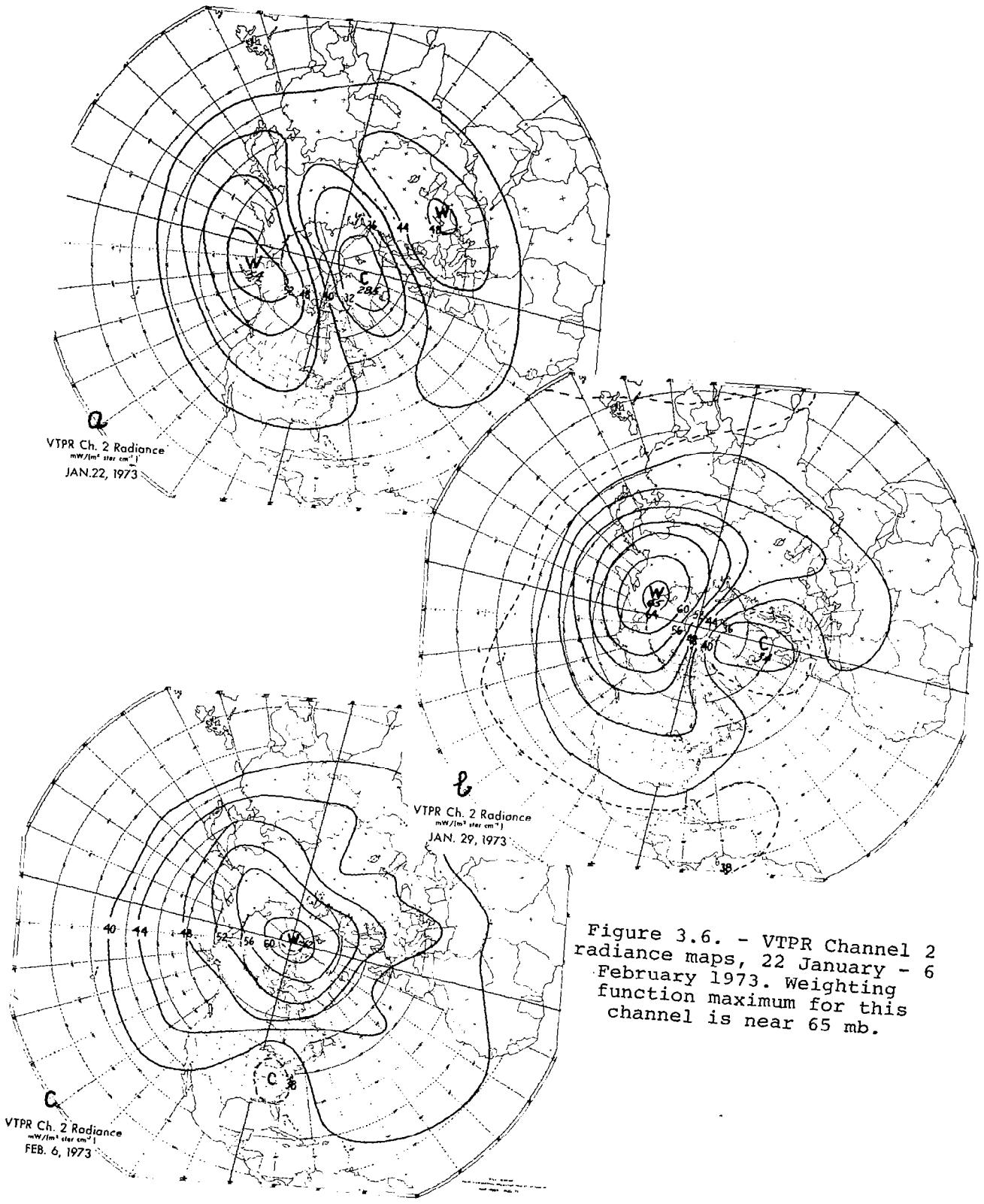

Figure 3.6. - VTPR Channel 2 radiance maps, 22 January - 6 February 1973. Weighting function maximum for this channel is near 65 mb.

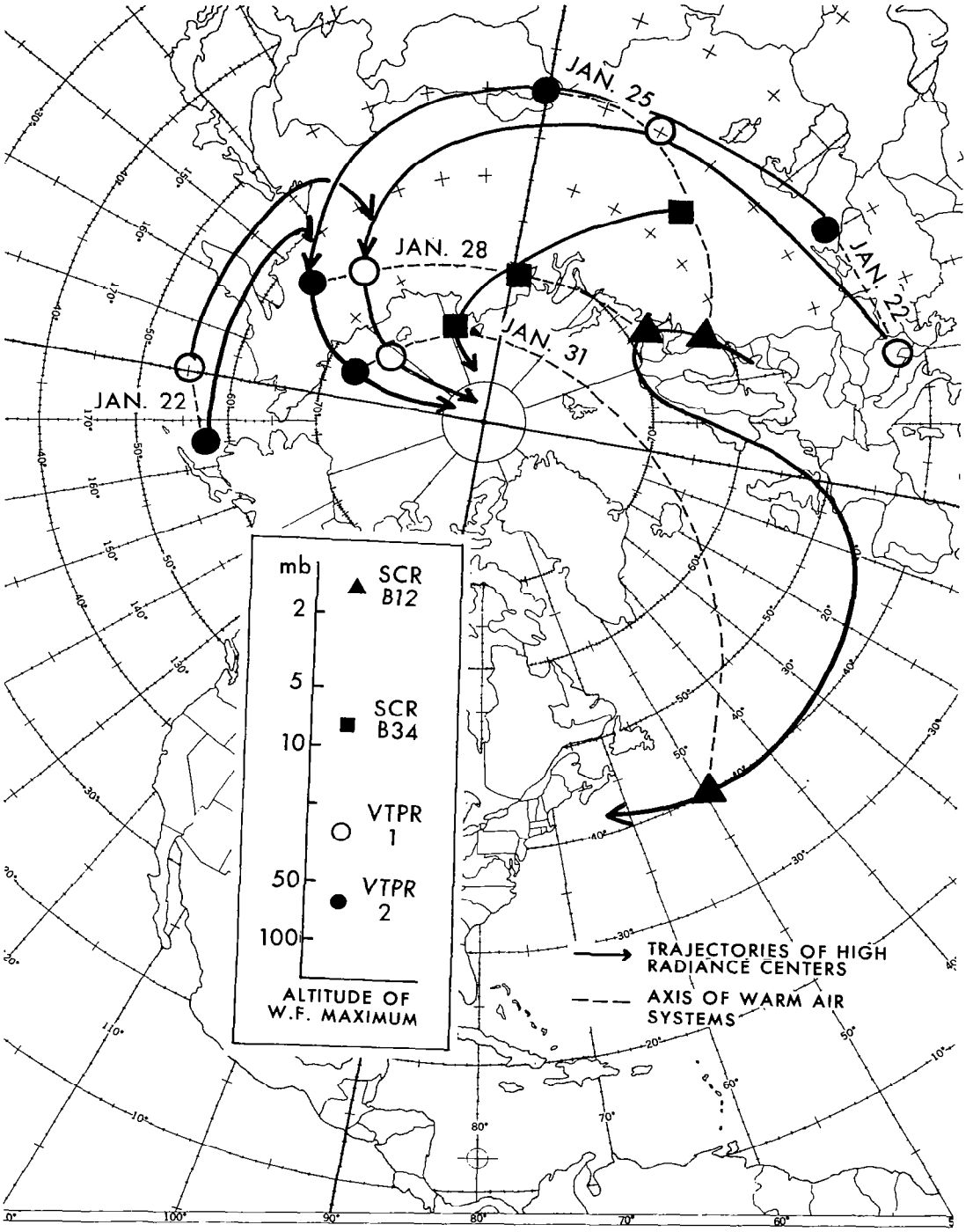

Figure 3.7. - Paths of high radiance centers for VTPR and SCR stratospheric channels in January 1973. Connecting dashed lines give approximate orientation of thermal ridges. (Note: 'W.F.' stands for 'weighting function.')

This pattern, observed in several major warmings since 1969 (ref. 11) is represented schematically in Figure 3.8a. The review of evidence regarding the movement of stratospheric thermal systems in recent warming cases and in cases as early as 1949 (ref. 35) indicates two principal types of development, (1) the mode just described for 1973, in which warm air moves poleward in an apparent wavenumber 1 pattern, and (2) a mode perhaps best represented by the warming of January - February 1963 (ref. 36). In (2), depicted in Figure 3.8b, the traveling wave has a strongly meridional trajectory in or near the area of the North Atlantic Ocean. In 1963, the North Atlantic and east Siberian thermal systems (delineated by stratospheric radiosonde data) arrived seemingly independently in the polar region, forming a single thermal system at 10 mb after a pronounced wavenumber 2 pattern was observed in the pressure field.

For (1) above, we speak of an apparent wavenumber 1 pattern, because it is evident that the resultant pattern is a consequence of interaction between traveling waves with wavenumber greater than 1, and the wavenumber 1 standing wave.

Some discussion has been made earlier of the difficulty of classifying warmings. Since minor events may have much in common with major events, a rigid separation is not desirable. However, considering that most of the mass of the stratosphere is found below the 10-mb level, it is reasonable to consider as major those events involving a reversal of the meridional temperature gradient below 10 mb and a circulation reversal at 10 mb or below.

Thus for the occurrence of a major event it appears necessary (though not sufficient) for the warming process to proceed from subpolar to polar latitudes. Polar warming, indeed, distinguishes a potential major event from minor ones. It is possible, however, for polar warming to occur in the upper stratosphere, as might be indicated, for example, in the highest radiation channel of the SCR, without a circulation reversal near 10 mb (see Figure 3.9a). This situation has been observed at least once yearly in the Northern Hemisphere, in recent years; and in the Southern Hemisphere it is commonplace after June. It is also possible for polar warming to occur at low stratospheric altitudes without sufficient intensity to culminate in a circulation reversal.

Another illustration of an upper stratosphere warming without an accompanying circulation reversal at 10 mb is given in Figure 3.9b, based on rocket soundings.

When intense warming is observed in subpolar latitudes, it is of interest to predict whether warming will proceed to the vicinity of the pole. A guide to this determination has been the intensity of the horizontal radiance gradient upon superposition of traveling and standing thermal waves (ref. 11). In each major warming observed during 1969-74, a gradient of 15 mW $(m^2\ ster\ cm^{-1})^{-1}$ $(10\ degrees\ latitude)^{-1}$ was attained in the uppermost radiance channels of the SIRS and VTPR instruments. In each case, the occurrence of such a gradient was followed by poleward migration of the high radiance centers, as seen on synoptic charts. Comparison with winds indicated by constant-pressure maps indicates that, in general, the movement of these centers is a reflection of some combination of horizontal temperature advection and adiabatic warming of subsiding air. (The contribution of diabatic heating is believed to be small or, in the polar night region, perhaps nil.)

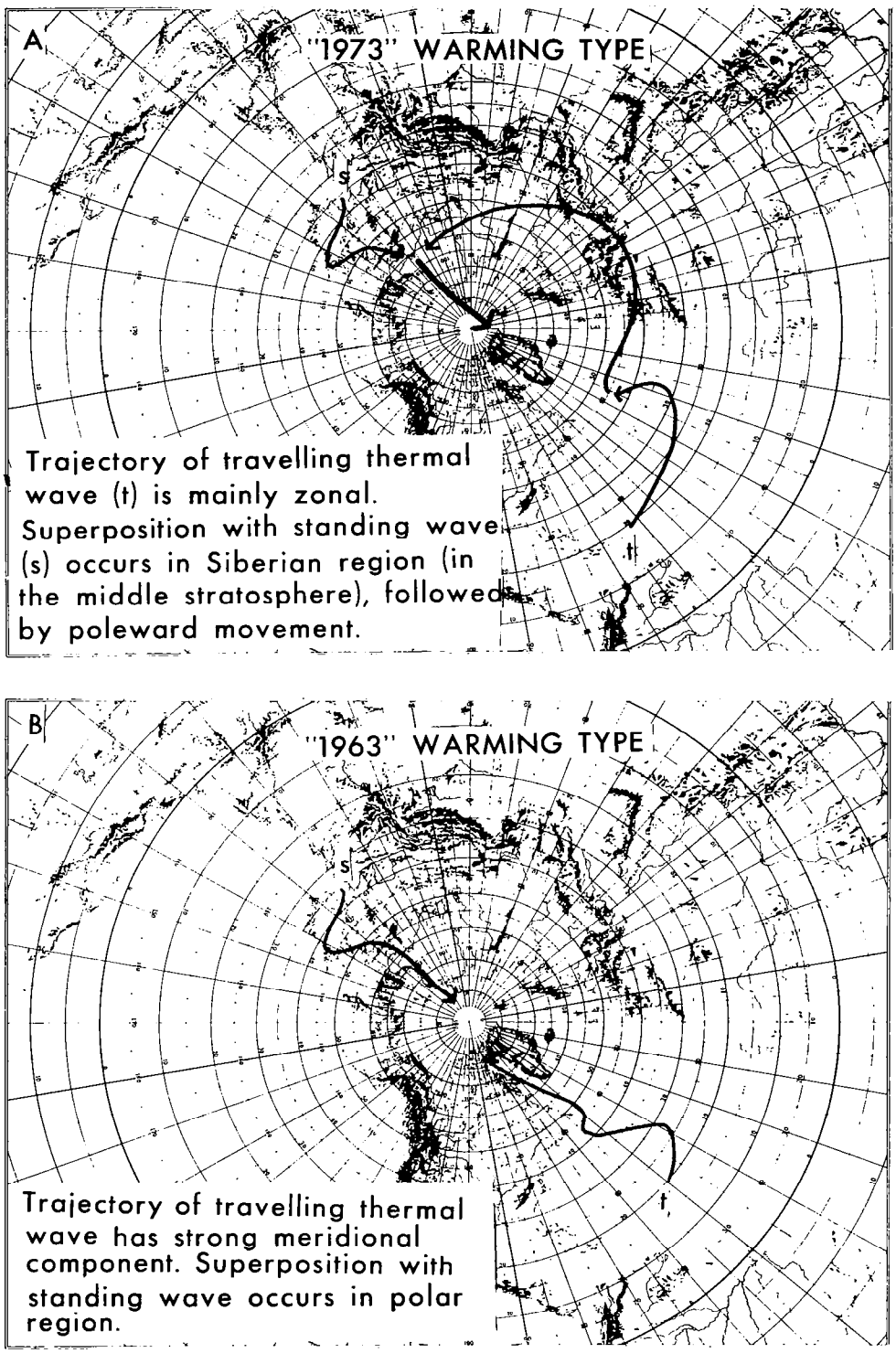

Figure 3.8. - Schematic trajectories of warm cells in 1973 and 1963 warmings. Paths represent movement of warm centers at (approximately) 30- or 10-mb level.

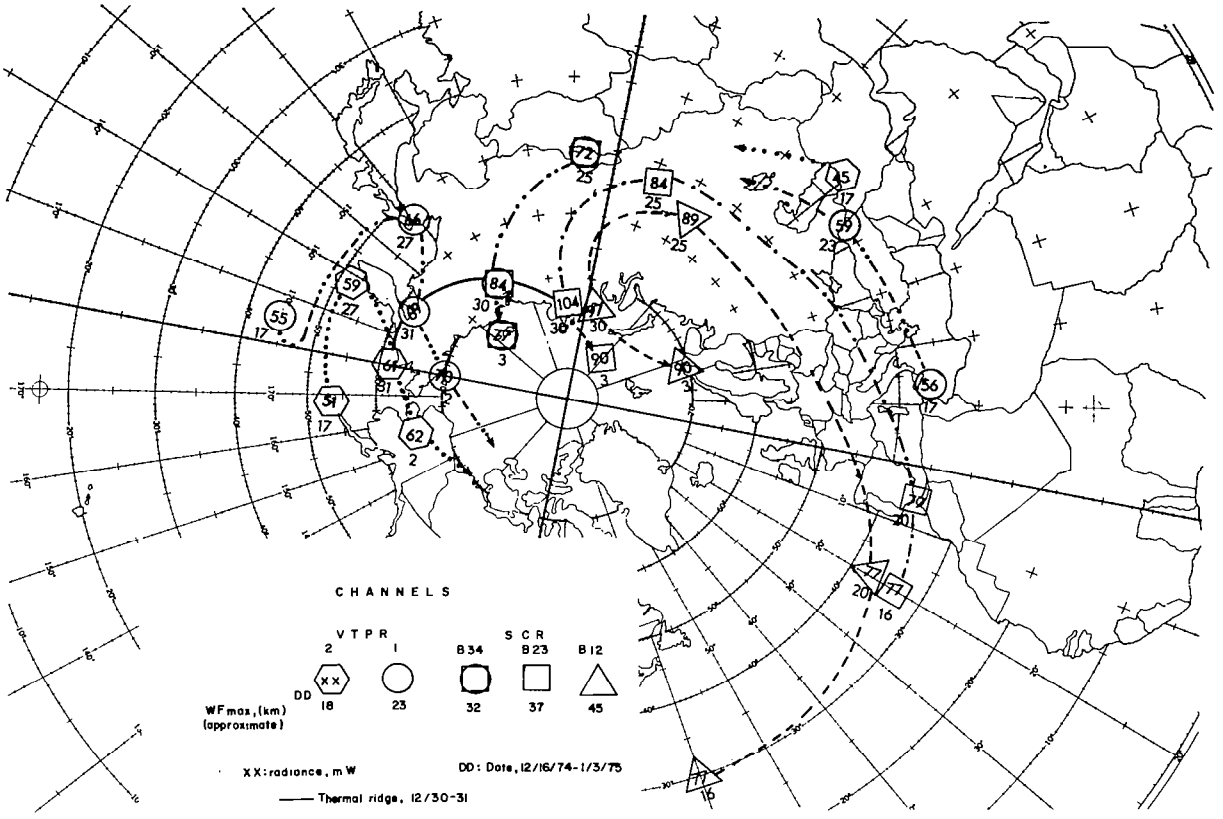

Figure 3.9a. - Trajectories of centers of maximum radiance in December 1974 - January 1975. Paths corresponding to radiation channels representative of lower stratosphere had only limited poleward penetration.

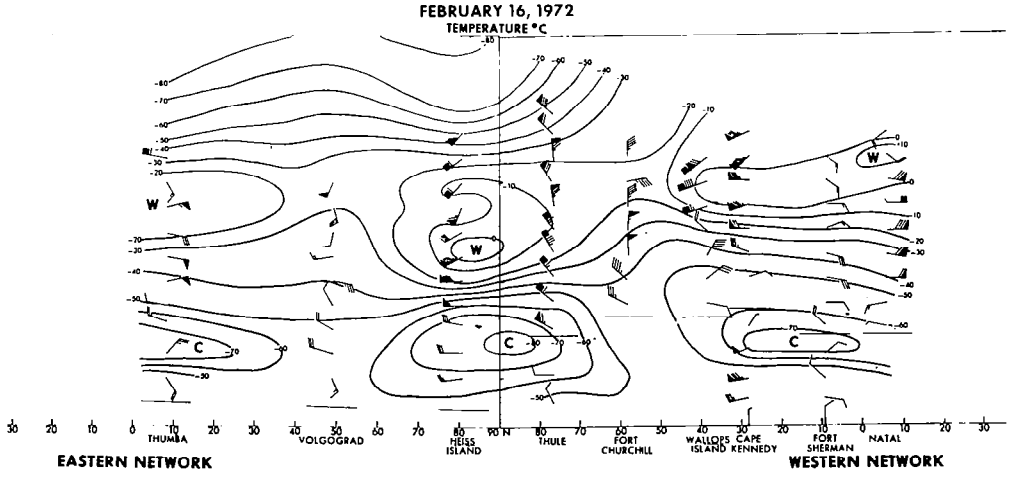

Figure 3.9b. - Space cross-section (Western and Eastern Hemispheres) for 16 February 1972. Numbers at bottom are degrees latitude.

The horizontal radiance gradient cited above corresponds to a horizontal gradient in the mean stratospheric temperature (100-2 mb) of 20°C (10 degrees latitude)$^{-1}$; and through the thermal wind equation corresponds to a mean vertical wind shear of 7 m s^{-1} km^{-1}. Since baroclinic instability is favored by strong vertical shear, it is possible that the condition described may be a key factor in the occurrence of "major" warming characterized by a "breakdown" of the polar vortex.

Synoptic Conditions in the Troposphere

Not much is known about attendant conditions in the troposphere, except for two factors mentioned below. The isolation of features in the troposphere which might lead to stratospheric warming is difficult because of the masking effect of wavenumbers higher than those prevailing in the stratosphere (mainly 1 and 2); also, the smaller amplitude of tropospheric features. We do know the following: (1) in the early warming stages, or just prior to a warming, there is often a strong conversion of zonal available potential energy to eddy available potential energy in the troposphere and a strong eddy flux of geopotential from the troposphere to the stratosphere (the energy budget will be discussed elsewhere in this monograph). (2) There is a significant inflation of the pressure surfaces in the middle and upper troposphere in advance of stratospheric warming, especially in the region of the North Atlantic and southern Eurasia. Early evidence presented by Muench (ref. 37) for the warming of January - February 1958 suggests that this process proceeds in waves 1 and 2 from the lower troposphere to the stratosphere, with a lag of 3-5 days (Figure 3.10). His depiction of wave amplitudes was confined to January 2-28 and one latitude (50°N). A more general analysis, covering longer periods and other latitudes, is needed to establish some relationship between stratospheric and tropospheric events. Such an analysis, besides indicating wave amplitudes and phases, should also seek to identify the particular tropospheric features associated with stratospheric warmings.

A significant rise of the tropospheric pressure may be exhibited in the form of "blocking", a condition that is difficult to quantify. This condition has been defined in several ways (see reference 38 for a discussion of problems in evaluating blocking). Essentially it is a state of the circulation characterized by persistent high pressure in some preferred region (e.g., 50°W - 20°E), in which basically zonal flow is interrupted by persistent meridional flow. Labitzke (ref. 39) made interesting observations concerning the tropospheric synoptic situations before and after warmings. One was the occurrence of blocking some 10 days after a number of warmings, perhaps suggesting some form of stratospheric "feedback." Equally interesting was the observation of very deep cyclonic systems, shown in 3-day mean 500- or 300-mb maps, underlying regions of incipient stratospheric warming. To characterize the tropospheric flow, "zonal index" values may be used; these provide a crude measure of the average geostrophic flow between specified latitudes. Although this may not be a satisfactory parameter for studying tropospheric-stratospheric interaction, it is noteworthy that Quiroz (ref. 40) showed oscillations of this index at 700 mb which were in phase with oscillations in the upward geopotential flux through 100 mb, preceding thermal oscillations in the stratosphere (Figure 3.11). Improved use of this index might involve a more judicious choice of pressure level and latitude domain in its calculation.

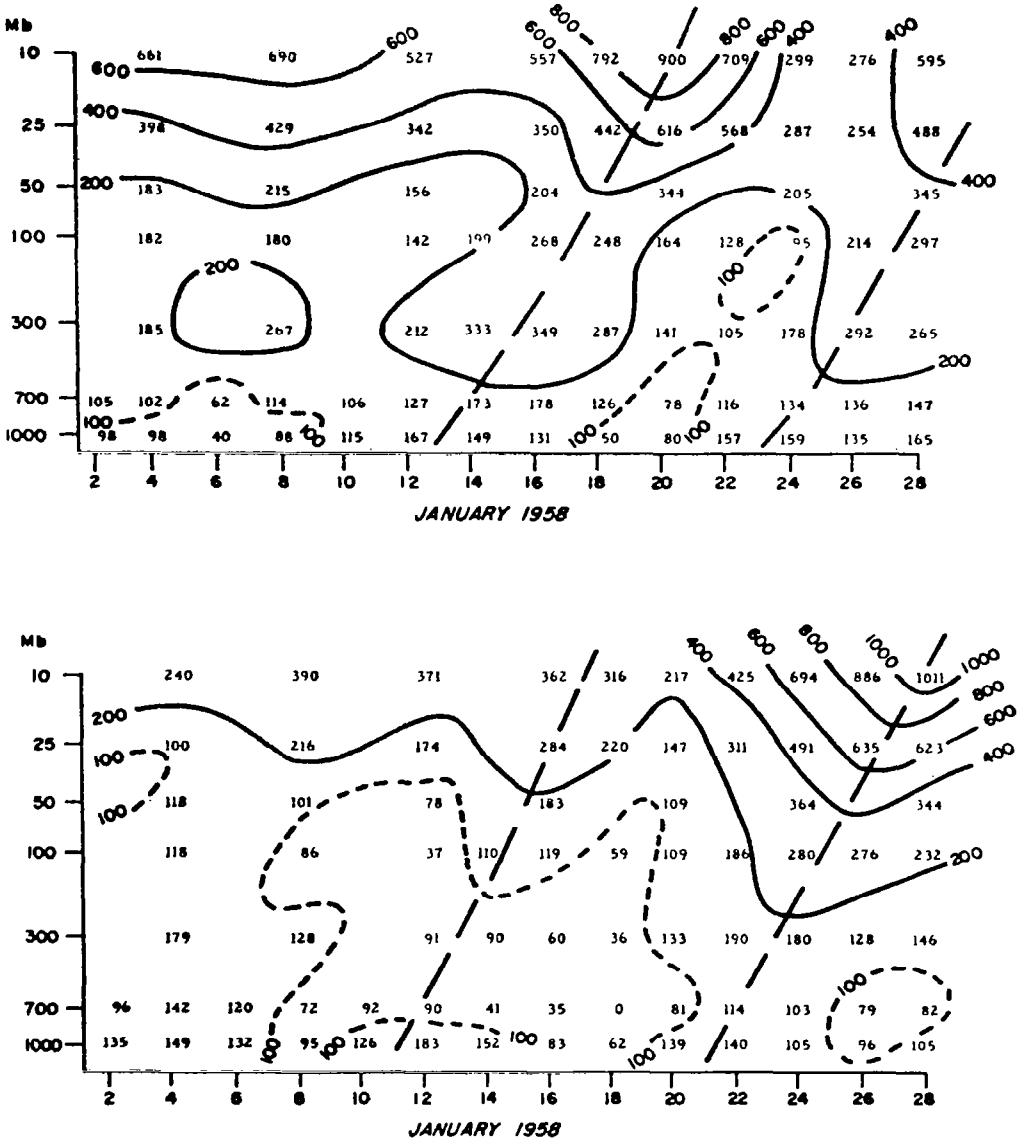

Figure 3.10. - Height amplitudes, in meters, of wavenumber one (upper) and wavenumber two (lower) at 50°N during January 1958. (Source: Ref. 37.)

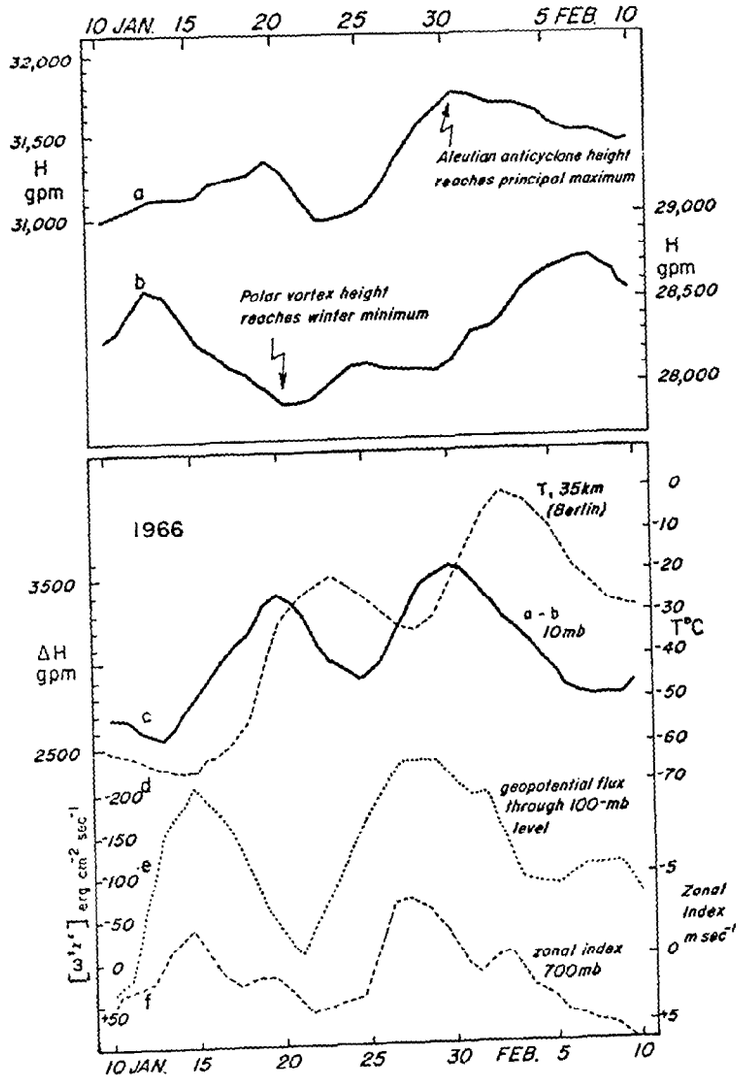

Figure 3.11. - Tropospheric and stratospheric parameters during early 1966. (a) maximum height of 10-mb surface north of 45°N; during period depicted, this was the height of the Aleutian-Siberian anticyclone. (b) central height of 10-mb polar vortex. (c) difference, (a) minus (b). (d) Berlin, Germany, temperature, 35 km. (e) vertical flux of geopotential, integrated over latitudes 17.5°-82.5° N, through the 100-mb level, wave number 1. Negative values refer to upward flux. (f) polar zonal index (55°-70°N), 700 mb, Western Hemisphere. Note parallelism of (e) and (f), both leading (c) by 3-5 days. Berlin temperatures, 35 km, lag (c) by about 3 days. Low zonal index values in mid- and late January were associated with blocking of westerlies. (Source: Ref. 40.)

Consistent with the observation of a strong rise in the height of the tropospheric pressure surfaces is the amplification of wave 2 in dynamic simulations of stratospheric warmings (ref. 41). Matsuno (ref. 42), for example, introduced a perturbation with amplitude 300 m at 300 mb which led to a simulated warming and circulation reversal resembling the major event of 1963. In Newson's (ref. 43) simulation of a warming resembling the major event of 1973, amplitudes of 200-300 m spontaneously occurred at levels in the upper troposphere. (See section on Numerical Modeling.)

Circulation Effects

In each winter one or more events are observed in which there is unusually strong amplification of the Siberian-Aleutian standing thermal wave. Some poleward component of movement of the reinforced wave will be discerned, but the trajectory of the warm air in the middle or lower stratosphere will retain a basically zonal character. In contrast, the path of warm air in the upper stratosphere may diverge poleward and may even indicate westward retrogression, within a westerly vortex. An example of this behavior was shown in Figure 3.9a, depicting the paths of warm centers during an important "minor" warming event in December 1974 - January 1975. In this figure, paths of high radiance centers are shown for VTPR Channel 2 (WF maximum in lower stratosphere) and SCR Channel B12 (WF maximum in upper stratosphere).

Figure 3.12a (30-mb chart for 1 January) shows a relatively undisturbed polar vortex, but Figures 3.12b-d (5, 2, and 0.4 mb, ∿ 1 January 1975) show that in connection with this "minor" warming the circulation was greatly affected in the upper stratosphere. Over the Alaskan Arctic, the circulation changes from westerly, ∿50 m/sec, in the lower stratosphere, to weak northerly winds at 5 mb.

Another important type of circulation change may occur with warming of the lower stratosphere which is confined to subpolar latitudes. Indeed, there is evidence that the "Aleutian" anticyclone undergoes quasi-periodic modulations associated with the superposition of weak thermal waves. Hirota et al. (ref. 44) have shown periodic fluctuations of the anticyclone center which result in alternating westerly or easterly wind components over Japan. With intense development and eastward displacement of the anticyclone, even stations in North America as far east as Wallops Island, Virginia may observe anomalous wind flows with a strong northerly component. At a station in the southern United States, such as White Sands, New Mexico, easterlies may replace the more usual westerlies.

In a more general sense, the stratospheric wind at any site in middle latitudes may undergo fluctuations which can be traced to (1) tropospheric pressure variations and/or (2) pressure gradient changes explainable by minor, albeit quasi-systematic thermal changes within the stratosphere. A significant upper-stratosphere circulation change at any rocket site can usually be related to the passage of a thermal wave within the stratosphere. There is often a similarity of repeating oscillations in wind and temperature discernible in time-height sections at individual rocket sites. The oscillatory character of the thermal structure will be discussed in a later section.

Figures 3.13-3.14 depict the breakdown of the polar vortex in the warmings of January - February 1963, and January - February 1973. Characteristic stages of the circulation breakdown are listed below. Reference is to the 10-mb level unless otherwise specified.

(1) Polar vortex is well developed and quasi-circular (may be elongated at levels below 10 mb). Central height has reached wintertime minimum ($\leq$ 28,500 gpm).

(2) Polar vortex becomes elongated, especially at levels below 10 mb. From hydrostatic considerations, elongation suggests a dominant contribution in wave 2 below 10 mb. Triangularity suggesting an additional contribution in wave 3 is also often indicated. The thermal contributions need not occur

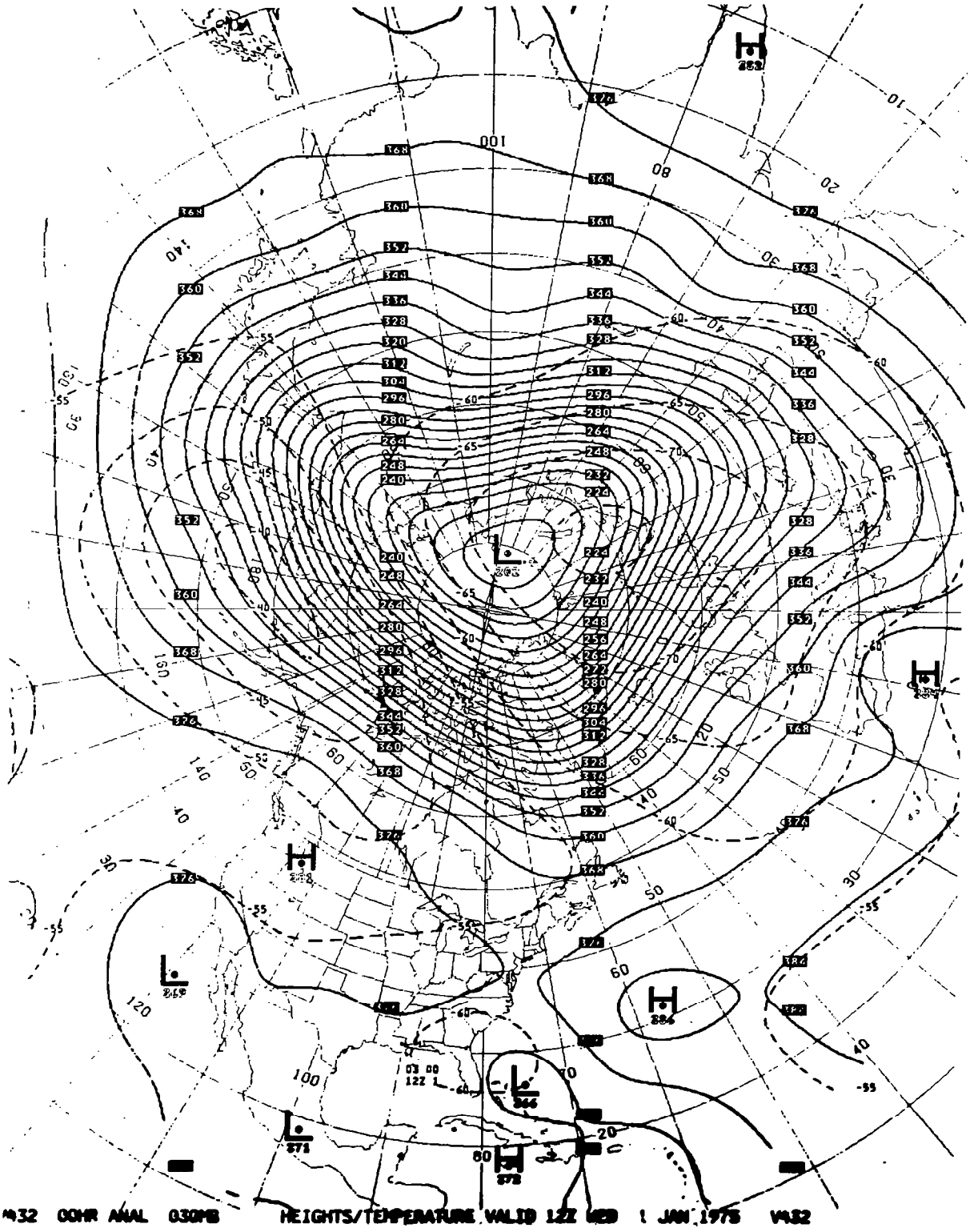

Figure 3.12a. - 30-mb map for 1 January 1975, objectively analyzed according to the method described in Ref. 15.

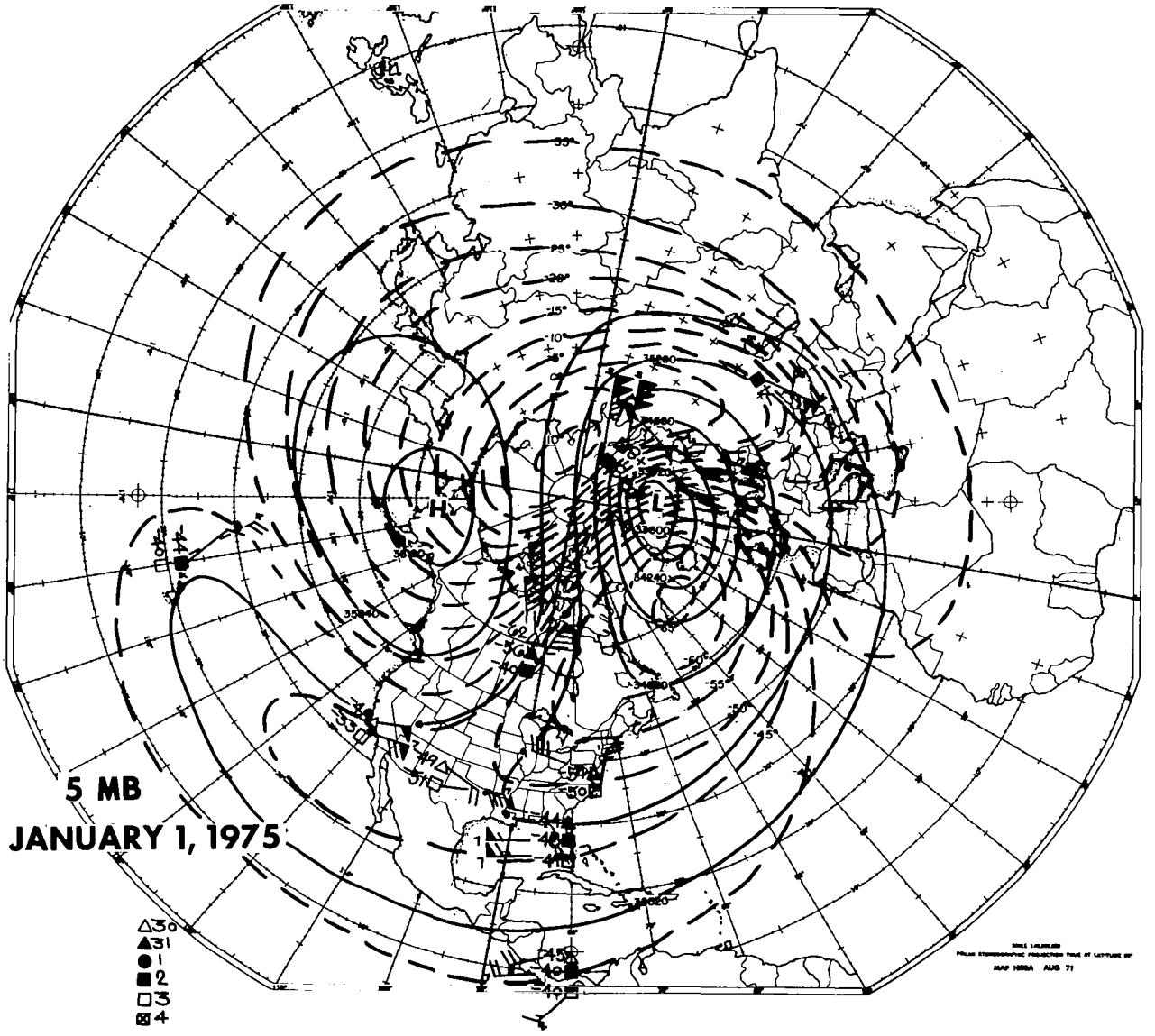

Figure 3.12b. - 5-mb map for 1 January 1975. Analysis is for rocketsonde data as plotted, with dates indicated according to the key at lower left. First-guess field of heights is based in part on thicknesses derived from VTPR Channel 2 radiances. First-guess field of temperatures is based on a combination of VTPR Channel 1 and Channel 2 data, together with regressions which relate in situ data to radiance fields.

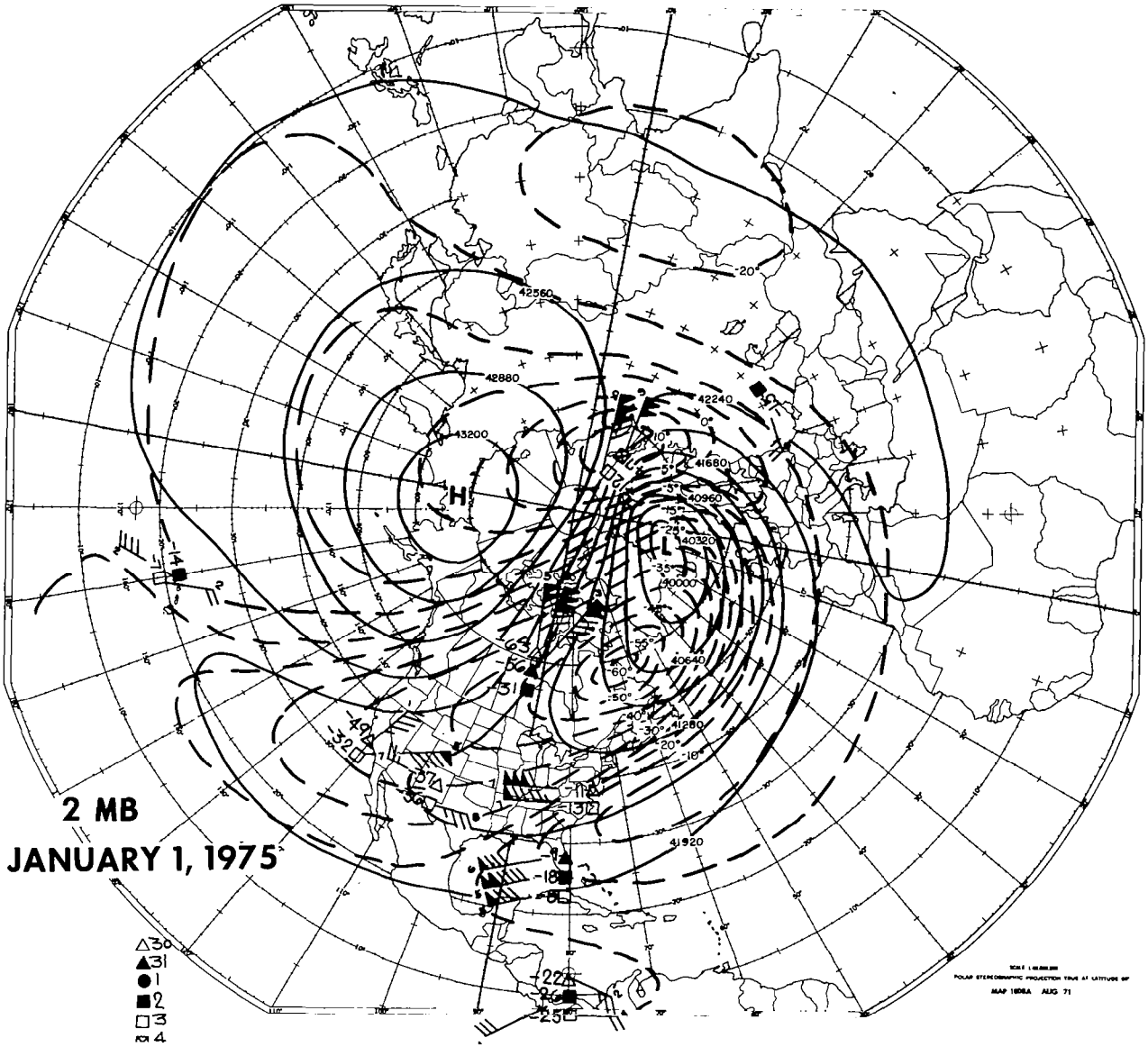

Figure 3.12c. - 2-mb map for 1 January 1975. Analysis same as b), except first-guess field of heights is related to VTPR Channel 1 rather than Channel 2.

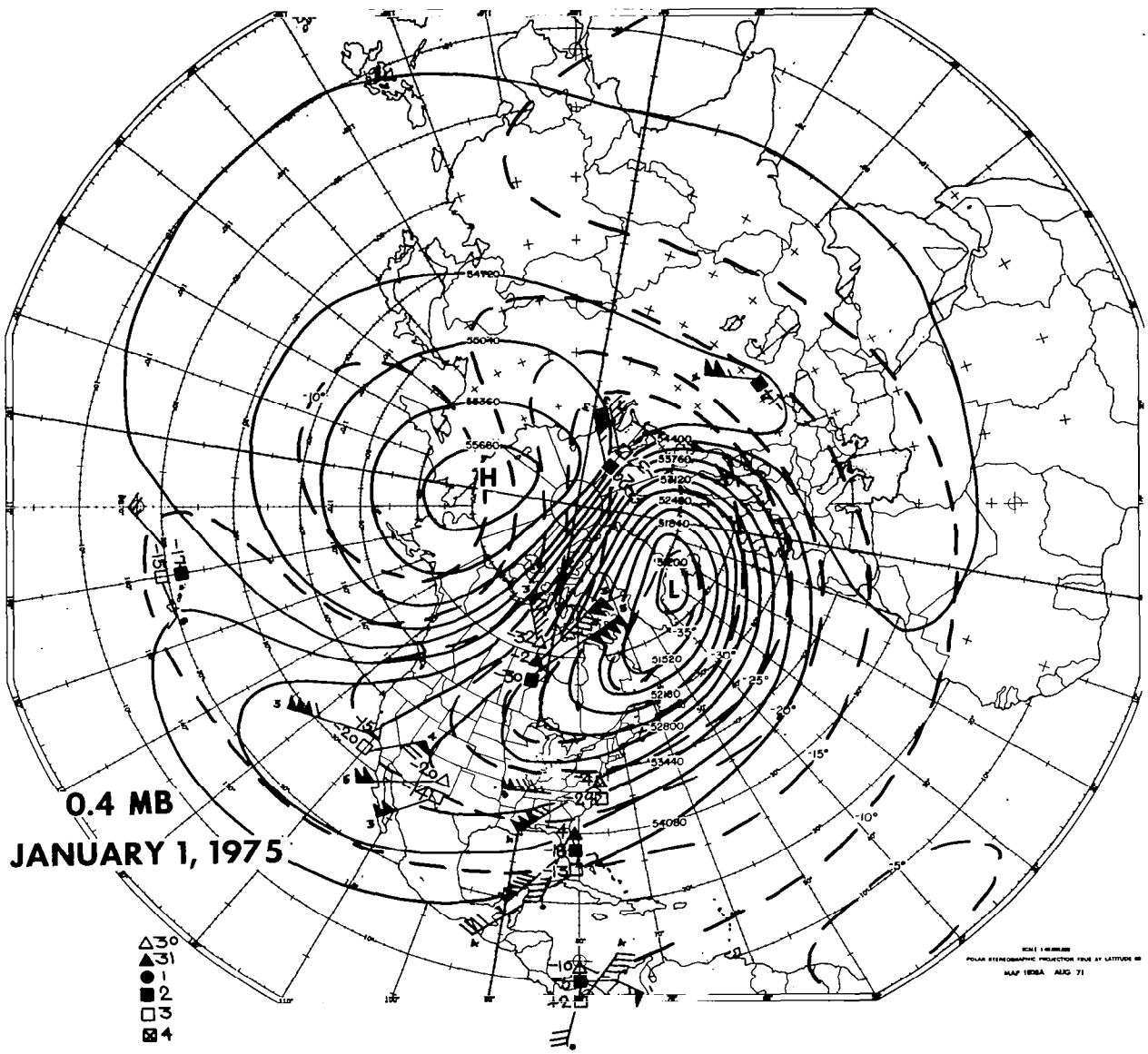

Figure 3.12d. - 0.4-mb map for 1 January 1975. Analysis same as b), except first-guess field of heights is related to both VTPR Channels 1 and 2.

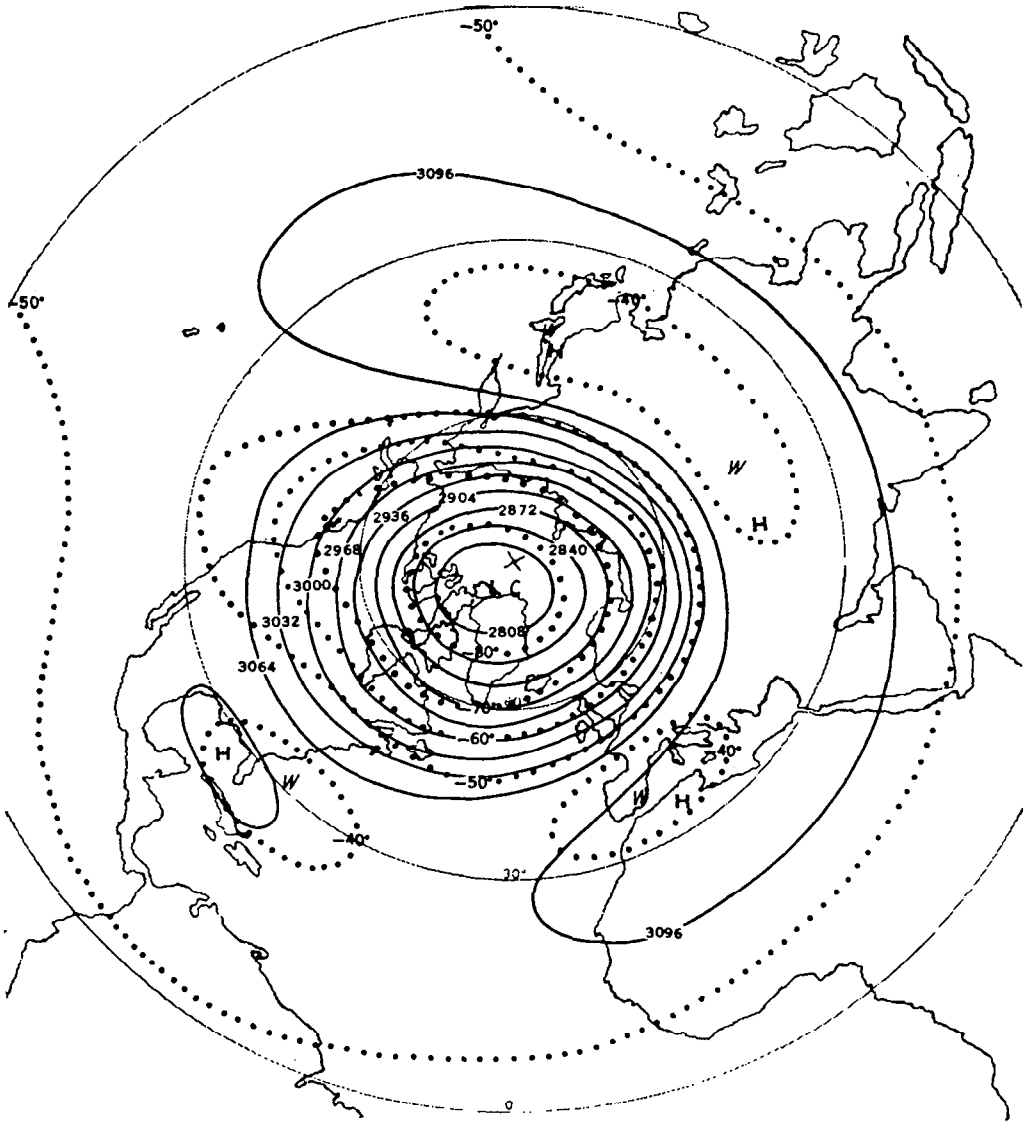

Figure 3.13a. - 10-mb chart for 0000 GMT, 8 January 1963. Contours are solid lines at intervals of 32 decameters. Isotherms are dotted lines at intervals of 10°C. (Source: Ref. 14, 1963: Meteor. Abhandl., Band XL, Heft 1.)

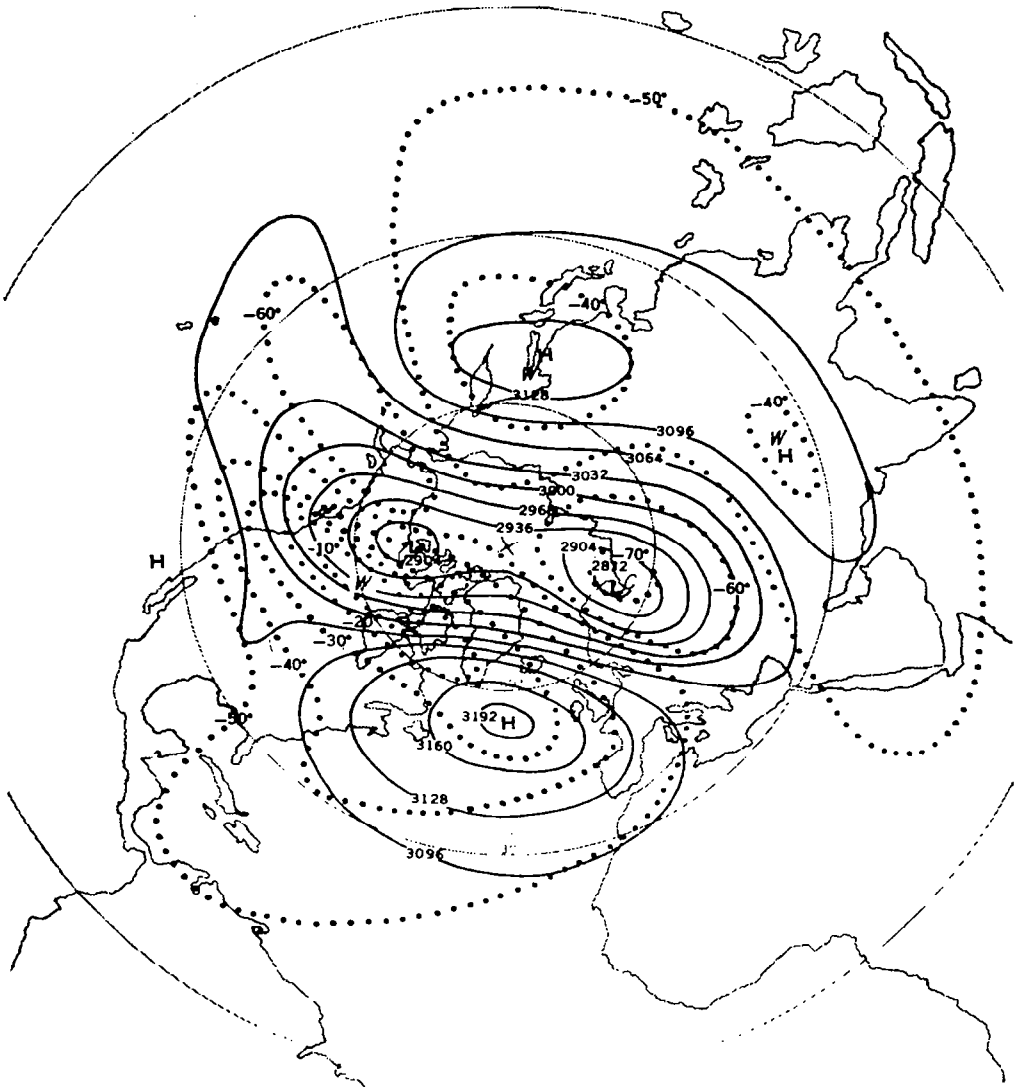

Figure 3.13b. - 10-mb chart for 0000 GMT, 23 January 1963. Explanation as in Figure 3.13a. Same source.

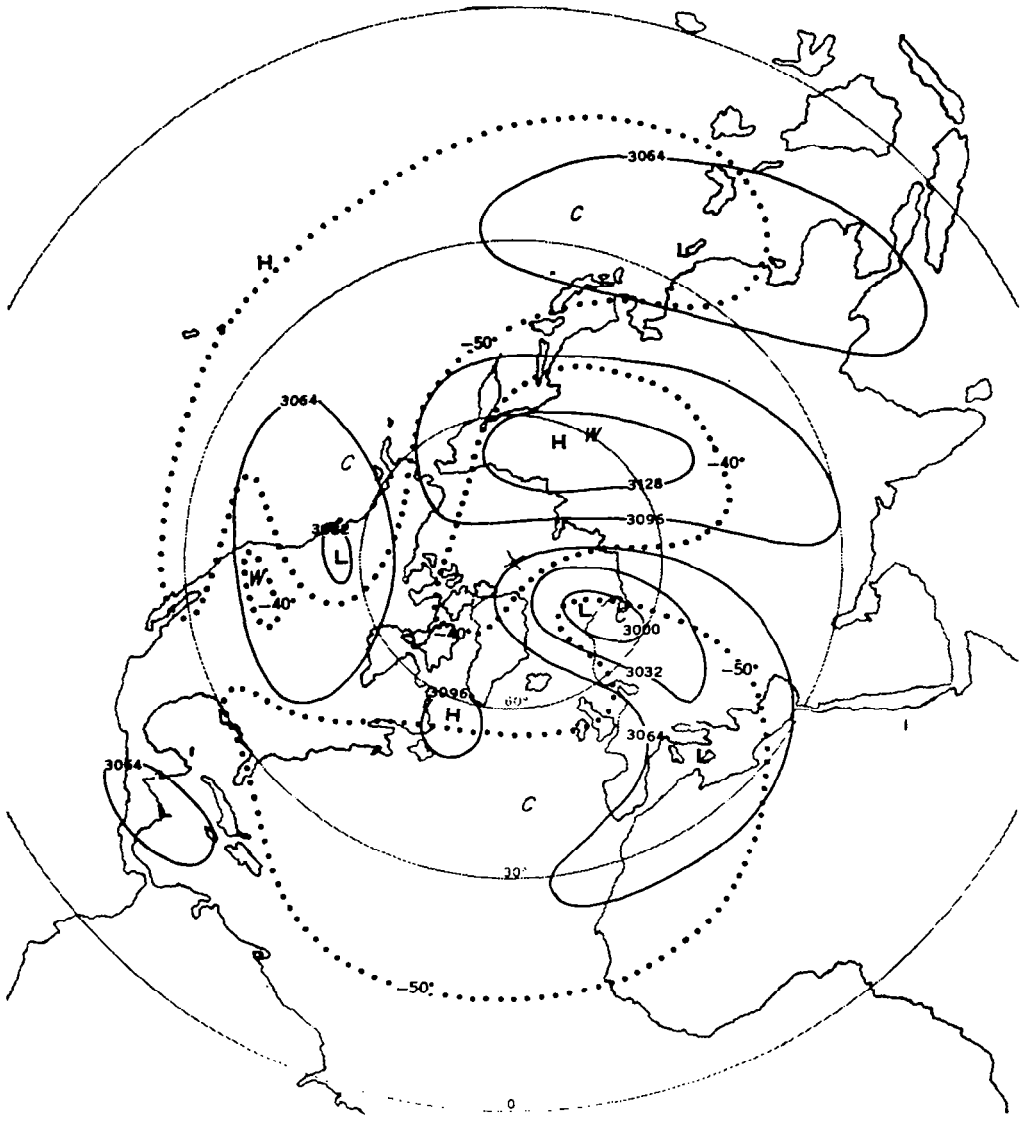

Figure 3.13c. - 10-mb chart for 4 February 1963.
Explanation as in Figure 3.13a. Same source.

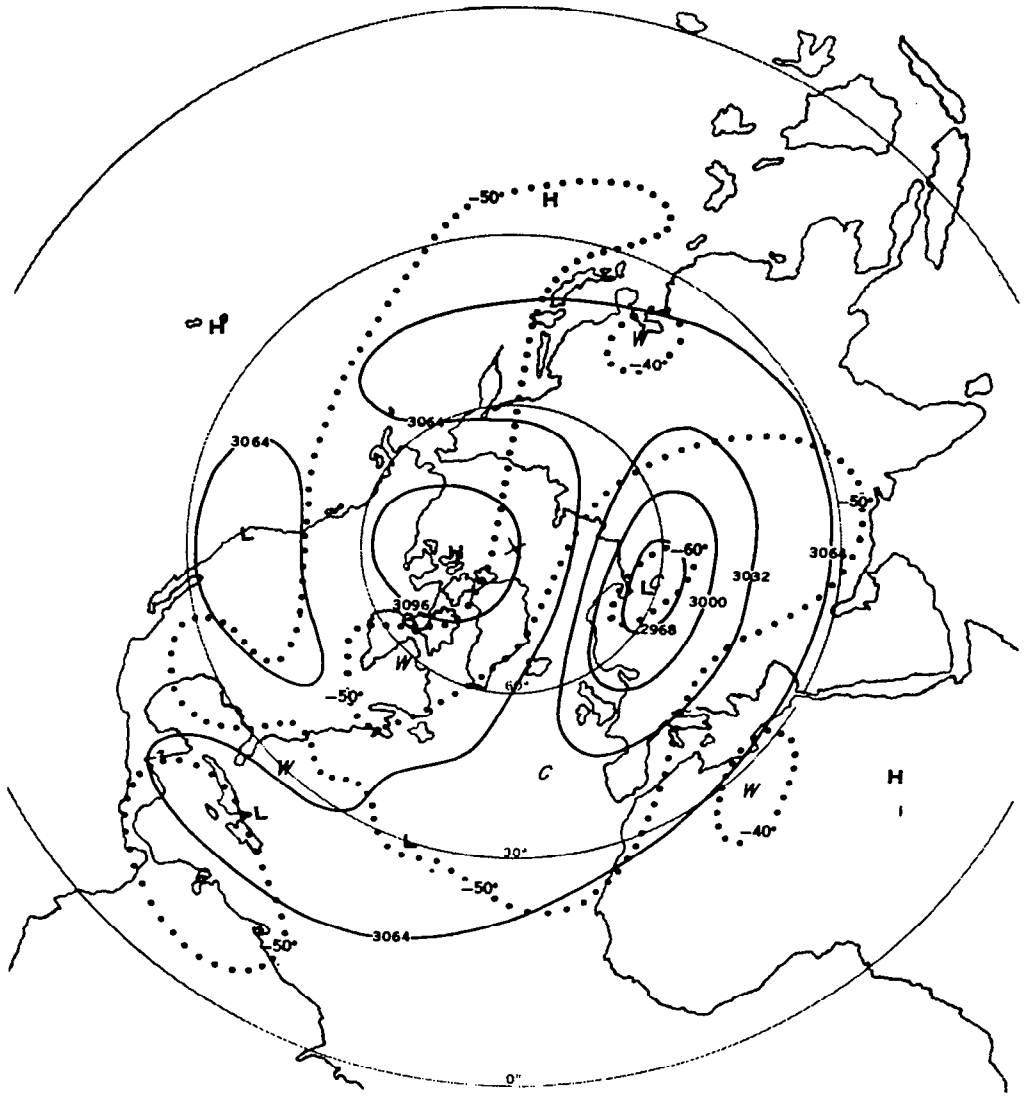

Figure 3.13d. - 10-mb chart for 11 February 1963.
Explanation as in Figure 3.13a. Same source.

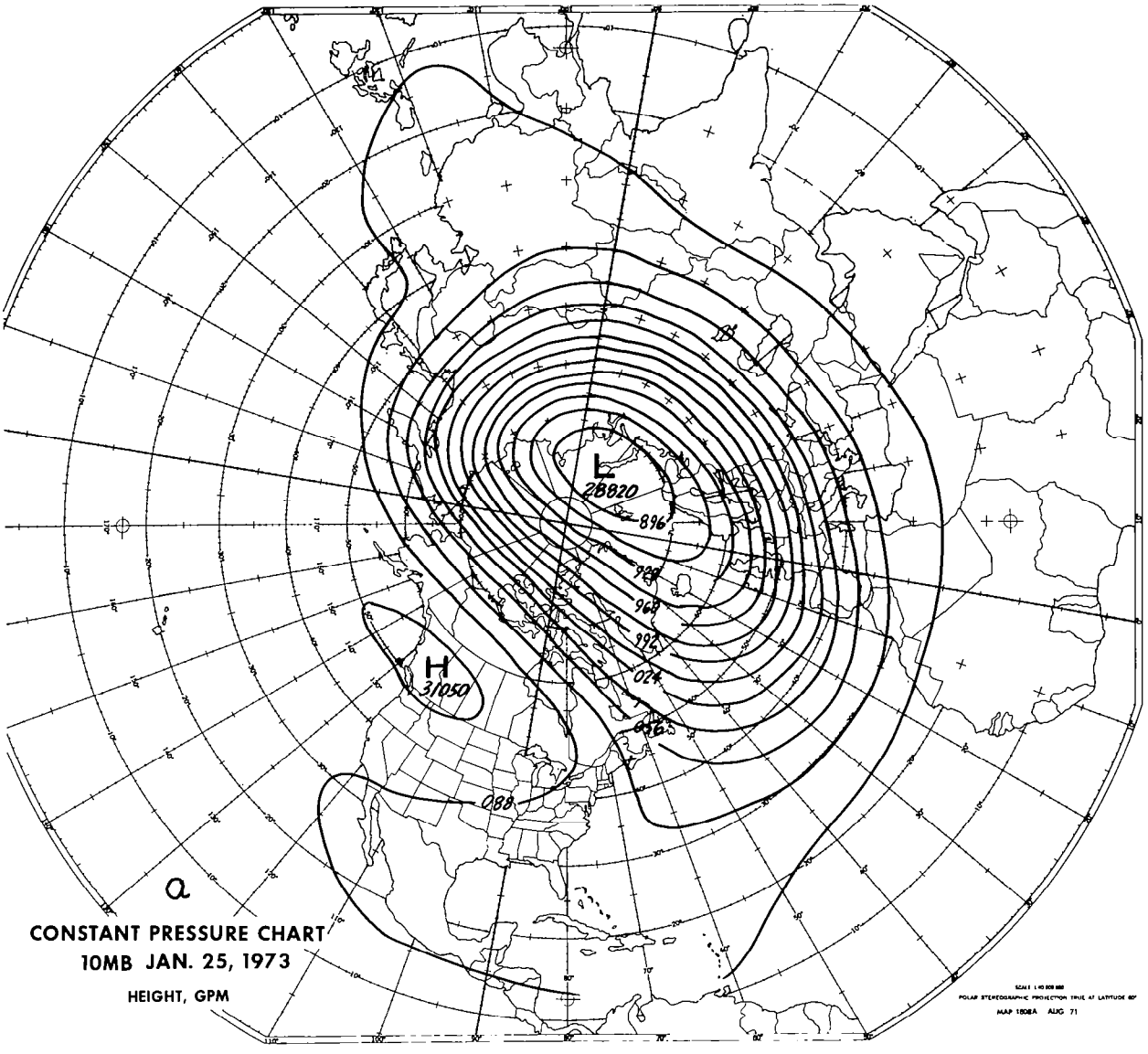

Figure 3.14a. - 10-mb map for 25 January 1973.

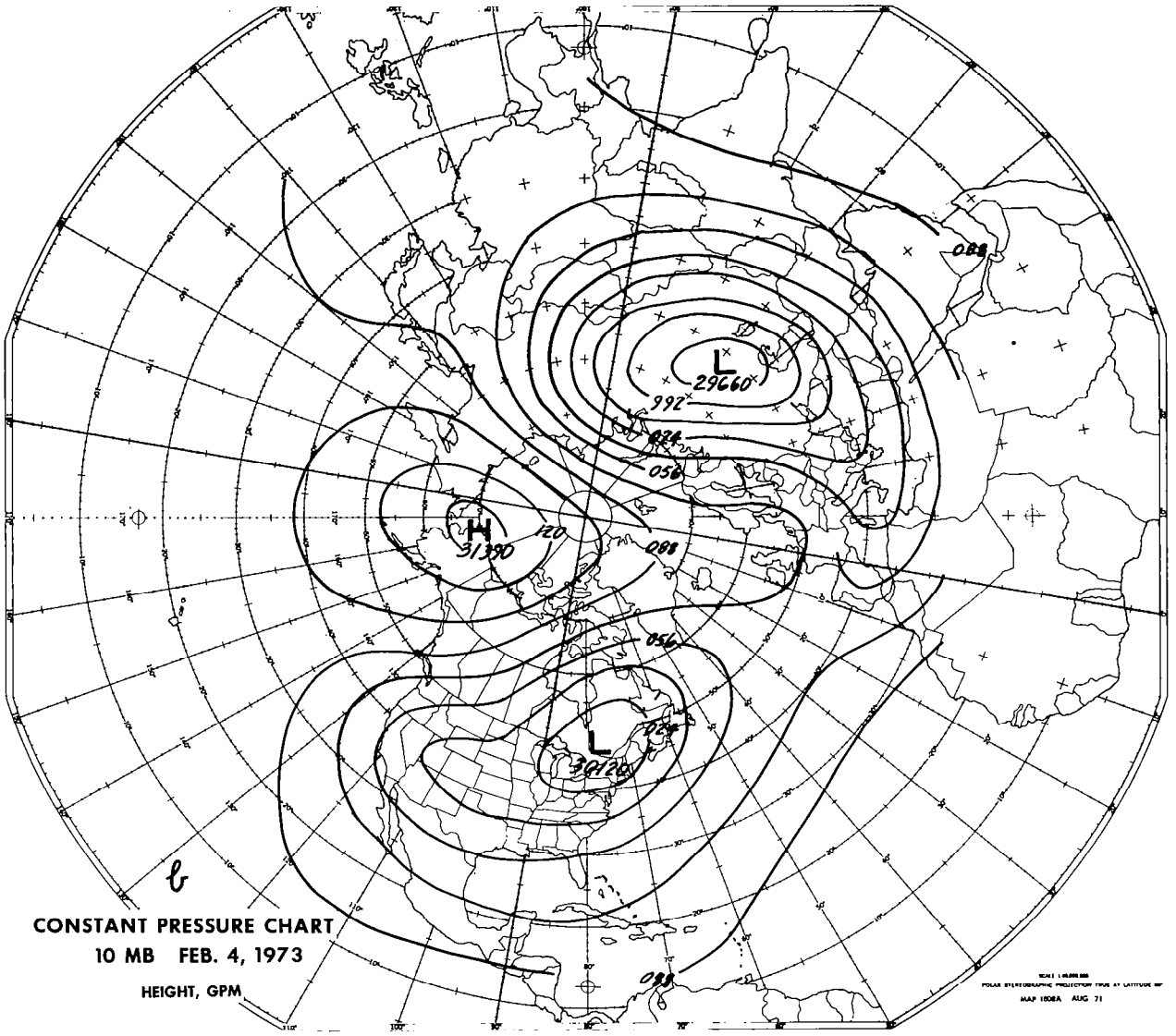

Figure 3.14b. - 10-mb map for 4 February 1973.

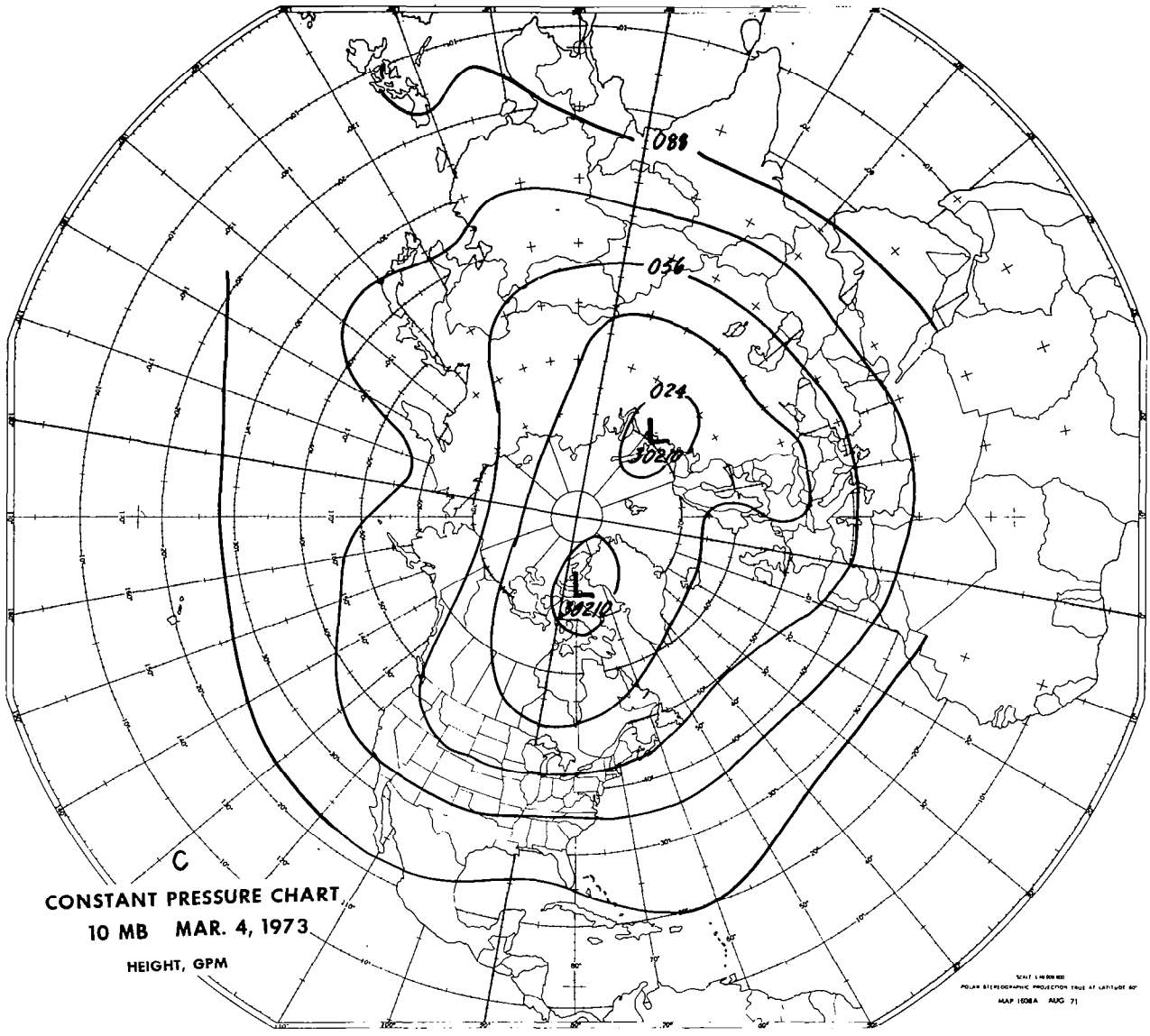

Figure 3.14c. - 10-mb map for 4 March 1973.

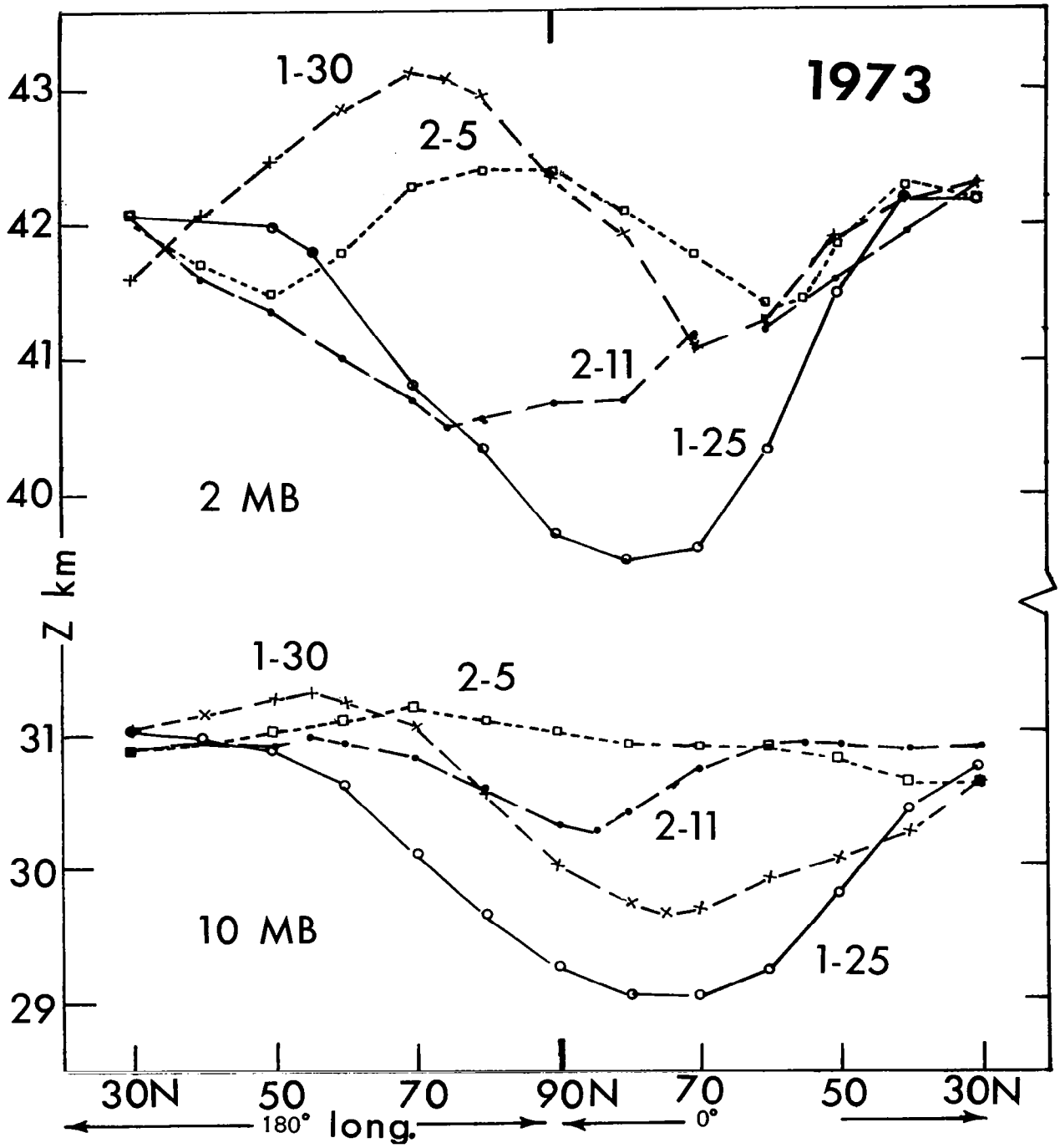

Figure 3.14d. - Height of 10- and 2-mb surfaces along 180° and Greenwich meridians on selected dates.

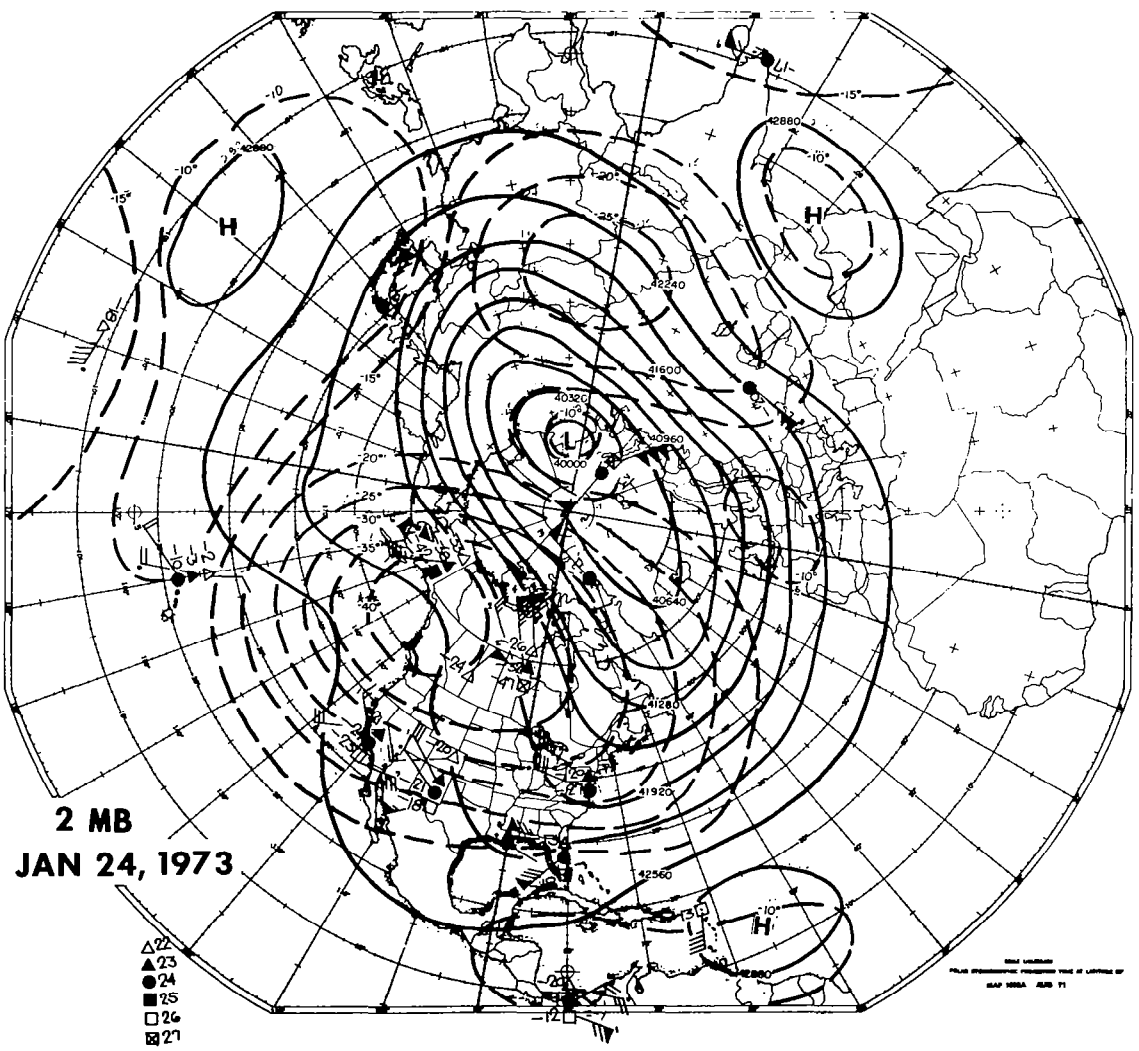

Figure 3.14e. - 2-mb map for 24 January 1973.
Explanation as for Figure 3.12c.

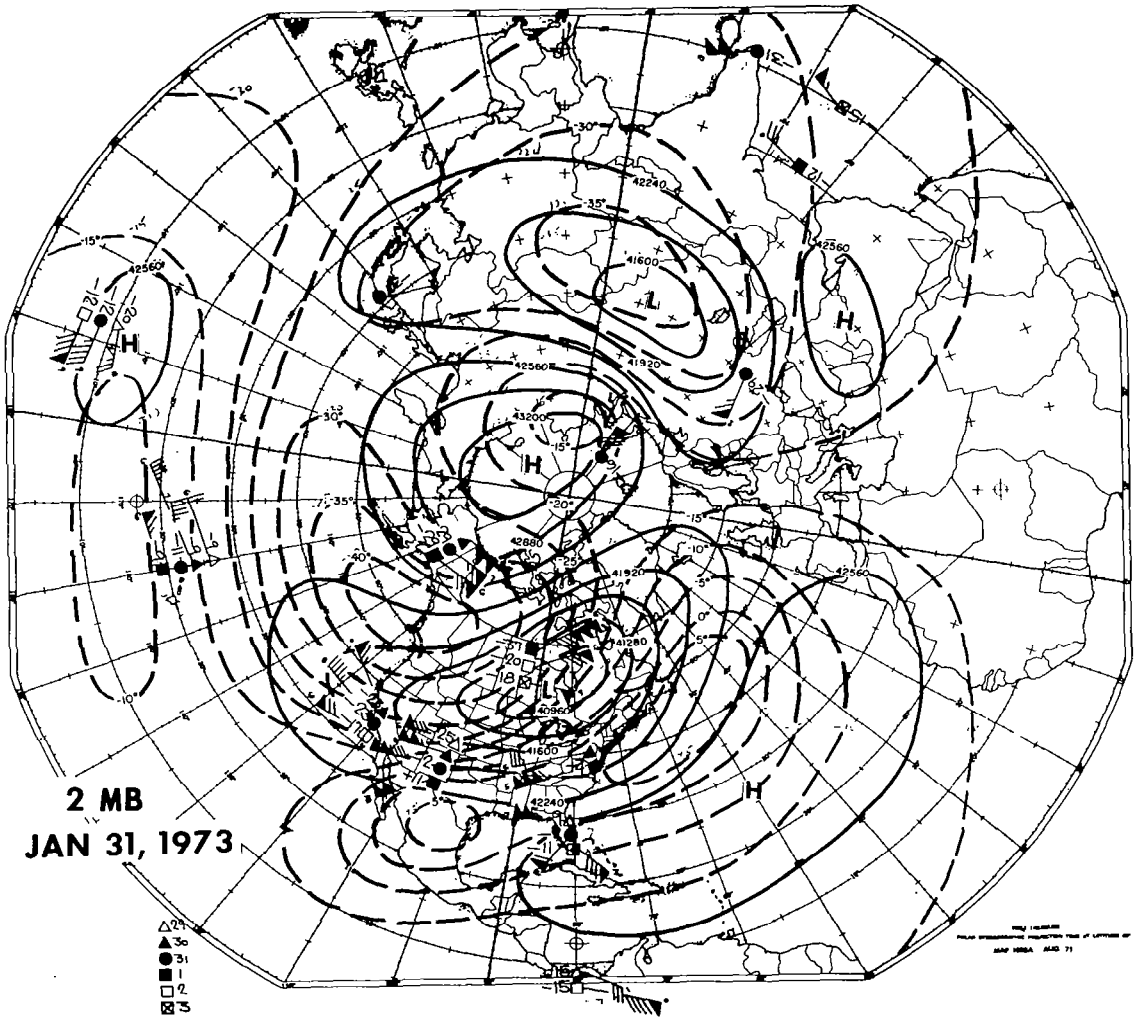

Figure 3.14f. - 2-mb map for 31 January 1973.
Explanation as for Figure 3.12c.

in the same layer. For example, the elongation of the polar vortex at 10 mb often reflects a warm anomaly in the Siberian-Aleutian area within the stratosphere, together with a tropospheric warm anomaly over North Africa and southern Europe, in the presence of a relatively "flat" stratospheric thermal field or even low stratospheric temperatures in that area. Climatological data are consistent with this concept; moreover, the data even show a strong tendency to stratospheric-tropospheric "compensation."

(3) Vortex is split. This appears to happen in two principal modes, exemplified by the warmings of 1973 and 1963. In the former case anticyclonic buildup encroaches from the North Pacific region at 10 mb (farther west above 10 mb, in accordance with the general slope westward with height of the "Aleutian" system). As warming proceeds poleward in the middle or lower stratosphere, ridging over the Arctic occurs. In 1973, as discussed earlier, such a process followed after superposition of an eastward travelling thermal wave with a quasi-stationary wave in the Siberian-Pacific region (Figures 3.6 and 3.15). In 1963, poleward anticyclonic buildup occurred from both Siberia and the North Atlantic, in accordance with the prevailing thermal patterns (Figure 3.13).

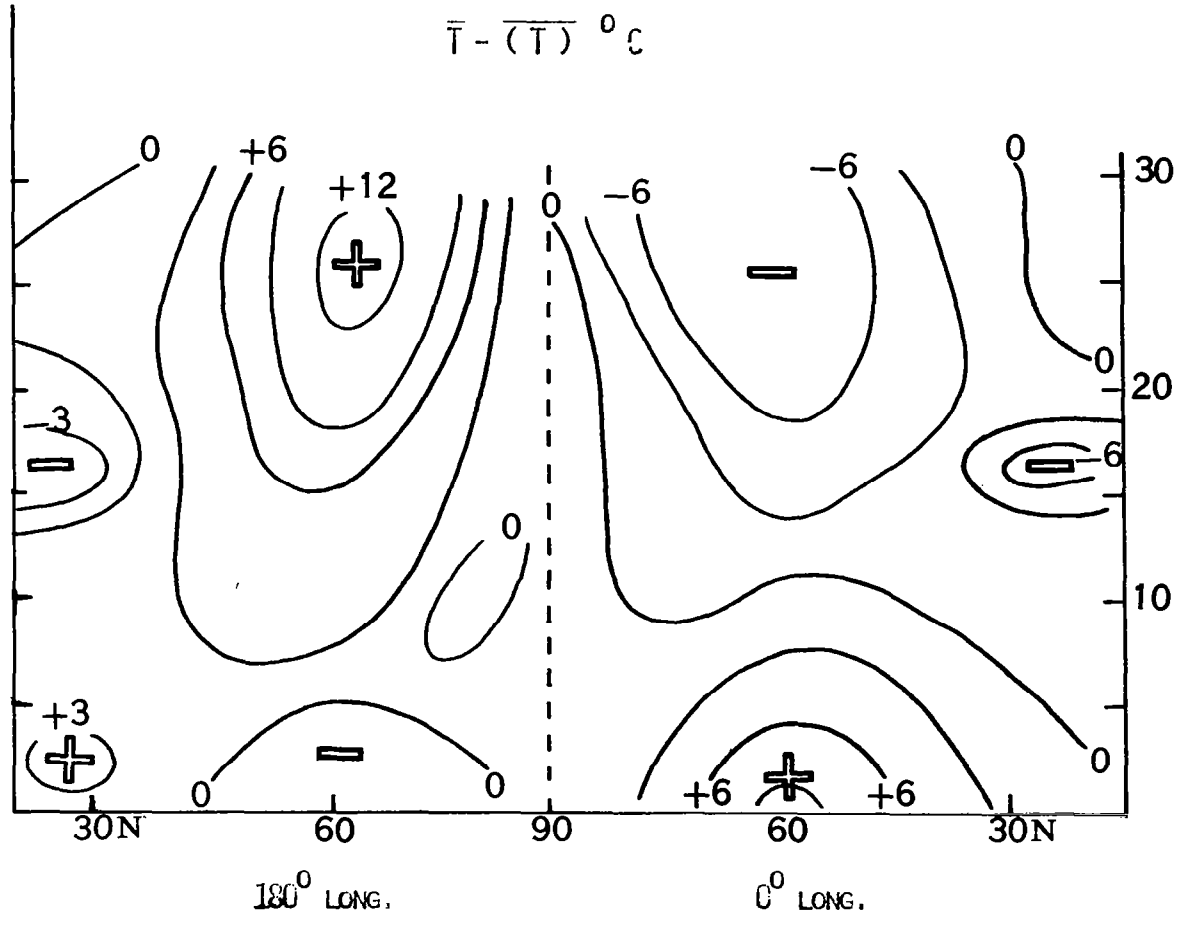

Figure 3.15. - Height structure of temperature anomalies along the 180° and Greenwich meridians, determined from departure of mean temperature at the specified longitude from the zonal mean. Constructed from data in Meteor. Abh. (Berlin Univ.), Vol. 100. (See Ref. 14.)

(4) Anticyclonic flow dominates during several days in the polar region, while residual low-pressure cells retreat to lower latitudes, "filling" somewhat. In 1963, low cells filled almost to the point of disappearing. Anticyclone system typically is established a few days earlier in the upper stratosphere, as is indicated by curves of the height of the 2 mb and 10 mb surfaces in 1973 in Figure 3.14d. Other observational data show that the anticyclone exhibits an increasingly circular shape from 30 to 2 mb.

(5) Reestablishment of polar cyclonic vortex of moderate intensity. The transition from (4) to (5) differs from case to case. In the 1973 warming the period of polar anticyclonic flow was followed by about a month of weak cyclonic flow at 10 mb depicted for March 4 in Figure 3.14c. The flow patterns at 2 mb (about 40 km) are depicted in Figures 3.14e-f for January 24-31. Note From Figure 3.14d that at 2 mb a stronger cyclonic circulation set in before mid-February (compare curves for 2-11), which was associated with rapid and strong cooling of the upper stratosphere, as depicted in Figure 8 of reference 11. In the case that a major warming begins quite late in winter, as in February - March 1974 and February - March 1975, a well-defined cyclonic vortex does not reappear at 10 mb (may reappear at higher levels), and the anticyclonic flow due to the warming may not easily be distinguished from the normal springtime reversal of the circulation.

Density Changes

During stratospheric warming very large changes in atmospheric density may occur which in extreme cases approach the magnitude of the seasonal variation. These changes are of practical importance in the evaluation of surface-heating of certain reentry vehicles, in ascertaining the mixing ratio of minor atmospheric constituents such as ozone, for determining electron production in the D- and E-regions of the ionosphere, etc. Like the pressure, the amount of density change is mainly a function of the amount of temperature change and the thickness of the perturbed layer, in accordance with the hydrostatic equation. Moreover, it has been shown analytically (refs. 45 and 46) that variations in density should closely parallel variations in pressure occurring at an altitude about one scale-height lower, and variations in temperature at about 2-3 scale-heights (about 20 km) lower. Thus a large temperature increase at 30 km should be accompanied by a large density increase near 50 km. Empirical verification was given in the above sources and in reference 47.

Illustrative data on density changes indicated by rocket observations in several warming cases were given in reference 47. Synoptic maps of density and density change to altitudes of 50 km (refs. 46 and 48) show density increases by as much as 70-80% in the polar region, in the major warmings of 1967-68 and 1973. The maps for 1973 were obtained by direct regression with VTPR satellite-measured radiances and have a standard error of 6% of the density if only radiances are used, less if a tropospheric predictor is included in the regression equations.

The Quasi-Periodic Character of Warming

The occurrence of quasi-periodic pulses of the structure of the Southern Hemisphere stratosphere was noted as early as the 1950's. In recent years the development of pulses of unusual amplitude has been depicted in detail with the aid of satellite radiation maps; and these have been identified as "minor warmings." Such pulses, recurring at about 15 days, are also evident in the Northern Hemisphere from SIRS and VTPR radiation data, and excellent corroboration has been given by van Loon et al. (ref. 49), in an analysis of several winters of 30-mb radiosonde temperatures. Moreover, Hirota and Sato (ref. 50) and Miller (ref. 51) have observed periodicities at about 15 days, the former in latitudinal means of the 30-mb zonal wind at 65°N and the latter in the 30-mb eddy kinetic energy integrated from 20°N to the Pole.

Figure 3.16 shows VTPR Channel 2 radiance variations observed at 65°N, 150°E during the 1973-74 winter. As discussed by Quiroz (ref. 11), of the 8 oscillations perceived at 65°N in the 4-month period, November 20 - March 20, two were considered to reflect important warmings. One beginning in late December indicated mid-stratospheric warming by 40-50°C in NE Siberia, but limited temperature and circulation effects at higher latitudes. The second event, beginning in mid-February, was considered a major warming, having many of the essential characteristics of the 1973 type discussed earlier in this section. Note from the North Pole trace that two bi-weekly thermal oscillations were required to eliminate or reverse the radiance gradient between 65°N and the Pole. This and similar information for other cases suggest that the full time-scale of major events is of the order of 2-6 weeks, although "sudden" and intense warming and cooling may occur within a single bi-weekly oscillation.

Since "sudden warmings" appear as a subset of the repeating oscillations in the stratospheric structure, research into the origin of these oscillations may prove to be a necessary step toward explaining the warming phenomenon.

Vertical Compensation and Propagation of Warming

Rocket data have shown that the domain of warming and cooling extends well into the mesosphere (refs. 18 and 40). They also indicate a typical vertical wavelength of about 45 km.* This is shown schematically in Figure 3.17a. Curve 1 shows a large positive departure from the reference curve at about 42.5 km, and negative departures at 20 and 65 km; the amplitude of the perturbation in reality is observed to be greatest in the upper or middle stratosphere (ref. 27). Curve 2 places the warming and cooling at

*Supporting data for this conclusion include (1) interlevel correlation coefficients calculated from wintertime rocket grenade temperature profiles and from rocketsonde profiles, and (2) individual "perturbed" profiles published by Labitzke (ref. 18). The former indicate correlations of -0.6 to -0.7 between temperatures at 25 and 45 km and temperatures at 45 and 70 km.

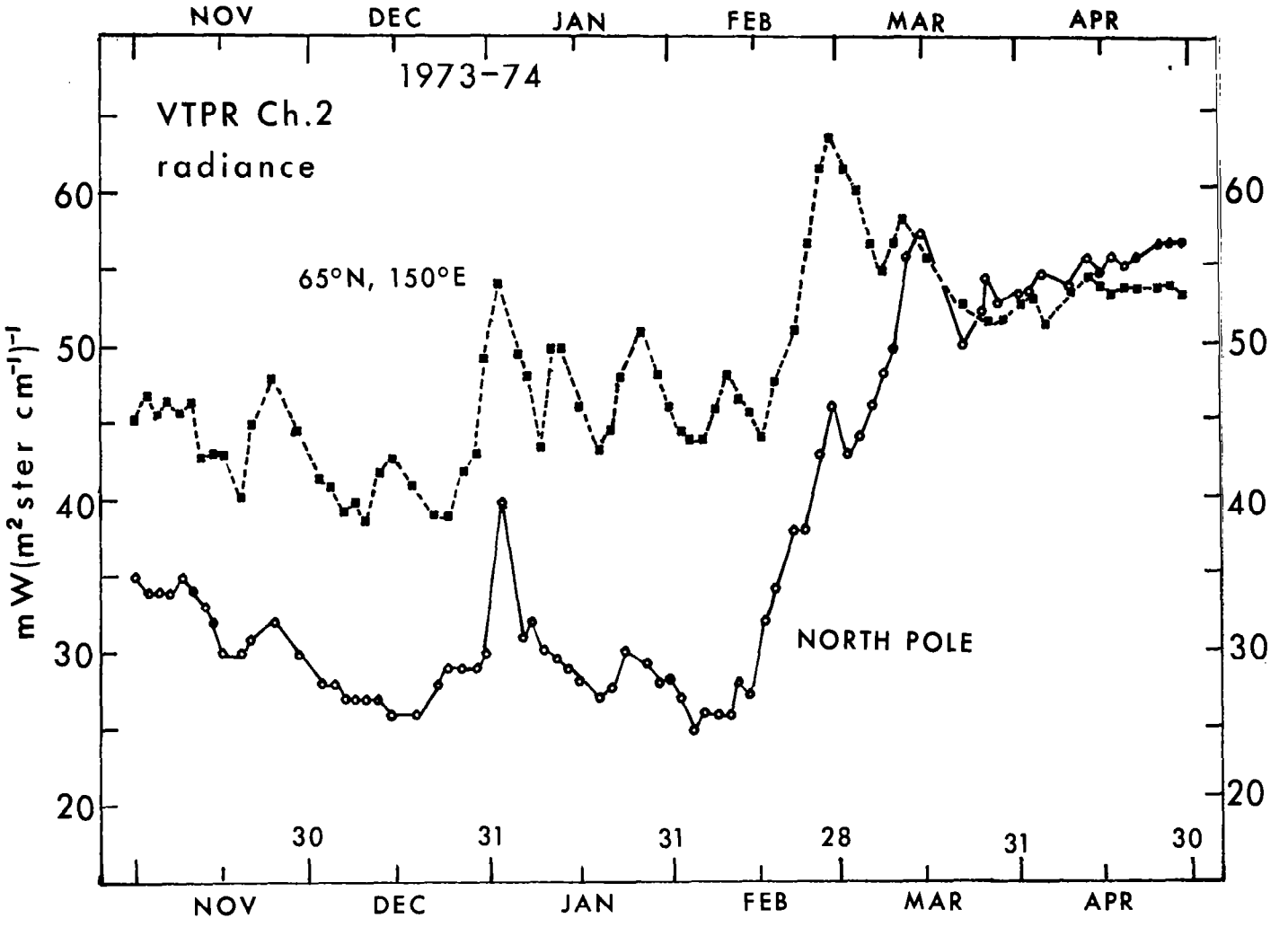

Figure 3.16. - VTPR Channel 2 radiance traces for the 1974-75 winter (ref. 39). Radiance shown is proportional to the mean temperature, 100-5 mb.

different heights. Note that warming in the lower stratosphere and cooling in the upper stratosphere, as in curve 2, should result in a nearly isothermal profile throughout the stratosphere, a condition of special interest to be discussed later. The temperature profiles at the right side of Figure 3.17a, observed during the warmings of 1969-70 and early 1973, correspond roughly to these two conditions. Between the occurrence of profiles 1 and 2 a variety of transitional profiles may be observed; and the fact that at fixed rocket stations they have been observed sequentially in time from 1 to 2 has been interpreted by some investigators as downward propagation of warming. However, the situation is rather complicated, as we shall now try to show.

Figures 3.17b-c, constructed from rocket temperature soundings (ref. 27), show evidence of warming at successively lower altitudes during a minor warming in January 1967 (Figure 3.17b) and during a major warming in late December 1967 - early January 1968 (Figure 3.17c). The question of the vertical propagation of warming is of interest in possibly providing clues as to the cause of warming. In most recent work it has been emphasized that upward-propagating planetary waves, along with an enhancement of the kinetic energy of the stratosphere due to the upward flux of geopotential (see Section 2), are probably vital features in the development of stratospheric warmings. Such results of course do not preclude the downward phase-propagation of the temperature waves themselves.

The satellite data of recent years offer a new means for investigating this question. Careful examination of radiance increases in different stratospheric channels shows that within the period of two weeks, at the time of a major pulse, warming develops nearly simultaneously at different altitudes of the stratosphere, in the upper stratosphere in one location, and in the lower stratosphere at some longitude farther east. This result, however, may simply arise from superposition of thermal waves with maximum amplitude at different altitudes. The Aleutian quasi-stationary system, for example, is known to have maximum amplitude in the middle stratosphere, near 30 mb. The traveling thermal waves outlined by the SIRS and VTPR stratospheric radiation data indicate a contribution usually centered at higher altitudes, as they approach from European longitudes. (This concept does not preclude the prevailing theoretical expectancy of planetary waves forced from below.) Once a reinforced standing wave is displaced from its preferred location, as has been observed in recent major warmings, the slope of the system can possibly account for the indication of downward (or upward) propagation of warming as the system moves over a fixed location. Evidently, more study of this question is needed.

The Vertical Motion

The field of vertical motion associated with stratospheric warmings is of interest for various reasons. Knowledge of the prevailing and perturbed vertical motions is essential for understanding the meridional circulation and for evaluating vertical and horizontal transport processes. Moreover, the vertical motion is a vital link in the explanation of local sudden warming. Consider the thermodynamic equation for vertical motion,

$$w = -(\Gamma-\gamma)^{-1}\underset{(1)}{(\partial T/\partial t} + \underset{(2)}{\vec{V}\cdot\nabla_H T} - \underset{(3)}{c_p^{-1}(dh/dt)}),$$

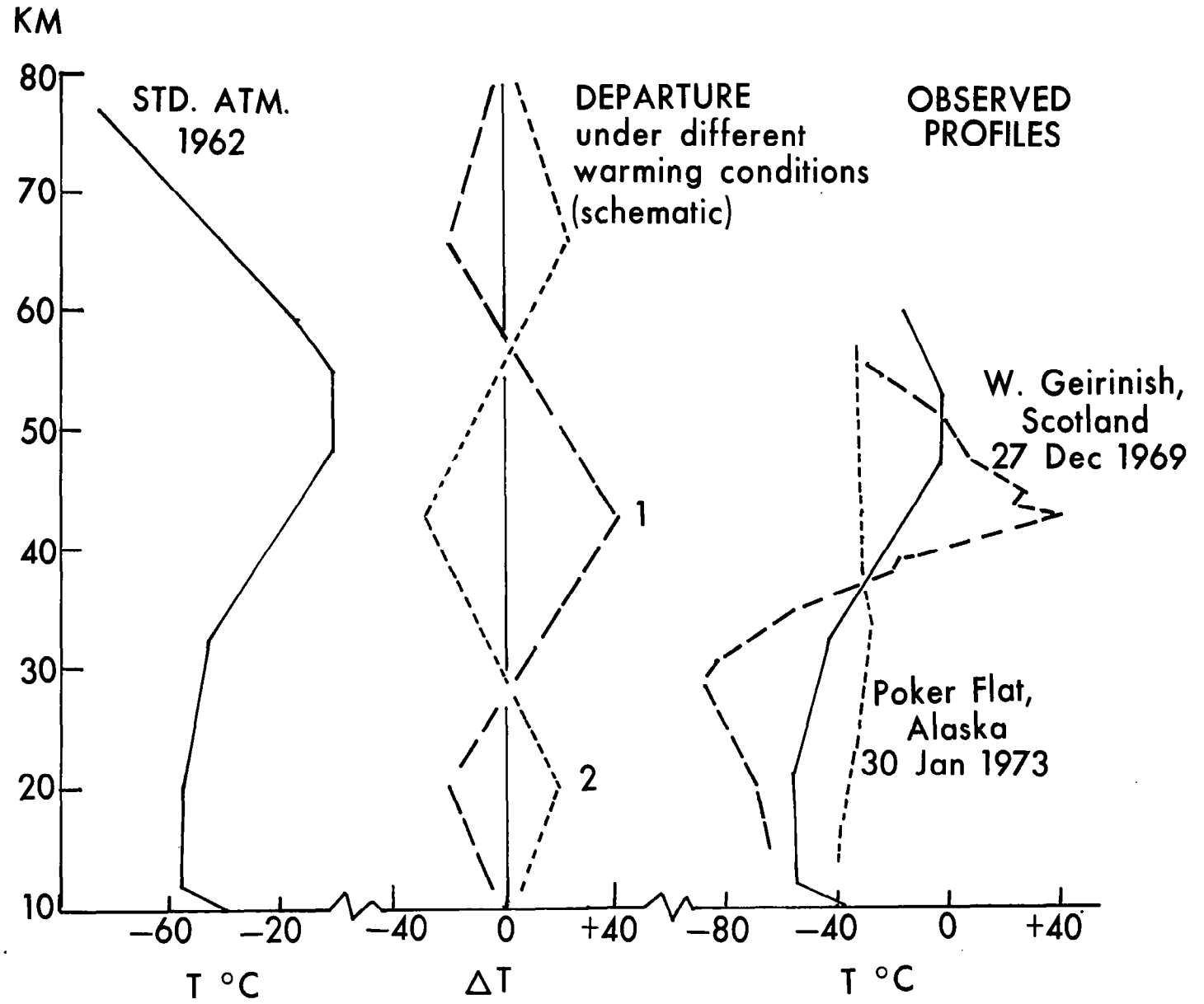

Figure 3.17a. - Details of vertical temperature structure (see text). Source: Ref. 41.

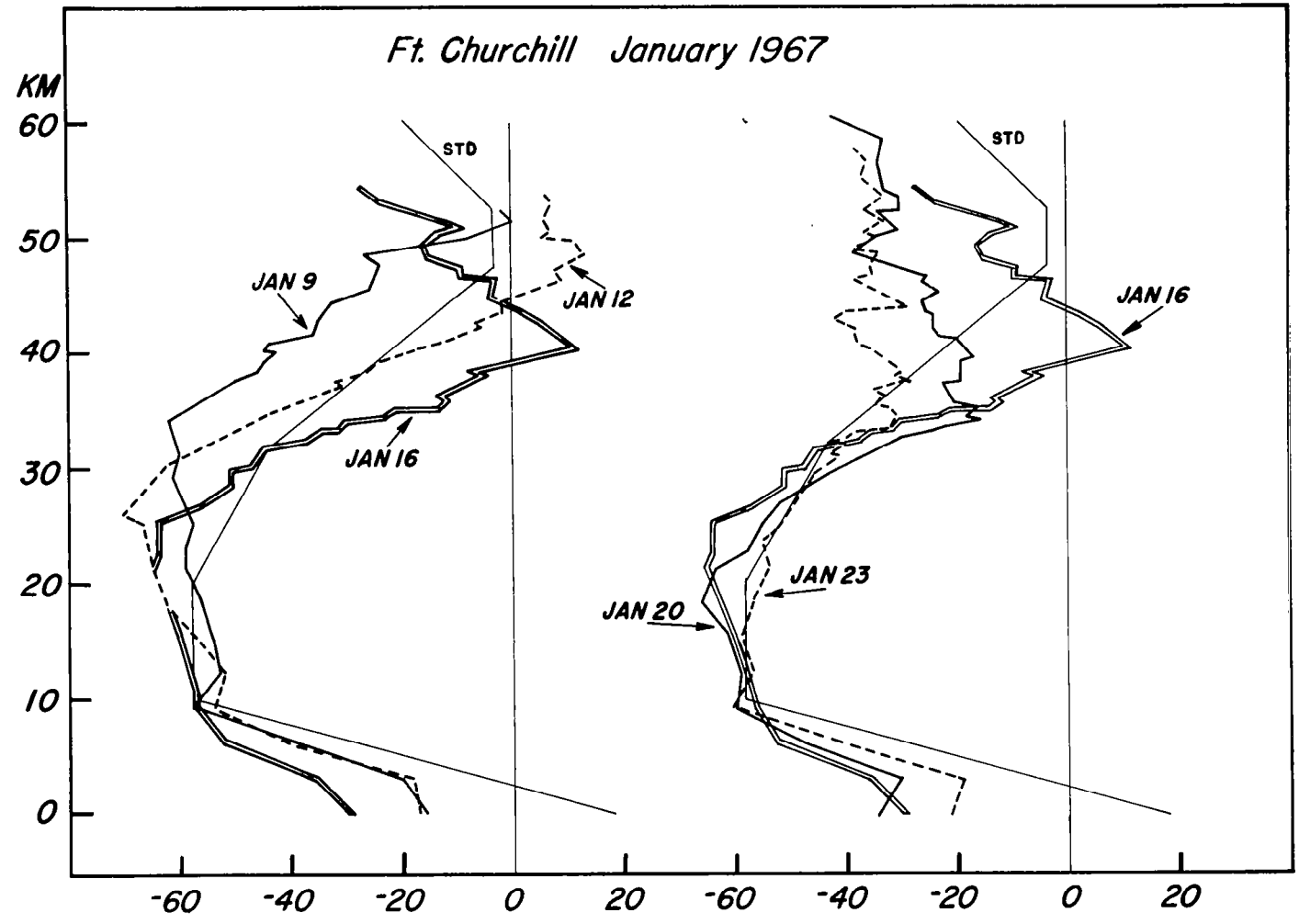

Figure 3.17b. - Temperature data from rocket soundings at Fort Churchill, Canada, suggesting downward propagation of warming. Source: Ref. 27.

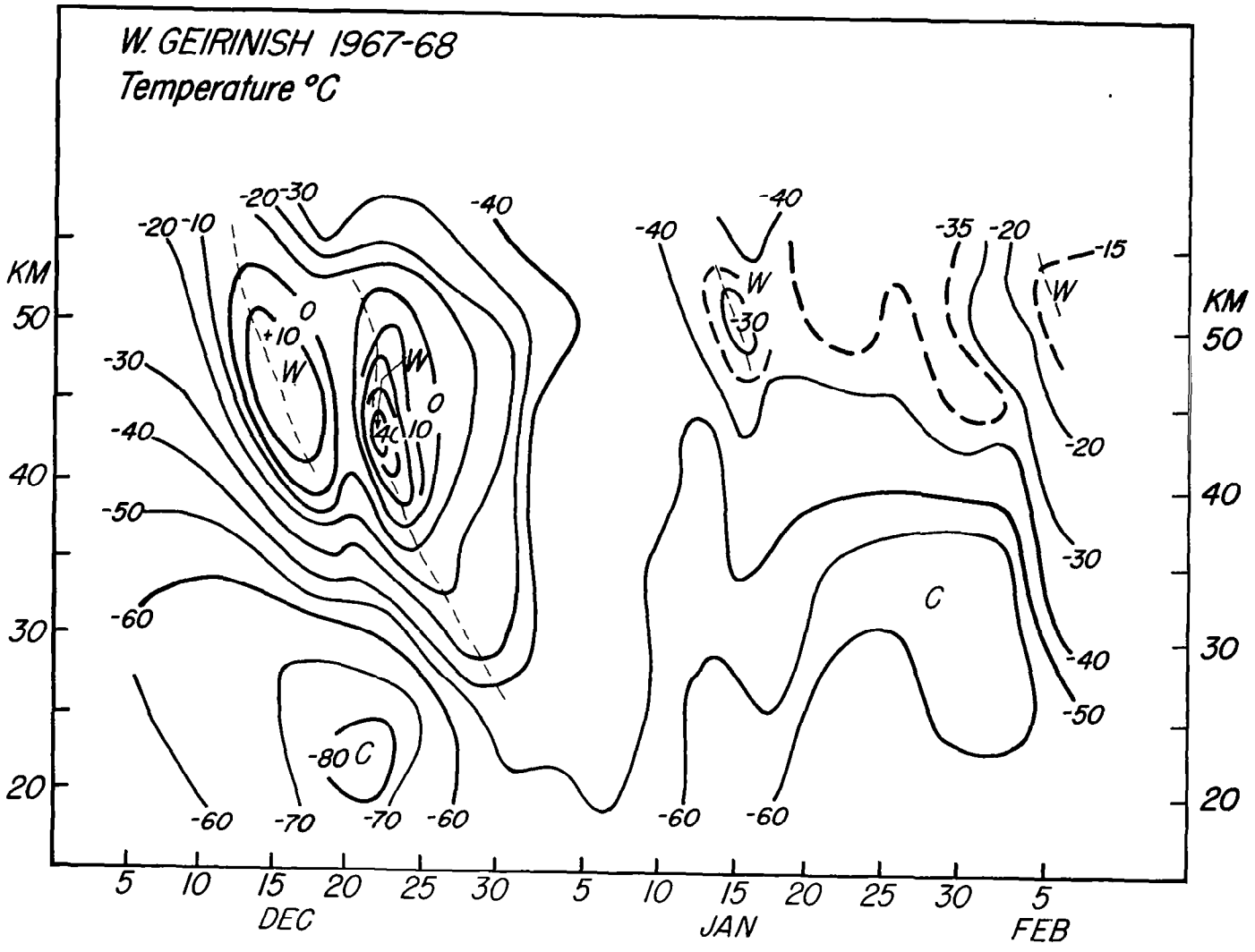

Figure 3.17c. - Temperature data from rocket soundings at West Geirinish, Scotland, suggesting downward propagation of warming. Source: Ref. 27.

where $(\Gamma-\gamma)$, the difference of the dry adiabatic and ambient lapse rates, is of order 10^{-4} deg/cm; (1) is the local temperature change, (2) the horizontal thermal advection, and (3) the diabatic heating. For winter and high latitudes, term (3) ordinarily ranges from about -1 deg/day in the lower stratosphere to -3 deg/day in the upper stratosphere, and during warming events can be shown to be small compared to (1) and (2). If (2) is also small, then the local temperature change must be explained essentially by adiabatic vertical motion (subsidence, if there is warming). If (2) dominates in importance, then the field of vertical motion is largely determined by the orientation of the height (pressure) field relative to the thermal pattern (see discussion below).

A summary of results of vertical motion calculations made by various authors for several warmings events is given in the Appendix. (This summary includes a simulated warming (Newson).) It is immediately evident that (1) there is a striking lack of uniformity with respect to the time, area, and height resolution of the calculations; and (2) not one truly comprehensive set of results has been published for a major warming event. Some authors have used the "omega equation," but it has yielded results that are similar to those given by the simpler equation written above. The error due to the neglect or uncertain evaluation of the diabatic heating is of the order of 1 cm/sec or less. Several authors (e.g., refs. 40, 50, and 52) have emphasized the difficulty of accurate evaluation of the advection term.

Some of the findings are as follows:

(1) Strong rising motions occur in high latitudes in response to strong horizontal advection from subpolar latitudes (refs. 40, 43, 53). Newson (ref. 41) calculated, on one day, magnitudes to about 20 cm/sec, at 44 km. Quiroz (ref. 38) obtained a maximum point value of 60 cm/sec, near 40 km, which may be unrepresentative of any substantial area.

(2) In medium or medium-high latitudes, subsidence has been considered by come authors as leading to local warming. Newson (ref. 43), on one day, found generally subsiding motions near 50°N with magnitudes up to 15 cm/sec at 44 km. At 41 km, Miller (ref. 54) found a downward value of 9 cm/sec in a 2-day sample during a minor warming.

(3) At radiosonde altitudes maximum rising or descending motions of about 2-8 cm/sec have been found by various authors.

(4) Some authors have suggested that there is a "typical" distribution with respect to pressure systems (e.g., downward west of a trough, upward east of a trough, as reported by Craig and Lateef (ref. 52) for the early stage of the 1957 warming. However, harmonic analysis of the vertical velocity and height fields (refs. 37, 55) showed precisely the opposite result, for waves 1 and 2. In reality, for the case that horizontal advection largely determines the vertical motion, various distributions of the latter may be expected. This is due to the fact that pressure and thermal patterns at a given stratospheric level need not have the same wavenumber, nor need they be evenly distributed in view of the role of the earth's orography in stratospheric processes.

(5) The calculations have thus far neglected conditions near the Equator (where they are especially difficult to make). Data for very low latitudes would be of interest because of the apparent tropical-polar interactions observed.

Warmings in the Southern Hemisphere

Various authors have alluded to multiple pulses in the Antarctic winter thermal structure. Even in early literature on the Antarctic stratosphere, some of these pulses were identified as "minor warmings." The final warmings of spring have been documented by Phillpot (ref. 56) and others. Only rather incomplete descriptions of mid-winter events have been possible, however, since Southern Hemisphere radiosonde data are usually not available for levels above 50 mb (ref. 56) and rocket data have been fragmentary (ref. 57). Preliminary documentation of these events based on satellite infrared measurements was first accomplished from TIROS 7 data (ref. 58) but thorough documentation was not possible until after the introduction of multi-channel radiometers such as the SIRS in 1969 and the SCR in 1970.

The oscillatory structure of the Southern Hemisphere stratosphere is vividly reflected in Figure 3.18, showing traces of the VTPR Channel 1 (I1) mean zonal radiance for equatorial (7.5°S), middle (52.5°S) and polar (82.5°S) latitudes, during the 1975 winter. Recall that I1 is proportional to $\overline{T}$ (100-2 mb). The average time interval between the principal radiance maxima at 82.5°S on July 29, August 16, 28, and September 9 and 29 is 15.5 days. Note the negative correlation between radiances at 7.5°S and 52.5°S. More significant probably is the lag in radiance maxima from low to high latitudes, about 6-8 days. This is consistent with our general observations for the Northern Hemisphere concerning the contribution of traveling thermal waves of low-latitude origin (ref. 11) to the development of warmings in subpolar latitudes.

A further illustration of these effects is suggested in Figure 3.19, depicting the gradual amplification of I1 (wave 1) at successively higher latitudes in the oscillation of late July 1975. The interpretation of such data in terms of stationary and traveling components requires special care.

In terms of synoptic map fields, the development of warmings in the Southern Hemisphere appear quite similar to the processes noted for the Northern Hemisphere (ref. 59). One notable difference is the indication of weaker standing components in the Southern Hemisphere, with the superposition of traveling and stationary waves resulting in lower radiance maxima in the combined systems during winter. Another difference is the limited poleward penetration of high radiance centers, which tend to retain a zonal trajectory except (1) during the final springtime warming and (2) at the highest levels, represented, for example, by SCR Channel A (Nimbus 4) or Channel B12 (Nimbus 5). Indeed, the repetitive incursion to south polar latitudes of high radiance values in these channels indicates a mean thermal state in the upper Antarctic stratosphere which after midwinter is warmer than in the Northern Hemisphere (ref. 60). For those interested in individual warming cases described with the aid of satellite data, such sources as the following may be consulted: refs. 9, 10, 61, 62, 63, and 64.

While the warmings referred to above can be shown to result in some distortion of the Antarctic polar vortex, a vortex breakdown has never been observed. Reasons for this failure have been discussed by Quiroz (ref. 59).

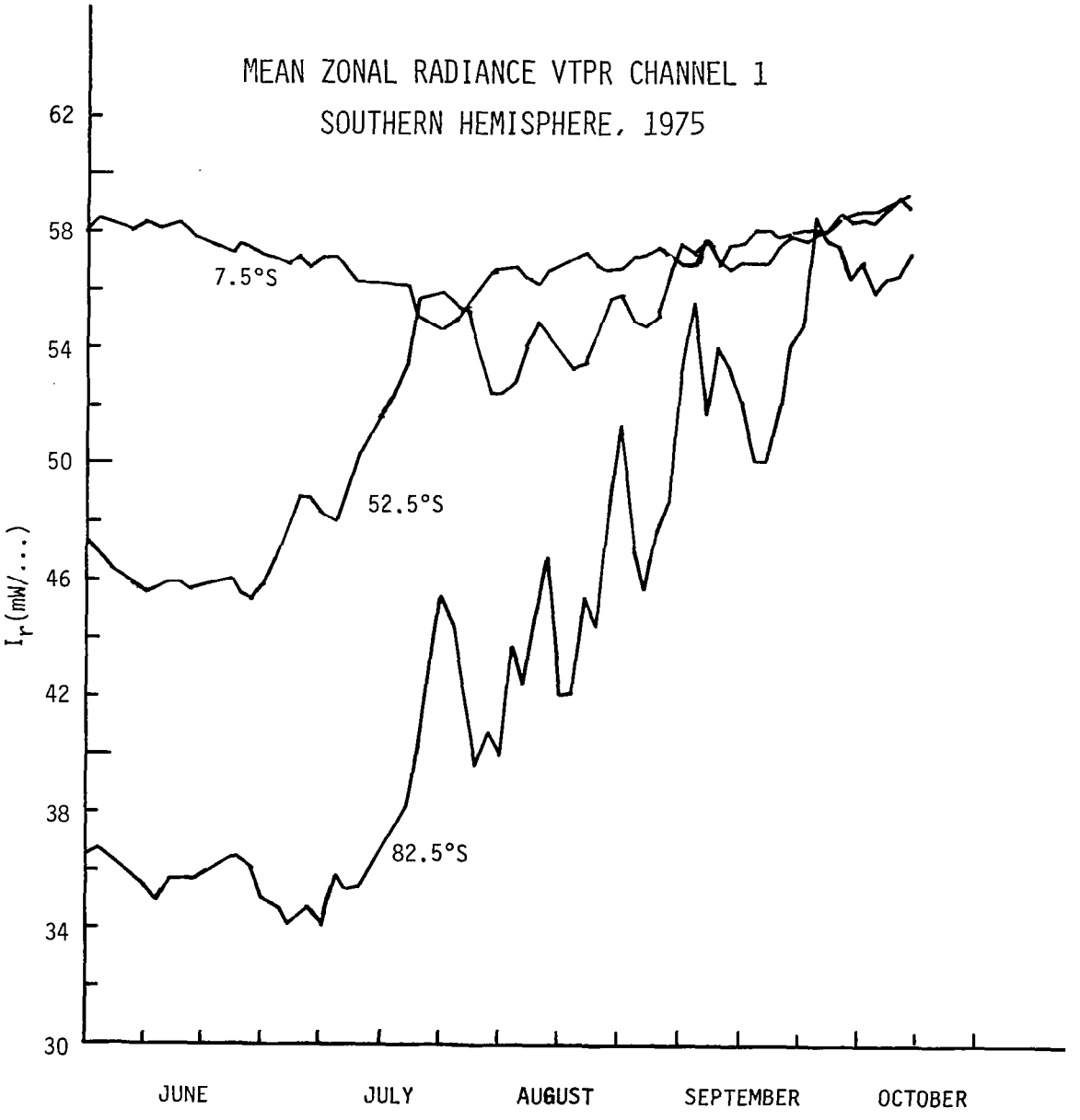

Figure 3.18. - Mean zonal radiance, $mW(m^2\ sr\ cm^{-1})^{-1}$, measured by VTPR Channel 1 during the 1975 Southern Hemisphere winter.

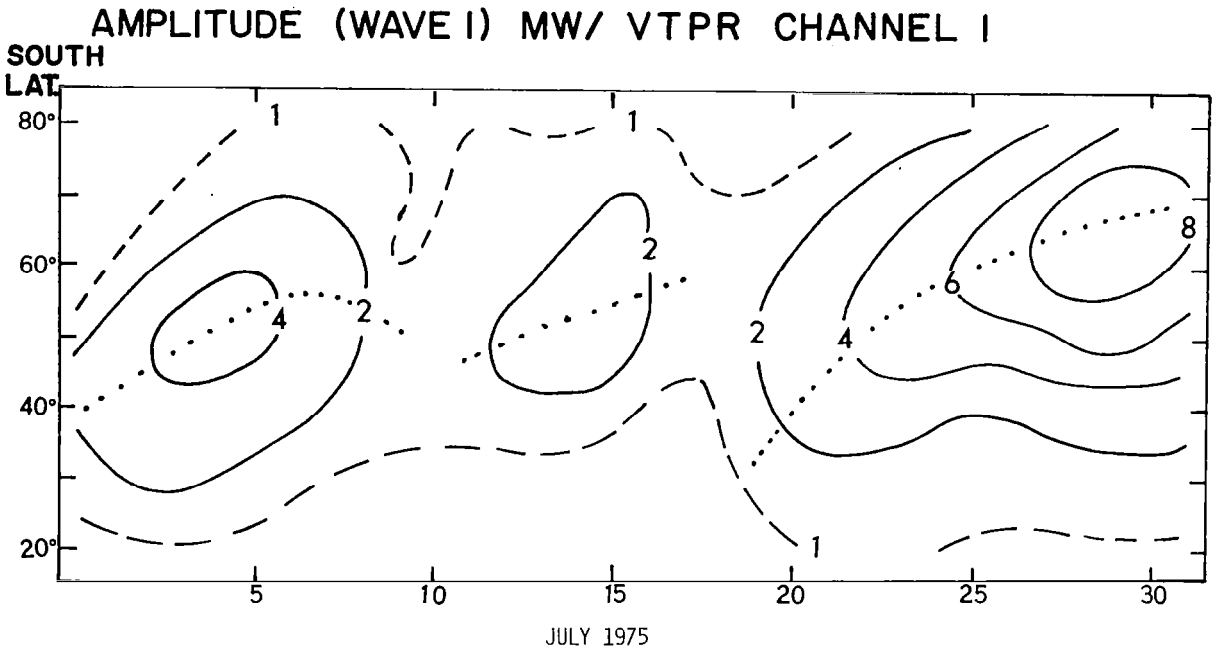

Figure 3.19. - Amplitude of wavenumber 1 in radiance (VTPR Channel 1), 20-80°S, July 1975.

Some Current Work

Beginning with the winter of 1975-76, the Upper Air Branch of the National Meteorological Center has been studying planetary wave developments in both the troposphere and the stratosphere of the Northern Hemisphere. Amplitudes and phases of zonal waves 1-4 have been examined, together with mean zonal fields. These data have been generated for the heights of the pressure surfaces and for temperature, the latter determined both from conventional maps to 10 mb and from satellite radiation measurements. Slope modulation and retrogressive and interactive properties in the planetary waves have been noted as significant in stratospheric warming developments. As with the model simulations mentioned above, an ultimate task is to identify the nature of the forcing accounting for planetary-wave amplification.

ENERGETICS - TROPOSPHERIC-STRATOSPHERIC INTERACTION

Background

Much of the early theoretical work on stratospheric warmings (STRATWARMS) dealt with tests for various kinds of dynamic instability--in particular, for baroclinic and barotropic instability. Perhaps the reason for this emphasis was the appearance of suddenness in the warmings--temperature increases of as much as 20 Celsius degrees per day at 10 mb at some locations (e.g., at Mould Bay, N.W.T., during the January 1963 warming). It is true that temperature changes averaged over the polar cap are not generally as dramatic, and a major warming tends to pass through its various stages of evolution (amplification, movement, decay) in a period of three weeks or more. Nevertheless, the sharp temperature changes in some locations at the onset of warming led some researchers to draw an analogy between the development of stratospheric warmings and the phenomenon of tropospheric cyclogenesis. The latter had been largely explained as a baroclinic instability phenomenon; it was hoped that similar explanations for STRATWARMS would be forthcoming.

A brief account of barotropic and baroclinic states and associated phenomena will now be given, to facilitate the ensuing discussion.

A barotropic state is one in which density is a function of pressure only, so there can be no horizontal temperature gradients on isobaric surfaces and consequently no vertical wind shear. Thus the Richardson number (ratio of the static stability to the square of the vertical wind shear) is not defined, though in practice a large Richardson number is said to characterize a "highly barotropic" atmosphere. Barotropy is, of course, an ideal state which is never perfectly attained by the real atmosphere.

Barotropic instability may be defined in terms of energy transformations which accompany any development in a barotropic atmosphere; or it may be defined as a state of the atmosphere in which conditions are conducive to the growth of disturbances in spite of the absence of vertical wind shear.

Whereas temperature gradients on isobaric surfaces must be present for the development of available potential energy, which is essential to the atmospheric overturning (warm air rising and cold air sinking) accompanying baroclinic development, these gradients are absent in a barotropic atmosphere. Thus the only source of energy for barotropic development is the basic horizontal current. As many authors have shown (e.g., ref. 65), a necessary condition for barotropic instability is that the gradient of the absolute vorticity must vanish somewhere in the atmospheric flow. This condition must be maintained in order that barotropic waves continue to grow at the expense of the basic horizontal current.

Barotropic instability phenomena are thus represented as involving a transfer of zonal kinetic energy to eddy kinetic energy. While this representation may be adequate in some cases, it seems doubtful that it is satisfactory for a study of instability in the polar-night stratospheric vortex. The reason for this is that the polar-night vortex is highly eccentric, giving rise to a substantial contribution to total kinetic

energy by wave number one. The "basic current" in this case may be better represented by wave one than by wave zero, and the flow of energy would occur out of wave one into the larger wave numbers.

The essential difference between barotropic and baroclinic development is that the former involves only transformations of kinetic energy, whereas the latter involves conversion of available potential energy to kinetic energy, as warm air rises and cold air sinks.

Vertical motion is paramount in any consideration of baroclinic and hydrostatic energy transformations, as the conversion from potential to kinetic energy must take place through terms of type

$$Rg^{-1}\int_{o}^{\overline{P}o} p^{-1}\ \overline{T\omega}\ dp, \text{ where } \omega = \frac{dp}{dt},$$

T = temperature, p = pressure.

These concepts can be made clearer, perhaps, by making reference to the Lorenz-type of energy-flow box diagram for the entire atmosphere:

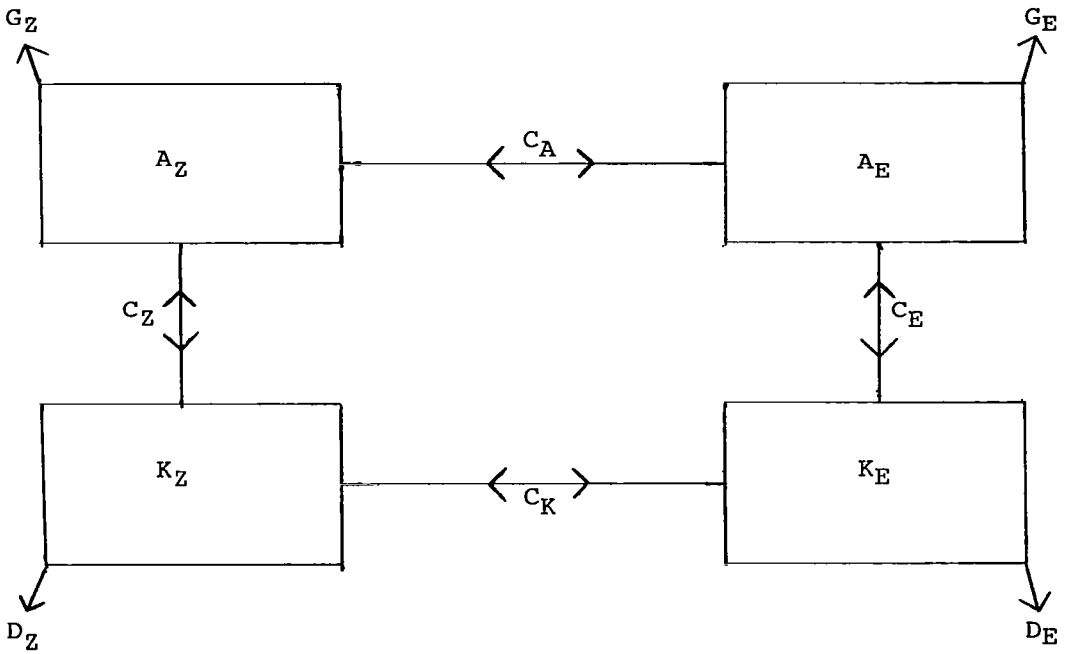

Figure 4.1.

Here, A_Z = zonal available potential energy, A_E = eddy available potential energy, K_Z = zonal kinetic energy, K_E = eddy kinetic energy, G_Z = generation of zonal available potential energy, G_E = generation of eddy available potential energy, D_Z = dissipation of zonal kinetic energy, D_E = dissipation of eddy kinetic energy, C_Z = conversion between zonal available potential energy and zonal kinetic energy, C_E = conversion between eddy available

potential energy and eddy kinetic energy, C_A = conversion between zonal available potential energy and eddy available potential energy, and C_K = conversion between zonal kinetic energy and eddy kinetic energy.

Examples will be given later with actual calculations shown for the various entries in this diagram. For the present discussion, it suffices perhaps to point out that the conversion terms C_A, C_E, C_K, and C_Z are of crucial importance, since they represent the direction of energy transformation, and give an indication of the contribution of each type of energy to the total process. A_Z, A_E, K_E, and K_Z are "storage terms"; sometimes ΔA_Z, etc. are computed over a period of several days and then compared with calculations for the amount of input and output as given by the C-terms and the G- and D-terms. While this representation is valid for the atmosphere as a whole, obviously it must be modified for application to a restricted portion of the atmosphere such as the stratosphere, so as to show the influence of boundary terms.

In a baroclinic development, with generation, dissipation, and boundary terms neglected for simplicity, the box-diagram might look like this:

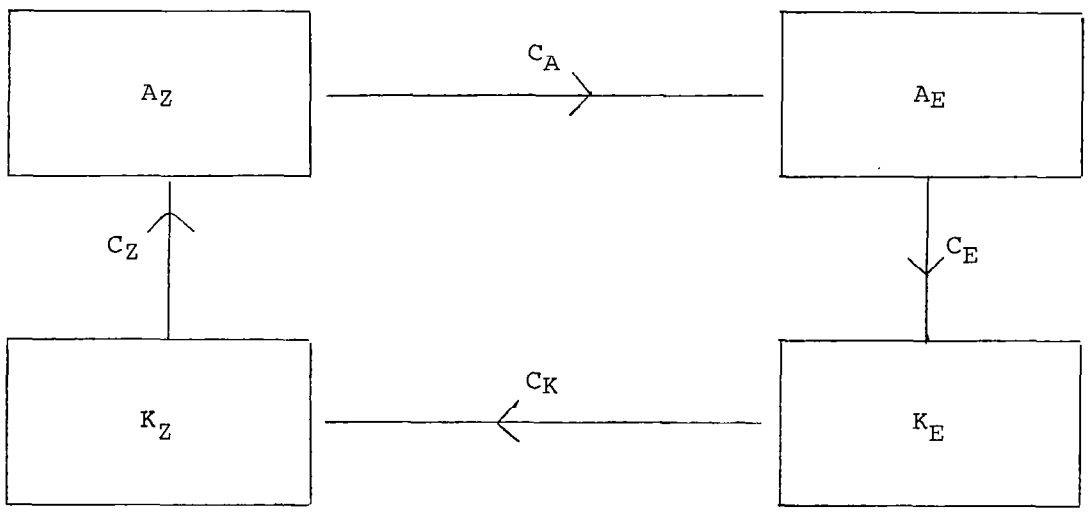

BAROCLINIC

Figure 4.2.

Indeed this kind of clockwise circuit describes the major processes of tropospheric circulation*: the conversion of A_Z to A_E (i.e., the contribution of small-scale perturbations of the temperature field to the total variance becoming larger than that of the zonally-averaged field); conversion of A_E to K_E, as warm air rises and cold air sinks, and the energy thus released is fed into the kinetic energy of the eddies; and, finally, the conversion of K_E to K_Z, whereby the strong current of mid-latitude westerlies (including the jet stream) is maintained. While it is misleading

*Tropospheric processes are used to illustrate the energy-cycle mainly because these processes are better known than stratospheric processes.

perhaps to try to separate the conversion processes in time, it may be helpful to think of C_A as corresponding to frontogenesis; of C_E as corresponding to cyclogenesis; and of C_K as the process responsible for the formation of jet streams.

What we think of as a typical barotropic development can be represented by a box diagram as follows:

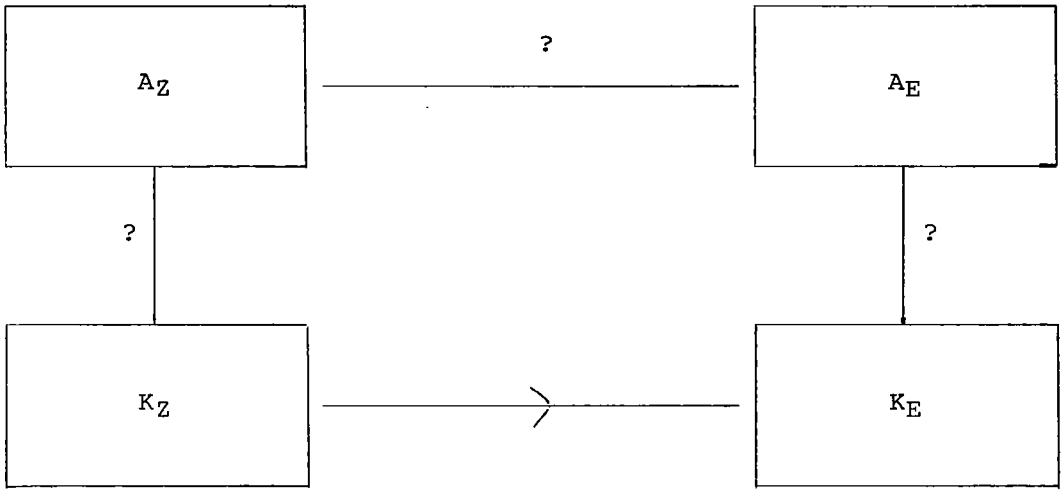

BAROTROPIC

Figure 4.3.

No arrows are drawn along the lines connecting the A- and K-boxes, since such transformations are alien to barotropic processes.

In light of what we have said above concerning the predominance of wave 1, at times, in the polar stratosphere, it might be advisable to construct diagrams such as this:

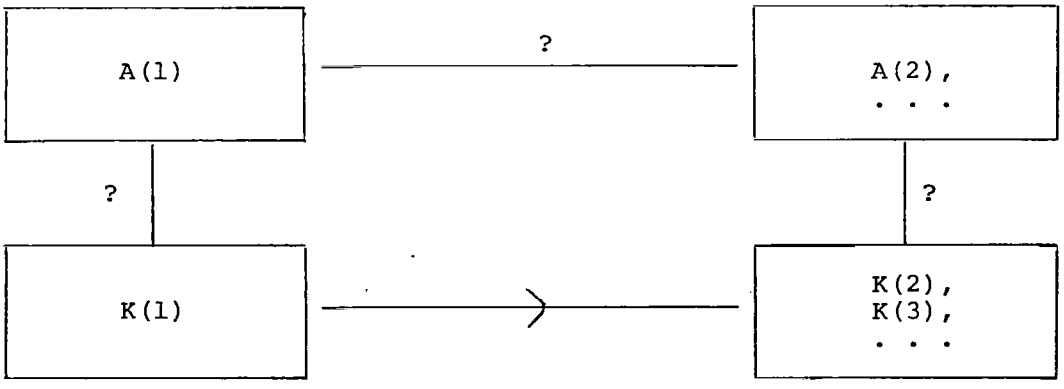

Figure 4.4.

The Energy Equations

For the sake of completeness, the basic equations for energy transformation will be given here. Reference 66 contains a more detailed account of the mathematical formalism, along with its physical interpretation.

The equations listed below are those for A_Z, A_E, K_Z, K_E, C_A, C_K, C_Z, C_E, G_Z, G_E, D_Z, and D_E discussed above in connection with the Lorenz-type box diagrams. Also we shall give an approximation for the upward flux of geopotential.

All the symbols in the following expressions have their usual meteorological denotation and/or connotation. We let [X] represent a zonal average of the parameter X, X* the deviation from this zonal average; thus

$$X = [X] + X^*;$$

similarly, we let $\overline{X}$ represent a long-term average of X, and X′ the deviation from this:

$$X = \overline{X} + X'$$

{X} denotes the total amount of X within the atmosphere. $\tilde{X}$ denotes an average over an entire isobaric surface, X″ a departure from this average. $\underset{\sim}{X}$ denotes a vector quantity.

The following expressions have been established (see ref. 66):

(1) $$A_Z = (1/2)c_p\{\Gamma_d(\Gamma_d-\tilde{\Gamma})^{-1}\ \tilde{T}^{-1}[T]''^2\}$$

and

(2) $$A_E = (1/2)c_p\{\Gamma_d(\Gamma_d-\tilde{\Gamma})^{-1}\ \tilde{T}^{-1}\ T^{*2}\},$$

where

$$\Gamma = -\frac{\partial T}{\partial Z} \text{ and } \Gamma_d = \frac{g}{c_p}$$

(3) $$K_Z = (1/2)\{[\underset{\sim}{V}] \cdot [\underset{\sim}{V}]\}$$

(4) $$K_E = (1/2)[\underset{\sim}{V}^* \cdot \underset{\sim}{V}^*]$$

(5) $$C_A = -c_p\{\tilde{T}^{-1}\ \tilde{\theta}([T^*v^*]''\ \frac{1}{a}\frac{\partial}{\partial\phi} + [T^*\omega^*]\frac{\partial}{\partial\phi_p})\cdot(\Gamma_d(\Gamma_d-\Gamma)^{-1}\ \tilde{\theta}^{-1}[T]'')\}$$

(6) $$C_K = -\{a\cos\phi\ ([u^*v^*]\ \frac{1}{a}\frac{\partial}{\partial\phi} + [u^*\omega^*]\frac{\partial}{\partial p})\left[\frac{u}{a\cos\phi}\right]$$

$$-\{a\cos\phi\ ([v^{*2}]\ \frac{1}{a}\frac{\partial}{\partial\phi} + [v^*\omega^*]\frac{\partial}{\partial p}$$

$$+\frac{\tan\phi}{a}[u^{*2}+v^{*2}])\left[\frac{v}{a\cos\phi}\right]\}$$

$$(7) \quad C_Z = -\{[\omega]\ [\alpha]\}$$

$$(8) \quad C_E = -\{\omega^*\alpha^*\}$$

$$(9) \quad G_Z = \{\Gamma_d(\Gamma_d-\tilde{\Gamma})^{-1}\ \tilde{T}^{-1}\ [Q]''\ [T'']\}$$

$$(10) \quad G_E = \{\Gamma_d(\Gamma_d-\tilde{\Gamma})^{-1}\ \tilde{T}^{-1}\ Q^*\ T^*\}$$

$$(11) \quad D_Z = -\{[\underset{\sim}{V}] \cdot [\underset{\sim}{F}]\}$$

$$(12) \quad D_E = -\{\underset{\sim}{V}^* \cdot \underset{\sim}{F}^*\}$$

To derive an expression for the upward flux of geopotential from the troposphere to the lower stratosphere (usually the boundary is taken as 100 mb, so that the expression represents the transfer of kinetic energy), we start with the thermodynamic energy equation

$$(13) \quad \frac{\partial\theta}{\partial t} + \frac{u}{a\cos\phi}\frac{\partial\theta}{\partial\lambda} + \frac{v}{a}\frac{\partial\theta}{\partial\phi} + \omega\ \frac{\partial\theta}{\partial p} = h,$$

where

$$h = c_p^{-1}\left(\frac{dQ}{dt}\right)p_o^{\kappa}p^{-\kappa}.$$

Assuming geostrophic motion and $[\omega]=0$, and expanding (13) in terms of zonal averages, we obtain:

$$(14) \quad [\omega^*z^*] = \left(\frac{\partial[\theta]}{\partial p}\right)^{-1}\{[u]\ \frac{f}{g}[v^*\theta^*] - \left(\frac{\partial\theta}{\partial t}z^*\right) + [h^*z^*]\}$$

Since it has been found that the second two terms on the right are negligible, we get

$$(15) \quad [\omega^*z^*] = \left(\frac{\partial[\theta]}{\partial p}\right)^{-1}\{[u]\ \frac{f}{g}[v^*\theta^*]\}$$

for our approximation. This equation was first derived through different methods and within a different context by Eliassen and Palm (ref. 67). (It should be noted that in this section 'ϕ' denotes latitude, 'θ' denotes potential temperature, whereas elsewhere in this monograph 'ϕ' denotes geopotential height, 'θ' denotes latitude.)

Results of Energy Calculations

Table 4.1 represents an attempt to summarize some of the research in stratospheric energetics accomplished over the past 15 years. This table is not intended to be comprehensive; but it does include some information about the most important papers, those which are most often cited in the literature (e.g., refs. 6, 8, 68, 69, 70, and 71).

TABLE 4.1.

AUTHOR	PERIOD COVERED	AREA COVERED
(a) Jensen (1960)	Jan 58; Apr 58	20°-90°N
(b) Teweles (1963)	Jan-Feb 58	15°-90°N
(c) Miyakoda (1963)	Jan 58	15°-90°N
(d) Reed et al. (1963)	Jan-Feb 57	35°-80°N
(e) Oort (1964)	July 57 - Jun 58	N.H.
(f) Lateef (1964)	Jan 16 - Feb 15, 57	North America
(g) Julian-Labitzke (1965)	Jan-Feb 63	N.H.
(h) Murakami (1965)	Dec 57 - Feb 58	N.H.
(i) Perry (1967)	Jan 63	N.H.
(j) Quiroz (1969)	Jan-Feb 66	N.H.
(k) Mahlman (1969)	Jan 10 - Feb 19, 58	50°-90°N
(l) Hirota-Sato (1969)	Winters, 1963-67	20°-80°N
(m) Miller-Johnson (1970)	Dec 1, 67 Jan 13, 68	17.5°N-82.5°N
(n) Miller (1970)	Jan 64 - Dec 68	17.5°N-82.5°N
(o) Dopplick (1971)	Entire year, 1964	20°-90°N
(p) Miller et al. (1972)	Dec 69 - Jan 70	30°-90°N
(q) Iwashima (1974)	Nov 67 - Feb 68	30°-85°N
(r) Quiroz et al. (1975)	Jan 16 - Feb 5, 73 Dec 15, 74 - Mar 15, 75	22.5°-87.5°N, 20°-90°N; 82.5°N
(s) Klinker (1976)	Dec-Jan 70-71; Dec-Jan 74-75	15°-90°N

TABLE 4.1. (continued)

	LEVELS OR LAYERS	CALCULATIONS ENERGY-CONVERSION (C)	ENERGY-GENERATION (G)	A
(a)†	1000-50 mb	Yes	No	No
(b)	30, 50, 100, and 500 mb	K only	No	No
(c)	1000-25 mb	Yes	No	Yes
(d)	50 mb	Yes	Yes	Yes
(e)	100, 50, and 30 mb	Yes	Yes	Yes
(f)	100-50 and 50-25 mb	Yes	No	No
(g)	100-10 mb; 1000-100 mb	Yes	Yes	Yes
(h)	50, 100, and 500 mb	Yes	No	Yes
(i)	1000-10 mb	Yes	Yes	Yes
(j)	----------	No	No	No
(k)	100 mb and 50 mb	No	No	No
(l)	10, 30, 50, 100, and 300 mb	No	No	No
(m)	10 mb, 100 mb, 500 mb	No	No	No
(n)	10 mb, 100 mb	No	No	No
(o)	100-10 mb	Yes	Yes	Yes
(p)	30-2 mb, 100-30 mb, and 1000-10 mb	Yes	No	Yes
(q)	10, 30, 50, and 100 mb	Yes	Yes	Yes
(r)	100-30 mb 100 mb	Yes No	No No	Yes No
(s)	50-2 mb	Yes	No	No

†See page 78 for authors to whom (a) - (s) refer.

TABLE 4.1. (continued)

	CALCULATIONS					
	K	$\frac{\partial K(n)}{\partial t}$	n=	VERTICAL MOTION	MEAN MERIDIONAL CIRCULATION	VERTICAL FLUX OF GEOPOTENTIAL
(a)†	No	No	---	Yes	Yes	No
(b)	Yes	Yes	0-15	No	Yes	No
(c)	Yes	Yes	---	Yes	Yes	Yes
(d)	Yes	Yes	0-4	Yes	Yes	Yes
(e)	Yes	No	---	Yes	Yes	No
(f)	No	No	---	Yes	No	No
(g)	Yes	Yes	---	Yes	Yes	No
(h)	Yes	Yes	0-2	Yes	Yes	Yes
(i)	Yes	Yes	0-10	Yes	Yes	Yes
(j)	No	No	---	Yes	No	Yes
(k)	No	No	---	Yes	Yes	No
(l)	No	No	---	No	Yes	No
(m)	No	No	0-3	No	No	Yes
(n)	No	No	0-4	No	No	Yes
(o)	No	No	---	Yes	No	Yes
(p)	No	No	---	Yes	No	Yes
(q)	Yes	Yes	0-3	Yes	Yes	Yes
(r)	Yes	No	No	No	No	No
	No	No	No	No	No	Yes
(s)	Yes	No	No	No	No	Yes

†See page 78 for authors to whom (a) - (s) refer.

In connection with Table 4.1, reference should be made to Table 2.1, "Details of Stratospheric Warmings, 1952-1976" given in an earlier section of this monograph (Climatological Description). From this table it is easily seen that the first major warming observed after Scherhag's discovery of the phenomenon in 1952 was the event in January - February 1957.

The 1957 warming was studied intensively by Reed et al. (ref. 68) and Lateef (ref. 72). The study by Reed et al. was a milestone, since it was the first in the domain of wavenumber to provide enough information for the construction of the Lorenz-type box-diagrams. Figure 4.5, for 50 mb shows an essentially direct baroclinic-type energy transformation prevailing during the amplification phase of the 1957 warming (25 January - 4 February) and an indirect transformation during the phase of decay (4-9 February).

Teweles (ref. 73) showed that the development of wavenumber 2 during the 1958 warming also appeared to have been baroclinic in nature.

Oort's study (ref. 69) was significant largely on account of its scope. Although White (ref. 74), Starr (ref. 75), and Reed et al. (ref. 68) had published statistics showing that the lower stratosphere behaved like a refrigerator in the annual mean, Oort was the first to relate the countergradient flux of sensible heat to the entire energy cycle in a systematic and comprehensive fashion. This opened the door to investigation into the nature and range of influence on the stratosphere of the eddy flux of energy from below.

Julian and Labitzke (ref. 6) (hereafter sometimes referred to as 'J.-L.') quantified many of the observational details of the 1963 warming which had already been given by Finger and Teweles (ref. 36). Figure 4.6 gives the flow diagrams both for the stratosphere and the troposphere, during the phase of warming amplification (January 2-27), and during the phase of decay (January 27 - February 26). The similarity between these results for the stratosphere and those of Reed et al. should be noted. There is no difference in the directions of the arrows. The relative differences in the results of calculation may be attributed to the differences in the warmings; the 1963 warming was a much stronger event. (Differences in units should be noted; J.-L.'s results are for a layer, while the results of Reed et al. are for a single level (50 mb).)

Although J.-L., like Reed et al., used the seminal equations of Saltzman (ref. 76), their analysis was not performed for the entire domain of wavenumber. In order to extend their results throughout the wavenumber domain, and especially in order to calculate barotropic nonlinear kinetic energy transfer between eddy components, besides upward flux of geopotential from the troposphere and the many other quantities already calculated or estimated by J.-L., Perry (ref. 8) undertook once again a study of the 1963 warming. Figure 4.7 shows a summary of his results. It is to be noted that whereas in each of the box diagrams presented heretofore there have been only four boxes, here we see each box for K_E broken down according to wavenumber. Thus is shown schematically the nonlinear interaction between the eddies. Also to be noted is the term BG_E, standing for the eddy flux of kinetic energy from the troposphere into the stratosphere.

In agreement with J.-L., Perry found that the beginning of the 1963 STRATWARM was accompanied by both an increase in tropospheric K_E and by increased geopotential flux through the tropopause.

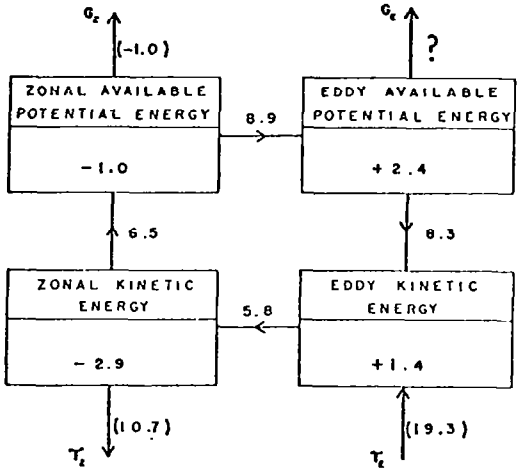

Energy flow diagram, 25 January-4 February 1957. Rates of energy change (ergs cm^{-2} mb^{-1} sec^{-1}) appear in boxes. Arrows indicate direction of energy flow. Figures by arrows give rates of energy conversion, transfer, or generation (ergs cm^{-2} mb^{-1} sec^{-1}). Figures in parentheses represent only crude estimates.

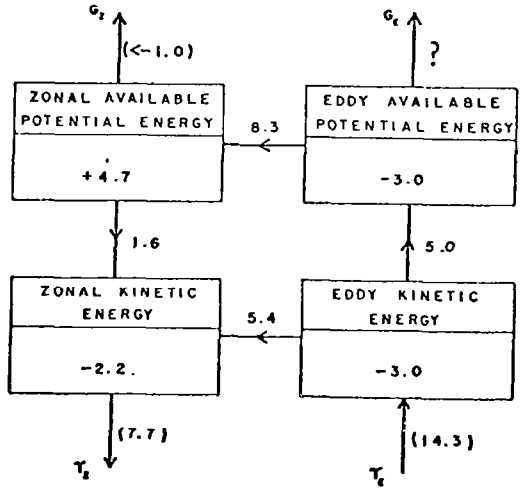

Same as above, except for 4-9 February 1957.

Figure 4.5. - Energy flow diagrams for the January - February 1957 warming, 50 mb only. Source: Ref. 68.

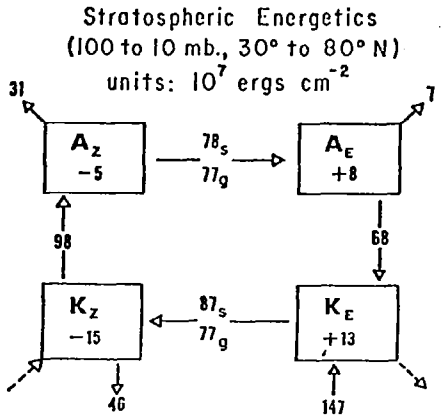

January 2 to 27, 1963

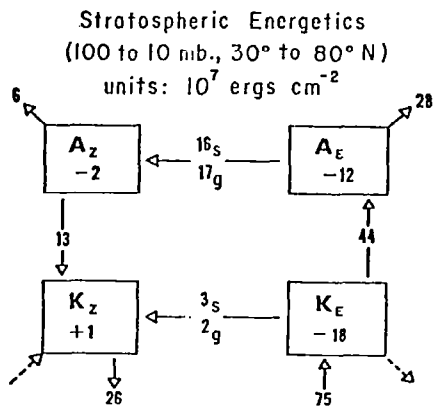

January 27 to February 26, 1963

Energy flow diagram for the stratosphere, 100 to 10 mb. Total energy converted or transferred in the interval given by integration of energy exchange rates is shown by arrows. Actual energy changes shown in the boxes. Arrows projecting from the corners of the boxes represent generative or dissipative processes. The values of the surface boundary integrals representing the net vertical flux of kinetic energy are entered beneath the kinetic energy boxes. Dashed arrows are inferred from balance requirements.

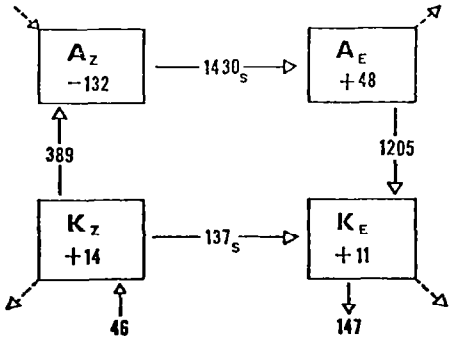

January 2 to 27, 1963

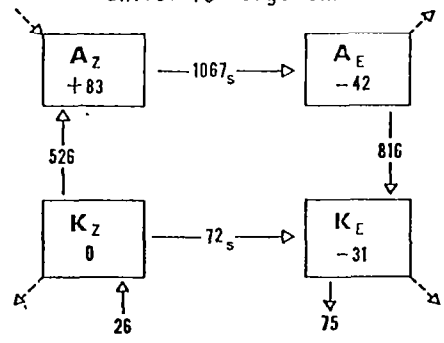

January 27 to February 26, 1963

Same as above, except for troposphere.

Figure 4.6. - Energy flow diagrams for the January - February 1963 warming, 1000-100 mb (troposphere) and 100-10 mb (lower stratosphere). Source: Ref. 6.

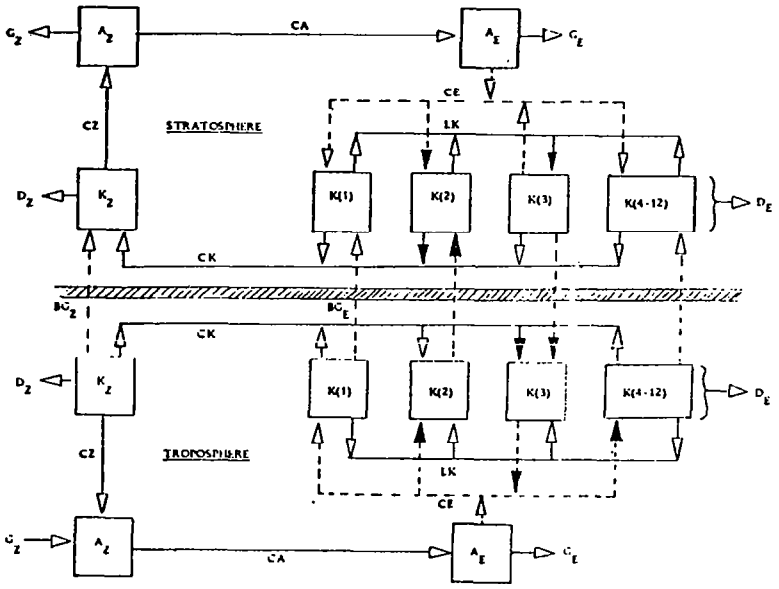

Schematic energy flow diagram for the stratosphere and troposphere in January 1963. Principal eddy energy processes are indicated by darkened arrows.

Figure 4.7. - Source: Ref. 8.

Perry was the first to demonstrate the importance of nonlinear interactions, and thus he corroborated Merilees' (ref. 77) conclusion that the stratosphere is largely nonlinear in character and that baroclinic processes are mainly forced by interaction with the troposphere.

In a manner similar to that of J.-L., Perry calculated the mean meridional circulation and found rising motion in the polar region and subsidence near 50°N. In addition, he found rising motion in the subtropical regions, and so was able to locate two indirect cells (as opposed to only one at higher latitudes which J.-L. had found).

Since in many ways Perry's study was the most comprehensive yet made in the field of STRATWARM energetics, and since it has been widely accepted by workers in this field, it seems appropriate to quote his concluding remarks concerning the 1963 warming:

"(1) In the early stages of the pre-warming eddy amplification, the stratosphere received eddy energy through pressure-interaction effects in wavenumbers one and three.

"(2) The growth of wavenumber two which dominated the later phases of the warming was due to baroclinic development and to vertical flux of geopotential in approximately equal parts.

"(3) Upward flux of eddy geopotential in wavenumber two was continuous from the lowest levels through the stratosphere, implying a coupling of the highest levels with the topography of the hemisphere.

"(4) Wavenumber three was driven by interactions with the zonal and other eddy components in both stratosphere and troposphere and played a significant part in carrying energy from regions of production to regions of dissipation.

"(5) Nonlinear interactions were significant in both stratosphere and troposphere, tending to transfer energy from cyclone waves to long waves in the troposphere, from the baroclinically active long stratospheric waves to wavenumber three. These interactions were a possible link between the variable energy-producing cycle waves of the troposphere and the long waves of the stratosphere.

"The energy processes deduced from the stratospheric warming period were not inconsistent with the instability hypotheses of Charney and Stern (ref. 78). However, the stratospheric warming was seen to be a long-duration, high-amplitude phenomenon in which diabatic and nonlinear effects were significant. It is therefore suggested that theoretical models capable of dealing with its entire scope should embody these processes explicitly."

We emphasize that the conclusions stated here are strictly based on just one case, namely the 1963 warming. Although other events have corroborated them, further investigations are required.

For reasons already indicated, it is of considerable interest to study, and, wherever possible, to monitor, stratospheric response to dynamic forcing from below. The best way to do this would seemingly be to compare the time rate of change of kinetic energy within a layer bounded below by the 100-mb surface with the upward flux of geopotential through that surface. Practical considerations, however, have sometimes dictated the use of a stratospheric circulation index (HIP) (ref. 79) in place of the calculated kinetic energy. The complete justification for this is given elsewhere (ref. 80); suffice it here to say that HIP is a normalized difference between the squared height amplitudes (C) of zonal wavenumber 2 and of zonal wavenumber 1 at 60°N and at 10 mb--viz., 3×10^{-4} $(C_2^2 - C_1^2)$. Furthermore, since it is known that the variance in height of a constant pressure surface gives an indication of the kinetic energy, and that most stratospheric energy usually lies in wavenumbers 1 and 2, it would seem reasonable to compare HIP with the difference between the upward flux in geopotential (at 100 mb) for wavenumber 1 and wavenumber 2--i.e., with $[\omega^* z^*]_{n=2} - [\omega^* z^*]_{n=1}$. (Here, $z^* = g^{-1}\phi^*$.) A basic underlying assumption here, of course, is that forcing in a certain wavenumber should be reflected in an increase of stratospheric kinetic energy of the same wavenumber. Thus we would expect, since a negative value of each energy flux term corresponds to an upward flux of geopotential, that the two indices would be negatively correlated. Also we would expect, in view of the time required for the forcing to elicit some response, that there should be some lag.

Figure 4.8 shows the results for January - March 1967. Lag correlations were computed for 387 points, and the most significant lag correlation coefficient was -0.41, for a lag of -2 days (negative lag indicates a lagging of HIP behind the energy flux).

A direct comparison of 10-mb kinetic energy with the term $[\omega^* z^*]$ for December 1967 - January 1968 was given by Miller and Johnson (ref. 70). The results are shown in Figures 4.9 and 4.10. The apparent response of K_E in wavenumbers 1 and 2 to forcing in wavenumbers 1 and 2 respectively--wavenumber 1 first being dominant, then wavenumber 2--should be especially noted.

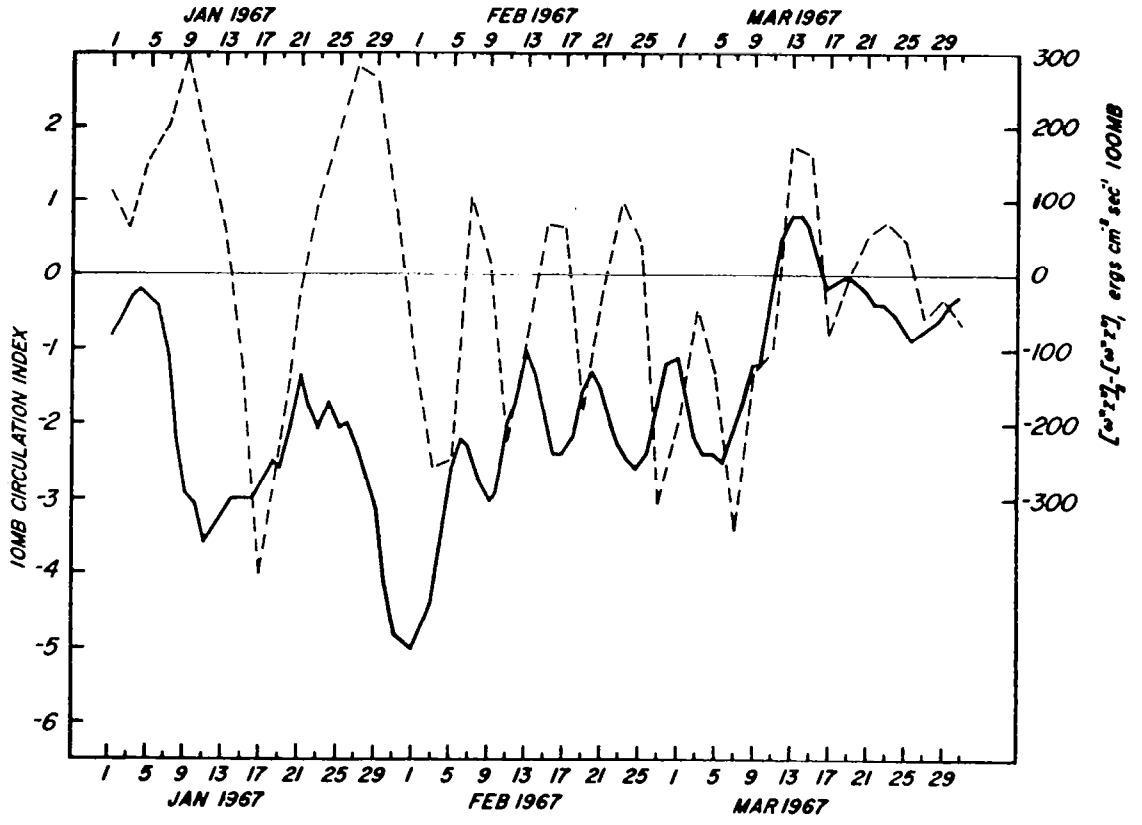

10-mb circulation index (solid line) vs the energy flux index defined by $[\omega^* z^*]_{n-2} - [\omega^* z^*]_{n-1}$ (dashed line) for the period January–March 1967.

Figure 4.8. - Source: Ref. 80.

Up to 1971, our view of the annual mean energy cycle for the stratosphere was that which had been given by Oort (ref. 69) already alluded to. Recognizing the importance of extending our knowledge of stratospheric behavior for all seasons, in order to interpret the calculations for any singular event (e.g., a STRATWARM), Dopplick (ref. 71) obtained the energy cycle for the entire year 1964. The main difference between Oort's and Dopplick's result is in the direction of the arrow between A_Z and A_E. It is believed that the explanation for this lies in the fact that Oort dealt with the 100-30 mb layer, Dopplick with the 100-10 mb layer; thus Oort would have neglected the 30-10-mb region, wherein A_Z is converted to A_E during winter in the vicinity of the polar-night jet. It should be noted here, however, that even though substantial amounts of K_E flow into the stratosphere from the troposphere, there is a conversion (again, in the annual mean) from K_E to K_Z and from K_E to A_E. Thus, in contrast to the amplification phase of most STRATWARMS studied, the annual mean energy cycle is not baroclinically direct, but rather is indirect.

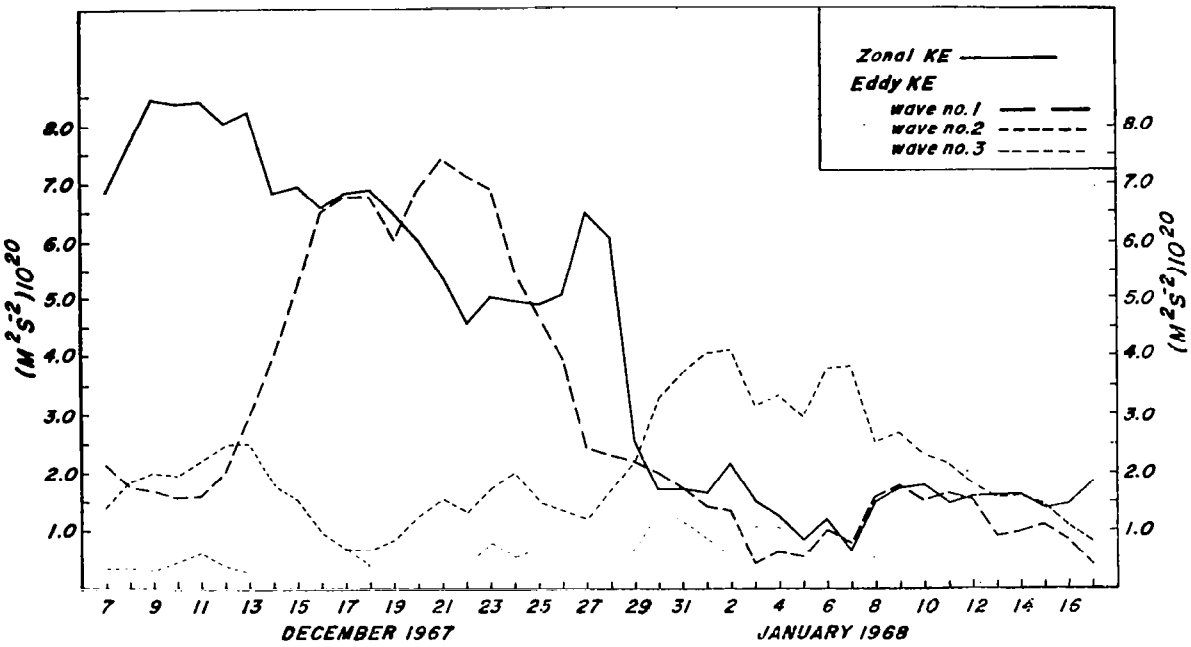

Figure 4.9. - 10-mb zonal and eddy kinetic energies for wavenumbers 1-3 during December 1967 and January 1968. All energies integrated over the region 17.5 - 82.5 degrees north. Units: $10^{20}m^2s^{-2}$. Source: Ref. 70.

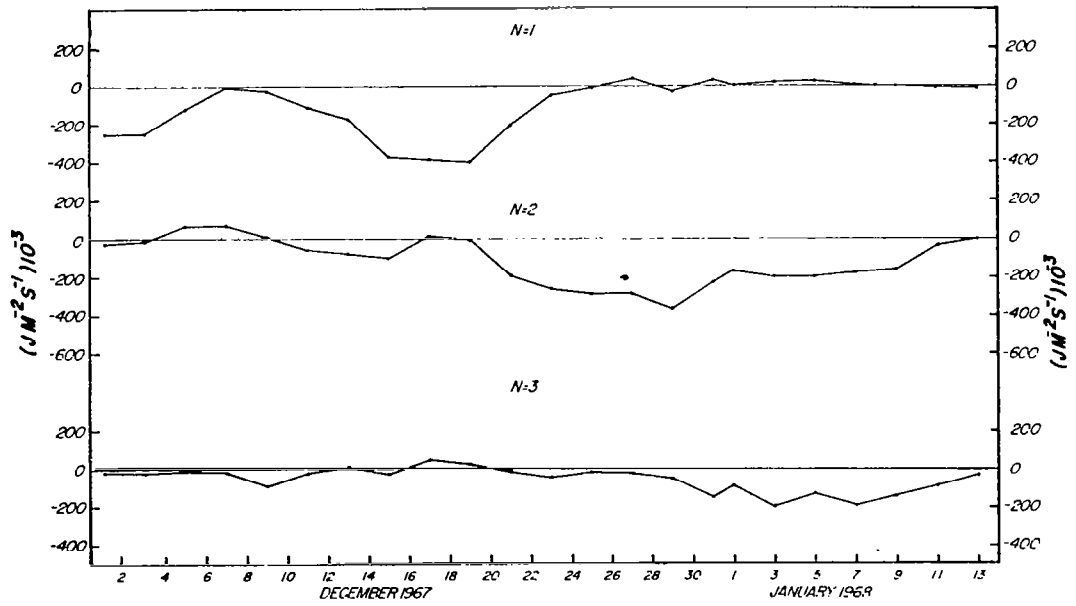

Figure 4.10. - Pressure-interaction term for wavenumbers 1-3 at 100 mb during December 1967 and January 1968. Units: $10^{-3}Jm^{-2}s^{-1}$. Source: Ref. 70.

Figures 4.11 and 4.12, taken from Miller et al. (ref. 7), shed further light on Dopplick's results, while adding considerable new information. Here energy calculations have been made for three layers during a minor STRATWARM--troposphere (1000-100 mb), lower stratosphere (100-30 mb), and upper stratosphere (30-2 mb). Figure 4.11 is for the amplification phase of the STRATWARM, Figure 4.12 for the phase of decay. It should be noted that the direction of the arrows does not change between phases for the troposphere; and this is consistent with our knowledge of the troposphere in winter as one involving baroclinically direct energy conversions. The basically passive nature of the lower stratosphere is well depicted in both figures--with a loss of K_E to A_E indicated for both periods. The upper stratosphere, however, manifests a strong baroclinically direct energy cycle during the amplification period, and a much weaker, rather ambiguous cycle during the period of decay.

The two principal conclusions of Miller et al. (ref. 7) were: (1) that the 1969-70 warming, like all the others that had been studied up to that time, appeared to be forced from below; and (2) that, in order for a warming to propagate from the upper stratosphere into the lower stratosphere (and hence to become major), the direction of energy conversion in the lower layer would have to change to the baroclinically direct sense.

Iwashima (ref. 81) studied the 1967-68 warming, and his results are similar to those of J.-L. (ref. 6) for the 1963 STRATWARM. In the Lorenz energy cycle for the later warming, the numbers are somewhat different, but the corresponding arrows point in the same direction. Iwashima's study was more complete in its calculations of energy fluxes, dissipation and generation; also it was based on a separation between stationary and traveling waves.

Up to 1968, most of the well-documented major STRATWARMS were principally wavenumber 2 phenomena, in the sense that the eddy kinetic energy of wavenumber 2 came to exceed the contributions of the other wavenumbers for at least a portion of the warming-cycle. The stratospheric circulation index (dubbed "height index parameter" or "HIP") was in fact based on the premise that major warmings must be predominantly wave-two warmings. Ironically enough, beginning about that time the stratosphere began to show a proclivity for producing mainly wave-one type warmings.

It should perhaps not be surprising that the energy calculations for wave-one type warmings may lead to results different from these for wave-two warmings. It will be recalled that both J.-L. and Perry found a strong baroclinic conversion $A_E \rightarrow K_E$ during the amplification phase of the 1963 warming between 100 mb and 10 mb. Figure 4.13 from Quiroz et al. (ref. 41) shows quite a different energy conversion, with $K_E \rightarrow A_E$ during the entire period of a major warming, January 16 - February 15, 1973. It should be pointed out, however, that for wave 1 alone, Quiroz et al. found a conversion $A_E \rightarrow K_E$ (rather, $A(1) \rightarrow K(1)$) up to January 20. Thus, even though the energy conversions are as shown (where A_E and K_E refer to all the wavenumbers > 1, i.e., all the eddies), there is evidence of baroclinically direct transformations in the predominant wavenumber, and therein lies a similarity between the results of Quiroz et al. and those which were concerned with mainly wave-2 type warmings. At the same time it must be borne in mind that a continuous positive energy flow $A_Z \rightarrow A_E \rightarrow K_E \rightarrow K_Z$, so much in evidence for some of the wave-2 warmings, is not discernible here even in wave 1. Quiroz et al. concluded that the 1973 warming must have differed in some fundamental respects from the warmings of, say, 1957, 1963, and 1967-68.

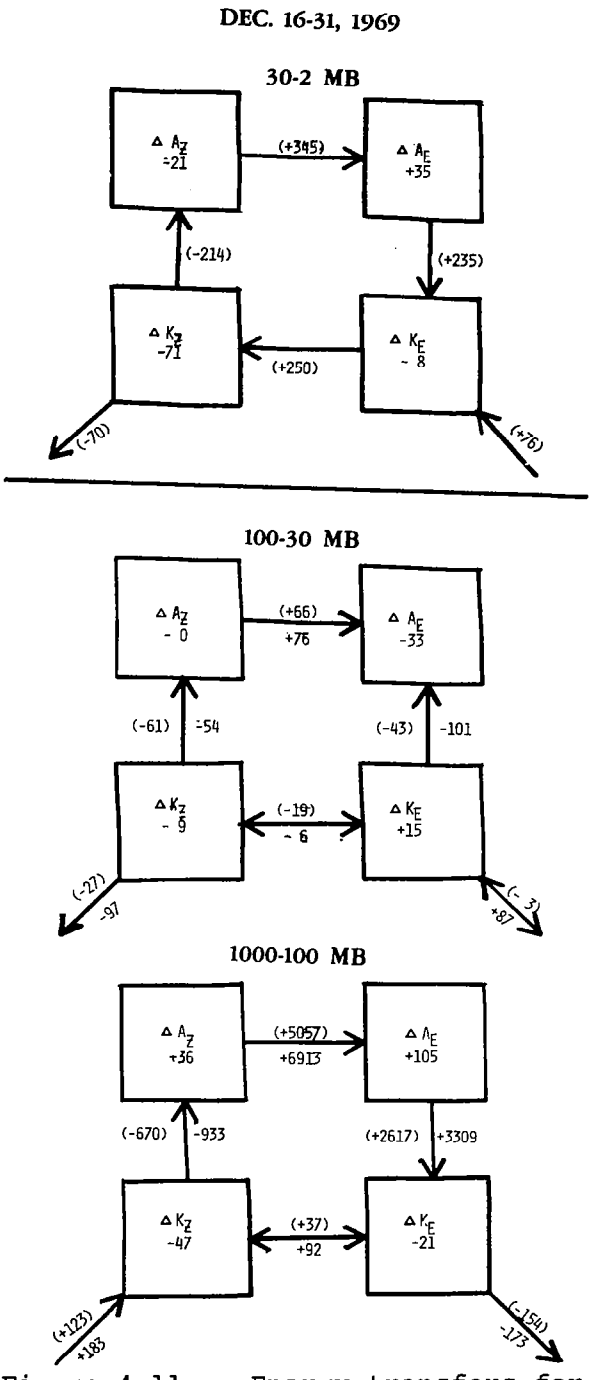

Figure 4.11. - Energy transfers for 1000-100, 100-30, and 30-2 mb layers averaged over 16-31 December 1969. Arrows represent direction of energy flow. Units: $10^{-3} Jm^{-2} s^{-1}$. Source: Ref. 7.

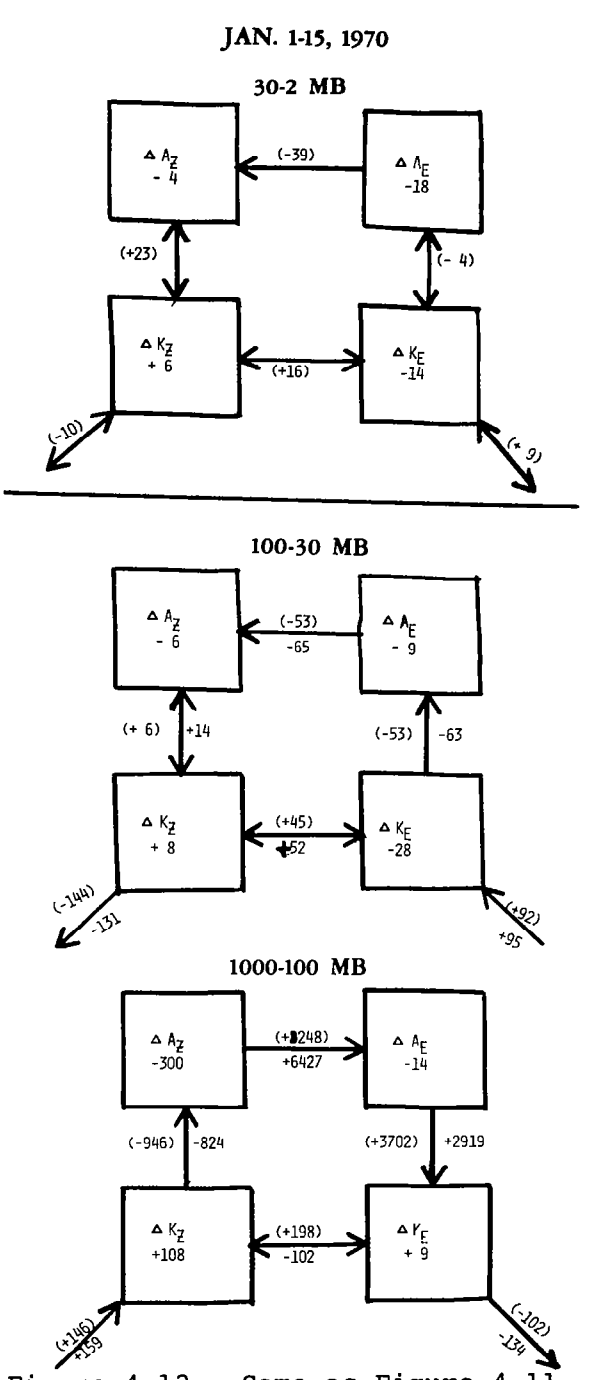

Figure 4.12. Same as Figure 4.11, but for the period 1-15 January 1970. Source: Ref. 7.

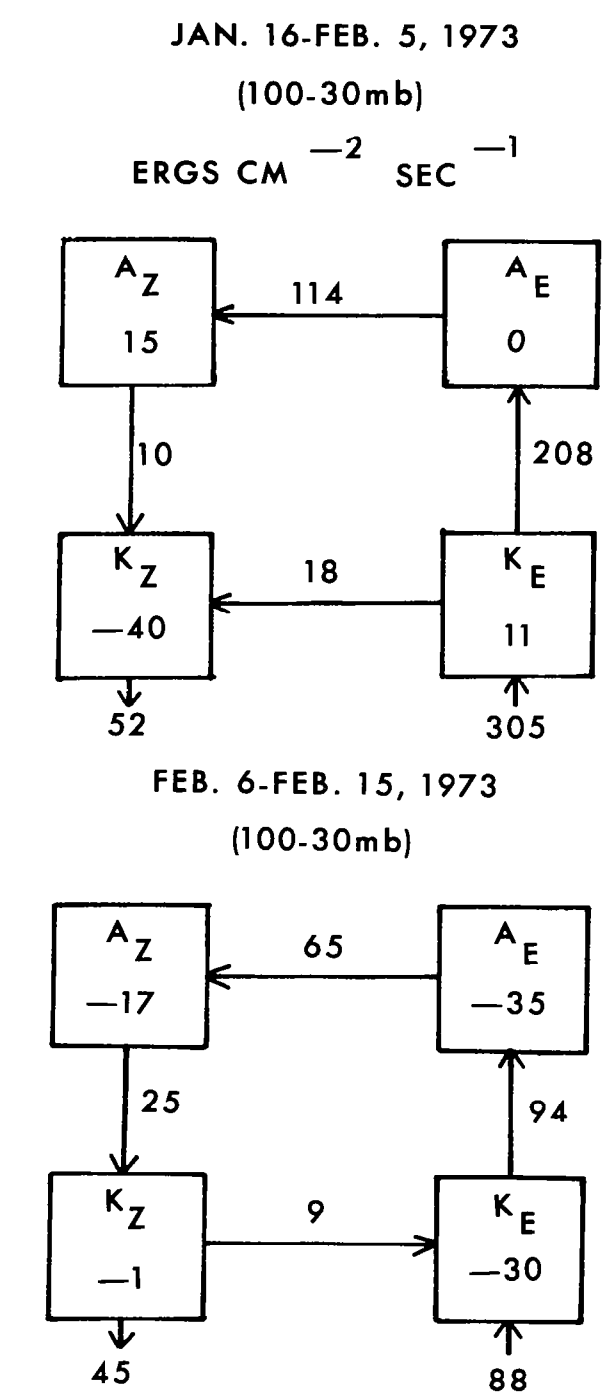

Figure 4.13. - Energy flow diagrams for periods leading up to the 1973 warming, and following the warming. Energy values are integrated for the periods indicated, between 22.5°N and 87.5°N for the layer 100-30 mb. Source: Ref. 41.

Since December 1974, a program of routine global energy computations has been conducted by the National Meteorological Center. One of the principal calculations is that of the eddy flux of geopotential through the 100-mb surface, integrated from 20°N to the North Pole. Figure 4.14 shows a trace of this quantity as a function of time. Also plotted in this figure are values of the zonal mean radiance at 82.5°N based on VTPR Channel 2 measurements (values are proportional to the 100-5 mb mean temperature).

While no clear and sharp relationship appears to subsist between the two traces in Figure 4.14, nevertheless, as Quiroz et al. point out, if one focuses only on what happens to the radiance-trace following a period of relatively high values of eddy flux of geopotential--such as between December 15 and January 5--then one may see something of interest. One would suppose that there are better indicators of stratospheric response to this flux than values of the Channel 2 VTPR radiances, however.

Klinker (ref. 82) has made an interesting comparison between the 1970-71 warming and the 1974-75 warming. The former was considered major, because it culminated in a circulation reversal at 10 mb. The latter was considered minor, since at 10 mb the temperature gradient was reversed only north of 60 degrees north latitude, without a corresponding breakdown of the polar vortex. Figure 4.15 shows cross-sections of longitudinally-averaged values of geopotential flux for the two warming events. "D=1" refers to Day One, i.e., the day the warming began. This day was judged to be December 30, 1970 for the earlier event, December 25 for the later event. Subsequent D-days were assigned at roughly one-week intervals. The isopleths of course give information not only about the geopotential flux, but also, indirectly, about the convergence of this flux. The much larger values of this convergence at D=1 and D=2 during the 1970-71 warming can perhaps explain the greater

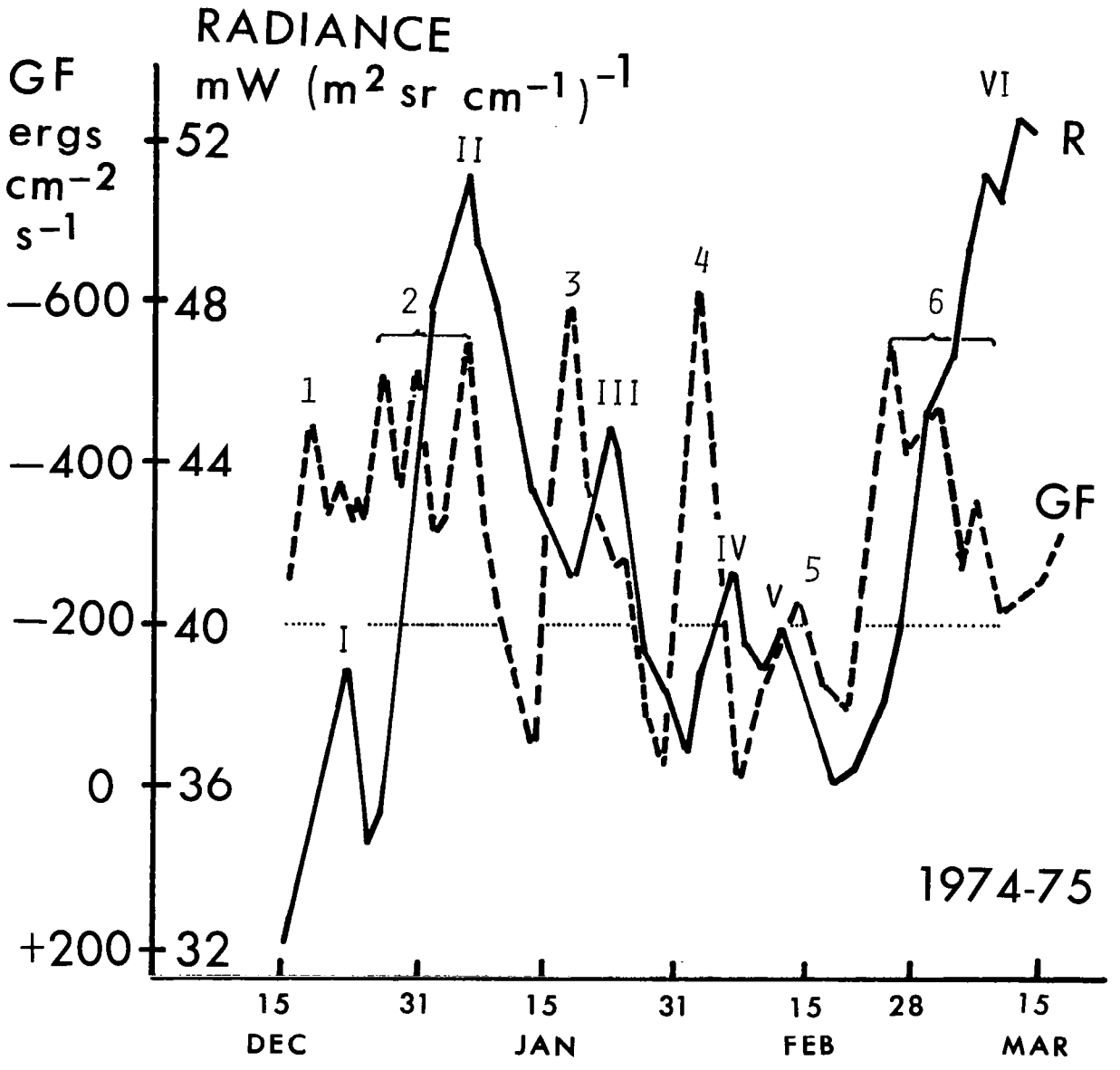

Figure 4.14. - Eddy geopotential flux through the 100-mb surface integrated from 20°N to the North Pole (dashed line), and zonal mean radiance at 82.5°N based on VTPR Channel 2 measurements (solid line). Note "width" (duration) of geopotential flux oscillations at ordinate value of -200 units. Source: Ref. 41.

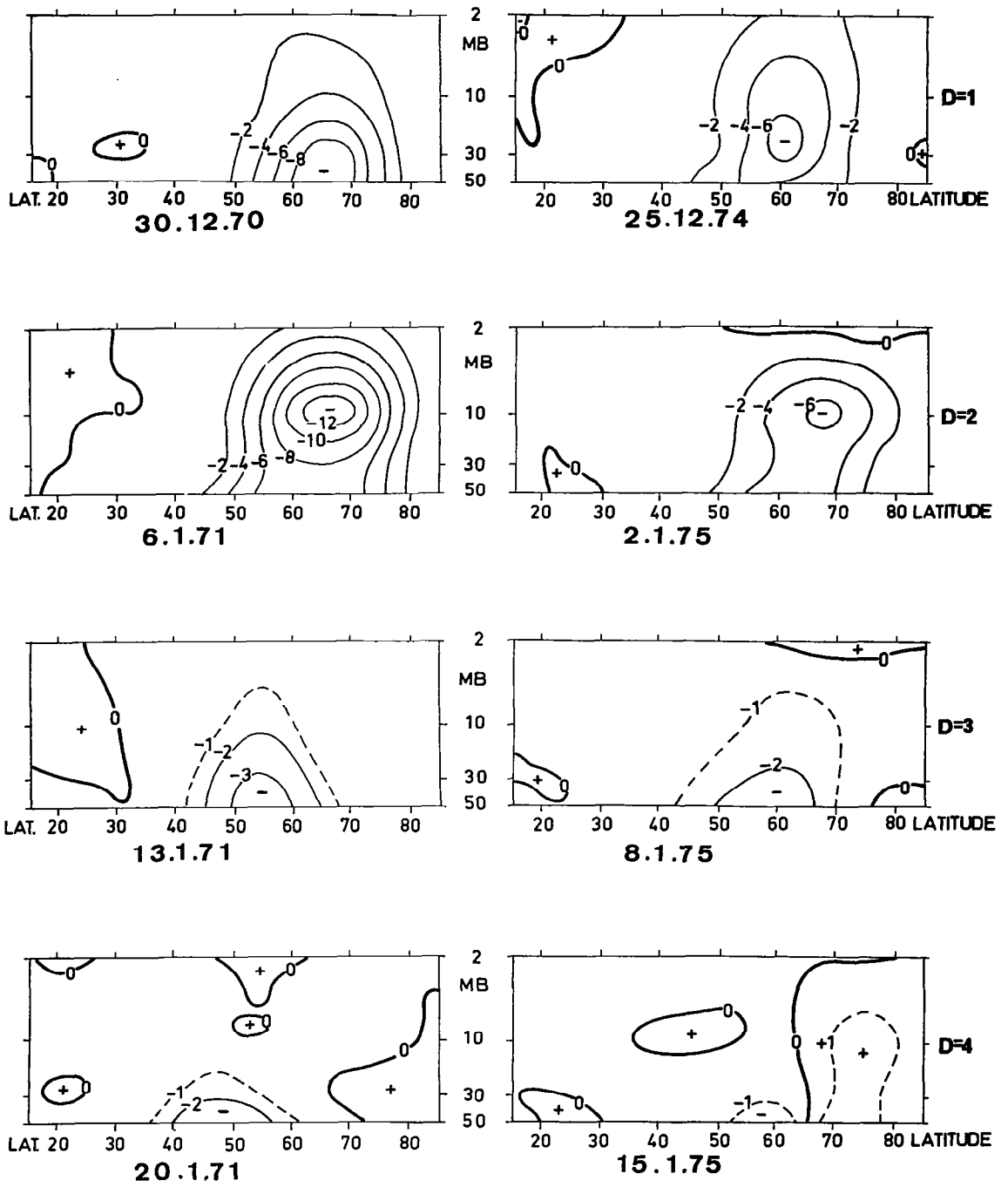

Figure 4.15. - Vertical structure of the eddy geopotential flux, 30 December 1970 - 20 January 1971 (left) compared with period 25 December 1974 - 15 January 1975 (right). "D"-days are assigned at approximate 1-week intervals (see right side of figure). Source: Ref. 82.

magnitude of this event. Thus, Klinker's study suggests the importance of examining flux convergence in STRATWARM studies.

The following picture of stratospheric energetics has emerged from the past 15 + years of investigation:

(1) The upper stratosphere (30-50 km, or 10-1 mb) while generally characterized by greater static stability than the lower atmospheric layers, resembles the troposphere inasmuch as it undergoes mostly baroclinic energy transformations.

(2) The lower stratosphere (16-30 km, or 100-10 mb) behaves, on a yearly average, as a refrigerator rather than as a heat engine, extracting heat from the cold equatorial region and transporting it to the relatively warm polar regions, thus maintaining the positive poleward temperature gradient against radiative dissipation. (This pattern holds for all periods and areas except for the winter at high latitudes.) Hence this layer must have an external energy source, which has been found to consist in tropospheric forcing (the flux of geopotential from below), rather than by internal energy transformations.

(3) The lower stratosphere in winter at high latitudes is sometimes characterized, like the upper stratosphere and troposphere, by baroclinic energy processes, especially during the amplification phase of stratospheric warmings.

(4) When a major STRATWARM occurs, baroclinic transformations prevail throughout the upper and lower stratosphere during the amplification phase of the warming, but, once the meridional temperature gradient is reversed, there begins a loss of eddy kinetic energy (K_E) to other forms of energy. (The transformation $K_E \rightarrow A_E$ is part of an indirect energy-cycle, as contrasted to the transformation $A_E \rightarrow K_E$, which is part of the baroclinically direct cycle.)

(5) The upward flux of geopotential from the troposphere to the stratosphere (often also referred to as "eddy flux of energy" or as "tropospheric forcing") appears to be important not only for maintaining the kinetic energy budget of the stratosphere, but also for the role it plays in the pre-amplification and amplification phases of STRATWARMS. It has been suggested that large amounts of this flux, sustained over several days, is a necessary (though not sufficient) condition for the occurrence of STRATWARMS.

This picture is very schematic, and certainly subject to modification. Many authors would place emphasis on different features. As far as actual calculations are concerned, many different results have been obtained, casting considerable doubt upon aspects of 1 - 5 above, or at least making them appear rather simplistic.

Since the apparent relationship between tropospheric forcing and the occurrence of STRATWARMS suggests the use of calculations of the upward flux of geopotential as a forecasting tool, considerable emphasis is placed on this aspect of the energy cycle in this monograph. The question arises, however, as to the source of the tropospheric forcing. Tropospheric blocking, as a response to intense baroclinic activity (increased vertical motion in the eddies), has been given the most attention, but a clear relationship between such blocking and STRATWARMS has not yet been established.

INTERACTIONS OF STRATOSPHERE WITH MESOSPHERE AND IONOSPHERE DURING STRATWARMS

Interaction with Neutral Mesosphere

A combination of rocket soundings and satellite data has made possible weekly synoptic analysis for isobaric surfaces up to 0.4 mb (approximately 54 km), well above the average stratopause height (48-50 km). It should be clear from the discussion already given that the principal deterrent to synoptic analysis above 54 km is the absence of reliable satellite data for such high levels. This situation is rapidly changing, however, with the introduction of more sophisticated sounders on the new-generation spacecraft.

Rocket soundings for altitudes above 70 km are still rather rare. Only very costly experimental-type rockets have the capability of sounding the entire stratosphere and mesosphere. Thus our knowledge of the mesosphere is severely limited by lack of data, compared to our knowledge of the stratosphere.

Our discussion here is restricted to what has been observed to happen in the mesosphere during periods of stratospheric warmings.

In order to place things in perspective, we first point out that both the tropopause height and the mesopause height appear to vary within much narrower limits than does the stratopause height. For example, the tropopause at high latitudes very rarely occurs below 6 km or above 12 km. Similarly--although this conclusion is far less certain--the mesopause hardly ever occurs below 70 km or above 90 km. On the other hand, the stratopause has been known to vary, according to the definition in terms of temperature maximum, between 20 km and 57 km.

The stratopause is known to be very high and very warm at the onset of a stratospheric warming at least over the area which comes to be ultimately affected by the warming, and possibly over the entire polar cap north of 60°N; it becomes very low and rather cold toward the end of the warming. It follows that the mesosphere it usually a relatively thin layer at high latitudes at the beginning of a STRATWARM, while the stratosphere is quite thick; then, as the STRATWARM progresses, the mesosphere gains in thickness at the expense of the stratosphere. Furthermore, while the stratospheric temperatures increase, the mesospheric temperatures decrease (ref. 18).

Figure 5.1 shows the variation of stratopause heights and temperatures during one stratospheric warming (January 1973). Here we see that the stratopause temperature increased markedly during the initial phase of the warming, then decreased as the stratopause height decreased. The stratospheric warming was accompanied by a mesospheric cooling, and the stratopause became less distinct.

Labitzke (ref. 84) has combined soundings from different winters to give the profiles for high and low latitudes, for the beginning, climax and conclusion of a "composite" warming, shown in Figure 5.2. The cold mesosphere accompanying the warm stratosphere is very much in evidence. In fact, there are opposite changes in temperature structure between high and low latitudes as well as between stratosphere and mesosphere.

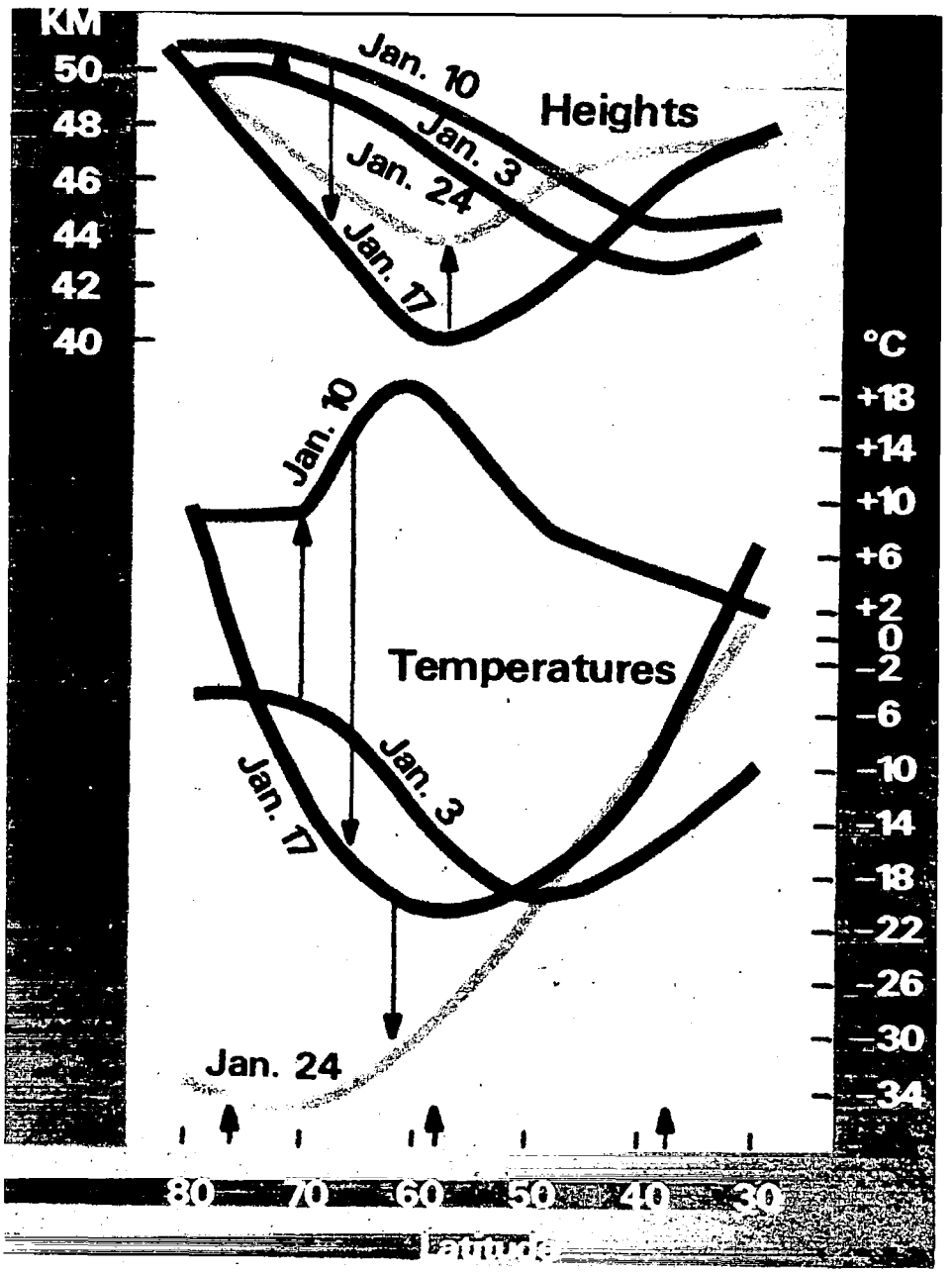

Figure 5.1. - Variation of stratopause heights and temperatures during a major stratospheric warming (January 1973). Source: Ref. 83.

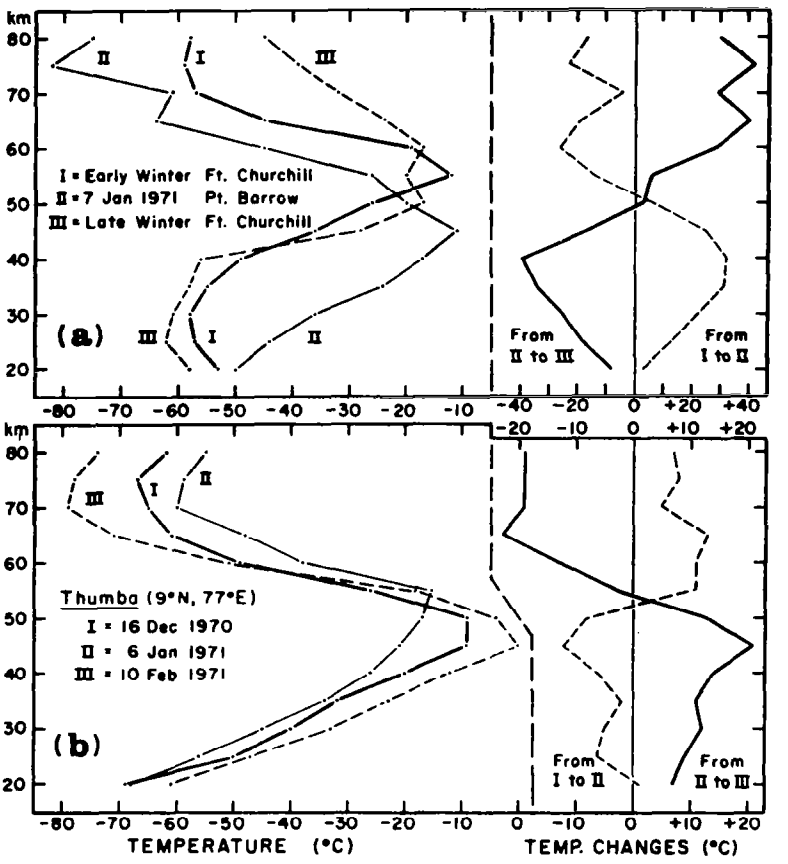

Figure 5.2. - (a)-Vertical temperature profiles: I, early winter (20 November 1968), Ft. Churchill; II, peak of warming (7 January 1971) Pt, Barrow; III, late winter minimum (1 February 1968, Ft. Churchill). Also the changes between I and II, and between II and III.
(b)-Vertical temperature profiles for Thumba, India, for the winter 1970/71.

It is tempting to conjecture, on the basis of pictures such as Figure 5.2, that 50-55 km is the level of interaction between stratosphere and mesosphere. That there must be some interaction is indicated by the opposite changes that occur in the two layers. But the precise mechanism for such interaction remains to be discovered.

Interaction With Ionosphere

There is a growing body of evidence supporting the hypothesis of interconnection between ionospheric (> 60 km) and upper stratospheric (roughly between 30 km and 50 km) phenomena.

Brown and Williams (ref. 85) have shown a well-defined correlation between the height of isopleths of electron density in the E-region (near 100 km) and pressure near 30 km (Figures 5.3 and 5.4). They argue, on the basis of what is known about the E-region (its conformity to the Chapman model), that this proves the existence of coupling between the lower and upper atmosphere--specifically, the sympathetic movements of isobaric surfaces from day to day in winter at stratospheric ($\sim$ 30 km) and ionospheric ($\sim$ 100 km) heights.

It has been suggested that neutral atmospheric density may be an important factor affecting electron density. However, the results of Brown and Williams suggest that temperature may be at least as important, since high pressures at 30 km are associated with STRATWARMS and low electron densities near 100 km. It might appear to follow that periods of STRATWARMS would be the least likely times for the D-region anomaly, but one must reflect that the D-region lies between the stratopause and the 100-km level, and there is no assurance that the D-region behaves like the E-layer. Moreover, it is known that the dominant daytime electron-ion production process in the D-region is photo-ionization of nitric oxide by Lyman-α. Thus it would seem that a study of the transport and distribution of nitric oxide would be more revealing than correlations of stratospheric-mesospheric temperatures, densities or pressure.

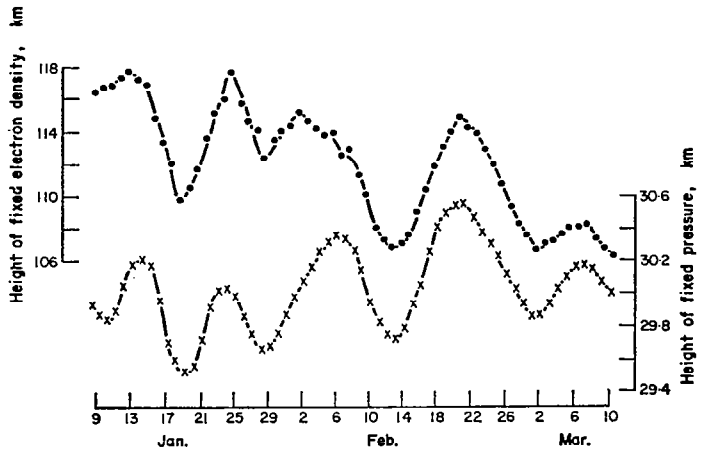

Figure 5.3. - Variation of height of isopleths of electron density (N = 4.5 x 10^4 cm^{-3}) and pressure (10-mb surface) over Aberystwyth, January-March 1965. Source: Ref. 85.

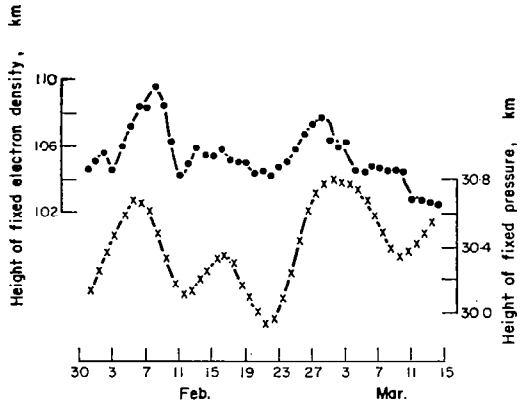

Figure 5.4. - Variation of height of isopleths of electron density (N = 6.5 x 10^4 cm^{-3}) and pressure (10-mb surface) over Aberystwyth, February-March 1966. Source: Ref. 85.

NUMERICAL MODELS

Introduction

In the most general sense, a numerical model is one that forecasts the behavior of atmospheric variables by numerical solution of the governing equations of hydrodynamics, subject to initial conditions and prescribed boundaries. However, our focus here will be on those models which result in a synoptic display of atmospheric variables (e.g., a "weather map") that can be compared against observation.

Our purpose is to present a very simplified overview of the several available models as an indication of the current success, or lack thereof, in simulating the stratospheric warming phenomenon. We will present only the very basic components necessary for understanding the models, and will focus on the results and their implications.

Within such a simplified framework, one must be aware of certain aspects of the warming phenomenon presently considered to be of prime importance, and the manner in which these particular features are simulated. The energy cycle during the warming events has been sketched in earlier sections (Synoptic Description and Energetics). Within the eddy kinetic energy equation the term that is now considered to be of perhaps major significance for the warming event is the term involving the convergence of eddy kinetic energy by the pressure-work term (or wave energy flux, as it is sometimes referred to). This term is of double importance, since in addition to representing the physical effect of transferring energy upward from the troposphere to the stratosphere, it involves the horizontal transport of sensible heat and thus has thermodynamic implications.

Thus it is clear that we should observe closely the role of this term in current models, and, in particular, pay close attention to a) the forcing mechanism of this energy flux within the troposphere and b) the interaction of the vertical wave energy flux with the zonal flow. With reference to the latter point, we shall pay special attention to the prescribed boundary conditions and their possible effect on the convergence of the wave energy flux.

In the sense that we will be describing those models that are pertinent to the resolution of the stratospheric warming phenomenon, it is helpful to categorize them into 3 types:

(1) Prognostic - those that employ as an initial condition an observed meteorological field (pressure, temperature, and wind) and attempt to forecast the warming from that point. Under this category is the study of Miyakoda, Strickler and Hembree (ref. 86).

(2) Climatological - those that start from some general physical state such as thermal equilibrium, and attempt by long-range integration of the governing equations to arrive at patterns that resemble the climatological averages of the stratosphere. As it happens, during the integration period of some of these experiments, certain variations in the stratospheric synoptic patterns resembling those observed during stratospheric warmings are occasionally realized. Of this type, we will discuss the results of Newson (ref. 43), Manabe and Hunt (ref. 87), Cunnold et al. (ref. 88).

(3) Hypothesis Testing - those that employ the numerical models to test the impact of certain specific features implicit in the model such as

boundary conditions, radiation effects, etc. Included in this type are the results of Clark (ref. 89) and Matsuno (ref. 42), as well as several models based on Matsuno's.

Various Models

Prognostic Models. - The prediction model considered under this category is the 9-level primitive equation model of Miyakoda, Strickler, and Hembree, originated at the Geophysical Fluid Dynamics Laboratory (ref. 86). Table 6.1 presents the standard heights and pressures of this model where p is the pressure and p_* the surface pressure. We see that in this model there are only 3 levels in the stratosphere with the top at about 32 km. Inasmuch as we now recognized the importance of considering the entire stratosphere during a warming event, we might suspect at the outset that these results will have somewhat limited applicability, but it is interesting to consider their prognostic success.

TABLE 6.1. - STANDARD HEIGHTS AND PRESSURES OF THE NINE-LEVEL MODEL.
p: PRESSURE, p_*: SURFACE PRESSURE

Level k	p/p_*	Standard height (km)
1	.008916	31.60
2	.074074	18.00
3	.188615	12.00
4	.336077	8.30
5	.500000	5.50
6	.663923	3.30
7	.811385	1.70
8	.925926	0.64
9	.991084	0.07

For general information, the model is for the Northern Hemisphere, includes hydrologic processes and radiation effects, the latter based on climatological monthly means. Land-sea contrast is included as well as mountains. One important point to note is that the vertical motion is zero at p=o. This can be quite important, as the vertical resolution is such that we can expect any wave energy propagated upward from the troposphere to be, under the model constraints, absorbed in the lower stratosphere.

The goal of the experiment was to simulate the breakdown of the circumpolar vortex in the winter stratosphere for the case of March 1965. The experiment was run in two phases: the first (experiment A) employed as an initial state the observed pattern 2 days prior to that which they were trying to forecast, the second (experiment B) employed the initial conditions 5 days prior to the breakdown. The 5-day forecast was attempted on the basis that the initial time in experiment A was too close to the key day, that the elongation of the vortex had already begun (i.e., the most important moment, the onset of the vortex destruction, might have been missed). As an aside, this is an extremely important point when we consider the timing of observations during warming events, and we will return to it after consideration of the results.

The results of experiment A are presented in the next several diagrams, and the first, Figure 6.1, shows the observed 50-mb height patterns at the top and the predicted patterns on the bottom for the days after time zero - March 17, 1965. We see that the gross features of the patterns are maintained and, as shown on the second day, the predicted vortex appears to be elongating as is the observed. The predicted low values appear to be too low by about 60-120 meters and the Aleutian High seems too weak.

Figure 6.2 is a similar diagram, but for the 3rd and 4th days of the experiment, and we see that the predicted patterns are, in general, in good agreement with the observed bipolar vortex, although, again, the predicted low center is slightly too low and the Aleutian High is not really manifested.

The 50-mb results for experiment B are shown in the next 2 diagrams (Figures 6.3, 6.4) - in this case time zero is 3 days earlier - March 14, 1965. The patterns are shown at 2-day intervals. In this case, the disparities are quite striking by the 4th day with the predicted patterns already showing a 2-cell pattern and a 3rd low region where there is an observed high.

By the 6th, 8th, and 10th days, we see that the forecast charts show little similarity to the observed breakdown.

Figures 6.1 - 6.4 illustrate the height patterns, and the next diagram, Figure 6.5, depicts the observed zonal temperature (top) and experiment B's predicted values (bottom) at $\sim$ 9 mb. The observed sudden warming starts on the 5th day and culminates on the 7th, but in the prediction (and the authors state that the same is true for experiment A) there was almost a complete failure in the simulation of the sudden warming. The only consolation is a slight increase of temperature at days 5-7.

We will not dwell on the possible reasons for lack of success in experiment B, but it is undoubtedly related to many features of the model, including the vertical resolution. It is noteworthy, however, that the authors state that the predicted patterns in the troposphere to the stratosphere were, in all likelihood, poorly represented. This illustrates once again the need to consider the warming event within the context of the entire atmosphere, not as a phenomenon occurring within an isolated layer.

To return now to the point made earlier: one thing that seems clear from these results is that if initial analyses of the STRATWARM are provided only after it has begun, then it already may be too late to gain insight into the origins of the phenomenon. We must be able to study the situation that leads up to the event and not merely the event itself.

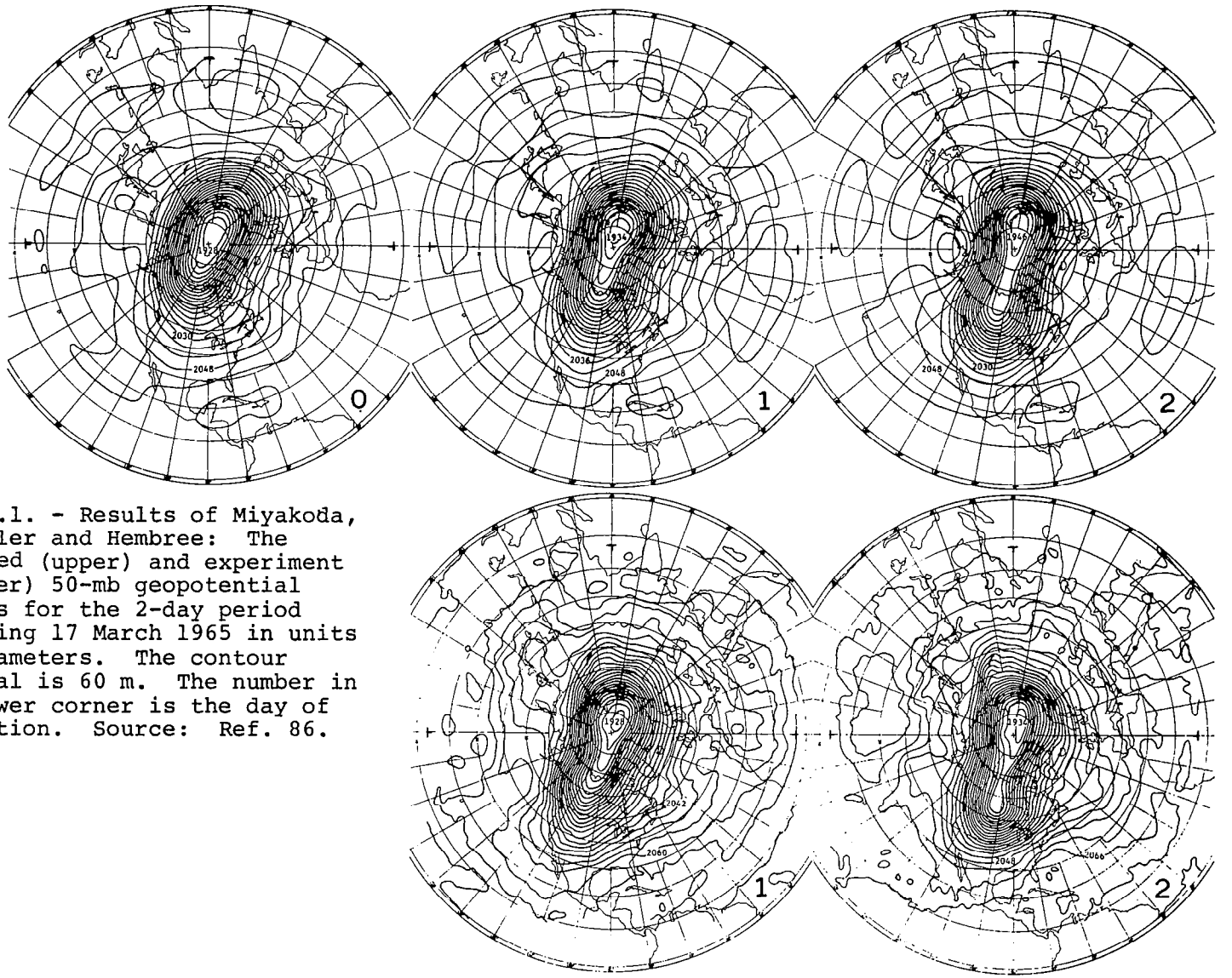

Figure 6.1. - Results of Miyakoda, Strickler and Hembree: The observed (upper) and experiment A (lower) 50-mb geopotential heights for the 2-day period beginning 17 March 1965 in units of decameters. The contour interval is 60 m. The number in the lower corner is the day of prediction. Source: Ref. 86.

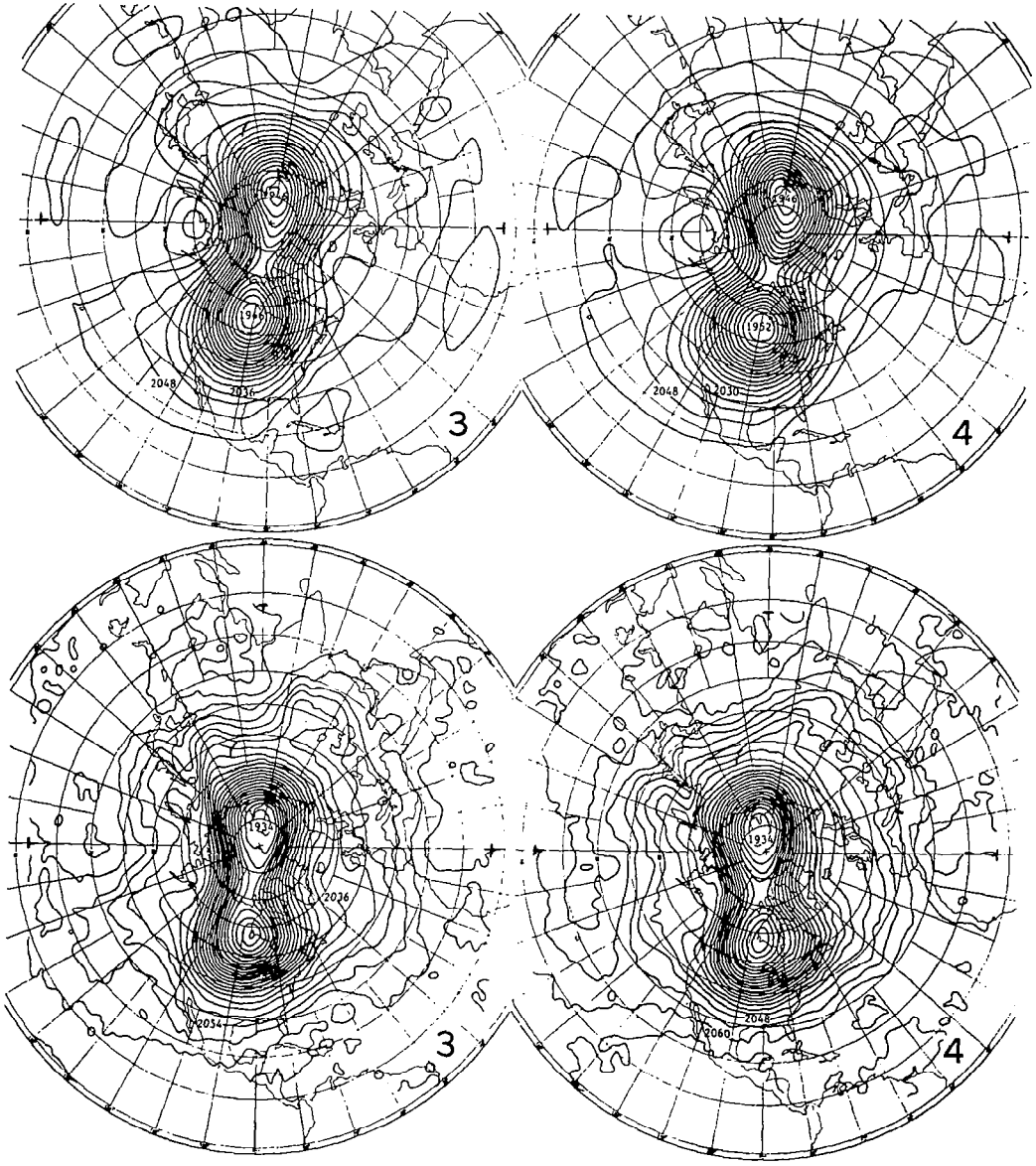

Figure 6.2. - Same as Figure 6.1, except for the following two days. Source: Ref. 86.

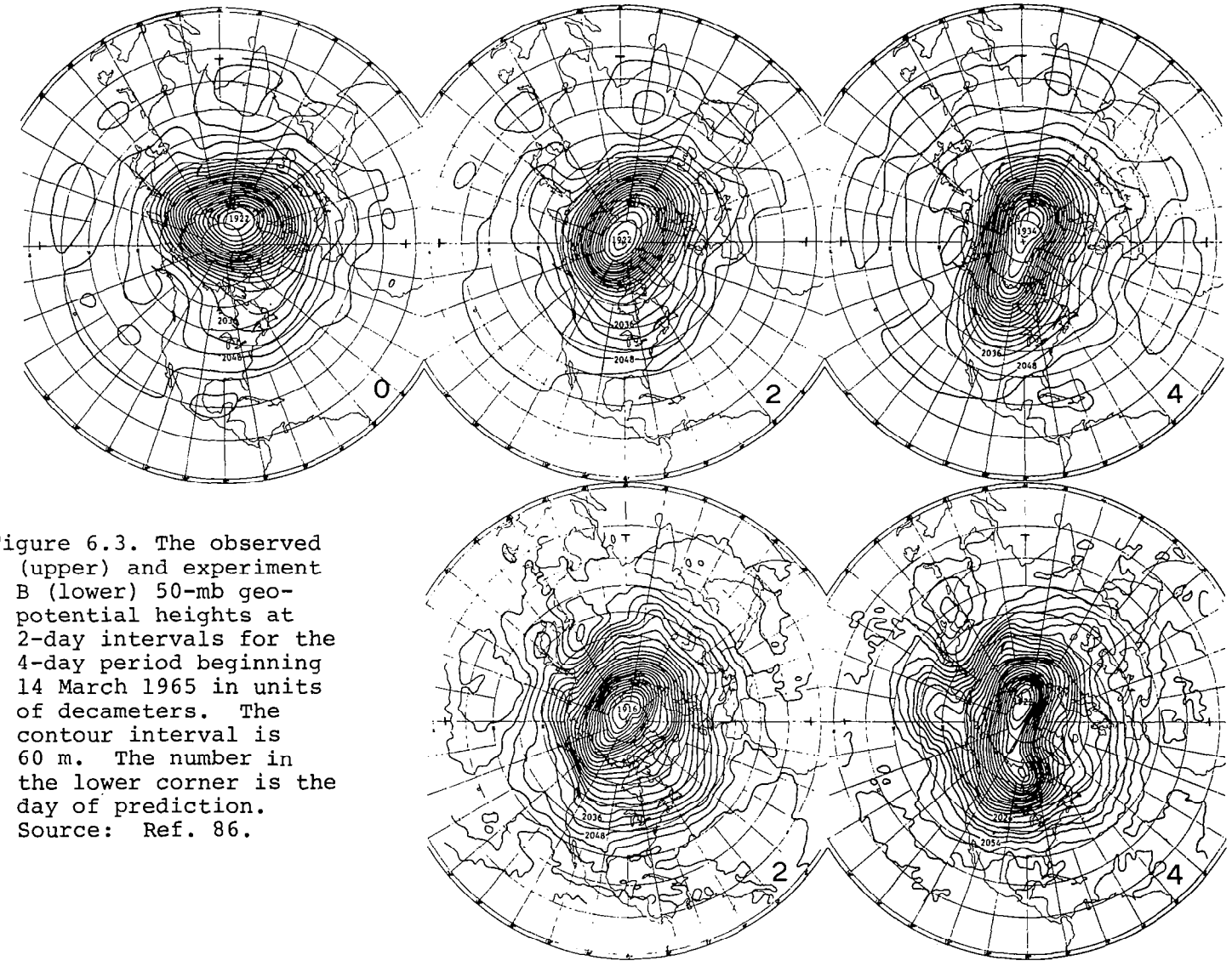

Figure 6.3. The observed (upper) and experiment B (lower) 50-mb geopotential heights at 2-day intervals for the 4-day period beginning 14 March 1965 in units of decameters. The contour interval is 60 m. The number in the lower corner is the day of prediction. Source: Ref. 86.

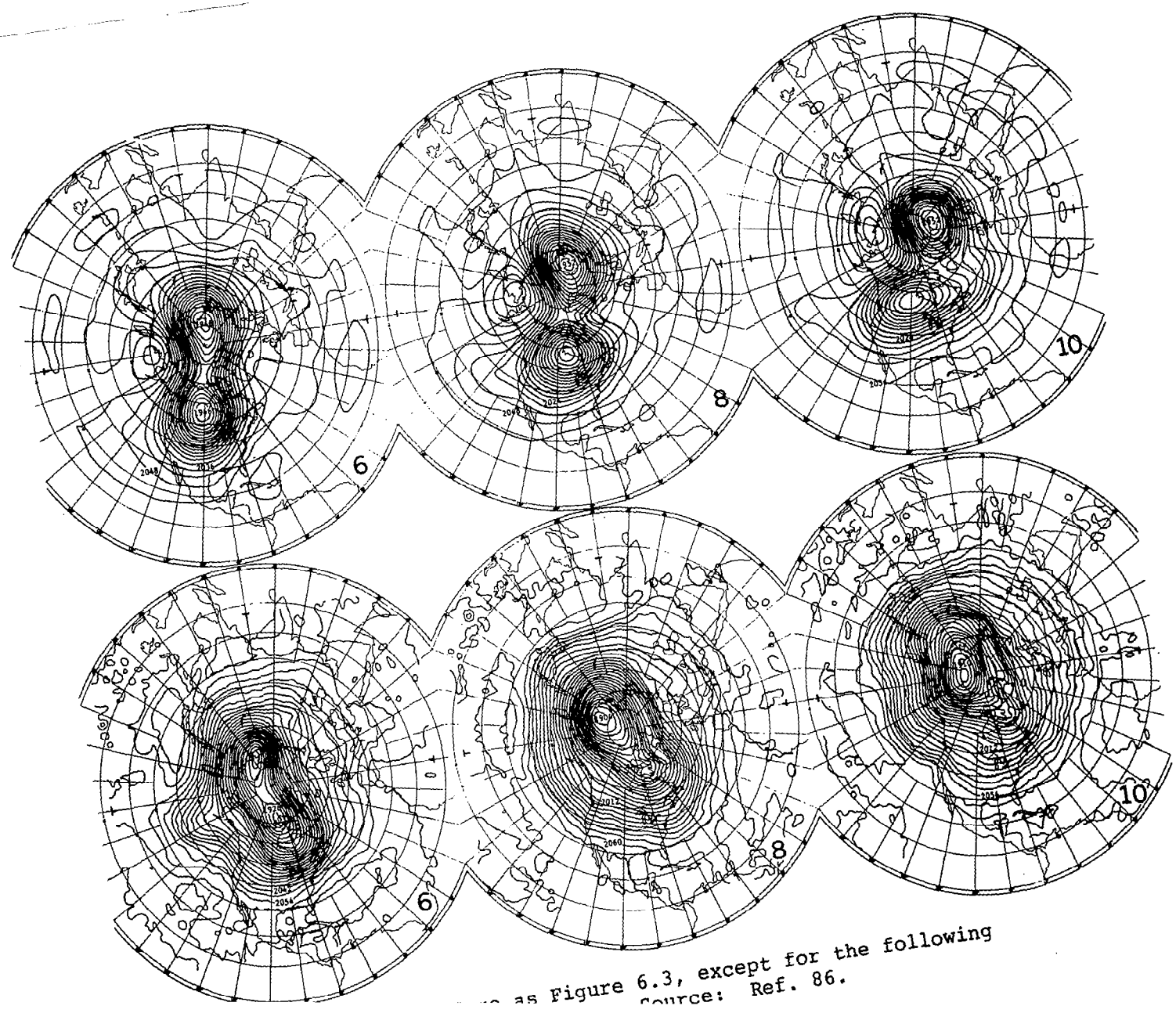

as Figure 6.3, except for the following
Source: Ref. 86.

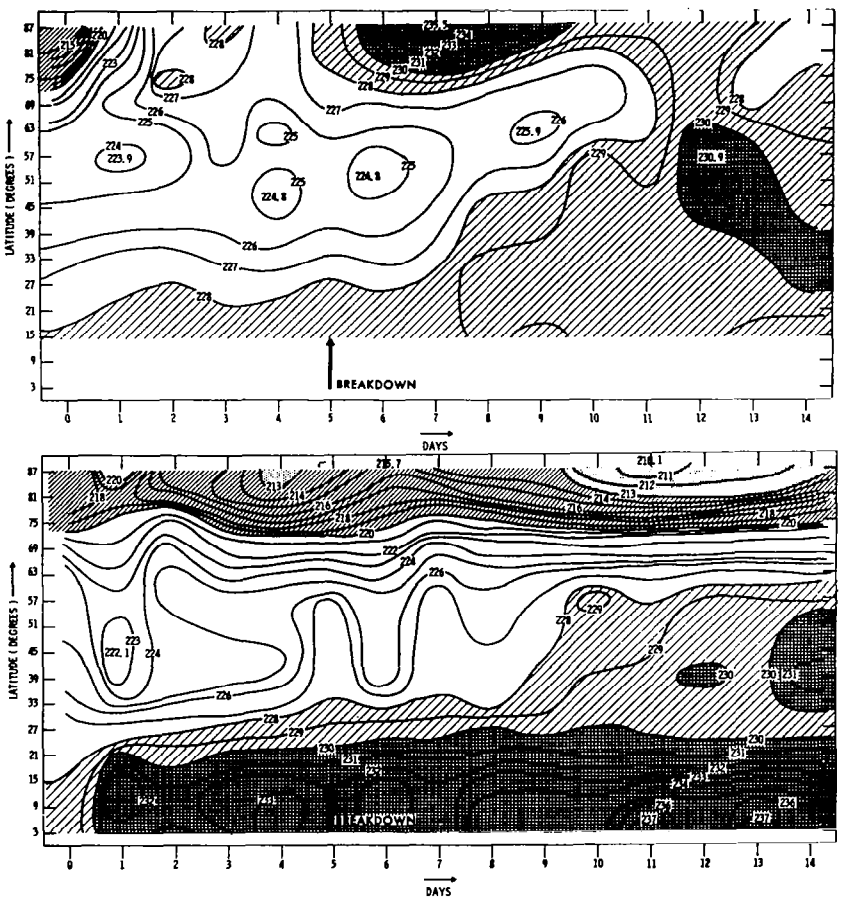

Figure 6.5. - The zonal average of temperature, observed (upper) and experiment B (lower), at level 1 in °K. Source: Ref. 86.

Climatological Models. - We discuss first the model of Manabe and Hunt (ref. 87). The overall prediction model employed in this study is basically very similar to that already described for the previous model. However, there are some very important differences. The first is that this is an 18-level model, as shown in Figure 6.6, with considerably greater resolution in the stratosphere. The top now is in the mid-stratosphere, $\sim$ 38 km, as compared with the previous one whose top level was at $\sim$ 32 km. Also, in this model neither mountains nor land-sea contrast are included, and it is basically dry. These latter items are pointed out, because it is now considered that they might be very important in determining the form and magnitude of the wave-energy flow from the troposphere to the stratosphere, and it is of interest to note the results when these items are not included.

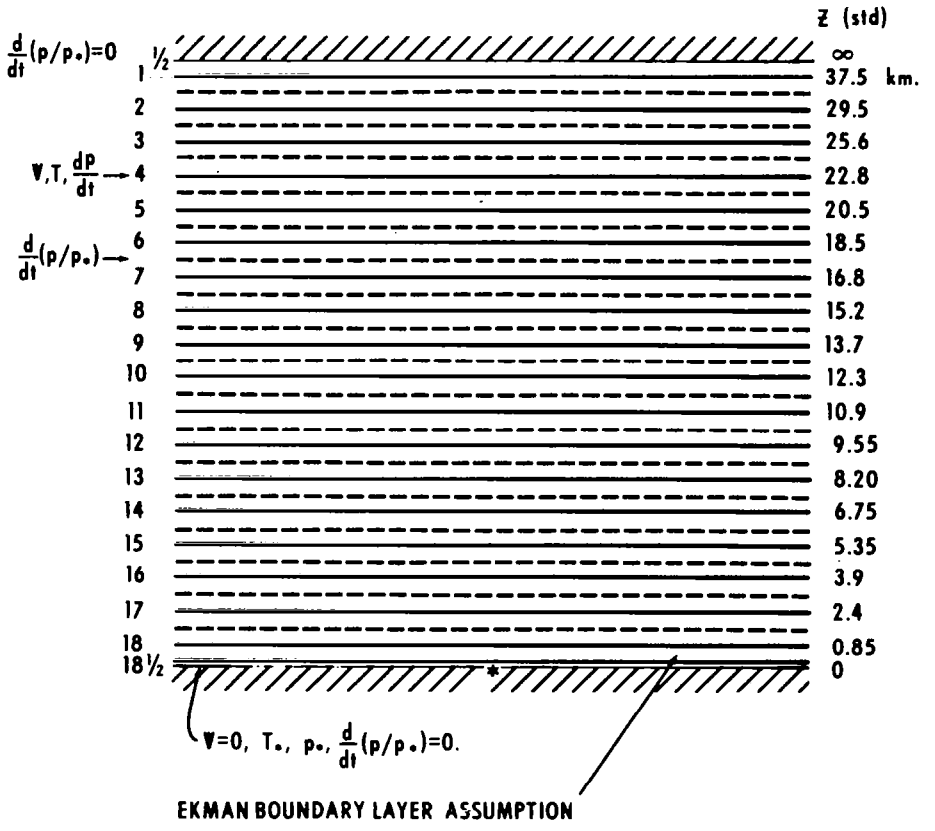

Figure 6.6. - The Q levels used in the Manabe-Hunt model and their approximate heights. The levels at which the model variables are predicted are indicated. Source: Ref. 87.

For this experiment, the model was started from the time-averaged zonal mean values of the zonal wind, pressure and temperature obtained by extrapolating and interpolating the data from the 9-level model, and a random temperature perturbation was applied at each point after 5 days to trigger baroclinic instability. Although this produced the desired effect in the troposphere, very little response was noted in the top few levels.

Figure 6.7a indicates the hemispheric variation of temperature, geopotential height and meridional velocity for day 80 at level 1, ∿ 37 km. This reveals that both temperature and geopotential height fields were fairly symmetrical at this time. Subsequent to this day the development appeared somewhat faster and the fields presented at 140 days (Figure 6.7b) show the amplification of the westerly wave, elongation of the polar vortex and the two-cell pattern in the height and temperature fields.

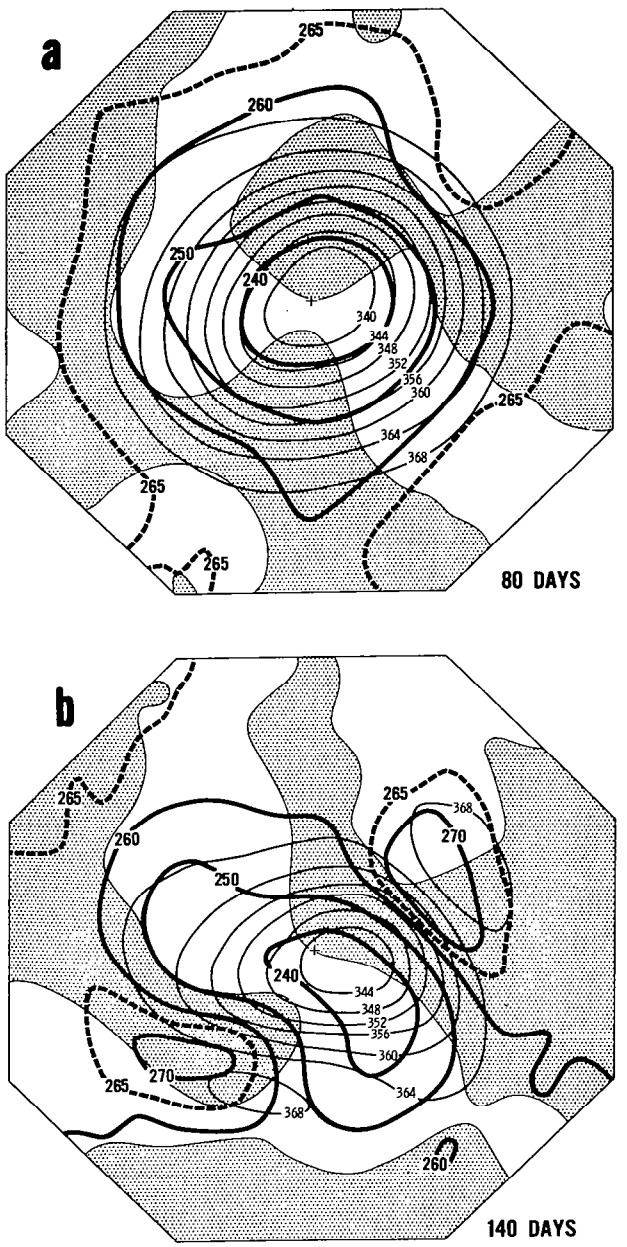

Figure 6.7. - The hemispheric variation of temperature (thick isolines), meridional velocity, and geopotential height (thin isolines) for the top level of the model at two different times illustrating the changes produced by the forcing from below. Shaded areas are regions of northwards velocity. Units: temperature, °K; geopotential height, 100 m). Source: Ref. 87.

If the effects shown in this diagram are attributable to a sudden onset of baroclinic instability, then it would be expected that the CE term for these levels (i.e., the conversion from AE to KE) would show a corresponding increase to supply energy for the development of the flow pattern. There was some increase in the release of potential energy during this period (Figure 6.8), but the corresponding change in the eddy pressure interaction term leaves no doubt that it is the supply of energy from the lower levels that is responsible for the observed perturbations. For the top level about 6 times as much energy came from below as was created in situ. This suggests that the increase in the conversion term at these times was caused by the changes produced in the flow patterns by forcing from below, rather than by genuine baroclinic development. The consequent increase in the eddy kinetic energy in the top three levels of the model is illustrated in the lower figure, and it is clear that it is closely related to the upward flux of energy. The reason for the sudden increase in the energy transfer from below is unknown, but it might be indicative of the kind of interaction which takes place in the middle stratosphere prior to a stratospheric warming. In this regard it is interesting to note that subsequent to the decline of the second impulse, the flow field in level 1 gradually returned to a more zonally symmetric state similar to that given in the previous figure. The possibility therefore exists that the first numerical simulation of a stratospheric warming may have occurred in this model, albeit accidentally.

The next results we will present under the category of Climatological Models are those of Newson (ref. 43), obtained from a general circulation model developed at the British Meteorological Office.

Basically, this model is a 13-level primitive equation model

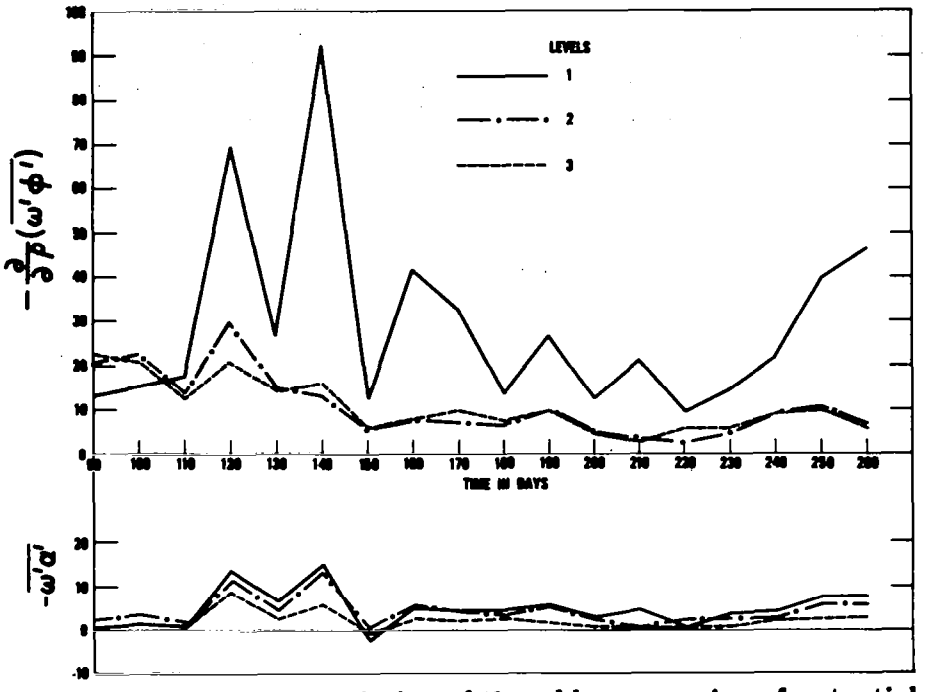

The time variation of the eddy conversion of potential energy and the eddy pressure interaction term for the top three levels of the model. Values are based on 10-day time averages. (Units: 10^{-1} erg cm.$^{-2}$ mb.$^{-1}$ sec.$^{-1}$)

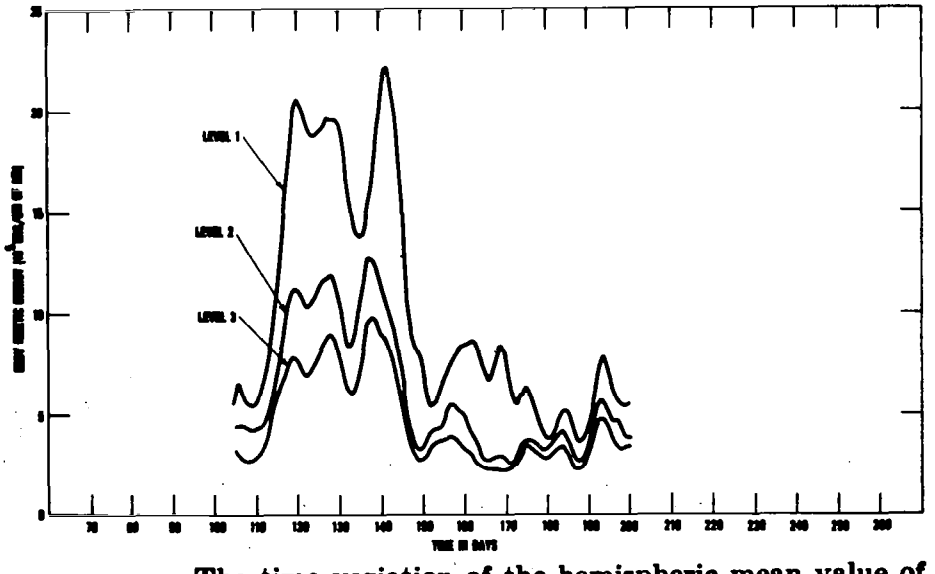

The time variation of the hemispheric mean value of the eddy kinetic energy for the top three levels of the model. (Units: 10^5 ergs/gm.)

Figure 6.8. - Source Ref. 87.

extending, as shown in Table 6.2, from approximately 1 to 44 km with good resolution in the stratosphere. It is for the Northern Hemisphere and includes topography, moisture and land-sea contrast. For the purposes of the particular experiment which we will discuss here, radiation was included via Newtonian cooling, and solar heating was set to January climatological values. As in the previous studies, the vertical motion was set equal to zero at the top.

TABLE 6.2

Level	σ	Approximate ICAO height in km if surface pressure is 1000 mb
1	0.0015	44
2	0.0058	35
3	0.011	30
4	0.020	27
5	0.032	24
6	0.049	21
7	0.074	18
8	0.117	15
9	0.196	12
10	0.319	9
11	0.493	6
12	0.695	3
13	0.896	1

The model was started from zonally averaged climatological values for January and was integrated out to about 160 days. In the stratosphere there was a slow intensification of the polar vortex. However, this process came to a halt at about 50 days' integration time, and from then to about 78 days the predicted state appeared to be one of quasi-equilibrium, possibly representing the model's January simulation.

Figure 6.9 depicts the 2-mb pattern of day 70 within this quasi-equilibrium period. The characteristic intense polar night vortex is apparent, although the central values of -80°C seem far too cold and the heights are correspondingly low. In addition, there is no evidence for an Aleutian anticyclone.

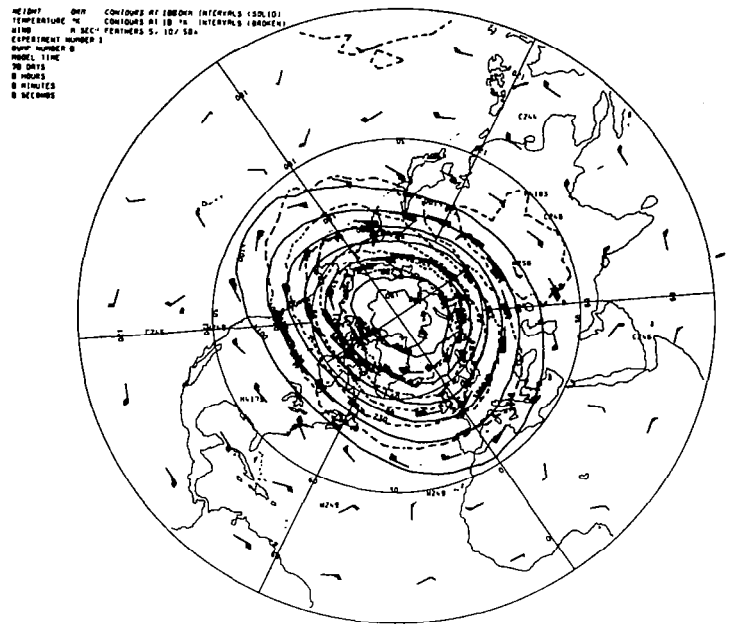

Figure 6.9. - Results from Newson's model: 2-mb chart for day 70. Source: Ref. 43.

Following this period, a sudden and dramatic change took place in the stratospheric circulation and temperature fields. This change is illustrated by Figure 6.10, which shows the 2-mb chart for day 90. The polar vortex has moved from the Pole and weakened considerably, while a high-pressure region has developed over Asia and is moving northward.

The same flow disruption and temperature rise occurred at all the stratospheric levels in the model, although the changes were less advanced at lower levels. Even at 100 mb there was an area of very warm air over the Bering Strait, and a marked ridge over the North Pacific. It is interesting to note that although this change became apparent almost simultaneously at all stratospheric levels, once initiated it proceeded much faster at high levels. Another feature of the change was the westward tilt with height of the axis of the warmest air. Overall, the changes that occurred in the model seem to resemble quite closely a stratospheric "sudden warming" event. (Quiroz, et al., ref. 41, discuss the resemblances more fully.)

The magnitude of the circulation disruption is depicted in Figure 6.11, which shows the latitudinally averaged zonal wind components at 90 days. The polar night jet has completed disappeared and has been replaced by easterlies almost everywhere in the stratosphere. Also there has occurred a reversal in the stratospheric temperature-gradient, with very pronounced warming near the Pole (Figure 6.12).

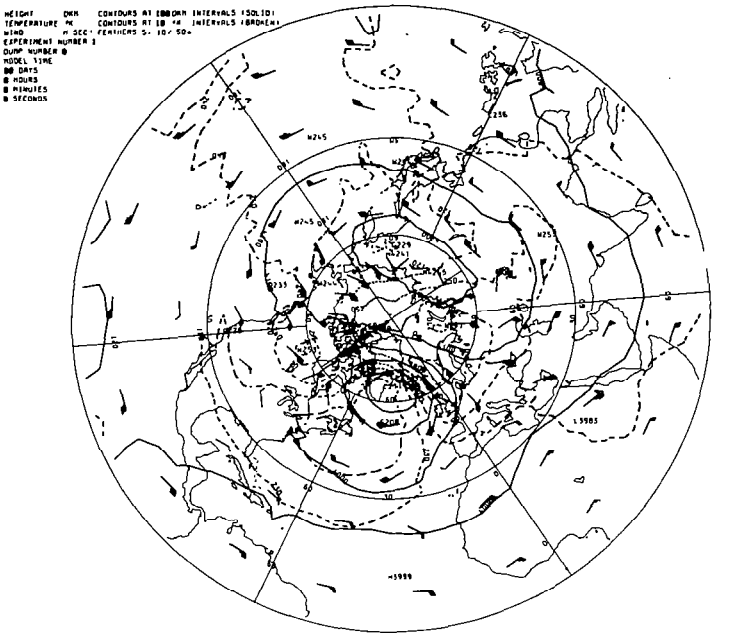

Figure 6.10. - 2-mb chart for day 90. Source: Ref. 43.

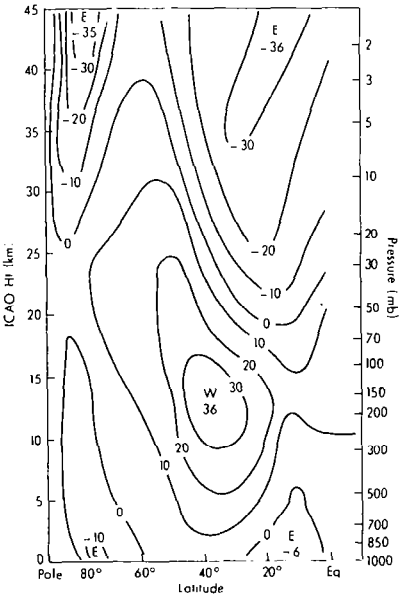

Figure 6.11. - Zonally meaned cross-section of zonal wind in m sec^{-1} for day 90. Source: Ref. 43.

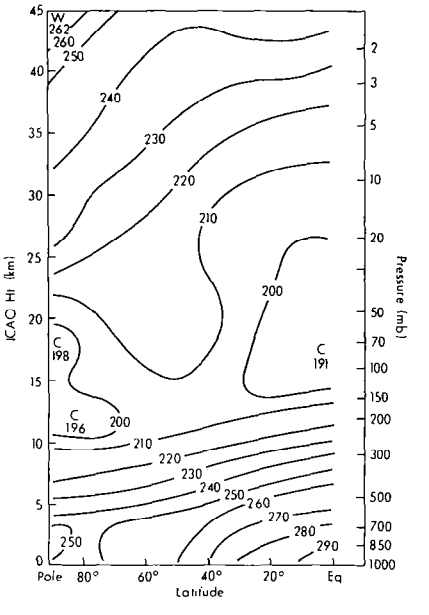

Figure 6.12. - Zonally meaned cross-section of temperature in °K for day 90. Source: Ref. 43.

The time required for the reassertion of more characteristic winter regime was much greater than seems to be characteristic of the real atmosphere. This aspect of the model's behavior is somewhat disappointing, in view of the fact that this experiment was a perpetual January simulation.

The essentially baroclinic nature of the circulation changes can be deduced from a study of Table 6.3 which gives values of energies and conversion terms in the top layer of the model (representing roughly 0-3 mb) during the warming period. The value of the baroclinic conversion term reached a maximum at day 80, coincident with rapid development of the warming. It is also evident from a study of values of the eddy kinetic energy that while the values of KE are increasing during this period, the loss from KE to KZ is much greater than the gain from PE thus indicating a source mechanism elsewhere. Presumably, this source would be the vertical flux of geopotential, but the author does not present values for this particular term. The relationships between changes in the various terms are similar to those calculated for the 1973 warming (Quiroz et al., ref. 41).

TABLE 6.3

Energies and Conversion Terms for Top Layer of the Model Atmosphere (representing 0 - 3 mb) During Warming Sequence

Day	P_Z	$C(P_Z,P_E)$	P_E	$C(P_E,K_E)$	K_E	$C(K_Z,K_E)$	K_Z	$C(P_Z,K_Z)$
70	435	138	39	85	308	-245	1760	-85
71	433	156	63	43	378	-175	1716	-80
72	426	155	90	68	476	-258	1656	-103
73	414	269	102	165	572	-449	1614	-146
74	398	258	126	74	613	-460	1601	-134
75	391	215	145	117	593	-472	1638	-150
76	385	199	148	69	543	-431	1693	-139
77	395	242	156	80	458	-494	1757	-158
78	402	320	151	193	387	-598	1795	-230
79	363	430	175	250	561	-653	1643	-285
80	197	564	279	425	1072	-1158	1294	-363
81	53	449	316	264	1527	-1167	1016	-262
82	9	114	300	19	1840	-670	709	-58
83	83	-142	198	-403	1726	-101	467	96
84	92	-222	312	-132	1366	38	349	62
85	54	-145	259	-110	1239	-45	293	55
86	54	-154	213	-178	1027	-126	333	90
87	81	-216	193	-271	854	-50	359	121
88	58	-142	147	-25	703	-190	392	55
89	17	-2	108	-49	681	-36	353	5

P_Z = zonal available potential energy
P_E = eddy available potential energy
K_Z = zonal kinetic energy
K_E = eddy kinetic energy
Units of above terms are 10^{-3} J gm^{-1}

$C(P_Z,P_E)$ = conversion from P_Z to P_E
$C(P_E,K_E)$ = conversion from P_E to K_E (i.e., "baroclinic" conversion)
$C(K_Z,K_E)$ = conversion from K_Z to K_E (i.e., "barotropic" conversion)
$C(P_Z,K_Z)$ = conversion from P_Z to K_Z
Units of above terms are 10^{-3} J gm^{-1} • day^{-1}

We turn next to the model of Cunnold, Alyea, Phillips and Prinn (ref. 88). This model is based on the "quasi-geostrophic" equations of motion where the variables are expressed in terms of spherical harmonics with maximum planetary wavenumber 6. The vertical extent, as shown in Table 6.4, is from the ground to $\sim$ 70 km utilizing 26 levels at $\sim$ 3 km height intervals. The effect of mountains is included in the model, and diabatic heating in the troposphere is parameterized as a linear function of temperature. Once again the vertical motion is set equal to zero at the top level.

TABLE 6.4. - PRESSURE, APPROXIMATE HEIGHT, AND STATIC STABILITY (K)† FOR MODEL LEVELS

Level j	Z	p (mb)	z (km)	K
1	10.14	0.04	71.6	41.0
2	9.73	0.06	69.0	43.1
3	9.33	0.09	66.3	46.1
4	8.92	0.13	63.5	48.2
5	8.52	0.20	60.6	49.7
6	8.11	0.30	57.6	50.0
7	7.70	0.45	54.5	52.0
8	7.30	0.68	51.4	64.9
9	6.89	1.01	48.2	82.9
10	6.49	1.52	45.0	90.3
11	6.08	2.28	41.9	88.2
12	5.68	3.43	38.8	85.3
13	5.27	5.14	35.9	82.9
14	4.87	7.71	33.0	81.4
15	4.46	11.6	30.2	80.5
16	4.06	17.3	27.5	78.1
17	3.65	26.0	24.8	75.1
18	3.24	39.0	22.2	70.9
19	2.84	58.5	19.6	64.9
20	2.43	87.8	17.1	58.0
21	2.03	132	14.6	46.4
22	1.62	198	12.0	37.4
23	1.22	296	9.3	29.9
24	0.81	444	6.4	20.9
25	0.41	667	3.4	20.9
26	0.00	1000	0.1	(23.9)

†$K = \frac{dT_s}{dZ} + \frac{R}{C_p} T_s$

The set of chemical reactions included in the model is presented in Table 6.5. We see that in addition to the standard Chapman reactions, they have include 3 NO_x reactions and above 50 km the two HO_x reactions. Not included is the effect of HNO_3, which would have greatly complicated the model.

TABLE 6.5. - REACTIONS USED IN THE MODEL. M DENOTES ANY THIRD BODY AND $h\nu$ AN ULTRAVIOLET PHOTON.

	Reaction	Reference†
1.	$O_2 + h\nu \rightarrow 2O$	Ackerman (1971); Kockarts (1971)
2.	$O + O_2 + M \rightarrow O_3 + M$	Garvin and Hampson (1973)
3.	$O_3 + h\nu \rightarrow O_2 + O$	Ackerman (1971)
4.	$O + O_3 \rightarrow 2O_2$	Garvin and Hampson (1973)
5.	$NO + O_3 \rightarrow NO_2 + O_2$	Schofield (1967)
6.	$NO_2 + O \rightarrow NO + O_2$	Davis (1973)
7.	$NO_2 + h\nu \rightarrow NO + O$	Hall and Blacet (1952)
8.	$OH + O \rightarrow O_2 + H$	McElroy et al. (1974)
9.	$HO_2 + O \rightarrow O_2 + OH$	McElroy et al. (1974)

†These references are to be found in the "Additional Bibliography," pages 163-166.

Initially, the temperature field is set equal to a Standard Atmosphere Temperature profile and the stream functions are set equal to zero. The model is started up from 44 days prior to the spring equinox (early February) and a model year is composed of twelve 30-day months.

A typical daily synoptic map of geopotential height for the end of January (Figure 6.13) shows the typical zonal flow in summer and planetary wave structure in winter. (It should be noted that in these results orographic effects were inadvertently omitted, and the Southern Hemisphere is modeled from a summer Northern Hemisphere, rather than as a true January Southern Hemisphere.)

When the model was run for a period of several years, evidence was obtained which suggested rapid stratospheric temperature changes. Figure 6.14 depicts annual cycles of temperature at 50°N and two longitudes 80°E and 100°W. The data shown are from year 2 of the calculations at $\sim$ 2 mb. The model results give large warmings during several periods in both the Northern and Southern Hemispheres (Figure 6.15). The warmings appear to propagate westward with time and occur several days later at the 10-mb level than at the higher 2-mb level. It is not clear, however, whether the above warmings actually reach the polar region and result in easterly winds there.

Hypothesis Testing. - The first model to be discussed under this specialized topic is that of Clark (ref. 89). This was the forerunner of the model used by Cunnold et al. (ref. 88); hence, we will focus on some of the principal differences in the gross features of the models. For a description of the differences in calculations of ozone absorption, etc., the reader is referred to the original papers.

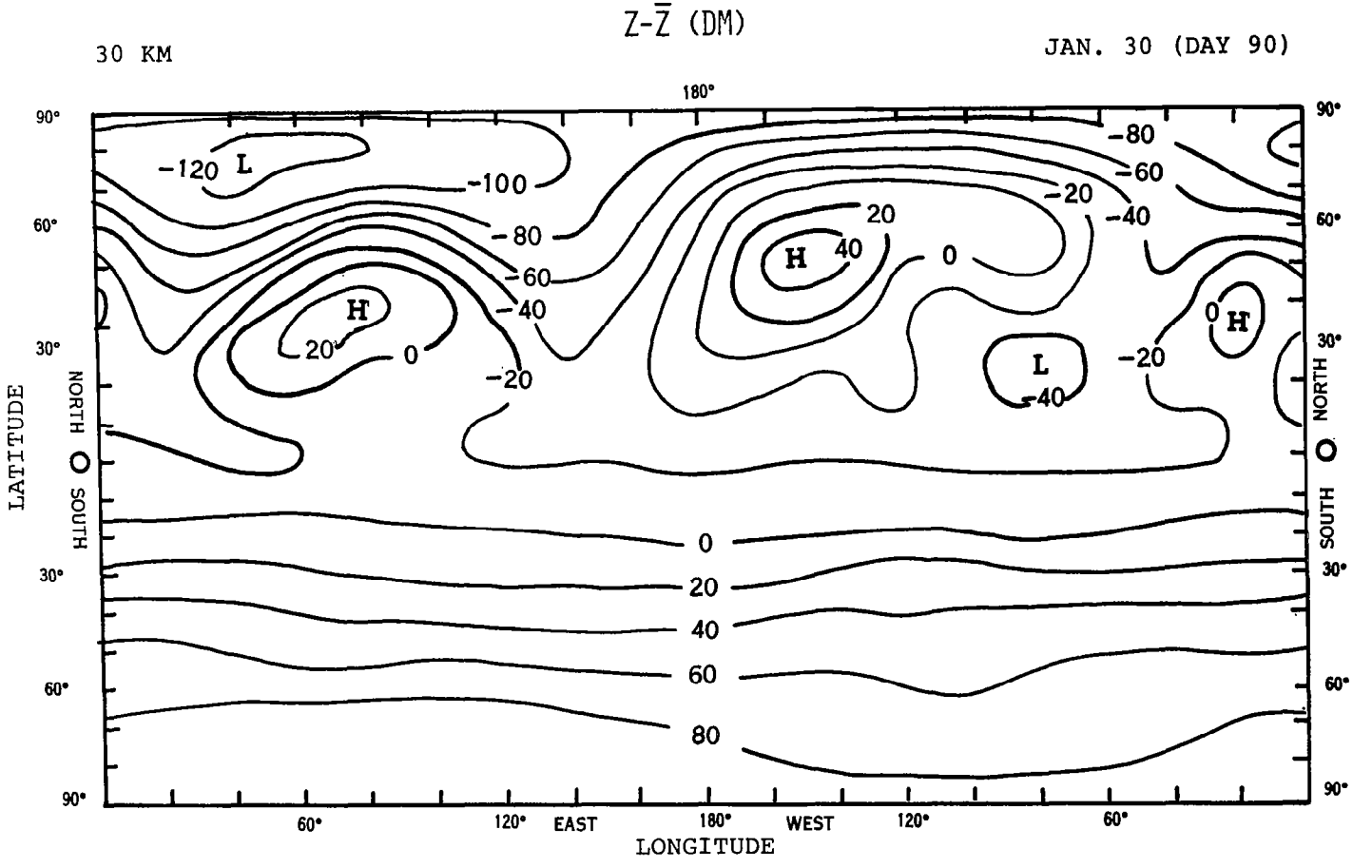

Figure 6.13. - A typical daily synoptic map of geopotential height (deviations from the mean zonal mean $\overline{Z}$ in decameters), showing the typical summertime zonal flow (Southern Hemisphere), and the wintertime planetary wave structure (Northern Hemisphere). Source: Ref. 88.

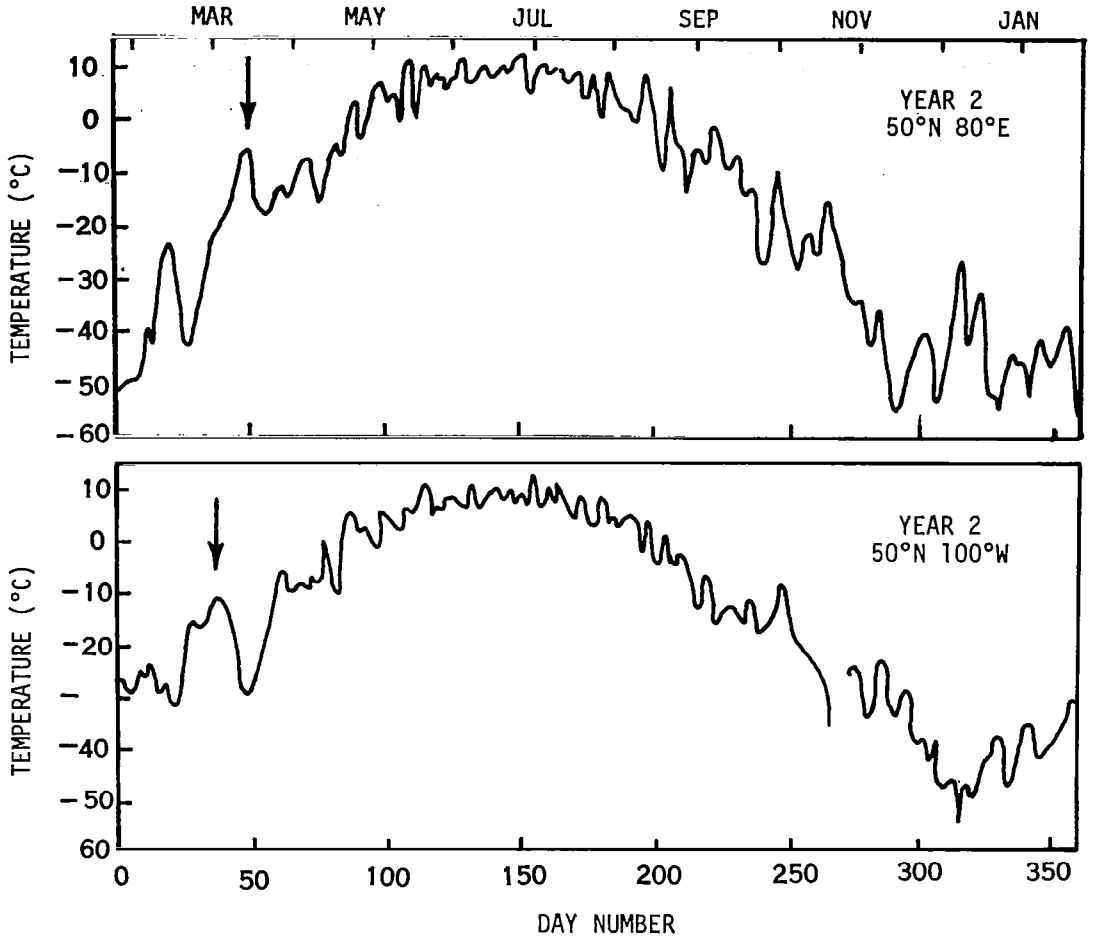

Figure 6.14. - Time-series of 2-mb temperatures, at 50°N, 80°E (top), and at 50°N, 100°W (bottom). Source: Ref. 88.

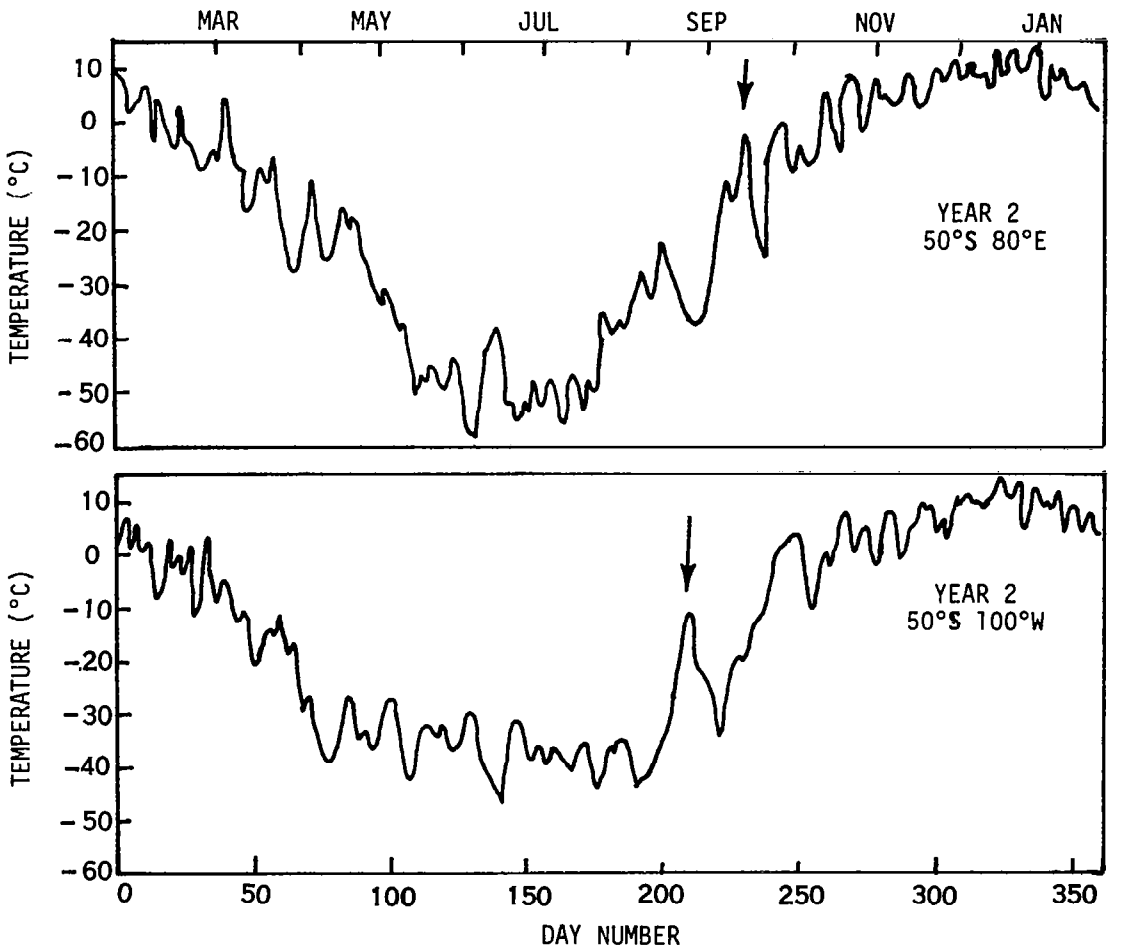

Figure 6.15. - Same as Figure 6.14, except for 50°S, 80°E (top) and 50°S, 100°W (bottom). Source: Ref. 88.

Figure 6.16 shows the vertical resolution of this model, with major emphasis on the stratosphere. Here the longitudinal wavenumbers are restricted to 1, 2, 3, and 6; and the effect of NO_x chemistry is not included. In addition, a Newtonian heating term (wave 2) is included at 5 and 25 mb to account for possible reflected solar radiation. The maximum amplitude of this disturbance is $\sim$ 10°K near 60°N with warm regions over western Europe and Alaska.

The model was first run as a climatological model and then as a test of the warming phenomenon.

The climatological model was initiated from a state of joint radiative-photochemical equilibrium, and, after the 120th day of the experiment, occasional spontaneous minor warmings occurred near the Pole. They usually originated at the height level of $\sim$ 5 mb and propagated downward reaching 100 and 200 mb from 4 to 7 days later.

Figure 6.17 illustrates, in terms of isolines of the departure of the polar temperature from equilibrium, one spontaneous warming that began on day 143. The temperature wave attained a maximum amplitude of 12°K at 25 mb. Little response was noted at 200 mb, and the troposphere was largely unaffected.

Stated simply, 1) the spontaneous warmings were related to increased forcing of the stratosphere by the troposphere, and 2) the rapid rises near the Pole were associated with adiabatic compressional heating in the mean meridional circulation (sinking motion at the Pole). At no time, however, did a spontaneous high-latitude warming develop into a major stratospheric warming (which would have reversed the latitudinal temperature gradient and replaced the polar vortex with an anticyclone).

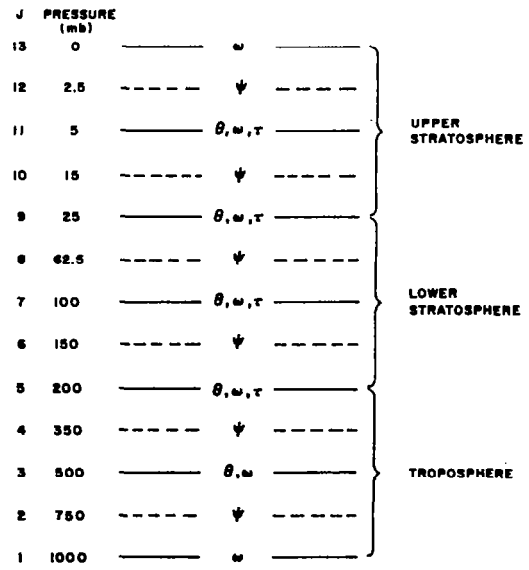

Figure 6.16. - Vertical resolution of Clark's model. Source: Ref. 89.

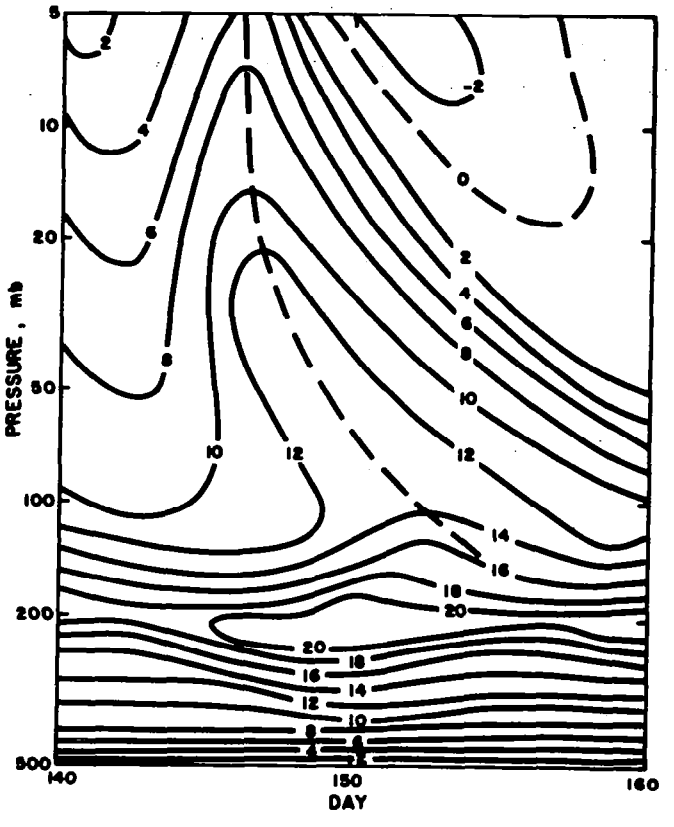

Figure 6.17. - Departure of polar temperature from equilibrium (°K) during spontaneous warming. Source: Ref. 89.

Following the suggestion by Charney and Stern (ref. 78) that the stability of an internal jet is strongly influenced by the temperature gradient near the ground, polar equilibrium conditions were altered on day 180 to simulate a cooling by 20°K through a deep layer extending from the ground to 500 mb. The zonally-averaged stream function field was then adjusted to maintain the geostrophic balance between the wind and thermal fields at all levels. The result was an increase in the maximum jet speed at 2.5 mb by 30 m sec^{-1} and a strengthening of the north-south wind shear at all latitudes. The experiment was then run for an additional 50 days to day 230.

After day 200, rapid temperature rises of 10° to 20°K occurred in the lower stratosphere near the Pole, with highest temperatures attained on day 209, Figure 6.18. This warming rapidly intensified as it spread upward to the upper stratosphere and resulted in polar warmings of 40° and 60°K at 25 and 5 mb, respectively. Maximum temperatures at 5 mb were attained on day 219, about 10 days later than at 200 mb. The most rapid heating occurred at 5 mb at a rate of about 50°K in 5 days. The latitudinal temperature gradient at 25 mb was completely but only briefly reversed, while at 5 mb it changed sign north of 50° latitude only.

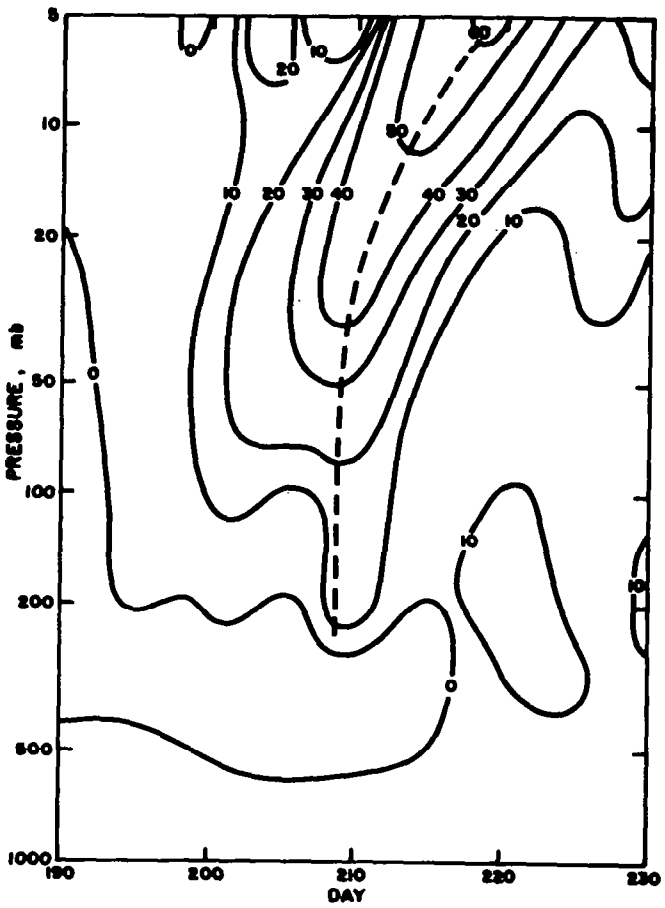

Figure 6.18. - Departure of polar temperature from equilibrium on day 180 (°K) during stratospheric warming. Source: Ref. 89.

Prior to the warming, the stratospheric flow pattern consisted of strong westerlies circulating about an eccentric polar vortex. As the warming proceeded from day 210 to day 220, the vortex elongated into a principally wavenumber-2 pattern and split into two centers over Asia and North America. At the same time, the warm Alaskan ridge extended northward to the Pole, isolating cold pools over Asia and North America and leaving a warm pocket near the Pole.

The stratospheric jet was weakened considerably by the warming and temporarily shifted southward. It did not, however, break down completely, and it regained some strength toward the end of the experiment. A weak easterly flow of about 10 m sec^{-1} appeared for a short period near the Pole in the upper stratosphere.

The two-cell mean meridional circulation persisted through most of the warming except during the period of maximum temperature rises when it reversed to give strong subsidence at the Pole in the same manner as in the spontaneous high-latitude warmings.

The energy cycle of the lower stratosphere on day 207, at the peak of the warming in this region, indicates that the major energy transfers were from the troposphere at the rate of over 3000 erg cm^{-1} sec^{-1}. This is approximately 4 times greater than the largest transfers ever observed during any warming period and thus raises questions about the applicability of these results. For example, it would be interesting to determine the relationship of the tropospheric-stratospheric interaction and the observed upward propagation of the warming at the Pole noted earlier.

Matsuno (ref. 42) has carried out an extensive numerical simulation, based on the concept of interaction between vertically-propagating planetary-waves and the zonal wind. Such interaction is believed to occur when the waves reach a critical level at which the relative zonal wind velocity is zero (i.e., at which the phase velocity of the waves is equal to the zonal wind velocity).

Before we consider the results from his numerical experiment, it is helpful to study the proposed mechanism of interaction in a very simple way.

Consider an atmosphere bounded laterally by vertical walls at two latitudes, and extending infinitely in the vertical direction (Figure 6.19, from Matsuno, ref. 42). Assume that the basic wind is a function of height only and that the planetary wave, propagated from far below, transports no horizontal momentum. Forcing of the mean height change then occurs only when horizontal heat transport varies with height.

Consider a situation in which the basic wind profile has a critical level at the height z_c. In this case, by the mechanism proposed, the heat flux jumps from a positive value to zero in crossing z_c (Figure 6.20). The zonal mean heights tend to rise in higher latitudes and to fall in lower. Corresponding to this distribution of $\partial\bar{\phi}/\partial t$, negative $\partial\bar{u}/\partial t$ (easterly acceleration) is distributed over almost all of the meridional section, with its core at middle latitudes. The time-change of zonal mean temperature is shown in the right side of this figure. Just below the critical level a region of marked warming is found at higher latitudes, while at lower latitudes cooling of the same magnitude appears. The temperature tendency above the critical level is opposite to that below the level, but much smaller in magnitude.

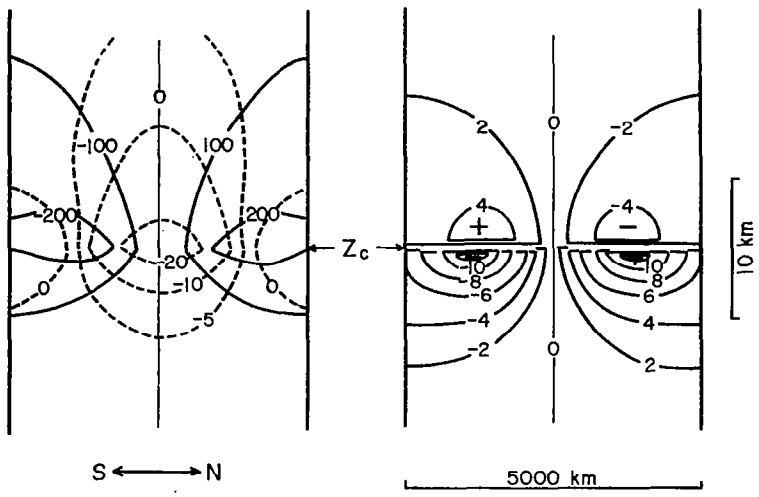

Figure 6.19. - Aspects of Matsuno's model: the changes of zonal mean fields caused by planetary waves incident on a critical level, as shown in the meridional plane. Left: time change of isobaric heights (solid lines, m day^{-1}), and that of zonal winds (dashed lines, m sec^{-1} day^{-1}). Right: time change of temperature (°C day^{-1}). The amplitude of the planetary wave at the critical level is assumed as 500 m. Source: Ref. 42.

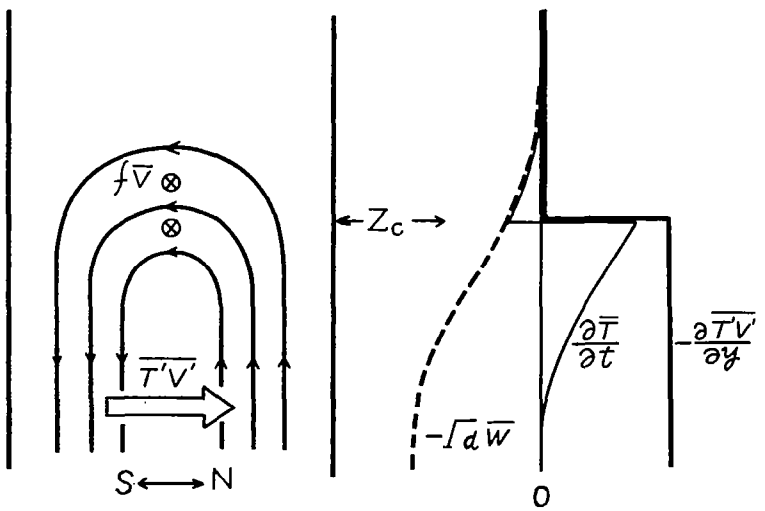

Figure 6.20. - Schematic illustration of the mean meridional circulation induced by the waves (left), and the vertical distribution of temperature change components (right) showing eddy heating (thick solid lines), mean vertical motion (dashed lines), and resultant temperature change (thin solid lines). Source: Ref. 42.

A schematic picture of the mean meridional circulation is illustrated in the left of Figure 6.20. Since upward propagating planetary waves accompany poleward heat transport (ref. 67), there is a heating tendency at higher latitudes and cooling at lower, as a result of flux divergence. These effects force zonal mean upward motion at higher latitudes and downward motion at lower latitudes. The forced vertical motions diminish above the critical level because the heat transport vanishes there. Then there must be a flow from higher to lower latitudes near the critical level for the continuity of mass flux. The Coriolis force acting on this "wave-induced meridional circulation" is the origin of the easterly acceleration.

The temperature change results from the balance between the eddy heating and the effect of the mean vertical motion. Below the critical level the former effect exceeds the latter and hence warming occurs at higher latitudes. Above this level, only vertical motion causes temperature changes. Note that temperature changes are very small at atmospheric levels far removed from the critical level.

Next consider the situation where the basic wind is everywhere westerly. The planetary waves are in a transient state of upward propagation. In other words, assume that the waves are generated and transmitted from far below and that the leading edge of the waves has reached a certain height z_f by the time under consideration. Far below z_f the waves may decrease with height in the vicinity of z_f. The forcing to the zonal mean field is essentially the same as the one in the former situation. The only difference is that in this case the forcing is distributed through a finite range of z near z_f, while in the former case it was so concentrated at the critical level that it was expressed in terms of the delta function. Therefore, the zonal wind acceleration and the temperature change caused by the present forcing should be similar to those shown in Figure 6.19 and 6.20, except that they are more diffused. Thus it is concluded that upward propagating planetary waves accompany easterly acceleration of zonal winds and warming of the air in the higher latitude side, when the waves are in a stage of amplification.

So far, we have considered only those cases where no momentum transport is associated with the waves. If a horizontal flux of zonal momentum exists, the situation may be quite different.

In an attempt to verify this conceptual model, Matsuno employs a numerical model in which the adiabatic-geostrophic potential vorticity equation is integrated in time from 10 km to 100 km, employing prescribed boundary conditions.

The model's properties are shown in Table 6.6. The amplitude of the waves forced at the lower boundary is shown in Figure 6.21. The same forcing function is used for longitudinal wave components 1-3 although each wavenumber is treated in a separate calculation. The initial distribution of zonal wind, which can obviously play a very important role in the prescribed mechanism, is shown in Figure 6.22. Note the easterly winds in the tropics at $\sim$ 40 km, as they will be very relevant to the later discussion.

TABLE 6.6. - SUMMARY OF MATSUNO's MODEL

Important Model Properties: Spherical geometry, planetary-scale, (almost) quasi-geostrophic; designed to propagate vertically a single planetary wave (1, 2, or 3) introduced into the geopotential field at 10 km; and planetary waves forced changes in zonal wind field.

Grid Domain*: Vertical--$10 \leq h \leq 1\text{-}0$ km with 2.5 km resolution; horizontal--$0° \leq \theta \leq 90°$, with 5° resolution; and time step--1 hour.

Initial Conditions: No initial disturbances; specification of mean stream field (i.e., wind and temperature), critical.

Boundary Conditions*: Bottom--$\psi = F(\theta,t)$, $\partial\bar{\psi}/\partial t = 0$; top--$\psi = 0$, $\partial\bar{\psi}/\partial t = 0$; and Equator and Pole--$\psi = 0$, $\partial/\partial t(\partial\bar{\psi}/\partial\theta) = 0$.

Forcing Function: $F(\theta,t) = \sin[\pi(0\text{-}30°)/60°]\ \phi_{max}\ f(t)$ with f(t) specified similar to wavenumber 2 variation during warming of January-February 1963 and $\phi_{max} = 300$ m; tests indicate importance of tropospheric simulation for obtaining sudden warmings.

Results: In general, upward propagation of eastward acceleration, yielding slowing of westerlies and, in time, development of a critical layer at high altitude. Absorption of energy by critical layer than leads to heating. Easterly winds accelerated below level of critical layer, and layer continues to lower; thus, warming and wind reversal shift downward in time.

(1) Resemblances to Real Warming: Magnitude of temperature change about 40C to 80C (perhaps slightly high for wave 2); time of development, 15-20 days (perhaps a little slow for wave 2); height of warming layer, 30-40 km (good for wave 2); and moves northward with time.

(2) Differences from Observations of Warmings: Sudden, rather than gradual, weakening of westerly jet at high latitudes, and eventual establishment of easterly jet, exaggerated by model; exaggerated amplitude of warming and 80 mps easterlies at high latitudes; and does not show observed temperature differencs between the two warm centers of a wave 2 warming.

(3) Why doesn't warming occur every winter? Ordinarily planetary wave energy is refracted towards low latitudes, but exceptionally intense planetary waves at bottom and special configurations of mean zonal temperature and velocity fields yield propagation toward north.

*Legend:
- z = height
- θ = latitude
- t = time
- ψ = disturbance height of isobaric surface
- $\bar{\psi}$ = zonal average height of isobaric surface

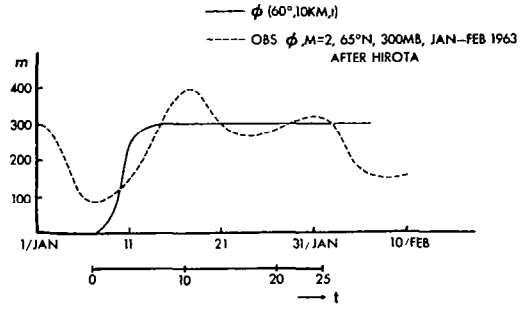

Figure 6.21. - Amplitude of the waves forced at the lower boundary (solid line). The dashed line shows the observed amplitude of the m = 2 wave at 300 mb in January-February 1963 (data from Dr. I. Hirota). Source: Ref. 42.

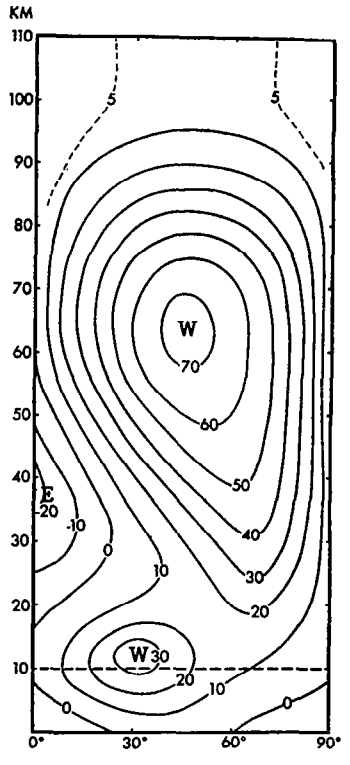

Figure 6.22 - Initial distribution of zonal winds, adopted as the initial condition for cases C1-C3. Source: Ref. 42.

Results of case 1 (zonal wavenumber 1) are shown in Figure 6.23, as time-height sections of $\bar{u}$ at 60°N and $\bar{T}$ at the Pole. Two separate easterly layers, accompanying each warming, are recognized at $\sim$ 25 and $\sim$ 65 km. Whether an easterly jet appears or not depends on the outcome of a complicated balance between the initial wind speed and accumulated amount of wave-induced acceleration. We might have two regions of easterlies, more or less independently. Apart from this peculiarity, the magnitude of temperature change ($\sim$ 40C) and the timing of the occurrences ($\sim$ 15 days for prewarming stage and $\sim$ 5 days for sudden warming) are reasonable. The easterly wind of 80 m sec^{-1} may be too strong.

In Figure 6.24 the results of case 2 (zonal wavenumber 2) are shown, in the same manner as in the former case. In the present experiment the warming occurred in one layer. The temperature rise of 80C at the Pole may not be too high, but easterly winds exceeding 60 m sec^{-1} are unrealistic, although some research indicates that easterly winds of this magnitude resulted during the January 1973 warming. It should be borne in mind that with this model we are dealing with a rather unrealistic situation, involving, for example, endless forcing, no dissipative effects whatever, etc. The height of the warming layer, 20-45 km, is comparable with that in the

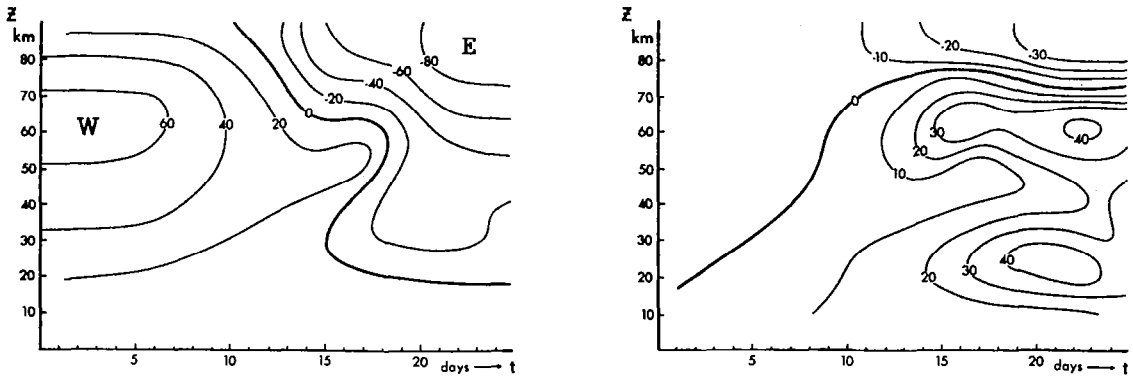

Figure 6.23. - Time-height sections of case C1: a) of the mean zonal wind at 60°N; b) of the temperature (deviation in °K from the initial temperature) at the Pole. Source: Ref. 42.

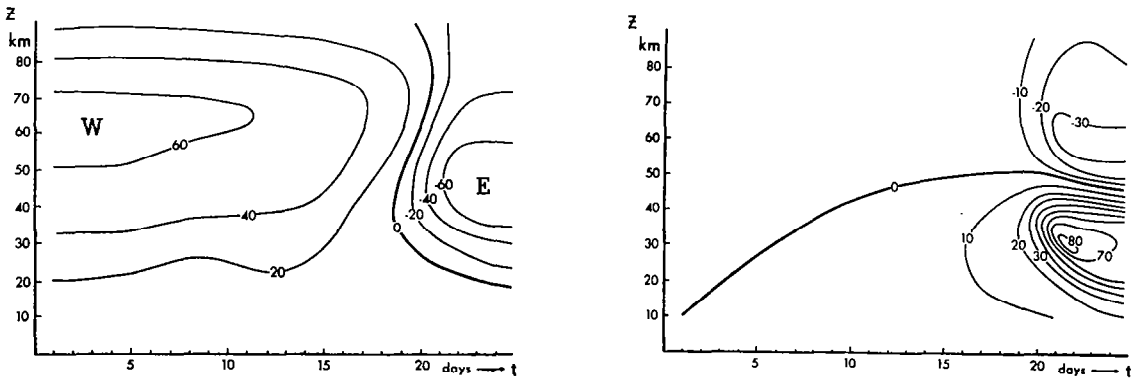

Figure 6.24. - Same as Figure 6.23, except for case C2. Source: Ref. 42.

observed event. The appearance of a cooling layer above the warming is at least consistent with an observation by Quiroz (ref. 40).

The results of case 3 (zonal wavenumber 3) are not spectacular and are not shown.

The functional form of the forcing in Matsuno's calculations was designed to fit roughly the zonal wavenumber 2 (m = 2) wave on the occasion of the 1963 sudden warming. This warming event was characterized by an unusual intensification of the m = 2 wave, almost exclusive of other components. (Compare the study of Byron-Scott, ref. 90.) Therefore, it seems worthwhile to study the synoptic patterns of the results of case C2. In Figure 6.25, heights and temperatures of the $\approx$ 13 mb surface at t = 10, 18, 20, and 22 days are shown.

It should be noted that the computed evolution of the event resembles the observed one in many respects: elongation and splitting of the polar cyclone, development of two anticyclones and their amalgamation over the polar region, slow westward movement of the entire system, etc.

Thus, these numerical results bear many similarities to the actual sudden warming event of 1963. However, in some respects, the results differ from the observed phenomena and also from what is expected from theoretical considerations. In the model it is postulated that the invasion of an intense disturbance will induce weakening of the westerly jet, and its eventual replacement by an easterly jet. However, the computed evolution is not so simple. By examining Figure 6.26, which is the time-latitude section of zonal winds at the 30 km level for case 2, one may note that the wind speed of the westerly jet decreases for the first 9 days, but then levels off. The disturbance seems to stop growing and to reach almost an equilibrium state. However, at lower latitudes, westerly winds continue to decrease and turn to easterlies. Since there are easterlies in the tropical region, the planetary waves decelerate the westerlies and produce further easterlies in the vicinity of the critical surface dividing westerlies from easterlies. The critical surface then shifts northward. After t = 15 days the disturbance increases again and propagates further upward owing to the weakening of westerlies in the middle latitudes. The weaker westerly winds are more favorable for wave propagation, as discussed theoretically by Charney and Drazin (ref. 91). Enhanced waves cause further deceleration until the polar night jet finally disappears at about t = 20 days. This chain of events occurred in the numerical model C2.

One may suppose that the existence of easterly winds in the tropical region and the mechanism described above are important factors in causing the sudden warming; however, the model calculation seems to exaggerate the effects. In tracing back, Matsuno finds that the origin of the discrepancy is the error in the computed wave 2 amplitude at earlier stages. The computed amplitude of the wave for T = 9-14 days, $\sim$ 50 m at 10 mb, is only half the observed value. It is therefore suspected that the present scheme of determining planetary wave propagation tends to underestimate the propagation of the m = 2 waves. If the amplitude of the wave were computed properly in the numerical model, the weakening of the westerly jet would occur sooner, and the critical-surface interaction in the tropical region might play a less important role in the present calculations.

In this model, the generation of a critical level in the high-latitude stratosphere is an essential requirement for the development of a sudden warming. Whether in fact this is a requirement of the real atmosphere

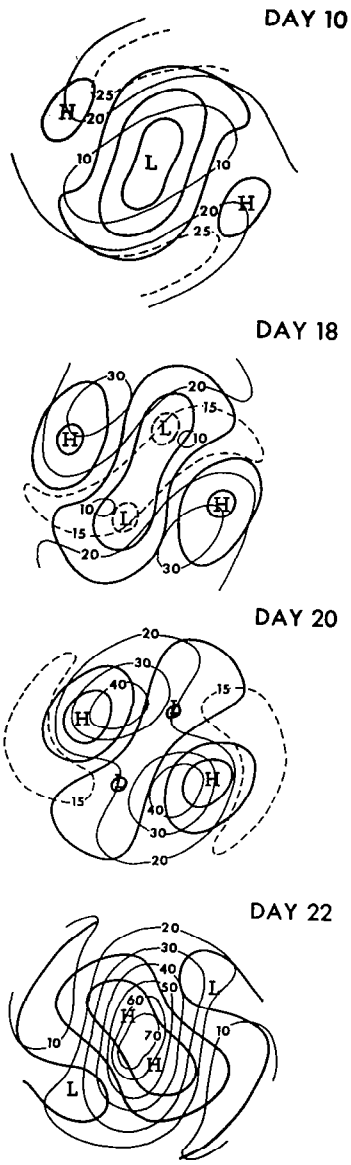

Figure 6.25. - Time evolution of isobaric height (500-m contours, thick lines), temperature (°C, thin lines), and the surface of $p = p_0 \exp(-30\ \text{km}/H) \approx 13$ mb for case C2. Temperature is shown as a deviation from its initial value at the Pole. The contours cover the area north of 30°N. Source: Ref. 42.

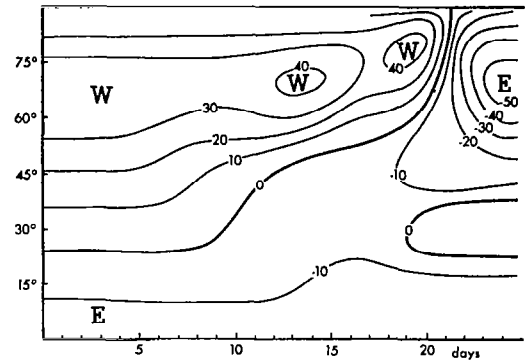

Figure 6.26. - Time-latitude section of mean zonal winds at $\bar{z}$ = 30 km for case C2. Source: Ref. 42.

remains to be seen. Furthermore, each wavenumber is considered separately. The author suggests that the simultaneous consideration of several wavenumbers (wave-wave interaction, in addition to wave-zonal flow interaction), or nonlinear treatments of planetary wave propagation, might have been more successful in simulating the wave-2 type warming.

Geisler (ref. 92) has developed a beta-plane model which, though simplified, preserves all of the qualitative features of the spherical model and produces quantitatively similar results for the beta-plane case of Matsuno (ref. 42). The purpose of the model is to study the effect of varying such parameters as the amplitude of the forcing wave, initial zonal wind configuration, and infrared cooling rates.

This model is a mid-latitude beta-plane channel with rigid vertical boundaries (cf. Table 6.7). Both zonal and eddy temperature fields are subject to dissipation by infrared damping, which is the only

TABLE 6.7. - SUMMARY OF BETA-PLANE MODEL WITH NEWTONIAN COOLING

(J. Geisler, "A Numerical Model of the Sudden Stratospheric Warming Mechanism," Journal of Geophysical Research, 79:4989-4999, November 20, 1974.)
Note: for notation, the original article must be consulted.

Assumptions: Quasi-geostrophic; mid-latitude, beta-plane (quasi-one-dimensional); north and south vertical boundaries; isothermal basic state; dissipative mechanisms--infrared damping of eddy and mean temperature fields, Newtonian cooling coefficient 6 day^{-1}; small-amplitude assumption; basic zonal flow $[u]_z$ independent of y; static stability $\sigma = kgH/p^2$ (H constant scale height of 7 km); no viscosity; $\psi' \sim$ vertical growth $\sim \exp(z/2)$; $\psi'(x,y,z,t) = \psi'(z/t) \exp(z/2) \cdot \sin(\ell y) \exp(ikx)$ (single wave); $u'v' = 0$; $\therefore q'v'$ due to $\partial/\partial z(v'T')$; and $\ell = k = 2$.

Boundary Conditions: At $z = 0$; $w' = f_o\rho \left(\frac{\partial}{\partial t} + [u]_z \frac{\partial}{\partial x}\right) \psi' - \rho g w'$; $Q' = 0$; surface heating independent of y; and $[w]_z = 0$ at $z = 0$ and $z = h$, (h = 130 km).

Initial Conditions: $\psi' = 0$ at $t = 0$; and w_s or heat source initiated at $t = 0$.

Wind Profile: $[u]_z = \{(\Delta U/2)[\ell + \tanh((z - z_c)/D)] + U_o\}$; $z = 5$ (35 km); $\Delta U = 62$ ms^{-1}; and $D = 1.8$ (12.6 km).

Standard Case: at $t = 0$ with $\ell = k = 2$; $U_0 = 19.7$ ms^{-1}; $U_0 + \Delta U \simeq 81.5$ ms^{-1}; and $w' = 0.25$ cm s^{-1}.

Conclusions: Frontal wave moves upward into stratosphere with oscillating potential vorticity transport below interacting with zonal flow. Increase in oscillating potential vorticity transport finally yields strong (irreversible) southward transport with maximum near 30-40 km. Zonal flow becomes easterly and warming descends. Variation of heat flux with altitude too gradual to permit ascribing descent of zero velocity line to critical layer absorption. Newtonian cooling attenuates warmings. Forcing must be maintained for at least 13 days. Resonant forcing secondary to amplitude of oscillatory transports.

dissipation process modeled. The initial zonal wind is a hyperbolic tangent profile increasing monotonically from a specified surface zonal wind, U_S (usually specified as 19.7 m s^{-1}), to approach asymptotically in the mesosphere a maximum zonal wind 62 m s^{-1} greater than at the surface.

Several different amplitudes of forcing functions are tested, both with and without Newtonian cooling. A stationary wave-two disturbance switched on at the lower boundary by either differential heating (land-ocean contrast) or vertical velocity (topography) causes a forced wave to move up into the stratosphere. Below the front of the forced wave, potential vorticity transport oscillates between northward and southward values and finally turns suddenly to a large southward value in the upper stratosphere. The zonal flow changes rapidly to easterlies with the region of easterlies decending into the middle stratosphere. At the same time, warming develops in the stratosphere and cooling in the mesosphere. This response is not substantially different with forcing under "resonant" conditions; i.e., conditions under which the excited waves are stationary.

Qualitatively realistic depictions of such parameters as mean zonal winds and temperatures are produced. However, whether or not Newtonian cooling is allowed, the model does not react in a manner that can be attributed to critical layer interaction. The variation of heat flux with height during the warming event is so small that it cannot be associated with absorption by a critical layer. Furthermore, the development of easterly winds occurs nearly simultaneously at all levels. Thus it is concluded that it is the transient waves excited by tropospheric forcing which "trigger" the subsequent breakdown of zonal flow. Consequently, both the strength of the zonal flow and the magnitude of the tropospheric forcing control the time of occurrence of the warming.

The results of this model are limited by the assumption that the eddy momentum flux is identically zero, and, therefore, all potential vorticity transport is associated with vertical variation of the eddy heat flux. Calculations in the present study show that both these terms are of similar magnitude and usually tend to be of opposite sign. Indeed, Charney and Drazin (ref. 91) and Dickinson (ref. 93) show that both terms are required in order to obtain the result of the vanishing of forcing of the mean zonal flow by the eddies. Hence the model omits one of the important sources of potential vorticity transport, which may limit the applicability of the results.

Another adaptation of Matsuno's model has been made by Holton (ref. 94). Again, a single harmonic wave interacts with the zonal flow, with a geometry similar to that of Matsuno, but the forecast equations are primitive rather than quasi-geostrophic. Another refinement is that gradient wind balance replaces the geostrophic balance used by Matsuno.

Holton's results are similar to Matsuno's, although the warming occurs later, and, in the case of the wave-one warming, is considerably weaker. Holton's results also cast doubt upon the validity of the "critical level interaction" mechanism proposed by Matsuno; however, there is a possibility that laterally propagating critical lines may be important.

Summary

There is at present no model that satisfactorily depicts or forecasts STRATWARMS. However, the partially successful efforts made to date suggest that researchers are heading in the proper direction. We undoubtedly require better observational results to feed back to the models. In particular, it is imperative that we obtain observational material on a) the question of the source of the tropospheric forcing mechanism that leads up to the increase in energy transfer to the stratosphere and b) how this wave energy flux interacts with the zonal flow. We can not, for example, simply depend on setting the vertical flux at the top = 0 to accurately depict the real atmosphere. The best obtainable information must be used in determining the boundary and initial conditions for the models.

The need is clear, then, for observational data with greater spatial and temporal resolution than has, heretofore, been available, and to higher altitudes.

OZONE IN CONNECTION WITH STRATWARMS

Of all the minor constituents in the stratosphere, ozone is by far the most important in terms of thermal energy. After being formed in the upper stratosphere or lower mesosphere, it is diffused or transported through vertical exchange processes to lower levels where it becomes a strongly conservative element and therefore serves as an excellent tracer. The importance of ozone to the biosphere is seen in the fact that it shields the earth from much of the sun's ultraviolet radiation. The possible anthropogenic breakdown or weakening of this shield has created a scientific controversy, with various theories formulated on the quantity of ozone depleted, the effects of depletion on the biosphere, and climatic impact.

Since the greatest circulation changes in the stratosphere occur during winter, it is expected that the largest and perhaps most important ozone changes will also occur during this period. The natural (non-anthropogenic) changes are of course important for an understanding of ozone sources and sinks. The natural variation must obviously be understood before any inferences can be made regarding anthropogenic influences.

As in other stratospheric measurements, the spatio-temporal density of conventional (in situ or ground based) measurements over the globe is extremely sparse and the differences between reported values from different techniques can be quite large, both for total ozone and for vertical profiles of ozone. Such measuring techniques will not be discussed here; the reader is referred to a discussion by Craig (ref. 95). Suffice it to say that the situation has changed within the past few years; conventional measuring techniques combined with satellite information now provide global coverage of data. Satellite data are not without their problems and limitations, but IRIS, BUV, and LRIR have provided a start for future instruments to provide us with better temporal and spatial coverage, and the data presently available from them have provided useful information.

Studies of individual stratospheric warmings in relation to ozone have been restricted to single stations or to restricted areas (refs. 96 and 97), until recently when BUV data became available for the 1970-71 warming (ref. 98).

Using data over Europe, Dütsch (ref. 96) showed a close spatial correlation between ozone and mean temperature of the 50 to 10 mb layer during the mid-winter stratospheric warming of 1957-58. For this same warming, London (ref. 97) investigated the changes occurring at the 25-mb level and obtained results similar to those of Dütsch. He found the centers of warming at 25 mb to be closely associated with centers of positive ozone anomalies.

By taking simple smoothed averages of all stations north of 40°N for three years, Züllig (ref. 99) took monthly plots of total ozone which included three winters, two of which had strong stratospheric warmings. He noted that strong increases of ozone occurred for those two years with strong stratospheric warmings (1962-63, 1967-68), whereas in 1966-67, when there was no marked warming, the increase of ozone was rather steady, without the sharp increases of the other two years (Figure 7.1). For the 1957-58 warming, Figure 7.2 consists of two maps by Dütsch showing the distribution of total ozone over Europe on January 17 and 20, 1958. The development of the center of high concentration over Belgium and the Netherlands

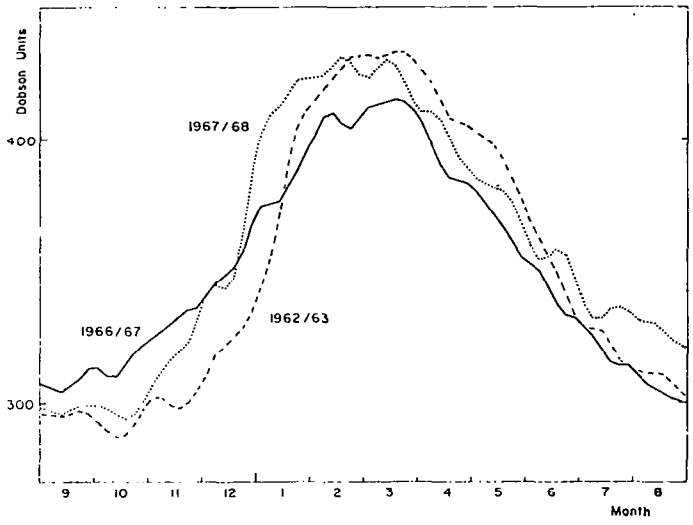

Figure 7.1. - Time cross-sections of the smoothed mean total ozone north of 40° latitude for the winters 1962-63, 1966-67 and 1967-68. (Source: Ref. 99.)

during the three days should be noted. In Figure 7.3, BUV data (ref. 98) for the 1970-71 warming show rapid increases for the winter months for the Northern Hemisphere versus a more steady and not so rapid increase for the Southern Hemisphere, verifying Züllig's observations that strong stratospheric warmings are accompanied by strong increases in ozone, since the Southern Hemisphere did not have as strong a warming as the Northern Hemisphere. For the same warming, Heath shows latitudinal plots of total ozone data with rapid variations at higher latitudes (Figure 7.4). Ghazi (ref. 100) has shown the total ozone field for the same warming to be closely correlated with the radiance field as given by VTPR Channel 2, which peaks in the lower stratosphere. This tends to verify the earlier work of Dütsch and London on ozone.

The enhanced changes during winter, the large gradients, and the large transports that apparently exist during STRATWARMS, all combine to make winter the most interesting and complicated of all seasons in the stratosphere, and perhaps the least understood in terms of interactions with ozone and other trace constituents. Synoptic maps were produced from BUV data for winter 1970-71. Figures 7.5-7.8 show mean monthly maps of total ozone together with mixing ratios at 5 mb for the months of December 1970 and January 1971. During January, when the stratosphere warming was in full force, an increase in total ozone is seen at higher latitudes. At 5 mb, increases are evident at high and low latitudes, with a decrease in the Aleutian area, indicating a depletion of ozone in this area.

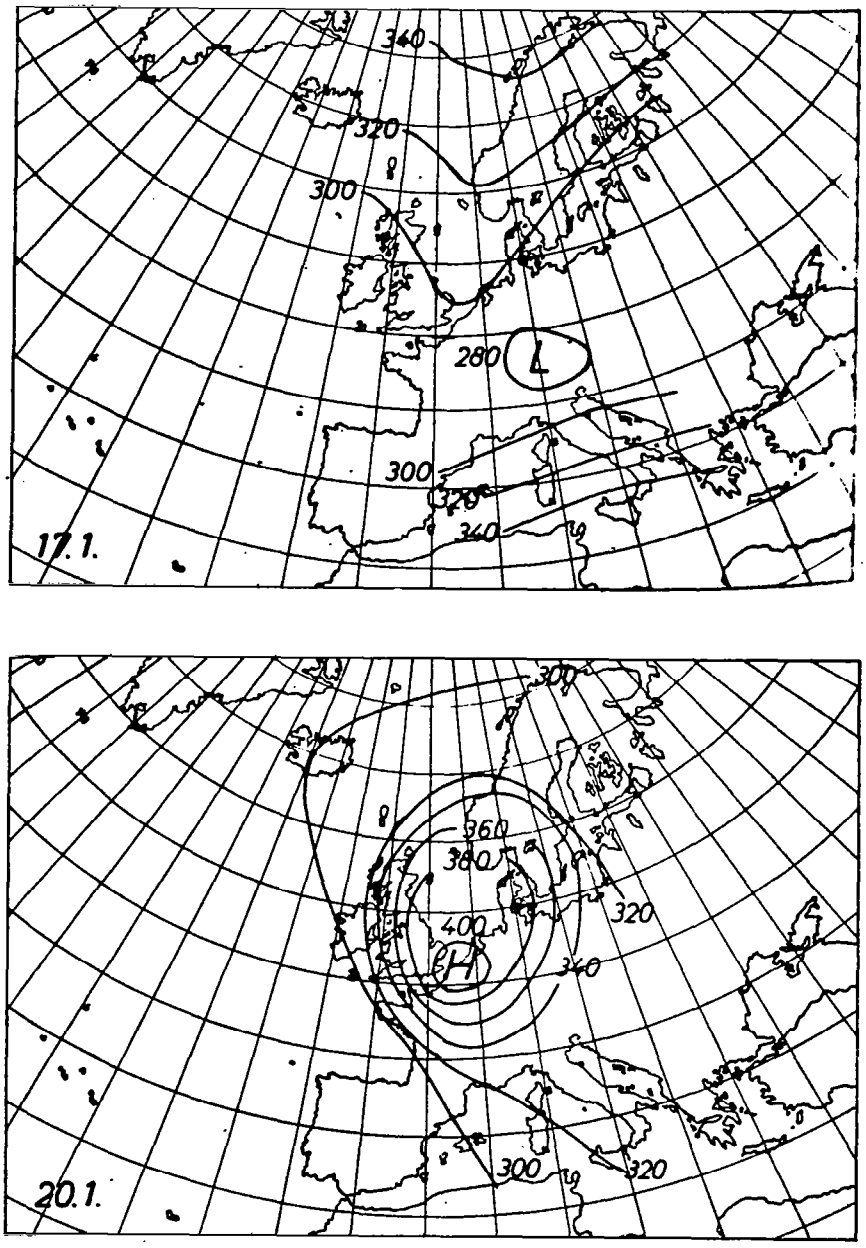

Figure 7.2. - Maps of total ozone over Europe, January 17 and 20, 1958. Units are 10^{-3} cm NTP. (Source: Ref. 96.)

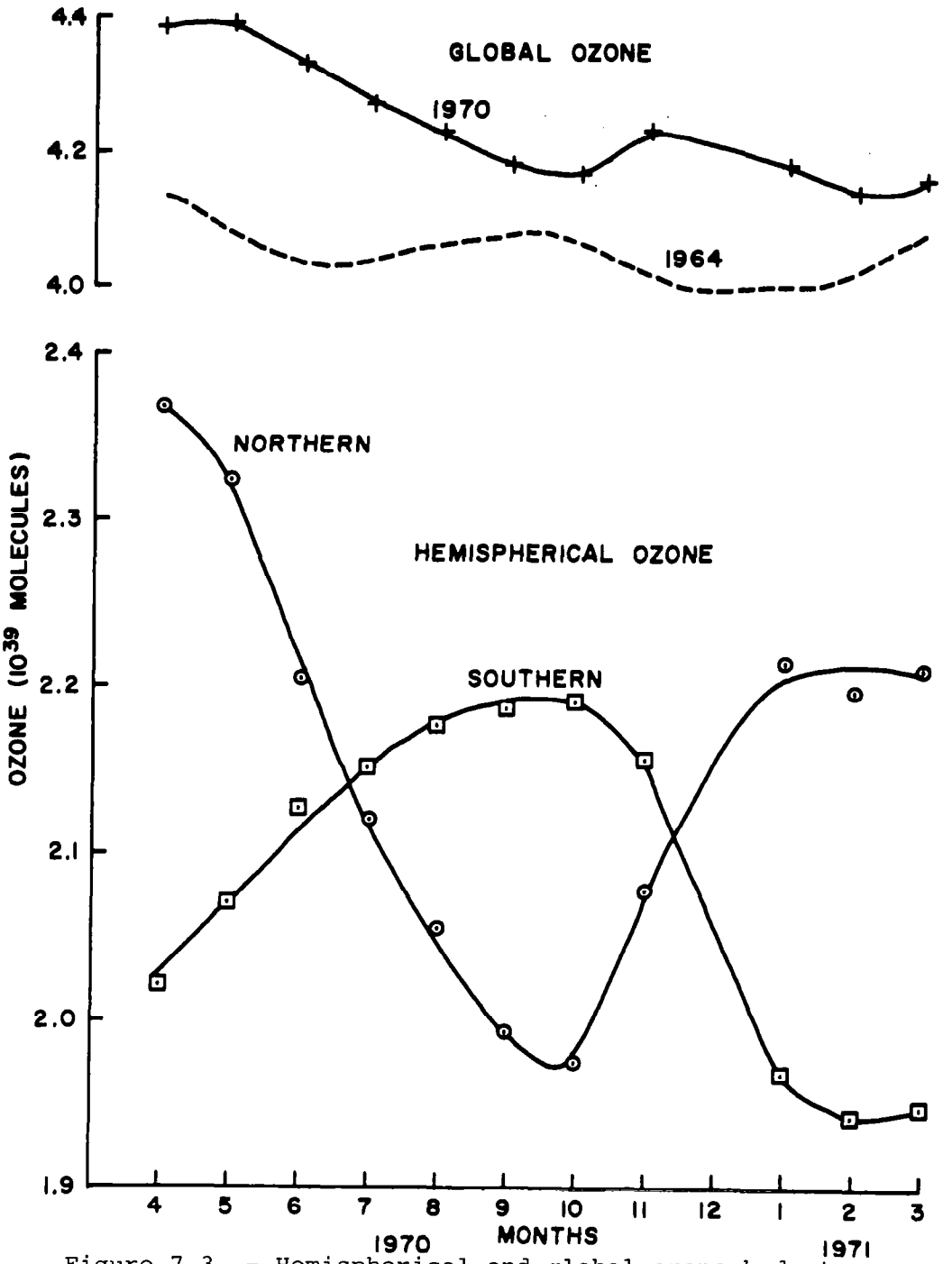

Figure 7.3. - Hemispherical and global ozone budget as derived from monthly means of the zonal means of total ozone. (Source: Ref. 98.)

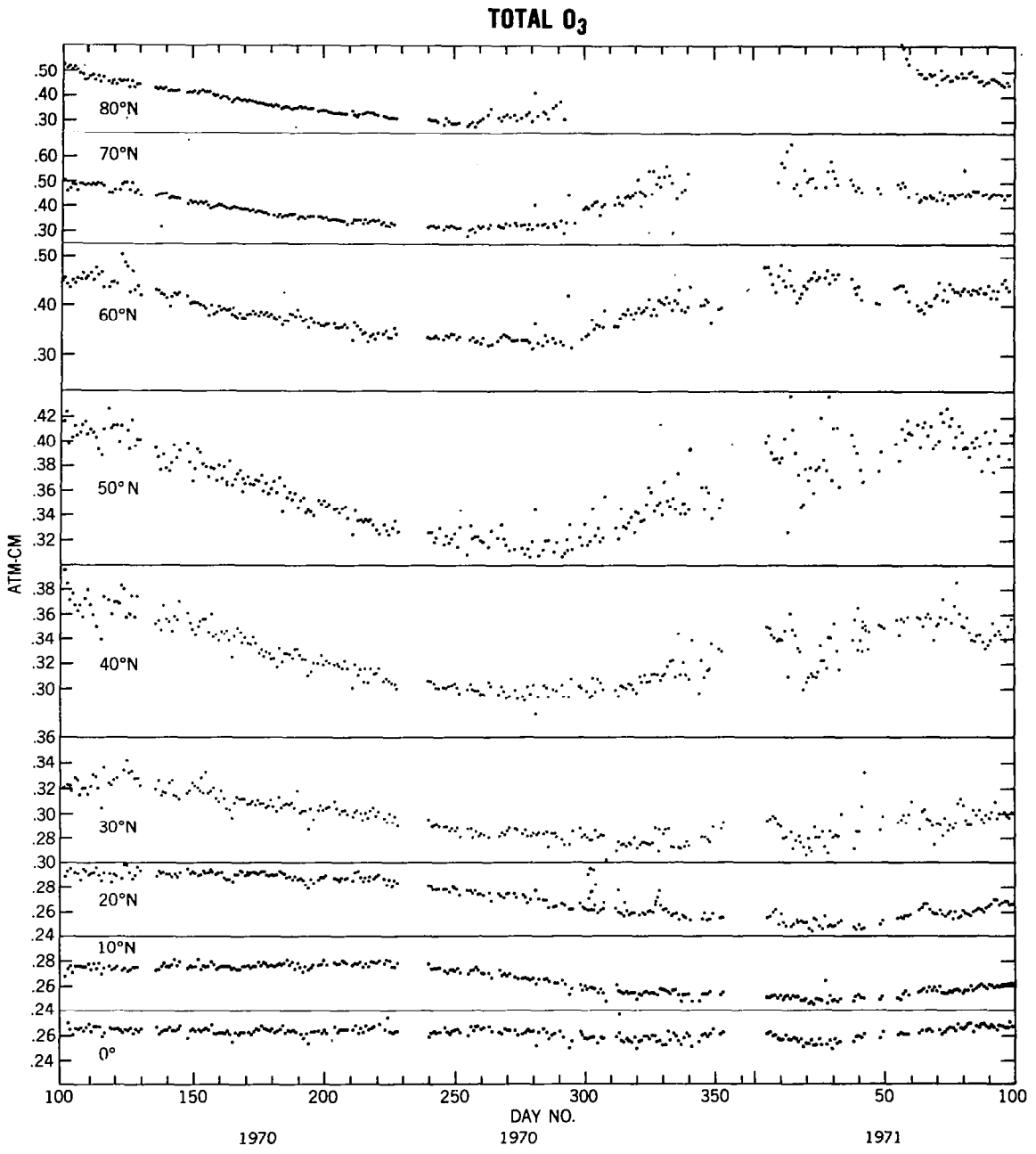

Figure 7.4. - Daily zonal means of total ozone in atm-cm for 10° intervals of latitude in the Northern Hemisphere. (Source: Ref. 98.)

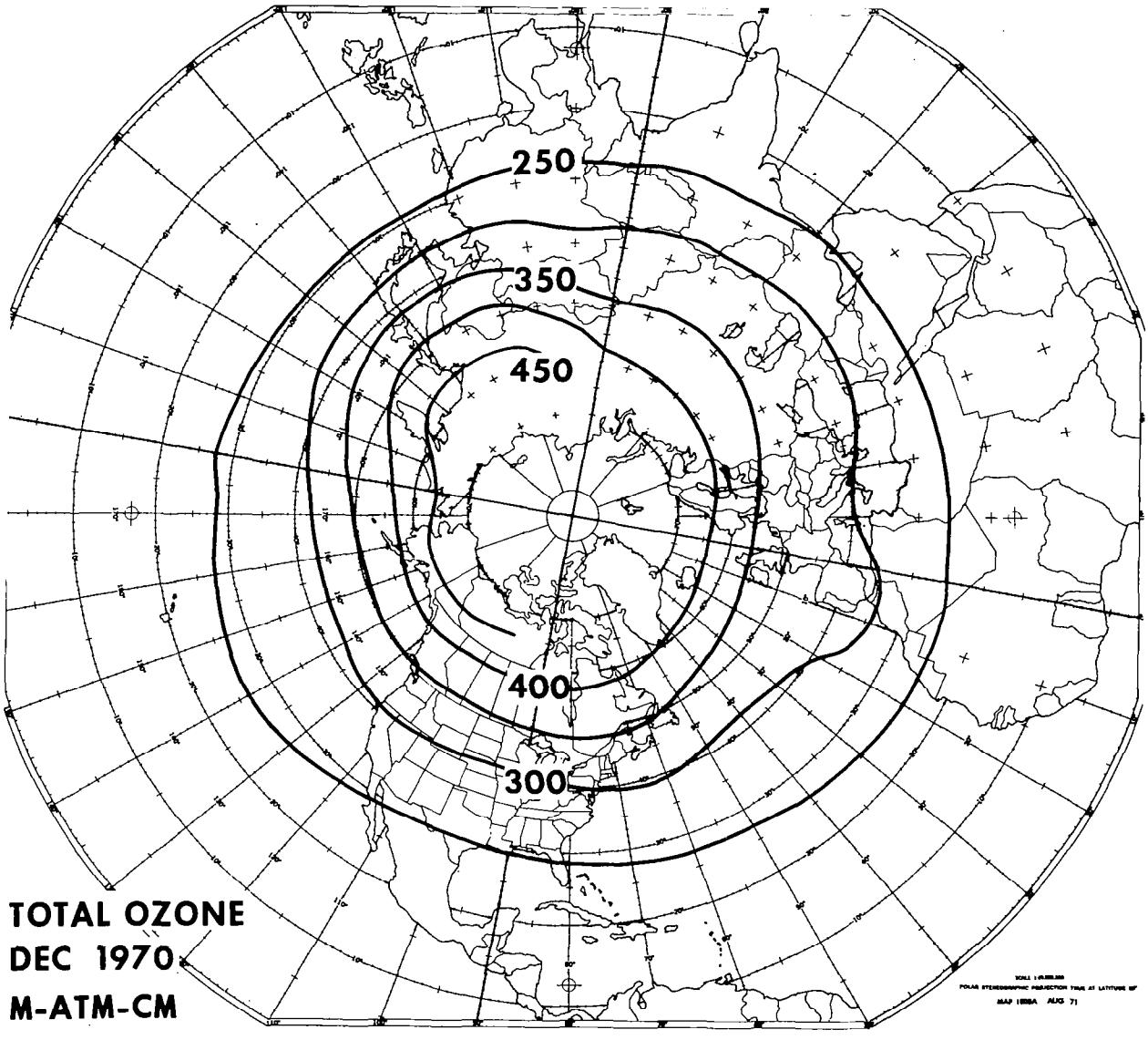

Figure 7.5. - Map of total ozone over the Northern Hemisphere for December 1970. Units are milliatmospheres-centimeters (matm-cm).

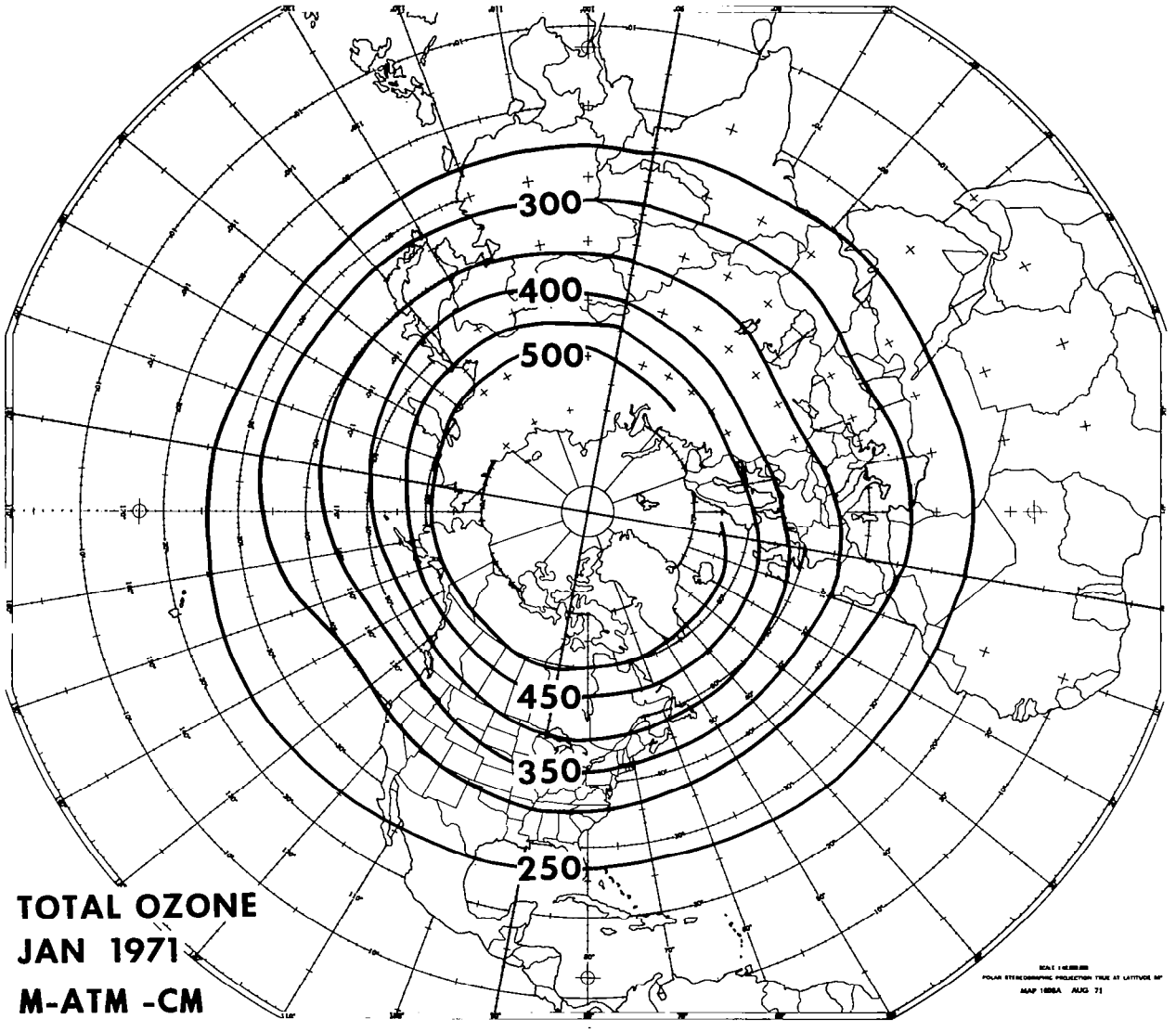

Figure 7.6. - Map of total ozone over the Northern Hemisphere for January 1971. Units are milliatmospheres-centimeters (matm-cm).

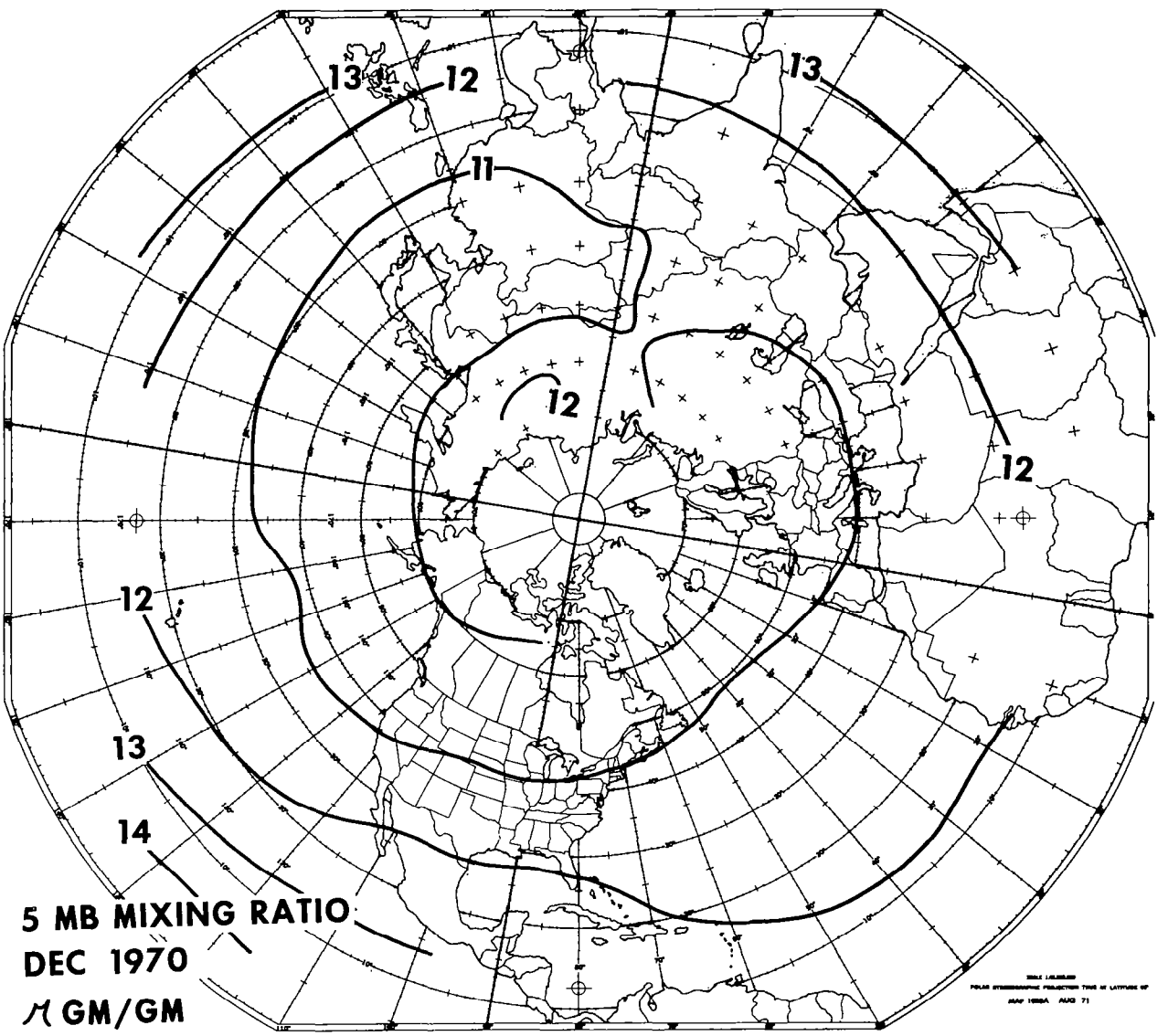

Figure 7.7. - Map of 5-mb mixing ratio over the Northern Hemisphere for December 1970. Units are micrograms/gram.

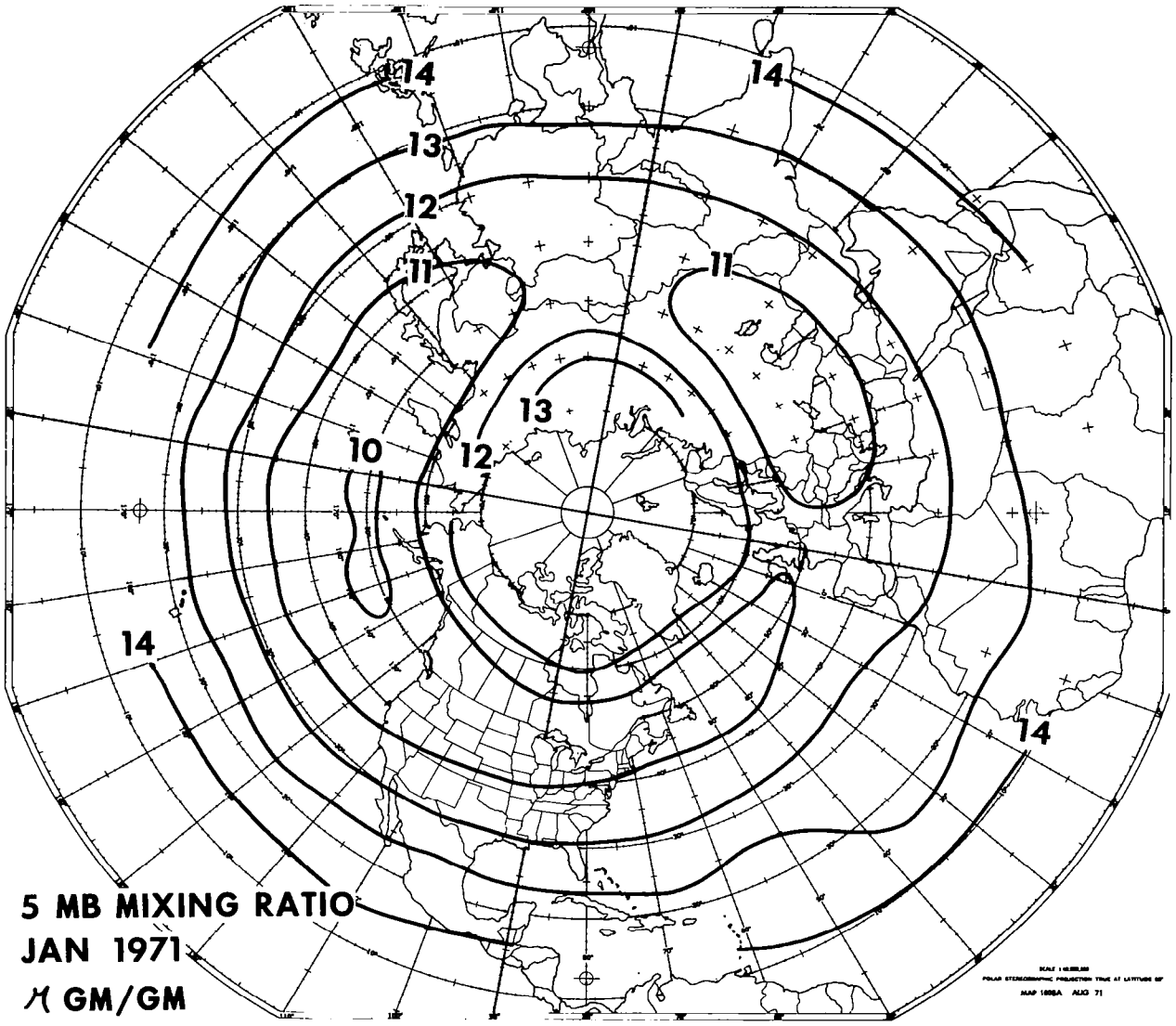

Figure 7.8. - Map of 5-mb mixing ratio over the Northern Hemisphere for January 1971. Units are micrograms/gram.

Perhaps the principal question to be answered with regard to stratospheric warmings is what role ozone plays in the warming phenomenon. Apparently it plays a role in the radiative equilibrium of the stratosphere up to the point when the warming begins. Once the warming begins, the changes take place so rapidly that the radiative effects of ozone probably play a secondary role compared to the dynamic changes.

It is obvious that many questions remain concerning the natural variations of ozone and its interactions with the atmosphere. Improved means of obtaining vertical profiles of ozone together with present and future satellites may help to answer some of the questions.

Interactions of other trace constituents with the stratosphere are even less well understood. The recent fluorocarbon controversy makes it even more necessary to understand some of the natural variations taking place.

STRATOSPHERIC WARMINGS AND MAN'S ACTIVITIES

Large-scale atmospheric changes have been noted in conjunction with stratospheric warmings at levels throughout the troposphere and ionosphere. Thus it is expected that stratospheric warming events will have an effect on man's activities that are dependent on atmospheric variables or on knowledge of those variables. Table 8.1 lists some of these activities (ref. 101).

Numerical weather prediction is an effort that requires data on a global scale including stratospheric levels. Modeling stratospheric processes, including the phenomenon of stratospheric warming, may be necessary to adequately account for energy transformations that take place in the general circulation. The degree to which these processes are realistically modeled may influence strongly the success which may be realized in long range predictions.

TABLE 8.1. - SCIENTIFIC/TECHNOLOGICAL PROJECTS AND ACTIVITIES DEPENDENT UPON KNOWLEDGE OF STRATOSPHERIC WARMINGS

Numerical weather prediction
Supersonic Transport operation
Space Shuttle reentry
Ionospheric radio propagation
Infrared horizon sensing for satellite navigation
Prediction of trajectories of high-level balloons
Infrasonic wave detection
Tracking of radioactive debris
Monitoring trace constituents (Ozone, CO_2, etc.)

The development and operation of aerospace vehicles designed to traverse stratospheric and mesospheric levels has created a need for high atmospheric information. Under anomalous environmental conditions, prediction of atmospheric variables as well as the flow of real-time environmental information may be desirable for the sake of economy as well as for safety reasons. Thus the development of high-altitude prognostic models commands a certain practical interest.

The reverse impact of aerospace vehicles and other human activities on the stratospheric environment is also of considerable interest. Destruction of stratospheric ozone by pollution of the environment carries

with it the danger of adversely affecting the biosphere. Since stratospheric warmings play such a profound role in the wintertime circulation, ozone production and redistribution may also be significantly affected. In fact, the redistribution of ozone during the course of a stratospheric warming event may also affect tropospheric temperature to some extent.

While we will discuss at length only the subjects of the impact of stratospheric warmings on numerical weather prediction, the SST, and the space shuttle, the other areas listed in Table 8.1 are also of great interest.

For example, infrared horizon sensors have been suggested for use in satellite navigation. The accuracy of this technique depends on knowledge of threshold radiance to be expected for specified angles of limb viewing. Under highly anomalous atmospheric conditions, such as those which prevail during stratospheric warming, there may be a large uncertainty in the radiance to be expected at the limb, so that navigational needs might not be met. This problem is receiving special attention with the aid of data that have become available from the Nimbus 6 LRIR instrument.

Other problems related to atmospheric changes are dependent on wintertime circulation characteristics. One of these has to do with monitoring trace constituents. One- and two-dimensional models of chemical reactions above the tropopause may give a first approximation to actual conditions, but dynamic effects undoubtedly play a major role in determining the actual atmospheric composition.

Ozone concentrations have been estimated by using one- and two-dimensional models. In order to assess questions such as the impact of aerospace vehicles (SST and the proposed space-shuttle) on the stratospheric concentration of ozone, the dynamics of the wintertime stratosphere must be better known. And since ozone reaction rates are very sensitive to ambient temperature, STRATWARMS especially must be given close attention.

Ionospheric physicists are interested in stratospheric warmings because of a possible relationship with large increases in the electron concentrations of the D- and E-regions. On the basis of observational evidence and some physical reasoning, a large density increase would be expected in the mesosphere (D-region) in association with a large temperature increase in the upper stratosphere. As discussed earlier, observations of concurrent changes of stratospheric parameters with ionospheric parameters have suggested a physical link between these atmospheric levels.

Tracking of infrasonic waves generated from natural or man-caused events (e.g., aurorae, high-altitude nuclear testing) requires knowledge of upper level winds and temperature to approximately 100 km (refs. 102, 103, 104). During STRATWARMS the return signals from the Baroms (infrasonic detector trace) take on a different character, and wind reversal at some upper level may be inferred. The estimation of the level that this phenomenon is taking place is made from independent observations. Thus knowledge of wind reversal and temperature anomalies associated with stratospheric warmings is necessary for proper use of this technique.

Numerical Weather Prediction

Numerical prediction models are used in service to the general public as well as to aviation, shipping, agriculture, and other industrial interests.

It has been shown that for weather prediction of more than a few days, observations on a global scale are needed. In addition, in order to provide long-range predictions (up to 2 weeks), stratospheric observations and processes must be taken into account. Increasing the vertical resolution and range of numerical models to incorporate stratospheric data, in addition to providing stratospheric forecasts, might at times improve shorter range forecasts of tropospheric weather. This could be achieved by properly accounting for those conditions at high altitudes which might in some ways through stratospheric-tropospheric interaction, have an influence on tropospheric weather.

Since 1974 the National Meteorological Center has used a 9-layer model with its effective top at the 50-mb level (approximately 20 km). Predictions from this model form the basis for some of the operational forecasts issued by the National Weather Service. In order to meet future requirements for longer-range forecasts and for forecasts at stratospheric levels, NMC has made plans to increase vertical range and resolution to a 16-layer model with the top layer centered at 10 mb.

The general circulation model used at the Geophysical Fluid Dynamics Laboratory, NOAA, is an 18-layer model with the top level at 4 mb (37.5 km). This model, like a number of others (see section on Models) was designed primarily for research purposes. It has been used with some success in simulating properties associated with stratospheric warmings. These models have also shown that more realistic simulation of tropospheric processes is possible only by including stratospheric-level information.

Supersonic Transport

With the introduction of regularly scheduled flights of the supersonic transport (SST), information on meteorological conditions of the lower stratosphere is now used to support routine civil aviation operations.

The International Civil Aviation Organization (ICAO) has specified the operational needs of SST for the en-route phase. As with subsonic aircraft, the information is to be given for 500-NM segments. For each 500 NM sector it is recommended that, in 90% of cases at least, errors in forecasting mean wind and temperature values should not exceed 20 knots and ±3°C, respectively. The corresponding effect on fuel consumption of the Concorde (ref. 105), cruise level slightly below 70 mb (18 km) for the 20 knot wind error is 1.7% and for ±3°C in temperature is 0 to 1.2%, depending on the average ambient temperatures (from 0 to 15°C greater than Standard, respectively). This is because the Concorde is not very sensitive to temperature variations below the standard temperature, but is rather sensitive to fluctuations at high temperature levels. Thus the high temperatures and anomalous winds associated with stratospheric warming will contribute to increased fuel consumption of the SST.

Figure 3.3 shows changes in temperature at 50 mb during a stratospheric warming in February 1974. It has been shown that, in order to meet ICAO requirements for the SST temperature forecast (+3°C), persistence from a previously analyzed map, even 12 hours old (available several hours after map time), are not sufficient for flight levels between 100 mb and 50 mb. Even though large-scale stratospheric warmings occur relatively infrequently over commonly-used flight-paths, it is still necessary to provide forecasts for them. It remains to be demonstrated, however, that numerical weather prediction models will be able to fill the need.

There is another important stratospheric phenomenon affecting the SST: small-scale (on the order of a few dozen nautical miles) temperature variations. Dousset et al. (ref. 105) have shown that the existence of "hot air bubbles" in the stratosphere could have an effect on the longitudinal and vertical separation of SSTs. Mach number variations closely follow temperature variations so that variations of 4°C could cause variations of .04 Mach, thus causing an altitude variation of up to 500 feet. With proposed vertical separations between SSTs of 2000 feet, maintaining this separation would depend on knowledge of temperature gradients between the aircraft. The frequency of these "hot air bubbles" and their relationship to stratospheric warmings remain to be determined.

Space Shuttle

The space shuttle is likely to be used in a variety of the United States' space missions scheduled during the 1980's. Following reentry into the earth's atmosphere and under influence of increasing atmospheric density, transition to atmospheric control of the space shuttle vehicle should occur between 120 and about 75 km, probably near 90 km. Atmospheric maneuvering takes place below 75 km, with a transition to powered cruise near 15 km. Ambient atmospheric conditions influence the exact characteristics of each flight. Figure 8.1 shows a typical low latitude flight trajectory in terms of time and altitude.

The major atmospheric problem of space shuttles has been considered to be surface heating of the reentry body. To a first approximation, the heating rate ($\dot{q}$) is proportional to the square root of ambient density (ρ) and to the cube of the vehicle velocity (v):

$$\dot{q} \propto \rho^{\frac{1}{2}} v^3$$

In middle and high latitudes during winter, the variability of density is so great from day to day and from one longitude to another that use of climatological profiles in forecasting can easily result in large errors. The greatest changes in density other than the annual component of change (winter extreme to summer extreme in high latitudes) are the variations associated with winter stratospheric warmings. Figure 8.2 (a, b, c) (ref. 105) show 50-km density maps before and after the sudden-warming phase of an event in January-February 1973. From January 25 to February 5, there was an increase in density near the North Pole by more than 50 percent. Anomalously high density at 50 km on February 5 can be expected to be

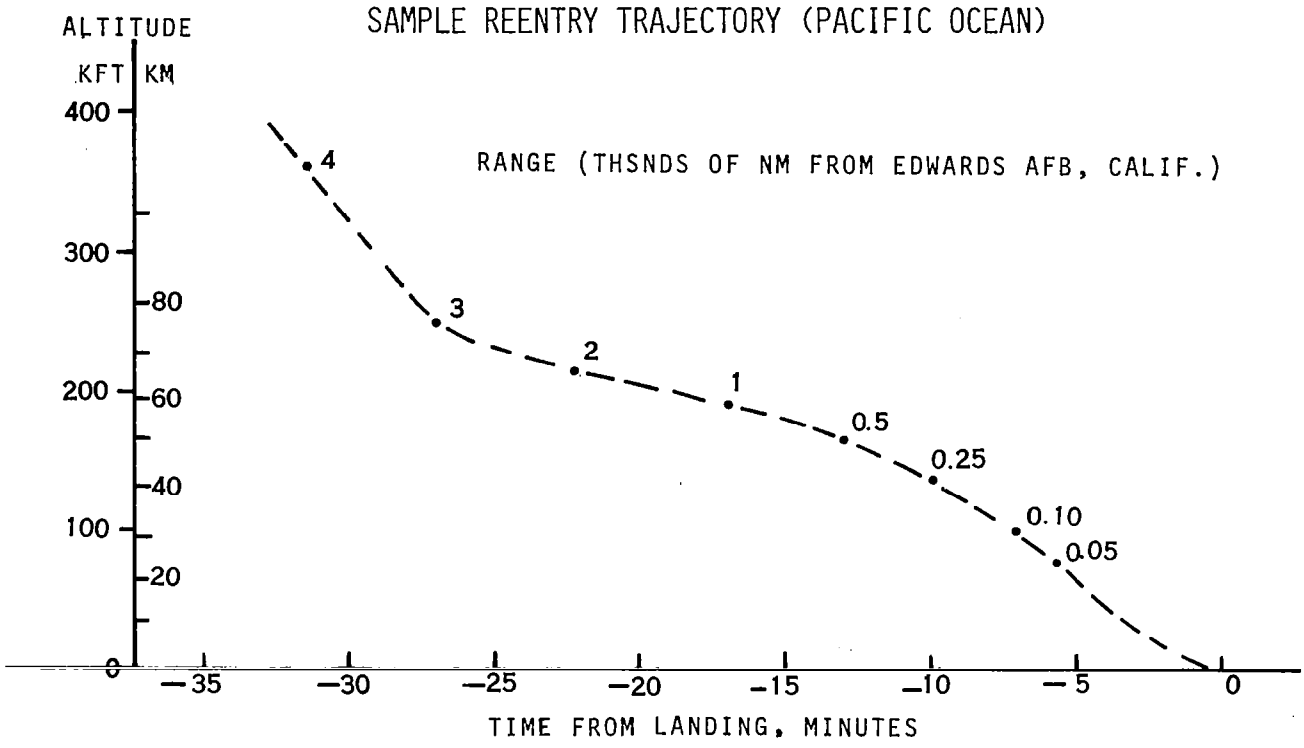

Figure 8.1. - A typical low-latitude flight trajectory, depicted as a time versus altitude cross-section.

accompanied by correspondingly low density near 75 km (owing to compensation effects). This is of interest in the present and future design of space shuttles.

It is likely that climatological profiles of density (refs. 106 and 107) will be adequate for reentry trajectories confined to low latitudes. Exceptions might occur at low latitudes of either hemisphere during periods of large scale stratospheric warming in the winter hemisphere. In Figure 8.3 (ref. 84) it is evident that significant temperature variations may occur even in low latitudes during such events. Note that compensating negative and positive temperature changes occur in the mesosphere, over 50 km, and in the stratosphere. Density profiles obtained for this set of profiles would show largest variations occurring at 50-60 km.

It should be emphasized, in connection with this, that design criteria (ref. 108) are such that the space shuttle is expected to operate safely under all foreseeable conditions.

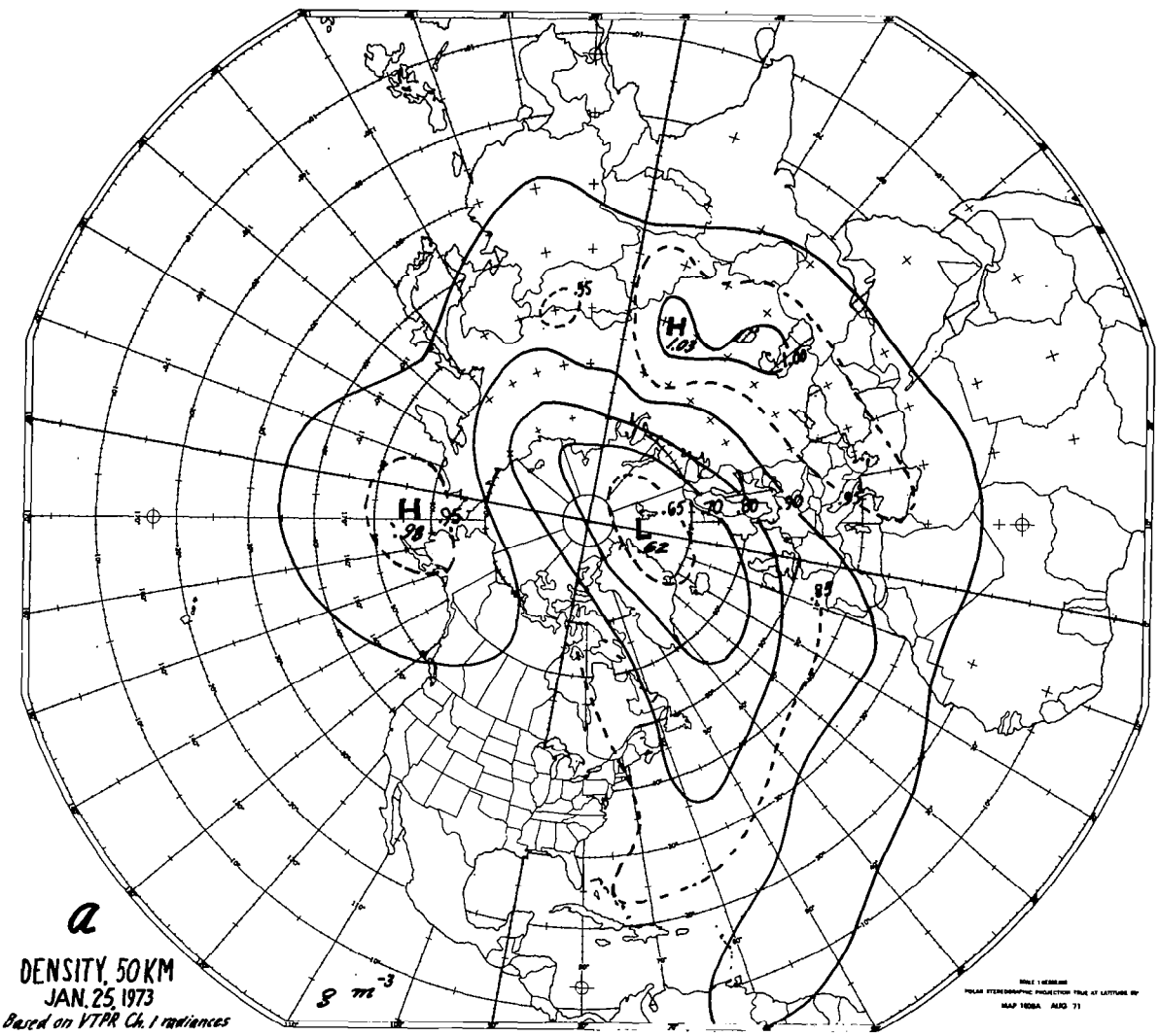

Figure 8.2a. - Density map for 50 km, January 25, 1973. Units are gm^{-3}. Based on satellite (VTPR Channel 1) radiances. (Source: Ref. 46.)

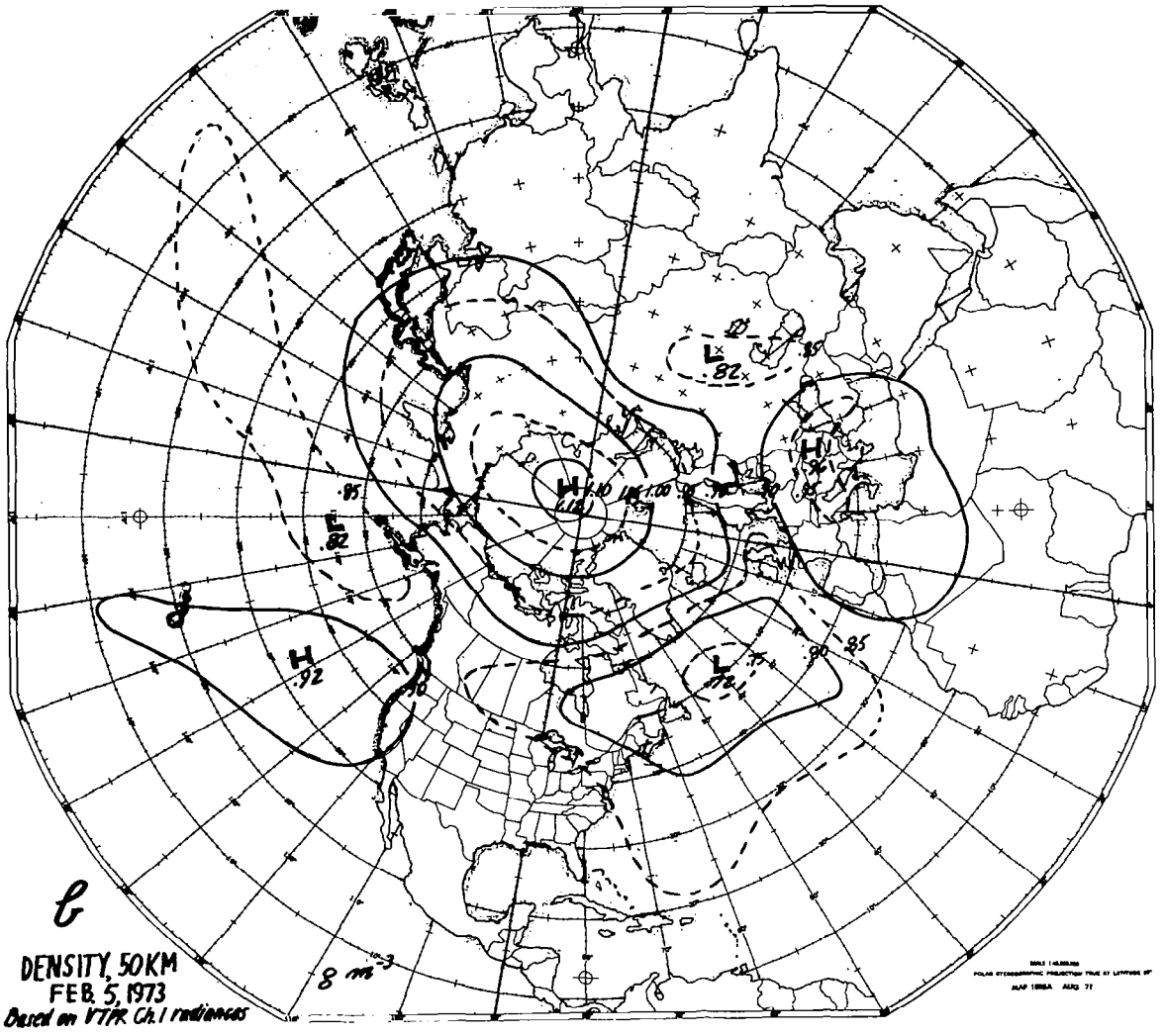

Figure 8.2b. - Same as 8.2a, except for February 5, 1973.

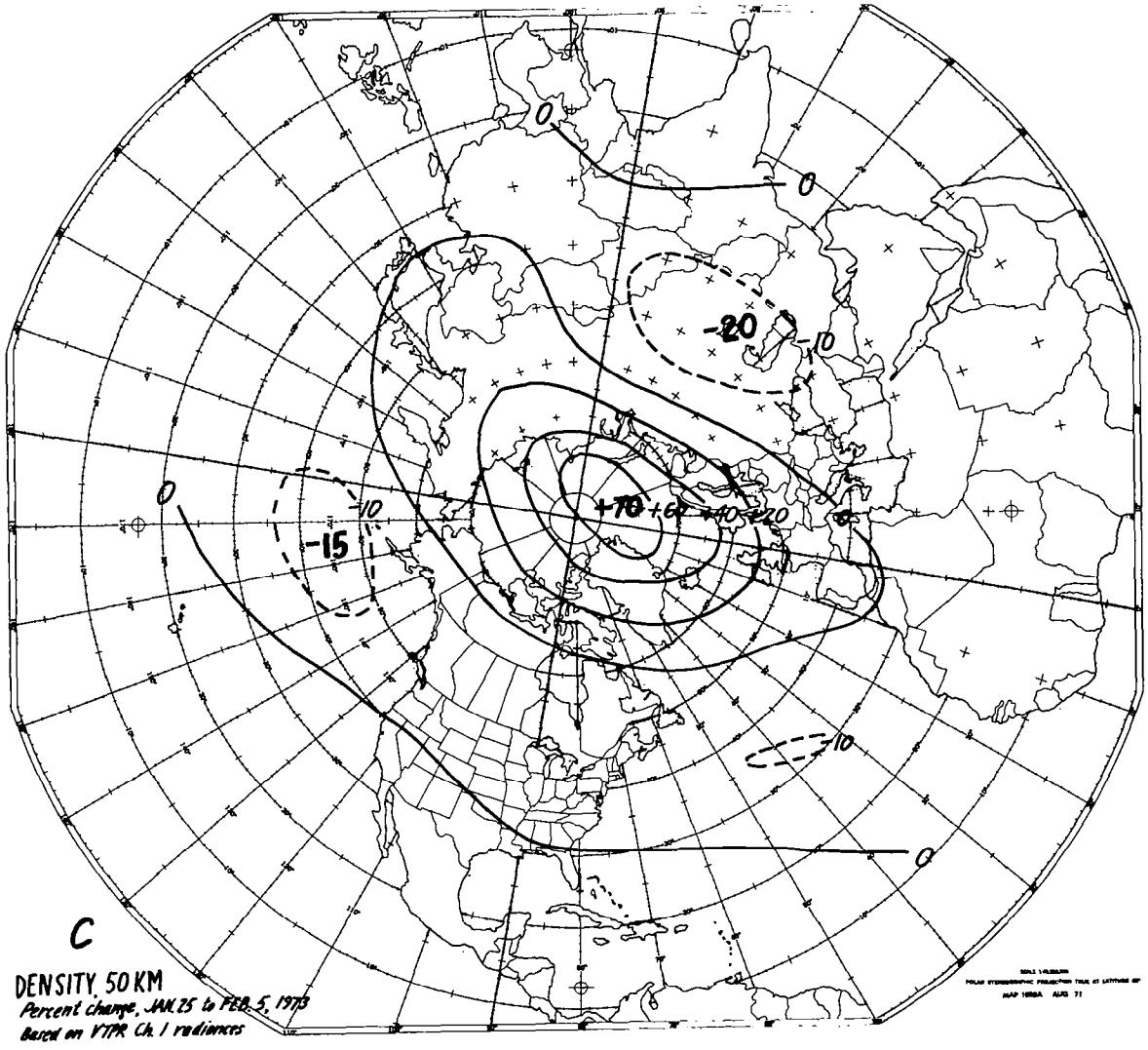

Figure 8.2c. - Percent change in density from January 25 to February 5, 1973.

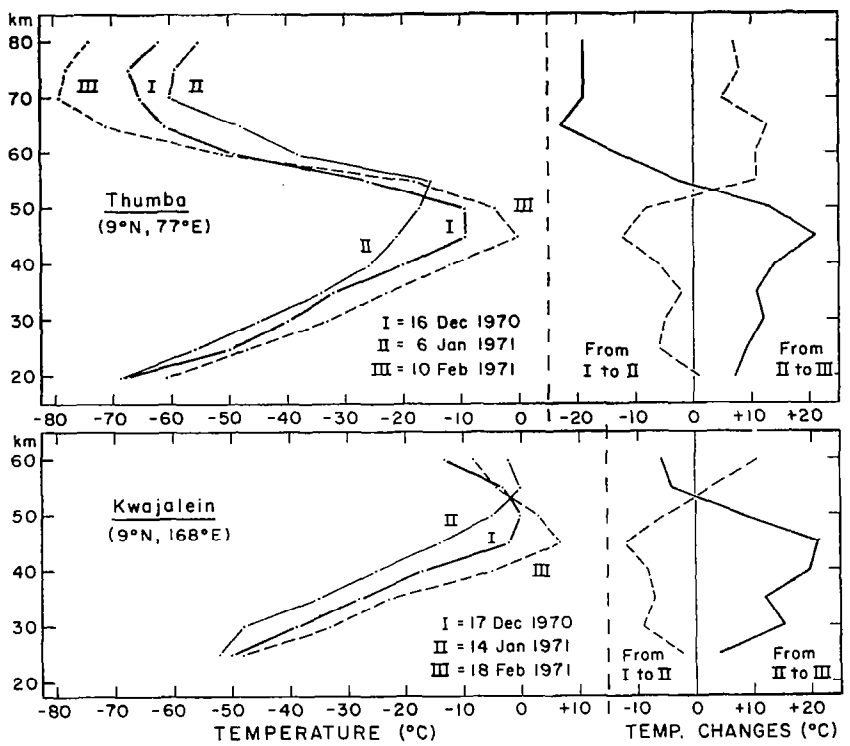

Figure 8.3. - Typical vertical temperature profiles at two typical stations, Thumba, India (Russian instrument) and Kwajalein, Marshall Islands (American instrument), for the winter 1970-71; I, early winter before the beginning of a warming; II, approximately at peak of warming; III, late winter minimum. Also changes between I and II, and between II and III. Source: Ref. 84.

APPENDIX

SOME VERTICAL MOTION RESULTS FOR STRATOSPHERIC WARMINGS

Source - (1) Event, (2) Calculations, and (3) Some results

Craig and Lateef, 1962

(1) January-February 1957
(2) Levels: 100, 50, 25 mb. Area: North America. Period: January 16 to February 15, 1957.
(3) Vertical motion largely explained by horizontal thermal advection. In early stage of warming regions of upward and downward motion tend to be found east and west of troughs respectively. In late stage, authors indicate the prevalence of a large area of uniformly downward motion, but from the advection pattern it is apparent that a large area of upward motion would probably have been observed in the European Arctic if the analysis area had extended to that region. Extreme values encountered were 4 cm/sec at 100 mb, 6 cm/sec at 50 mb, and 8 cm/sec at 25 mb.

Finger and Teweles, 1964

(1) January-February 1963
(2) Level: 10 mb. Area: Northern Hemisphere. Period: January 23 (in early stage of warming).
(3) Maximum upward motion, $\sim$ 8 cm/sec; downward, $\sim$ 6 cm/sec.

Mahlman, 1969

(1) January-February 1958
(2) Levels: 100, 50 mb. Area: Polar cap areas north of 50°, 60°, 70°N. Periods: January 10-20, January 20 - February 4, February 4-19.
(3) Mean areal vertical motion $\leq$ 0.5 cm/sec, largely determined by eddy heat flux. Rising motions near pole emphasized. Calculated motions are small because of areal smoothing.

Miller, 1970

(1) January 1967 (minor warming)
(2) Level: 2 mb. Area: Western Hemisphere. Period: January 11, 18; $\Delta T/\Delta t$ computed over 7-day interval.
(3) Vertical motion largely explained by horizontal thermal advection. Maximum upward motion, 9.4 cm/sec; down, 8 cm/sec.

Miller, Brown, and Campana, 1972

(1) December 1969 - January 1970
(2) Levels: 1000-2 mb (based on daily maps 1000-10 mb, 5-day maps 5 and 2 mb). Area: Northern Hemisphere. Period: December 15 - January 15; see below.

(3) Mean vertical motions over 2 periods (December 16-21; January 1-15) are presented schematically, without specific magnitudes, to indicate sense of meridional circulation.

Miyakoda, 1963

(1) January-February 1958
(2) Level: 34 mb. Area: Northern Hemisphere. Period: January 23-24, 1958 (in an early stage of warming).
(3) Variegated pattern, largely determined by the horizontal thermal advection, with velocities to 2 cm/sec.

Newson, 1974

(1) Simulated warming
(2) Level: 44 km for Day 82 (during early stage of sudden warming). Area: Northern Hemisphere.
(3) Generally upward motion in Arctic, maximum about 20 cm/sec; with descending motions in middle latitudes, up to about 15 cm/sec, in regions of warming.

Quiroz, 1969

(1) January-February 1966
(2) Levels: 20-44 km. Area: One station (Heiss Island, 81°N). Period: January 16 - February 9.
(3) Time-height section of vertical motion shows motions less than 5 cm/sec except for very strong upward motion up to 60 cm/sec near 40 km around February 1, associated with extremely strong horizontal thermal advection.

ACRONYMS AND ABBREVIATIONS

A	- average available potential energy per unit mass
BG	- work done by boundary pressure forces
BK	- change of kinetic energy due to boundary interactions
BUV	- Backscatter Ultraviolet
C	- energy conversion
CE	- conversion between eddy available potential energy and eddy kinetic energy
CK	- conversion between zonal kinetic energy and eddy kinetic energy
$\frac{\partial k(n)}{\partial t}$	- rate of change of kinetic energy in wavenumber n
G	- energy generation
GF	- eddy geopotential flux - same as $[\omega^*\phi^*] = g[\omega^*\Xi^*]$ - see page 76
GMT	- Greenwich Mean Time
ICAO	- International Civil Aviation Organization
IGY	- International Geophysical Year
IQSY	- International Years of the Quiet Sun
ITPR	- Infrared Temperature Profile Radiometer
K	- average kinetic energy per unit mass
LK	- transfer of kinetic energy between eddy harmonic components through nonlinear interactions
LRIR	- Limb Radiance Infrared Radiometer
MRN	- Meteorological Rocket Network
n	- wavenumber
NASA	- National Aeronautics and Space Administration
NEMS	- Nimbus-E (5) Microwave Spectrometer
Nimbus 1, 2, ...	- members of a series of experimental NASA (U.S.) satellites
NOAA	- National Oceanic and Atmospheric Administration; also used to designate series of operational polar-orbiting satellites (NOAA 1, 2, ...)

PMR	- Pressure Modulated Radiometer
RAOB	- Rawinsonde Observation
ROCOB	- Rocketsonde Observation
SCR	- Selective Chopper Radiometer
SIRS	- Satellite Infrared Radiometer Spectrometer
SST	- Supersonic Transport
STRATALERT	- stratospheric warming alert message
STRATWARM	- stratospheric warming
VTPR	- Vertical Temperature Profile Radiometer
ω	- instantaneous change of pressure with time, dp/dt; proportional to vertical velocity w: $\omega \sim -\rho g w$; where ρ = density, g = acceleration of gravity
w.f.	- weighting function
WMO	- World Meteorological Organization

REFERENCES

1. Scherhag, R.: Die Explosionsartigen Stratosphärenerwärmungen des Spätwinters 1951-52 (The Explosive-type Stratospheric Warming of Late Winter, 1951-52). Ber. Deut. Wetterd., vol. 6, pp. 51-63.

2. Teweles, S.: Anomalous Warming of the Stratosphere over North America in Early 1957. Mon. Wea. Rev., vol. 86, 1958, pp. 377-396.

3. Craig, R. A. and Hering, W. S.: The Stratospheric Warming of January-February 1957. J. Meteorol., vol. 16, 1959, pp. 91-107.

4. Teweles, S. and Finger, F. G.: An Abrupt Change in Stratospheric Circulation Beginning in mid-January 1958. Mon. Wea. Rev., vol. 86, 1958, pp. 23-28.

5. Trenberth, K. E.: Dynamical Coupling of the Stratosphere with the Troposphere and Sudden Stratospheric Warmings. Mon. Wea. Rev., vol. 101, 1973, pp. 306-322.

6. Julian, P. R. and Labitzke, K.: A Study of Atmospheric Energetics During the January and February 1963 Stratospheric Warming. J. Atmos. Sci., vol. 22, 1965, pp. 597-610.

7. Miller, A. J., Brown, J. A. Jr., and Campana, K.: A Study of the Energetics of an Upper Stratospheric Warming (1969-1970). Quart. J. Roy. Meteorol. Soc., vol. 98, 1972, pp. 730-744.

8. Perry, J. S.: Long-wave Energy Processes in the 1963 Sudden Stratospheric Warming. J. Atmos. Sci., vol. 24, 1967, pp. 537-550.

9. Fritz, S. and Soules, S.: Planetary Variations of Stratospheric Temperatures. Mon. Wea. Rev., vol. 100, 1972, pp. 582-589.

10. Barnett, J. H.: Hemispheric Coupling - Evidence of a Cross-equatorial Planetary Waveguide in the Stratosphere. Quart. J. Roy. Meteorol. Soc., vol. 101, 1975, pp. 835-845.

11. Quiroz, R. S.: The Stratospheric Evolution of Sudden Warmings in 1969-74 Determined from Measured Infrared Radiation Fields. J. Atmos. Sci., vol. 32, 1975, pp. 211-224.

12. Quiroz, R. S.: Meteorological Rocket Research Since 1959 and Current Requirements for Observations and Analysis Above 60 Kilometers. NASA CR-1293, 1969.

13. Staff, Upper Air Branch: Weekly Synoptic Analyses, 5-, 2-, and 0.4-Mb Surfaces for 1964, 1965, 1966, 1967, and 1968. ESSA Tech. Reps. WB-2, WB-3, WB-4, WB-12, and NOAA Tech. Rep. NWS-14, National Weather Service, 1967, 1969, 1970, and 1971.

14. Staff, Free University of Berlin: Meteorol. Abh., Verlag von Dietrich Reimer, Berlin, 1957-1975.

15. Finger, F. G., Woolf, H. M., and Anderson, C. E.: A Method for Objective Analysis of Stratospheric Constant-Pressure Charts. Mon. Wea. Rev., vol. 93, 1965, pp. 619-638.

16. Staff, Upper Air Branch: Monthly Mean 100-, 50-, 30-, and 10-Millibar Charts for 1964, 1965, 1966, 1967. ESSA Tech. Reps. WB-1 and WB-11, National Weather Service, 1967, 1969.

17. Staff, Upper Air Branch: Weekly Synoptic Analyses, 5-, 2-, and 0.4-Mb Surfaces for January 1972 through June 1973. NASA SP-3091, 1975.

18. Labitzke, K.: Temperature Changes in the Mesosphere and Stratosphere Connected with Circulation Changes in Winter. J. Atmos. Sci., vol. 29, 1972, pp. 756-766.

19. Badgley, F. I.: Response of Radiosonde Thermistors. Rev. Sci. Inst., vol. 28, 1957, pp. 1097-1084.

20. Teweles, S. and Finger, F. G.: Reduction of Diurnal Variation in the Reported Temperatures and Heights of Stratospheric Constant-Pressure Surfaces. J. Meteorol., vol. 17, 1960, pp. 177-194.

21. Finger, F. G., Mason, R. B., and Teweles, S.: Diurnal Variation in Stratospheric Temperatures and Heights Reported by the U.S. Weather Bureau Outrigger Radiosonde. Mon. Wea. Rev., vol. 92, 1964, pp. 243-250.

22. McInturff, R. M. and Finger, F. G.: The Compatibility of Radiosonde Data at Stratospheric Levels over the Northern Hemisphere. ESSA Tech. Memo. WBTM-DATAC 2, U.S. Weather Bureau, 1968.

23. Finger, F. G. and McInturff, R. M.: The Diurnal Temperature Range of the Middle Stratosphere. J. Atmos. Sci., vol. 24, 1968, pp. 1116-1128.

24. Krumins, M. V. and Lyons, W. C.: Corrections for the Upper Atmosphere Temperatures Using a Thin Film Loop Mount. Naval Ordnance Lab. Tech. Rep. 72-152, 1972.

25. Finger, F. G., Gelman, M. E., Schmidlin, F. J., Leviton, R., and Kennedy, B. W.: Compatibility of Meteorological Rocketsonde Data as Indicated by International Comparison Tests. J. Atmos. Sci., vol. 32, 1975, pp. 1705-1714.

26. Muench, H. S.: Temperature Measurements in the 30- to 40-Kilometer Region. Mon. Wea. Rev., vol. 99, 1971, pp. 158-160.

27. Quiroz, R. S.: The Determination of the Amplitude and Altitude of Stratospheric Warmings from Satellite-measured Radiance Changes. J. Appl. Meteorol., vol. 10, 1971, pp. 555-574.

28. Quiroz, R. S. and Gelman, M. E.: Direct Determination of the Thickness of Stratospheric Layers from Single-Channel Satellite Radiance Measurements. Mon. Wea. Rev., vol. 100, 1972, pp. 788-795.

29. Johnson, K. W.: Information Content of Vertical Temperature Profile Radiometer Data. Third Symposium on Meteorological Observations and Instrumentation of the American Meteorological Society, 1975, pp. 137-139.

30. Mason, R. B. and Anderson, C. E.: The Development and Decay of the 100-Mb Summertime Anticyclone over Southern Asia. Mon. Wea. Rev., vol. 91, 1963, pp. 3-12.

31. Taljaard, J. J., van Loon, H., Crutcher, H. L., and Jenne, R. L.: Climate of the Upper Air, Part 1 - Southern Hemisphere. Vol. 1: Temperatures, Dew Points, and Heights at Selected Pressure Levels. NAVAIR 50-1C-55, Naval Weather Service Command, Washington, DC, 1969.

32. Matsuno, T.: Vertical Propagation of Stationary Planetary Waves in the Winter Northern Hemisphere. J. Atmos. Sci., vol. 27, 1970, pp. 871-883.

33. Kasahara, A., Sasamori, T., and Washington, W. M.: Simulation Experiment with a 12-layer Stratospheric Global Circulation Model. J. Atmos. Sci., vol. 30, 1973, pp. 1229-1251.

34. Manabe, S. and Terpstra, T. B.: The Effects of Mountains on the General Circulation of the Atmosphere as Identified by Numerical Experiments. J. Atmos. Sci., vol. 31, 1974, pp. 3-42.

35. Wilson, C. and Godson, W.: The Structure of the Arctic Winter Stratosphere Over a 10-year Period. Quart. J. Roy. Meteorol. Soc., vol. 89, 1963, pp. 205-224.

36. Finger, F. G. and Teweles, S.: The Mid-winter 1963 Stratospheric Warming and Circulation Change. J. Appl. Meteorol., vol. 3, 1964, pp. 1-15.

37. Muench, H. S.: On the Dynamics of the Winter Stratospheric Circulation. J. Atmos. Sci., vol. 22, 1965, pp. 349-360.

38. Miyakoda, K.: Some Characteristic Features of Winter Circulation in the Troposphere and Lower Stratosphere. Tech. Rep. 14, Dep't Geophys. Sci., Univ. of Chicago, 1963.

39. Labitzke, K.: On the Mutual Relation Between Stratosphere and Troposphere During Periods of Stratospheric Warmings in Winter. J. Appl. Meteorol., vol. 4, 1965, pp. 91-99.

40. Quiroz, R. S.: The Warming of the Upper Stratosphere in February 1966 and Associated Structure of the Mesosphere. Mon. Wea. Rev., vol. 97, 1969, pp. 541-552.

41. Quiroz, R. S., Miller, A. J., and Nagatani, R. M.: A Comparison of Observed and Simulated Properties of Sudden Stratospheric Warmings. J. Atmos. Sci., vol. 32, 1975, pp. 1723-1736.

42. Matsuno, T.: A Dynamical Model of the Stratospheric Sudden Warming. J. Atmos. Sci., vol. 28, 1971, pp. 1479-1494.

43. Newson, R. J.: An Experiment with a Tropospheric and Stratospheric 3-dimensional General Circulation Model. Third Conference, Climatic Impact Assessment Program. U.S. Dep't of Transportation Rep. DOT-TSC-OST-74-15, pp. 461-473.

44. Hirota, I., Saotomi, K. Suzuki, T., and Ikeda, S.: Structure and Behavior of the Aleutian Anticyclone as Revealed by Meteorological Rocket and Satellite Observations. J. Meteorol. Soc. Japan, vol. 51, 1973, pp. 353-363.

45. Quiroz, R. S. and Miller A. J.: Height-lag Correlations of Density with Pressure and Temperature at Rocket Altitudes of the Stratosphere. J. Atmos. Sci., vol. 5, 1968, pp. 104-112.

46. Quiroz, R. S.: Estimation of Stratospheric-mesospheric Density Fields from Satellite Radiance Data. Mon. Wea. Rev., vol. 102, 1974, pp. 313-318.

47. Quiroz, R. S.: Modification of the Atmospheric Density Field in Response to Stratospheric Warmings. AMS-AIAA Fourth Nat'l Conf. Aerospace Meteorol., 1970, pp. 296-305.

48. Staff, Upper Air Branch: Stratospheric Density Maps for 1964-65 and for the Warming Event of December 1967. NASA TM X-1903, November 1969.

49. van Loon, D., Madden, R. A., and Jenne, R. L.: Oscillations in the Winter Stratosphere. Mon. Wea. Rev., vol. 103, 1975, pp. 154-162.

50. Hirota, I. and Sato, Y.: Periodic Variation of the Winter Stratospheric Circulation and Intermittent Vertical Propagation of Planetary Waves. J. Meteorol. Soc. Japan, vol. 47, 1969, pp. 390-402.

51. Miller, A. J.: Periodic Variation of Atmospheric Circulation at 14-16 Days. J. Atmos. Sci., vol. 31, 1974, pp. 720-726.

52. Craig, R. A. and Lateef, M. A.: Vertical Motion During the 1957 Stratospheric Warming. J. Geophys. Res., vol. 67, 1962, pp. 1839-1854.

53. Mahlman, J. D.: Heat Balance and Mean Meridional Circulation in the Polar Stratosphere During the Sudden Warming of January 1958. Mon. Wea. Rev., vol. 97, 1969, pp. 534-540.

54. Miller, A. J.: A Note on Vertical Motion Analysis for the Upper Stratosphere. Mon. Wea. Rev., vol. 98, 1970, pp. 616-620.

55. Hirota, I.: Planetary Waves in the Upper Stratosphere in Early 1966. J. Meteorol. Soc. Japan, vol. 46, 1968, pp. 418-429.

56. Phillpot, H. R.: The Springtime Accelerated Warming in the Antarctic Stratosphere. Int'l Antarctic Analysis Centre, Tech. Rep. 3, Bur., of Meteorol., Melbourne, 1964.

57. Quiroz, R. S.: The High-latitude Density Regime at Rocket Altitudes Inferred from Observations in Opposite Hemispheres. J. Appl. Meteorol., vol. 5, 1966, pp. 308-313.

58. Shen, W. C., Nicholas, G. W., and Belmont, A. D.: Antarctic Stratospheric Warmings During 1963 Revealed by 15-μ TIROS-VII Data. J. Appl. Meteorol., vol. 7, 1968, pp. 268-283.

59. Quiroz, R. S.: Stratospheric Warmings in the Southern Hemisphere Deduced from Satellite Radiation Data, 1969-73. Int'l Conf. on Structure, Composition, and General Circulation of the Upper and Lower Atmospheres, vol. 2, 1974, pp. 525-539.

60. Labitzke, K.: The Temperature in the Upper Stratosphere: Differences Between Hemispheres. J. Geophys. Res., vol. 79, 1974, pp. 2171-2175.

61. Miller, A. J., Finger, F. G., and Gelman, M. E.: 30-mb Synoptic Analyses for the 1969 Southern Hemisphere Winter Derived with the Aid of Nimbus III (SIRS) Data. NASA TM X-2109, 1970.

62. Quiroz, R. S., Weinreb, M. P., and Wark, D. Q.: Operational Radiance Maps of the Stratosphere, with Preliminary Details of a Major Stratospheric Warming. Space Research XIV, Akademie-Verlag, Berlin, 1974, pp. 31-37.

63. Fritz, S. and McInturff, R. M.: Stratospheric Temperature in Autumn--Northern and Southern Hemispheres Compared. Mon. Wea. Rev., vol. 100, 1972, pp. 1-7.

64. Harwood, R. S.: Temperature Waves in the Southern Hemisphere Observed by the Selective Chopper Radiometer on Nimbus IV. Int'l Conf. on Structure, Composition, and General Circulation of the Upper and Lower Stratospheres and Possible Anthropogenic Influences, Melbourne, Australia, 1974, pp. 540-555.

65. Holton, J. R.: An Introduction to Dynamic Meteorology. Academic Press, 1972.

66. Lorenz, E. N.: The Nature and Theory of the General Circulation of the Atmosphere. World Meteorological Organization, 1967.

67. Eliassen, A. and Palm, E.: On the Transfer of Energy in Stationary Mountain Waves. Geofys. Publ., vol. 12, 1960, pp. 1-23.

68. Reed, R. J., Wolfe, J. L., and Nishimoto, H.: A Spectral Analysis of the Energetics of the Stratospheric Sudden Warming of Early 1957. J. Atmos. Sci., vol. 20, 1963, pp. 256-275.

69. Oort, A. H.: On the Energetics of the Mean and Eddy Circulations in the Lower Stratosphere. Tellus, vol. 16, 1964, pp. 309-327.

70. Miller, A. J. and Johnson, K. W.: On the Interaction Between the Stratosphere and Troposphere During the Warming of December 1967-January 1968. Quart. J. Roy. Meteorol. Soc., vol. 96, 1970, pp. 24-31.

71. Dopplick, T. G.: The Energetics of the Lower Stratosphere Including Radiative Effects. Quart. J. Roy. Meteorol. Soc., vol. 97, 1971, pp. 209-237.

72. Lateef, M. A.: The Energy Budget over North America During the Warming of 1957. J. Geophys. Res., vol. 69, 1964, pp. 1481-1495.

73. Teweles, S.: Spectral Aspects of the Stratospheric Circulation During the IGY. Planetary Circulations Proj. Rep. 8, Mass. Inst. of Tech., 1963.

74. White, R. M.: The Counter-gradient Flux of Sensible Heat in the Lower Stratosphere. Tellus, vol. 6, 1954, pp. 177-179.

75. Starr, V.: Questions Concerning the Energy of Stratospheric Motions. Arch. f. Meteorol., Geoph., u. Biokl., Ser. A, vol. 12, 1960, pp. 1-7.

76. Saltzman, B.: Equations Governing the Energetics of the Larger Scales of Atmospheric Turbulence in the Domain of Wave Number. J. Meteorol., vol. 14, 1957, pp. 513-523.

77. Merilees, P. E.: Non-linear Barotropic Interactions. Publication in Meteorology No. 80, Department of Meteorology, McGill University, 1966, pp. 51-73.

78. Charney, J. G. and Stern, M. E.: On the Stability of Internal Baroclinic Jets in a Rotating Atmosphere. J. Atmos. Sci., vol. 19, 1962, pp. 159-172.

79. Johnson, K. W., Miller, A. J., and Gelman, M. E.: Proposed Indices Characterizing Stratospheric Circulation and Temperature Fields. Mon. Wea. Rev., vol. 97, 1969, pp. 565-570.

80. Miller, A. J.: The Transfer of Kinetic Energy from the Troposphere to the Stratosphere. J. Atmos. Sci., vol. 27, 1970, pp. 388-393.

81. Iwashima, T.: Observational Studies of the Ultra-long Waves in the Atmosphere (II). Part 2. Ultra-long Wave Energy Processes During the Stratospheric Sudden Warming. J. Meteorol. Soc. Japan, vol. 52, 1974, pp. 12-142.

82. Klinker, E.: The Energetics of the Stratosphere During the Warming Period 1974/75. COSPAR, Space Research XVII, Pergamon Press, 1977.

83. McInturff, R. M.: Recent Estimates of Stratopause Heights and Temperatures. National Weather Service, 1974.

84. Labitzke, K.: The Interaction Between Stratosphere and Mesosphere in Winter. J. Atmos. Sci., vol. 29, 1972, pp. 1395-1399.

85. Brown, G. M. and Williams, D. C.: Pressure Variations in the Stratosphere and Ionosphere. J. Atmos. Terr. Phys., vol. 33, 1971, pp. 1321-1328.

86. Miyakoda, K., Strickler, R. F., and Hembree, G. D.: Numerical Simulation of the Breakdown of a Polar-night Vortex in the Stratosphere. J. Atmos. Sci., vol. 27, 1970, pp. 139-154.

87. Manabe, S. and Hunt, B. G.: Experiments with a Stratospheric General Circulation Model, I. Radiative and Dynamics Aspects. Mon. Wea. Rev., vol. 96, 1968, pp. 477-502.

88. Cunnold, D. M., Alyea, F. N., Phillips, N. A., and Prinn, R. G.: A General Circulation Model of Stratospheric Ozone. International Conference on Structure, Composition and General Circulation of the Upper and Lower Atmospheres, and Possible Anthropogenic Perturbations, Melbourne, Australia, 1974, pp. 932-970.

89. Clark, J. H. E.: A Quasi-geostrophic Model of the Winter Stratospheric Circulation. Mon. Wea. Rev., vol. 98, 1970, pp. 443-461.

90. Byron-Scott, R.: A Stratospheric General Circulation Experiment Incorporating Diabatic Heating and Ozone Chemistry. Publs. Meteorol. No. 87, Arctic Meteorol. Research Gp., McGill Univ., 1967, 201 pp.

91. Charney, J. G. and Drazin, P. G.: Propagation of Planetary-scale Disturbances from the Lower into the Upper Atmosphere. J. Geophys. Res., vol. 66, 1961, pp. 83-109.

92. Geisler, J. E.: A Numerical Model of the Sudden Stratospheric Warming Mechanism. J. Geophys. Res., vol. 79, 1974, pp. 4989-4999.

93. Dickinson, R. E.: Theory of Planetary Wave-zonal Flow Interaction. J. Atmos. Sci., vol. 26, 1969, pp. 73-81.

94. Holton, J. R.: A Semi-spectral Numerical Model for Wave-mean Flow Interactions in the Stratosphere: Application to Sudden Stratospheric Warmings. J. Atmos. Sci., vol. 33, 1976, pp. 1639-1649.

95. Craig, R. A.: The Upper Atmosphere, Meteorology and Physics. Academic Press, 1965.

96. Dütsch, H. U.: Ozone and Temperature in the Stratosphere. Symposium on Stratospheric and Mesospheric Circulation, Meteorologische Abhandlungen der Freien Universität Berlin, Bd. XXXVI, 1963, pp. 271-291.

97. London, J.: Ozone Variations and Their Relation to Stratospheric Warmings. Symposium on Stratospheric and Mesospheric Circulation, Meteorologische Abhandlungen der Freien Universität Berlin, BD. XXXVI, 1963, pp. 299-310.

98. Heath, D. F.: Recent Advances in Satellite Observations of Solar Variability and Global Atmospheric Ozone. International Conference on Structure, Composition, and General Circulation of the Upper and Lower Atmospheres, and Possible Anthropogenic Perturbations, Melbourne, Australia, 1974, pp. 1267-1291.

99. Züllig, W.: Relation Between the Intensity of the Stratospheric Circumpolar Vortex and the Accumulation of Ozone in the Winter Hemisphere. Pure and Appl. Geophys., vol. 106-108, 1973, pp. 1544-1552.

100. Ghazi, A.: Nimbus 4 Observations of Changes in Total Ozone and Stratospheric Temperatures During a Sudden Warming. J. Atmos. Sci., vol. 31, 1974, pp. 2197-2206.

101. Quiroz, R. S.: On the Relative Need for Satellite Remote Soundings and Rocket Soundings of the Upper Atmosphere. Bull. Am. Meteorol. Soc., vol. 53, 1972, pp. 122-133.

102. Donn. W. L. and Shaw, D. M.: Exploring the Atmosphere with Nuclear Explosions. Rev. Geophys., vol. 5, 1967, pp. 53-82.

103. Donn, W. L. and Reid, D.: Microbaroms and the Temperature and Wind of the Upper Atmosphere. J. Atmos. Sci., vol. 29, 1972, pp. 156-172.

104. Tolstoy, I. and Herron, T. J.: Atmospheric Gravity Waves from Nuclear Explosions. J. Atmos. Sci., vol. 27, 1970, pp. 55-61.

105. Dousset, C., Joatton, R., and Stuckelberger, R.: Stratospheric Flight and Meteorology: Initial Data on Concorde. International Conference on Aerospace and Aeronautical Meteorology, American Meteorological Society, 1972.

106. COSPAR International Reference Atmosphere (CIRA). Akademie-Verlag (Berlin), 1972.

107. U.S. Standard Atmosphere Supplements. U.S. Government Printing Office, 1966.

108. Smith, O. E., Redus, J. R., Forney, J. A., and Dash, M. J.: Effects of Atmospheric Models on Space Shuttle Trajectories and Aerodynamic Heating. International Conference on Aerospace and Aeronautical Meteorology, American Meteorological Society, 1972.

BIBLIOGRAPHY

Ackerman, M.: Ultraviolet Solar Radiation Related to Mesospheric Processes. *Mesospheric Models and Related Experiments, G. Fiocco.* ed., Dordrecht, Reidel, 1971, pp. 149-159.

Barnett, J. J.: Large Sudden Warming in the Southern Hemisphere. Nature, vol. 255, 1975, pp. 387-389.

Barnett, J. J., Harwood, R. S., Houghton, J. T., Morgan, C. G., Rodgers, C. D., Williamson, E. J., Peckham, G., and Smith, S. D.: Stratospheric Warming Observed by Nimbus IV. Nature, vol. 230, 1971, pp. 47-48.

Davis, D. D.: New Rate Measurements on the Reaction of O(3P), O_3, and OH. AIAA Paper 73-501, June 1973.

Dickinson, R. E.: On the Exact and Approximate Linear Theory of Vertically Propagating Planetary Rossby Waves Forced at a Spherical Lower Boundary. Mon. Wea. Rev., vol. 96, 1968, pp. 405-415.

Dickinson, R. E.: Planetary Rossby Waves Propagating Vertically Through Weak Westerly Wind Wave Guides. J. Atmos. Sci., vol. 25, 1968, pp. 984-1002.

Dickinson, R. E.: Vertical Propagation of Planetary Rossby Waves Through an Atmosphere with Newtonian Cooling. J. Geophys. Res., vol. 74, 1968, pp. 929-938.

Dickinson, R. E.: Development of a Rossby Wave Critical Level. J. Atmos. Sci., vol. 27, 1970, pp. 627-633.

Dütsch, H. U.: Ozone Distribution and Stratospheric Temperature Field over Europe During a Sudden Warming in January/February 1958. Beitr. Phys. Atmos., vol. 35, 1962, pp. 87-107.

Finger, F. G., Gelman, M. E., and McInturff, R. M.: High-level Circulation Studies Based on Rawinsonde, Rocketsonde, and Satellite Observations. COSPAR, Space Research XIV, Akademie-Verlag, Berlin, 1974, pp. 17-29.

Fritz, S. and Soules, S. D.: Large-scale Temperature Changes in the Stratosphere Observed from Nimbus III. J. Atmos. Sci., vol. 27, 1970, pp. 1091-1097.

Garvin, D. and Hampson, R. F.: Atmospheric Modeling and the Chemical Data Problem. AIAA Paper 73-500, June 1973.

Green, J. S. A.: Large-scale Motion in the Upper Stratosphere and Mesosphere: An Evaluation of Data and Theories. Phil. Trans. R. Soc. Lond, A271, 1972, pp. 577-583.

Hare, F. K.: The Disturbed Circulation of the Arctic Stratosphere. J. Meteorol., vol. 17, 1960, pp. 36-51.

Hare, F. and Boville, B.: The Polar Circulation. W.M.O. Technical Note No. 70, 1965, pp. 42-78.

Hilsenrath, E.: Ozone Measurements in the Mesosphere and Stratosphere During Two Significant Geophysical Events. J. Atmos. Sci., vol. 28, 1971, pp. 295-297.

Hirota, I.: Dynamic Instability of the Stratospheric Polar Vortex. J. Meteorol. Soc. Japan, vol. 45, 1967, pp. 353-365.

Hirota, I.: The Vertical Structure of the Stratospheric Sudden Warming. J. Meteorol. Soc. Japan, vol. 45, 1967, pp. 422-435.

Hirota, I.: Planetary Waves in the Upper Stratosphere in Early 1966. J. Meteorol. Soc. Japan, vol. 46, 1968, pp. 418-430.

Hirota, I.: Exictation of Planetary Rossby Waves in the Winter Stratosphere by Periodic Forcing. J. Meteorol. Soc. Japan, vol. 49, 1971, pp. 439-449.

Holton, J. R.: The Dynamic Meteorology of the Stratosphere to Mesosphere. American Meteorological Society, 1975, 216 pp.

Johnson, K. W.: A Preliminary Study of the Stratospheric Warming of December 1967-January 1968. Mon. Wea. Rev., vol. 97, 1971, pp. 553-564.

Julian, P. R.: Some Aspects of Tropospheric Circulation During Mid-winter Stratospheric Warming Event. J. Geophys. Res., vol. 70, 1965, pp. 757-767.

Julian, P. R.: Midwinter Stratospheric Warmings in the Southern Hemisphere - General Remarks and a Case Study. J. Appl. Meteor., vol. 6, 1967, pp. 557-563.

Kockarts, G.: Penetration of Solar Radiation in the Schumann-Runge Bands of Molecular Oxygen. Mesospheric Models and Related Experiments, G. Fiocco, ed., Dordrecht, Reidel, 1971, pp. 160-175.

Labitzke, K. B.: On the Mutual Relation Between Stratosphere and Troposphere During Periods of Stratospheric Warmings in Winter. J. Appl. Meteor., vol. 4, 1965, pp. 91-99.

Labitzke, K. B.: Midwinter Warmings in the Upper Stratosphere in 1966. Quart. J. Roy. Meteorol. Soc., vol. 94, 1968, pp. 274-291.

Labitzke, K. B. and Barnett, J. J.: Global Time and Space Changes of Satellite Radiances Received From the Stratosphere and Lower Mesosphere. J. Geophys. Res., vol. 78, 1973, pp. 483-496.

Labitzke, K. and Schwentek, H.: Midwinter Warmings in the Stratosphere and Lower Mesosphere and the Behaviour of Ionospheric Absorption. Zeit. für Geophys., vol. 34, 1968, pp. 555-566.

Labitzke, K. and van Loon, H.: The Stratosphere of the Southern Hemisphere. Meteorol. Monogr., vol. 13, pp. 113-138, American Meteorological Society, Boston, Mass., 1972.

Mahlman, J. D.: Energetics of a "Minor Breakdown" of the Stratospheric Polar-night Vortex. J. Atmos. Sci., vol. 26, 1969, pp. 1306-1317.

Mahlman, J. D.: Heat Balance and Mean Meridional Circulation in Polar Stratosphere During Sudden Warming of January 1958. Mon. Wea. Rev., vol. 97, 1969, pp. 534-540.

Matsuno, T. and Hirota, T.: On the Dynamical Stability of Polar Vortex in Wintertime. J. Meteor. Soc. Japan, vol. 44, 1966, pp. 122-128.

McElroy, M., Wofsy, S., Penner, J., and McConnell, J.: Atmospheric Ozone: Possible Impact of Stratospheric Aviation. J. Atmos. Sci., vol. 31, 1974, pp. 287-303.

McInturff, R. M. and Fritz, S.: The Depiction of Stratospheric Warmings with Satellite Radiance Data. International Conference on Aerospace and Aeronautical Meteorology, American Meteorological Society, Boston, 1972, pp. 113-114.

McIntyre, M. E.: Baroclinic Instability of an Idealized Model of the Polar-night Jet. Quart. J. Roy. Meteorol. Soc., vol. 98, 1972, pp. 165-174.

Murakami, T.: Energy Cycle of the Stratospheric Warming in Early 1958. J. Meteorol. Soc. Japan, vol. 45, 1965, pp. 205-231.

Murgatroyd, R. J.: The Structure and Dynamics of the Stratosphere. The Global Circulation of the Atmosphere, London, Royal Meteorol. Soc., 1970, pp. 159-195.

Murray, F.: Dynamic Stability in the Stratosphere. J. Geophys. Res., vol. 65, 1960, pp. 3273-3305.

Nitta, T.: Dynamical Interaction Between the Lower Stratosphere and the Troposphere. Mon. Wea. Rev., vol. 95, 1967, pp. 319-338.

Phillpot, H. R.: Antarctic Stratospheric Warming Reviewed in the Light of 1967 Observations. Quart. J. Roy. Meteorol. Soc., vol. 95, 1969, pp. 329-348.

Reed, R. J.: On the Cause of the Stratospheric Warming Phenomenon. International Symposium on Stratospheric and Mesospheric Circulation, Berlin Free University, Meteor. Abh., vol. 36, 1963, pp. 315-334.

Sawyer, J. S.: The Dynamical Problems of the Lower Stratosphere. Quart. J. Roy. Meteorol. Soc., vol. 91, 1965, pp. 407-416.

Schofield, K.: An Evaluation of Kinetic Rate Data for Reactions of Neutrals of Atmospheric Interest. Planet. Space Sci., vol. 15, 1967, p. 643.

Sheppard, P. A.: Dynamics of the Upper Atmosphere. J. Geophys. Res., vol. 64, 1959, pp. 2116-2121.

Simmons, A. J.: Planetary-scale Disturbances in the Polar Winter Stratosphere. Quart. J. Roy. Meteorol. Soc., vol. 100, 1974, pp. 76-108.

Trenberth, K. E.: Global Model of the General Circulation of the Atmosphere Below 75 Kilometers with an Annual Heating Cycle. Mon. Wea. Rev., vol. 101, 1973, pp. 287-305.

Webb, W. L.: Structure of the Stratosphere and Mesosphere. Academic Press, 1966.

1. Report No.	2. Government Accession No.	3. Recipient's Catalog No.
NASA RP-1017		

4. Title and Subtitle	5. Report Date
STRATOSPHERIC WARMINGS: SYNOPTIC, DYNAMIC AND GENERAL-CIRCULATION ASPECTS	January 1978
	6. Performing Organization Code
7. ~~Author(s)~~ Editor: Raymond M. McInturff	8. Performing Organization Report No.
	10. Work Unit No.
9. Performing Organization Name and Address Upper Air Branch, National Meteorological Center National Weather Service, NOAA Washington, DC 20233	11. Contract or Grant No. P55,946(G)
	13. Type of Report and Period Covered
12. Sponsoring Agency Name and Address National Aeronautics and Space Administration Wallops Flight Center Wallops Island, VA 23337	14. Sponsoring Agency Code

15. Supplementary Notes

16. Abstract

Current knowledge of stratospheric warming phenomena is presented. This is set against the background of stratospheric climatology, which includes an account of "normal" stratospheric variation at middle and high latitudes. Synoptic descriptions consist largely of case-studies, which involve a distinction between major and minor warmings. Results of energetics studies show the importance of tropospheric-stratospheric interaction, and the significance of the pressure-work term near the tropopause. Theoretical studies have suggested the role of wave-zonal flow interaction as well as nonlinear interaction between eddies, chemical and photochemical reactions, boundary forcing, and other factors. Numerical models have been based on such considerations, and these are discussed under various categories. Some indication is given as to why some of the models have been more successful than others in simulating warmings. The question of ozone and its role in warmings is briefly discussed. Finally, a broad view is taken of stratospheric warmings in relation to man's activities.

17. Key Words (Suggested by Author(s))

Stratospheric Warming
Atmospheric Circulation
Synoptic Meteorology
Atmospheric Models
Sounding Rockets
Satellite observation
Climatology
Rawinsondes

18. Distribution Statement

Unclassified - unlimited

STAR Category 47

19. Security Classif. (of this report)	20. Security Classif. (of this page)	21. No. of Pages	22. Price*
Unclassified	Unclassified	174	$6.75

* For sale by the National Technical Information Service, Springfield, Virginia 22161

NASA-Langley, 1978

18 1 1U,E,SPGEN,010978 S00903DS 740731
DEPT OF THE AIR FORCE
AF WEAPONS LABORATORY
ATTN: TECHNICAL LIBRARY (SUL)
KIRTLAND AFB NM 87117